COMPLEXES OF GROUP 10 METALS WITH NON-CLASSICAL AND THIOETHER-FUNCTIONALIZED N-HETEROCYLIC CARBENE LIGANDS

JAN CHRISTOPHER BERNHAMMER

(DIPL.-CHEM., PHILIPPS-UNIVERSITÄT MARBURG)

A THESIS SUBMITTED FOR THE DEGREE OF

DOCTOR OF PHILOSOPHY

DEPARTMENT OF CHEMISTRY

NATIONAL UNIVERSITY OF SINGAPORE

2014

DECLARATION

I hereby declare that this thesis is my original work and it has been written by me in its entirety, under the supervision of A/P Huynh Han Vinh, Chemistry Department, National University of Singapore, between 2011 and 2014.

I have duly acknowledged all the sources of information which have been used in the thesis.

This thesis has also not been submitted for any degree in any university previously.

The content of the thesis has been partly published in:

1) Bernhammer, J. C.; Huynh, H. V. *Dalton Trans.* **2012**, *41*, 8600.
2) Bernhammer, J. C.; Huynh, H. V. *Organometallics* **2012**, *31*, 5121.
3) Bernhammer, J. C.; Frison, G.; Huynh, H. V. *Chem. Eur. J.* **2013**, *19*, 12892.
4) Bernhammer, J. C.; Huynh, H. V. *Organometallics* **2014**, *33*, 172.
5) Bernhammer, J. C.; Huynh, H. V. *Organometallics* **2014**, *33*, 1266.
6) Bernhammer, J. C.; Frison, G. ; Huynh, H. V. *Dalton Trans.* **2014**, *43*, 8591.
7) Bernhammer, J. C.; Chong, N. X.; Jothibasu, R.; Zhou, B.; Huynh, H. V. *Organometallics* **2014**, *33*, 3607.
8) Bernhammer, J. C.; Singh, H.; Huynh, H. V. *Organometallics* **2014**, *33*, 4295.
9) Bernhammer, J. C.; Huynh, H. V. *Organometallics* **2014**, Article ASAP.

Jan C. Bernhammer		/ /2014
Name	Signature	Date

La science n’a pas de patrie, parce que le savoir est le patrimoine de l’humanité, le flambeau qui éclaire le monde.

(Louis Pasteur)

Acknowledgements

I thank my supervisor, A/P Huynh Han Vinh, for his guidance throughout my research, many fruitful discussions, helpful remarks, and for being an impressive source of chemical inspiration and creativity. He has given me the possibility to explore the fascinating chemistry of N-heterocyclic carbenes, and helped me overcome the challenges along the way.

I'm thankful for the SINGA scholarship provided by NUS and A*STAR, and the opportunity to work and study in Singapore.

Dr. Gilles Frison was so kind to accept me as a visiting researcher into his lab at Ecole Polytechnique for several months. He provided me with training in theoretical chemistry, and was always helpful in answering any questions pertaining to this matter even after my return to Singapore.

I also thank the technical staff at the various analytical laboratories. Ms. Han Yanhui and Dr. Wu Ji'en ensured smooth operation of the NMR facilities and provided assistance when needed. Similarly, Ms. Wong Lai Kwai from the mass spectrometry lab provided help with the operation of mass spectrometers and GC-MS. I thank Ms. Leng Lee Eng and Ms. Zing Tan Tsze Yin for performing elemental analyses, and I'm especially grateful to Mr. Bruno Donnadieu, Ms. Tan Geok Khong, and Prof. Koh Lip Lin for obtaining and refining the molecular structures presented in this work. Other technical and administrative staff members at the Department of Chemistry that shouldn't go unmentioned are the always helpful Mr. Ramasamy Dhasaratha Raman of the glassblowing workshop, Mr. Phua Wei De Victor who provided lab supplies and always a cheerful word, and Suriawati Binte Saad who helped me with administrative matters.

My past and present labmates are thanked for their contributions to my research and their advice. I'm especially grateful to Dr. Yuan Dan and Haresh S/O Sivaram for helping me to get started in the lab, and to Guo Shuai, Ning Xi Chong, Zhou Binbin, and Harvenjit Singh, with whom I have worked together on publications.

I thank my friends in Singapore, in Germany, and elsewhere, for their continuous support, their company, and their encouragement. And finally, I thank my family for their unwavering assistance and their belief in me, not only during my graduate studies, but throughout my whole academic career.

Table of Contents

Summary

Since their isolation in pure form two decades ago, N-heterocyclic carbenes (NHCs) have risen to prominence as one of the most important classes of ligands in transition metal catalysts, and found widespread application as organocatalysts. This thesis describes a theoretical approach to a better understanding of these ligands, as well as experimental contributions to the development of group 10 complexes with electron-rich NHCs as well as sulfur- and nitrogen-functionalized NHCs, and the application of these complexes in a variety of catalytic reactions.

Chapter 2 describes the study of the electronic structures of 14 N-heterocyclic carbene ligands derived from five-membered azoles with varying numbers of nitrogen atoms in the heterocycle by DFT calculations. After identifying key electronic parameters and their variation with molecular structures, the binding of these NCHs to early and late transition metal fragments is described in detail based on results from energy decomposition analyses and ETS-NOCV calculations.

The first part of chapter 3 builds on previous research concerning ligand donor strength determinations by means of ^{13}C NMR spectroscopy, and correlates the donor strengths of substituted pyrazoles with their nucleophilicities as estimated by their reactivities towards ethyl bromide, ethyl iodide and trimethyloxonium tetrafluoroborate. In the second part, the synthesis of pyrazolin-3-ylidene complexes of palladium(II) by means of oxidative addition and by silver carbene transfer is described. A small library of complexes with varying coligands was prepared, and the activity of these complexes in the direct arylation of pentafluorobenzene was studied.

The fourth chapter is focused on indazolin-3-ylidene ligands and their coordination chemistry with palladium(II). Mixed NHC-phosphine complexes were prepared and their and catalytic applications for Sonogashira cross-couplings and the hydroamination of alkynes are described in this chapter. Additionaly, a library of indazolin-3-ylidene complexes bearing different pendant tertiary amine functionalities were prepared by post-functionalization of a common precursor complex. These complexes were used as precatalysts for the direct arylation of 1-methylpyrrole.

Chapter 5 describes the synthesis of thioether-functionalized benzimidazolium salts, the coordination chemistry of the corresponding NHCs with platinum(II), palladium(II) and nickel(II), and applications of the resulting complexes in catalysis. Three distinct coordination modes exist for these complexes. For platinum(II), the chelating κ^2-*C*,*S* coordination mode is

exclusively observed in the solid state of the mono-NHC complexes, albeit evidence exists that other forms might exist in solution. The palladium(II) complexes show either the chelating κ^2-*C*,*S* coordination mode, or dimeric species bridged in which the coordination sites of the ligand are bound to different metal centers. For nickel(II), homo-bis(NHC) complexes with pendant thioether functionalities were prepared. Platinum(II) complexes were found to be active catalysts for intermolecular hyroaminations and hydrosilylations, palladium(II) complexes catalyzed hydroaminations and direct arylations of 1-methylpyrrole, and nickel(II) complexes were used as precatalysts for the Suzuki-Miyaura coupling.

Additionally, the coordination chemistry of structurally related *C*,*S*,*C*-pincer ligands with palladium(II) was studied computationally, and the interconversion between the pincer and pseudopincer forms was found to be correlated to the ligand donor strength of the ligands' NHC moieties.

Compounds Synthesized in this Work

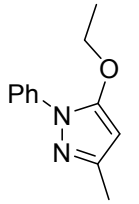

60

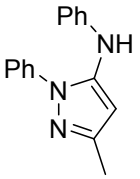

63

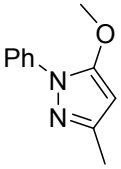

64

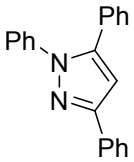

68

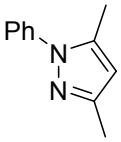

69

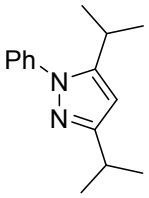

70

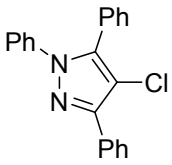

71

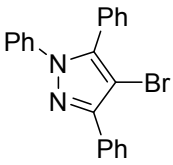

72

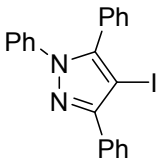

73

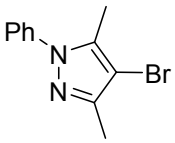

75

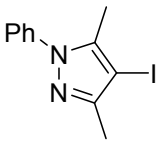

76

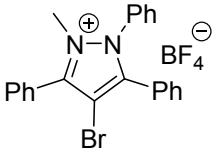

79

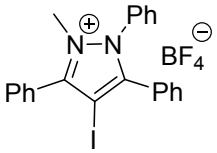

80

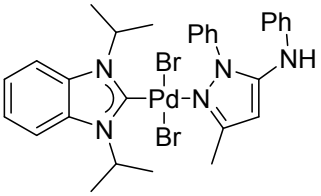

81

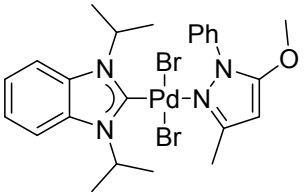

82

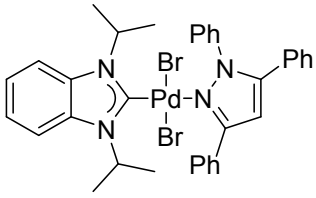

83

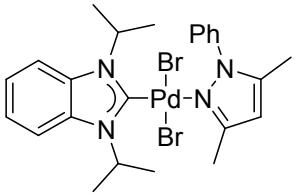

84

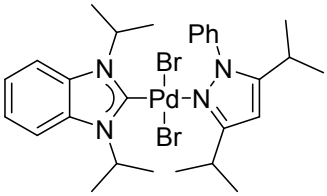

85

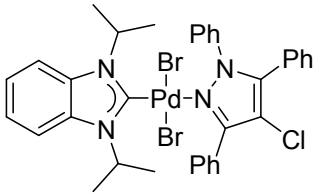

86

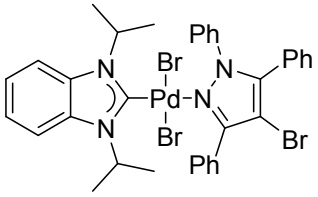

87

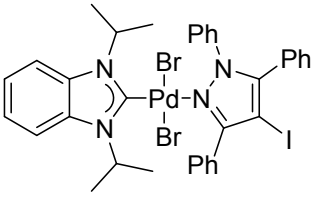

88

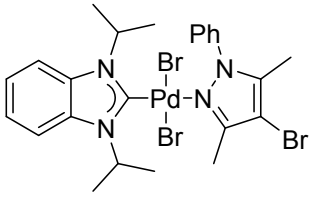

89

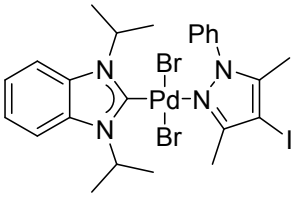

90

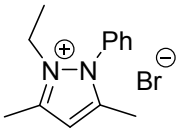

91

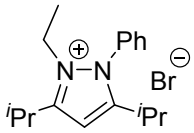

92

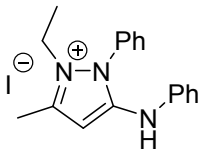

93

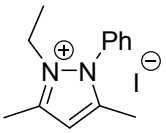

94

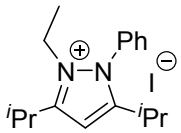

95

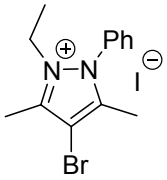

96

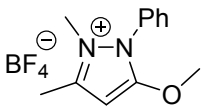

97

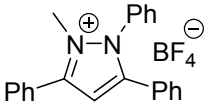

98

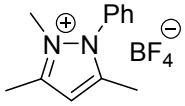

99

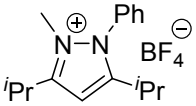

100

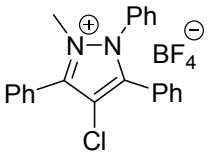

101

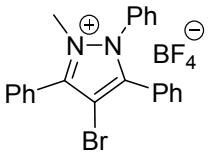

102

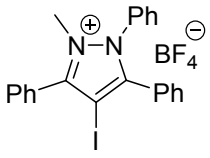

103

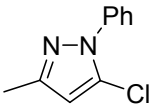

104

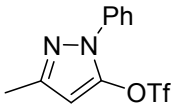

105

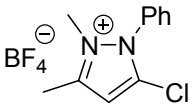

107

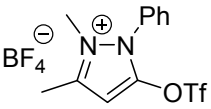

108

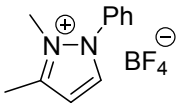

109

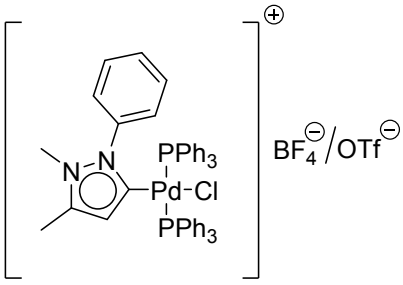

112

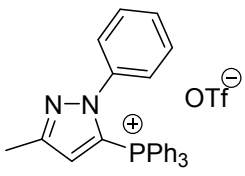

114

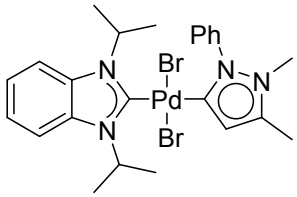

116

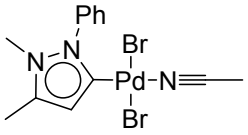

117

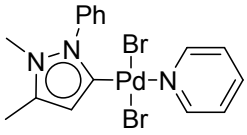

118

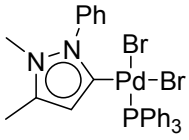

119

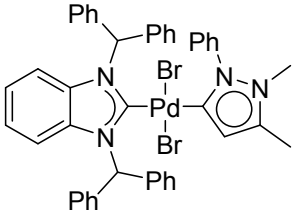

120

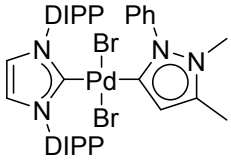

121

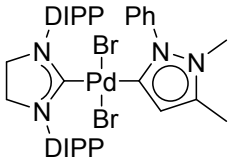

122

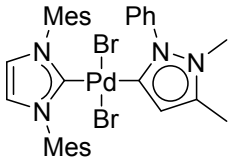

123

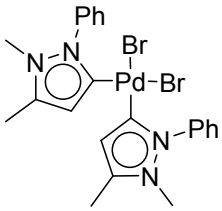

124

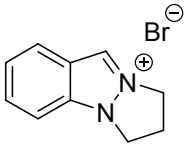

131

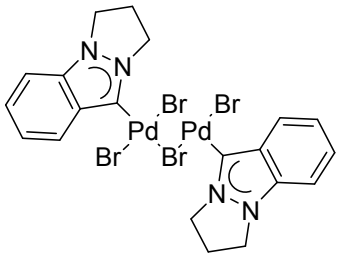

133

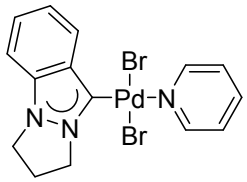

135

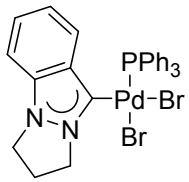

136

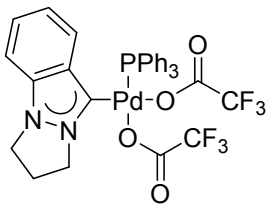

137

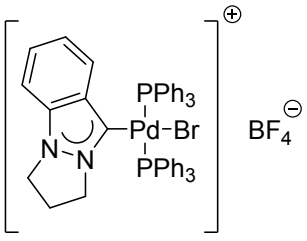

138

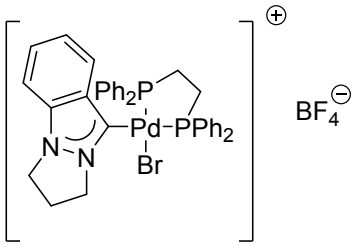

139

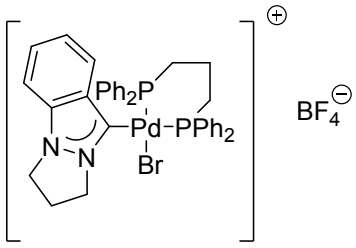

140

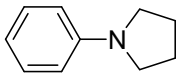

166

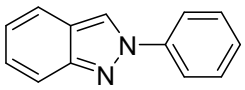

179

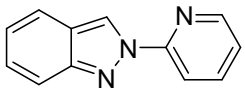

181

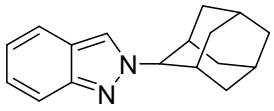

182

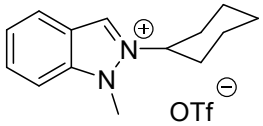

187

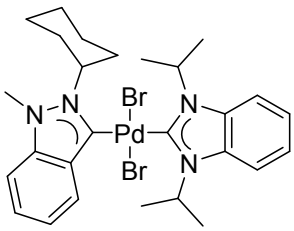

188

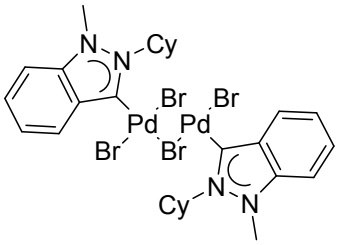

189

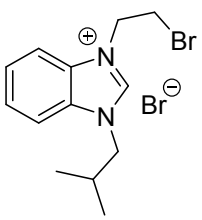

200

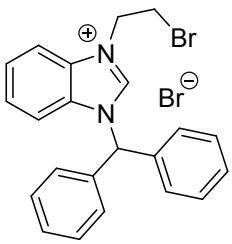

201

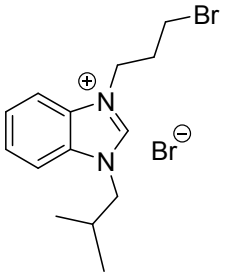

203

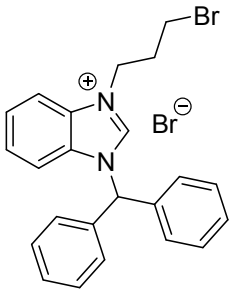

204

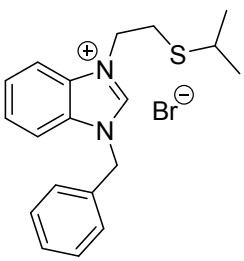

205

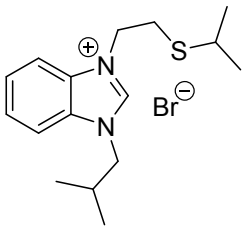

206

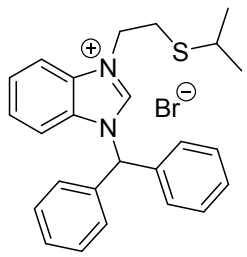

207

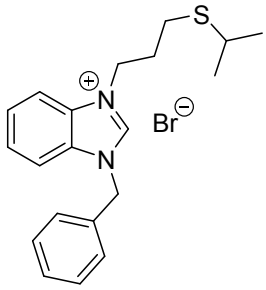

208

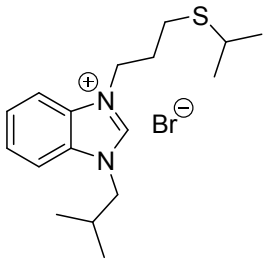

209

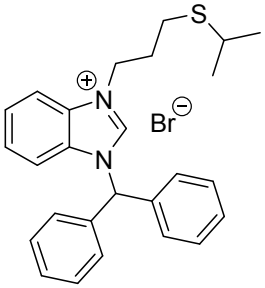

210

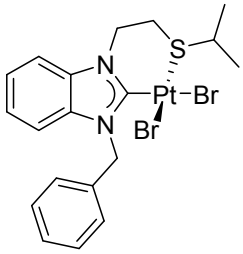

211

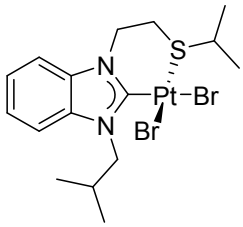

212

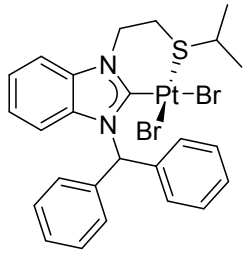

213

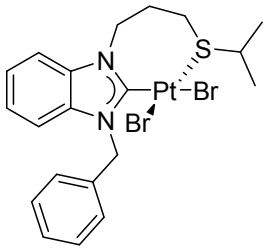

214

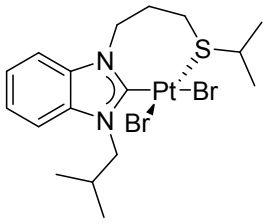

215

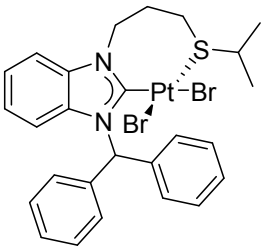

216

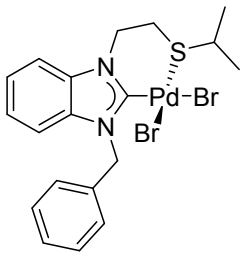

221

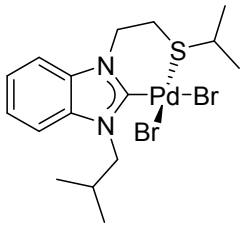

222

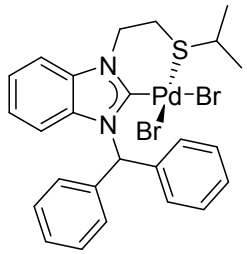

223

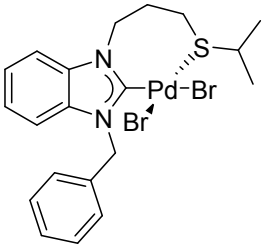

224

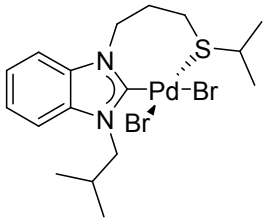

225

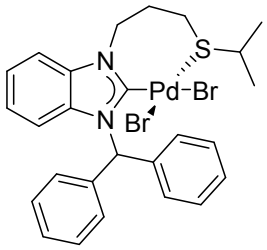

226

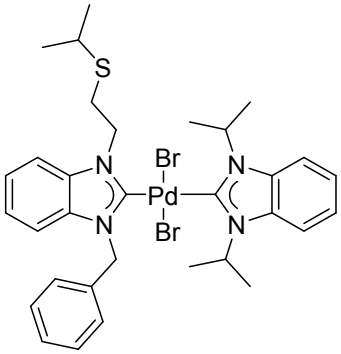

227

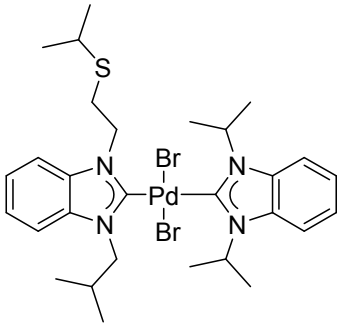

228

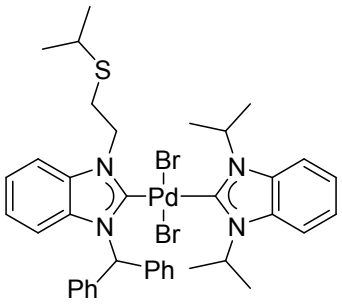

229

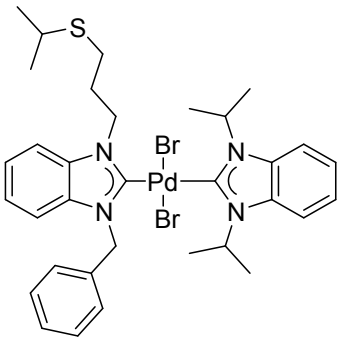

230

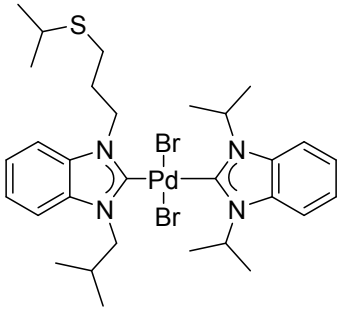

231

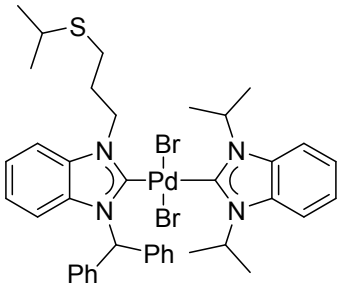

232

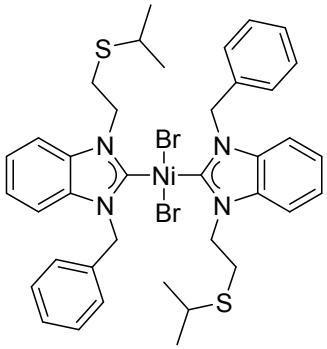

233

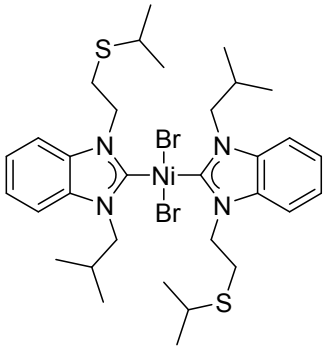

234

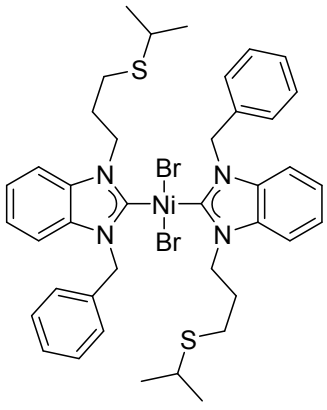

236

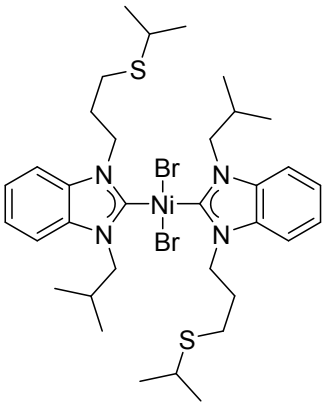

237

List of Tables

List of Figures

List of Schemes

List of Abbreviations

Anal. Calcd.	analysis calculated
Ar	aryl
Bn	benzyl
br	broad
^{i}Bu	*iso*-butyl
^{n}Bu	*n*-butyl
^{t}Bu	*tert*-butyl
cf.	compare (Latin *confer*)
Cy	cyclohexyl
δ	NMR chemical shift in ppm
d	doublet (NMR)
dba	dibenzylideneacetone
DCM	dichloromethane
dd	doublet of doublets (NMR)
DEAD	diethyl azodicarboxylate
DIPEA	diisopropylethylamine
DIPP	2,6-diisopropylphenyl
DMA	dimethylacetamide
DMF	dimethylformamide
DMSO	dimethylsulfoxide
EA	ethyl acetate
e.g.	for example (Lation *exempli gratia*)
EI	electron ionisation (mass spectrometry)
equiv.	equivalent(s)
ESI	electrospray ionisation (mass spectrometry)
et al.	and others (Latin *et alii*)
etc.	and so on (Latin *et cetera*)
GC-MS	gas chromatography – mass spectrometry
h	hour

i.e.	that is (Latin *id est*)
J	coupling constant (NMR)
m	multiplet (NMR)
Me	methyl
Mes	2,4,6-trimethylphenyl
min	minute
MS	mass spectrometry
MW	microwave irradiation
m/z	mass to charge ratio
NMR	nuclear magnetic resonance
PA	proton affinity
Ph	phenyl
Pr	propyl
^{i}Pr	isopropyl
s	singlet
t	triplet
TBAB	tetrabutylammonium bromide
TBACl	tetrabutylammonium chloride
TBAF	tetrabutylammonium fluoride
Tf	triflate
THF	tetrahydrofurane
TLC	thin layer chromatography
TMEDA	tetramethylethylenediamine
TMS	trimethylsilyl

1. Introduction

Carbenes are neutral, divalent carbon species with six valence electrons. Besides their two covalent bonds, they possess two non-bonding electrons, which can either be of the same spin, resulting in a triplet state, or spin-paired, giving rise to a singlet state.[1] The simplest carbene is thus methylene, and more complex carbenes can be formally derived from this system by replacing the hydrogen groups with more complex substituents.

The resulting species R_2C: can adopt either a linear or a bent geometry, which can be understood when considering the hybridization at the carbene centre. The linear geometry arises when bonding occurs using two sp-orbitals, leaving two energetically degenerate p orbitals (p_x and p_y) to accommodate the non-bonding electrons. In this case, the Pauli exclusion principle allows only the electron configuration $p_x^1 p_y^1$, since the spin-pairing energy cannot be offset by a difference in orbital energies. Since both electrons have the same spin, the ground state of such a carbene is always a triplet state (Fig. 1.1).

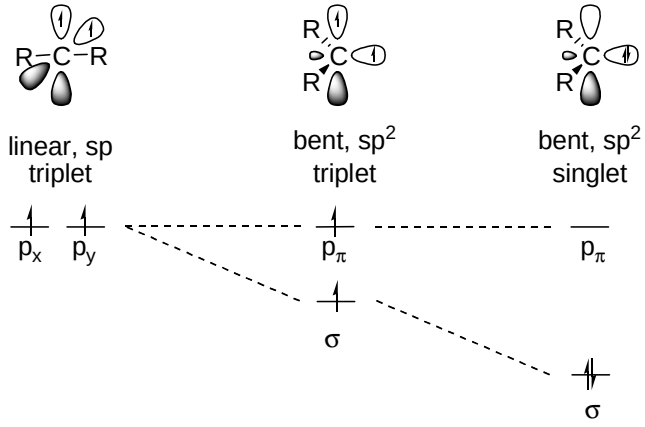

Fig. 1.1. Geometry, orbital energies, and electronic configuration of carbenes.

The altogether more common bent geometries arise from sp^2-hybridization. In this case, the orbitals available to the unpaired electrons are no longer equal. Instead, there are a purely p orbital (p_π) and an sp^2-orbital (σ). The σ orbital is lower in energy than the p_π orbital due to its partial s-character. Two distinct ground states are possible for bent carbenes ,depending on the energy gap between the σ and p_π orbitals. If the energy gap is too small to offset the spin-pairing energy, a triplet state of the configuration $\sigma^1 p_\pi^1$ is the ground state, otherwise, the configuration

$\sigma^2 p_\pi^0$ is more stable and the ground state is a singlet state (Fig. 1.1). An energy difference of 2 eV is sufficient to stabilize the singlet state, while energy gaps between σ- and p_π-orbitals below 1.5 eV are almost always indicative for a triplet ground state.[2] Other electronic states are theoretically possible, but these are energetically to unfavorable to be of importance.

Steric and electronic factors influence the energy gap between the frontier orbitals. Where electronic effects are negligible, the steric bulk of the substituents at the carbene center is the governing factor. Bulky substituents enforce a more linear geometry which reduces the s character of the σ-orbital, favouring the triplet state. Bulky di-tert-butylcarbene has a larger than ususal CCC angle and is a triplet carbene, while dimethylcarbene is more bent and in a singlet ground state.[3]

Inductive and mesomeric effects of the substituents have a stronger influence on the frontier orbital energy gap. The σ orbital can be stabilized inductively by electron-withdrawing substituents due to the resulting increase in s character. Since the energy of the p_π orbital is largely unaffected by these changes, an energetically lower σ orbital means a larger orbital energy gap. Conversely, electron-rich substituents destabilize the σ orbital, narrowing the orbital energy gap and favoring the triplet state.[4]

Mesomeric effects can influence both the geometry and the electronics of the carbene, and generally favor singlet ground states.[5] In the presence of π-accepting substituents, the degeneracy of the p_x and p_y orbitals in the linear state is broken, giving rise to a linear singlet carbene. On the other hand, the p_π orbital can be destabilized by receiving electron density from π-donating substituents, thereby increasing the orbital energy gap and stabilizing the singlet state.

Depending on their ground state spin multiplicity, carbenes exhibit different properties and reactivity.[6] The open-shell triplet carbenes are electrophiles and diradicals, and show insertion reactions, dimerizations, reactions with other radicals, or C-H and O-H cleavage. The closed-shell singlet carbenes possess a σ lone pair which can act as a nucleophile, and an unoccupied p_π orbital acting as an electrophile. Consequently, the ability to act both as a Lewis acid and a Lewis base makes singlet carbenes ambiphiles.

Due to their highly reactive nature, carbenes commonly occur as highly reactive intermediates in a variety of organic transformations such as the Simmons-Smith cyclopropanation or the carbene insertion into C-H and heteroatom-hydrogen bonds.[7,8] However, for a long time attempts at carbene syntheses failed, until it was believed they were to unstable to be isolated and studied in

substance. However, the stabilization of the σ orbital by electronegative substituents, and the destabilization of the p_π orbital by π-donors, have not only the effects of widening the singlet-triplet gap as described above, but it also leads to a reduction of both the nucleophilicity and the electrophilicity of the (singlet) carbene. Consequently, substituents more electronegative than carbon, which also possess a lone pair available for π-donation can stabilize carbenes through a "push-pull" mechanism, i.e. pulling electron density from the carbene lone pair by a inductive effects, and pushing electron density into the unoccupied orbital through mesomeric effects.

In 1960, Wanzlick came close to achieving the synthesis of a free carbene stabilized in this manner by thermolysis of 1,3-diphenyl-2-trichlormethylimidazolidine **(1)**.[9] The α-elimination of chloroform was correctly predicted to lead to the formation of carbene **2** – however, this reaction was immediately followed by the dimerization to yield a stable enetetramine **3** (Scheme 1.1).

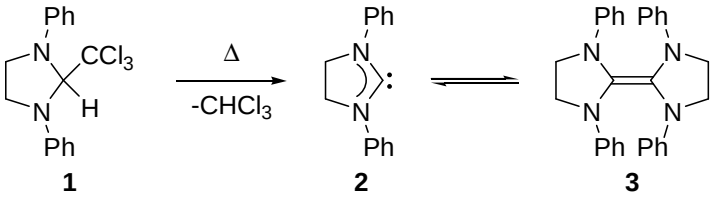

1 **2** **3**

Scheme 1.1. Elimination of chloroform to give free carbene, followed by dimerization.

Such dimerization reactions are not uncommon for carbenes, and generally there exists a dynamic equilibrium between free carbenes and electron-rich olefins.[10] In Wanzlick's case however, it was later established that the equilibrium lies exclusively with **3**.[11]

Thus, it fell to Bertrand *et al.* to prepare the first free, heteroatom-stabilized carbene in 1988.[12] The photolytic or thermolytic decomposition of the phosphorus-substituted diazomethane **4** yielded a carbene which could be stored for weeks at ambient temperature under inert atmosphere (Scheme 1.2).

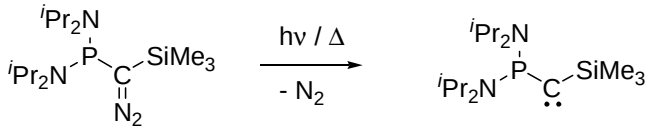

4 **5**

Scheme 1.2. Preparation of the first stable free carbene.

Despite their unprecedented stability, **5** and related compounds are neither readily available, nor particularly easy to handle. Carbene chemistry really started in earnest with the isolation of the first free N-heterocyclic carbene (NHC) by Arduengo and coworkers at DuPont. The synthesis of imidazoline-2-thiones by reaction of an *in situ* generated carbene with elemental sulfur was observed to proceed in good yields, despite the presence of air and moisture in the reactor. This observation signified an exceptionally high stability of the carbene intermediate, and building on this realization, an imidazioline-2-ylidene protected by two bulky adamantly substituents was prepared (Scheme 1.3). Indeed, the compound was found to be indefinitively stable, and could be studied by X-ray diffraction.[13]

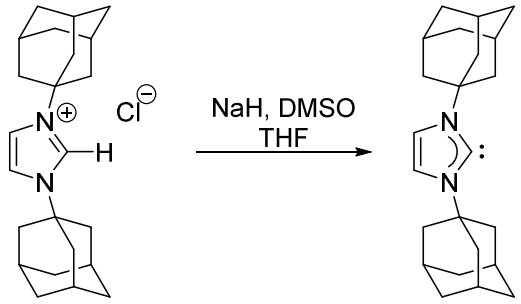

6 **7**

Scheme 1.3. Synthesis of the first stable free N-heterocyclic carbene.

Carbene **7** is stabilized by various factors, including the steric shielding by the bulky wingtip substituents, the presence of two amino groups imparting "push-pull" stabilization, a cyclic system enforcing a bent geometry, and an aromatic 6 π-electron system in which the carbene p_π orbital participates.

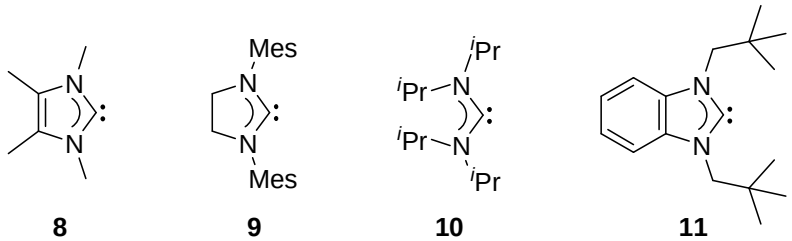

8 **9** **10** **11**

Fig. 1.2. Early examples of isolable free carbenes.

Subsequently, it was shown that not all of these factors were requisite and free NHCs could be synthesized lacking some of these features (Fig. 1.2).[14] The presence of stabilizing heteroatom substituents is by far the most important factor. Nevertheless, it should be noted that unsaturated and benzanullated NCHs as well as acyclic diaminocarbenes require sterically bulky wingtip substituents to prevent dimerization, because of the reduction or absence of aromaticity in these compounds.[15]

Carbene complexes were synthesized long before the isolation of **7**. The coordination to a metal center prevents decomposition of the carbene by reaction with moisture or oxygen. An early example of a metal-templated carbene synthesis, though unrecognized at the time, was Tschugajeff's synthesis of mono- and bis(carbene) complexes of platinum(II). The attack of hydrazine on metal-bound isocyanide yielded an acyclic diaminocarbene, but the correct structure was determined only half a century later.[16] The first targeted synthesis of a carbene complex was achieved in 1964 by Fischer and Maasböl by nucleophilic attack of methyl lithium on a tungsten(0)-bound carbonyl ligand, followed by protonation and alkylation to give a methoxymethylcarbene ligand.[17] Ten years later, Schrock *et al.* reported the synthesis of a carbene complex of tantalum(IV), in which the carbene only bears hydrogen and alkyl substituents.[18] Fischer's and Schrock's carbenes became the prototypes for two distinct classes of carbene ligands (Fig. 1.3).[19]

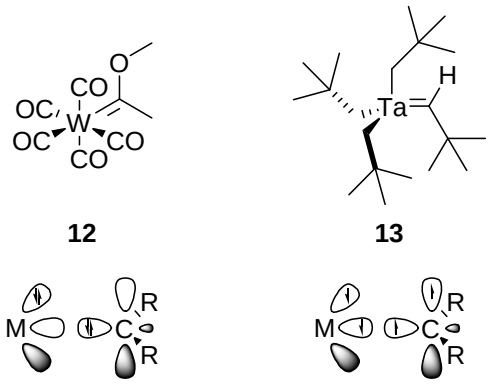

Fig. 1.3. Fischer and Schrock carbenes.

Fischer carbenes are singlet carbenes bearing at least one π-donating substituent at the carbene center. They are typically bound to middle to late transition metals in low oxidation states, which bear additional π-accepting ligands, and their interaction with the metal center consists of a σ-

donation of the carbene lone pair to the metal center, and a π-backdonation from a filled metal orbital to the empty p_π orbital of the carbene.

By contrast, Schrock carbenes are triplet carbenes, bound to early transition metals in high oxidation states, and the complexes typically incorporate π-donating ligands. The carbene is not stabilized by π-donors, but bears alkyl or hydrogen substituents. The bonding to the metal center can be thought of as an interaction between the singly occupied metal orbitals of the appropriate symmetry with the singly occupied σ and p_π orbitals of the carbene.

N-heterocyclic carbenes are a subclass of Fischer carbenes, though they differ from most other Fischer carbenes due to their strong stabilization by π-donors. While they are exceptionally strong σ-donors, π-backdonation is weak, and the metal-carbon bond is better represented as a single instead of a double bond.

The synthesis of NHC complexes followed shortly after the first reports of **12**. In 1968, Öfele reported the synthesis of a chromium(0) NHC complex and Wanzlick succeeded in obtaining a mercury(II) bis(NHC) complex (Scheme 1.4).[20] In both cases, the imidazolin-2-ylidene ligands wer generated by deprotonation of imidazolium cations by basic metal precursors – mercury(II) acetate and pentacarbonylhydridochromium(0), respectively.

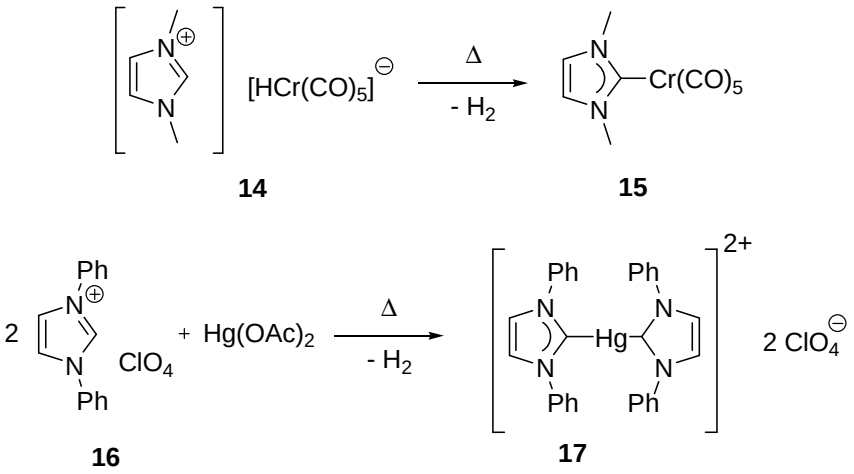

Scheme 1.4. Öfele's and Wanzlick's NHC complex syntheses.

A few years later, the Lappert group demonstrated that NHC complexes can indeed be obtained by cleavage of an electron-rich olefin, thus confirming that the equilibrium between such electron-rich olefins and carbenes postulated by Wanzlick is indeed possible (Scheme 1.5).[21] The

reaction between a chlorido-bridged platinum(II) dimer and the electron-rich olefin **18** formally derived from dimerization of 1,3-diphenylimidazolindin-2-ylidene yielded a mixed phosphine-NHC complex when heated to reflux in xylene.

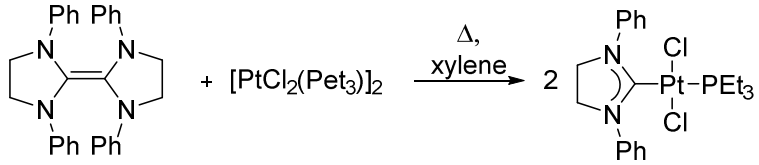

18 **19**

Scheme 1.5. NHC complex synthesis by cleavage of an electron-rich olefin.

From these humble beginnings, and especially since the isolation of the first infinitely stable free carbene, NHCs have become one of the most versatile and widely employed class of ligands in organometallic chemistry and catalysis,[22] and in their free form they are well established as organocatalysts.[23] Part of this success story is the remarkable ease with which free NHCs can be prepared from readily available azolium salts.[24,25] The most common NHCs are imidazolin-2-ylidenes (**A**), imidazolidin-2-ylidenes (**B**), benzimidazolin-2-ylidenes (**C**) and 1,2,4-triazolin-5-ylidenes (**D**), and for their precursor salts, synthetic approaches are available (Fig. 1.4).

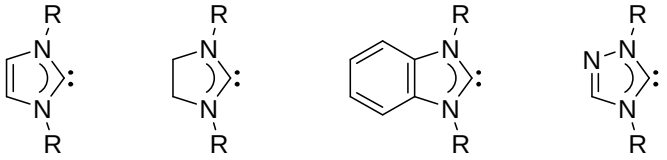

A **B** **C** **D**

Fig. 1.4. The most common NHC backbones.

Two major strategies are possible to obtain carbene precursor salts, both of which usually involve only air- and moisture-stable reagents. The desired salts can either be obtained by ring-closing reactions leading directly to cationic species, or by quarternization of a nitrogen atom in a suitable heterocycle.

Symmetrically substituted imidazolium salts can be conveniently obtained by an acid-catalyzed three-component condensation reaction involving two equivalents of aromatic or aliphatic amine, and one equivalent each of glyoxal and paraformaldehyde, or a two step process involving the

synthesis of a 1,4-diazadiene first, followed by reaction with paraformaldehyde or another suitable C1 building block.[26] By reduction of the diazadiene prior to the ring-closing step, imidazolinium salts are also available using this approach. However, this approach is plagued by comparatively low yields and the formation of copious amounts of side products, which are tedious to remove. A more convenient approach to imidazolium salts was found in the replacement of the catalytic acid in the condensation step by trimethylsilychloride, leading to a marked increase in yields and product purity (Scheme 1.6).[27] By contrast, imidazolinium salts are readily available from the condensation of formamidines with dichloroethane in the presence of an external base, or with formamidine serving as sacrifical base itself.[28]

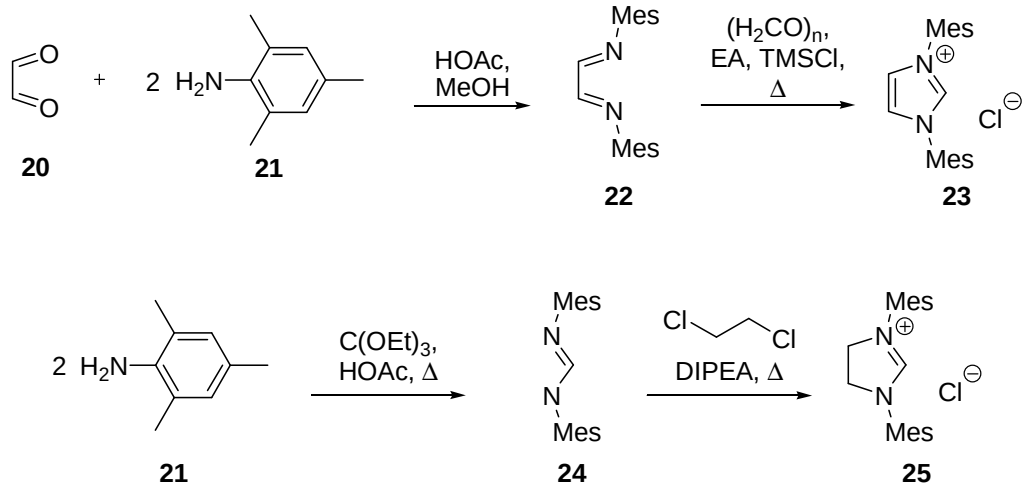

Scheme. 1.6. Synthesis of imidazolium and imidazolinium chlorides.

For benzimidazolium salts and triazolium salts, successive alkylation reactions are more commonly used than cyclization reactions, since these azoles are more difficult to obtain from condensation reactions. A synthetic protocol for benzimidazolium salts bearing sterically bulky secondary alkyl substituents has been developed by Huynh *et al.* and involves a two step, one pot reaction sequence.[29] After being deprotonated by potassium carbonate, benzimidazole is alkylated by a large excess of isopropyl bromide (Scheme 1.7). A large excess of alkylating agent, as well as the addition in two portions, is required to counteract the loss of isopropyl bromide as propylene resulting from the base-induced elimination reaction. Similarly, 1,2,4-triazolium halides can be readily obtained by the regioselective alkylation of either 1- or 4-substituted triazoles.[30]

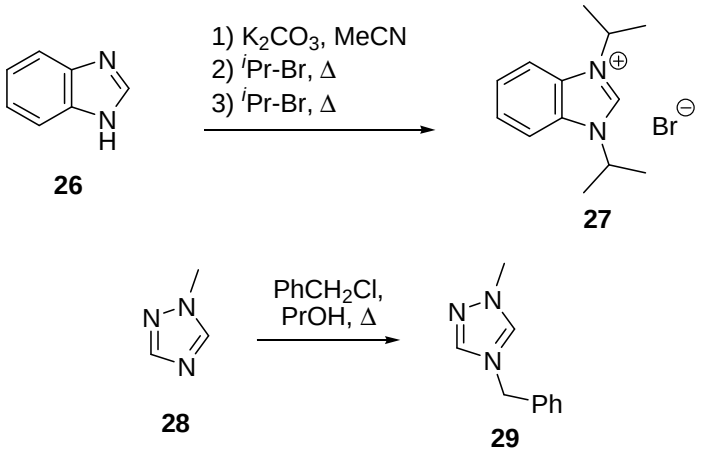

26 **27** **28** **29**

Scheme 1.7. Synthesis of azolium salts by quarternization.

The flexibility of these approaches makes a wide variety of NHCs readily available, which can differ substantially in their electronic and steric properties, as well as their reactivities.[31] An example of reactivity differences is the tendency to dimerize, which is pronounced for imidazolidin-2-ylidenes, less pronounced for benzimidazolin-2-ylidenes, and basically nonexistent for imidazolin-2-ylidenes and 1,2,4-triazolin-5-ylidenes, and closely related to the degree of aromatic delocalization in azole.[15]

Modifying the electronic properties of NHCs is of great interest for their application in catalysis, and marked changes in their donating abilities can be achieved by modifications of the NHC backbone. [32] The incorporation of electron-withdrawing or –donating substituents in the backbone,[33] the incorporation of additional hteroatoms or heteroatoms other than nitrogen into the azole ring,[34] and even different sizes of the heterocycle are among the various possibilities.[35] A more detailed discussion of how some of these modifications influence the electronic structure of carbenes and how these changes influence the metal-carbon bond is presented in chapter 2.

Particularly interesting NHCs are species which deviate from the traditional diaminocarbene pattern. Imidazolin-4-ylidenes (**E**), which are based on the same backbone as imidazolin-2-ylidenes, but in which the carbene is adjacent to only one nitrogen atom, have attracted considerable attention.[36] Due to the lower electronegativity of carben compared to nitrogen, the inductive effects stabilizing the σ orbital are reduced, and the increased electron density in this orbital leads to an increase in σ-donation.[2b,22b, 37] The complexes of such ligands are more electron-rich then traditional NHC complexes, and were found to outperform them often in

catalytic applications.[38] Others example of such carbenes with reduced heteroatom stabilization are 1,2,3-triazolin-5-ylidenes (**F**),[39] pyrazolin-3-ylidenes (**G**),[40] indazolin-3-ylidenes (**H**),[41] and pyrazolin-4-ylidenes (**I**) (Fig. 1.5).[42] In chapters 3 and 4, various contributions to the chemisty of pyrazolin-3-ylidenes and indazolin-3-ylidenes are presented.

Due to the absence of any nitrogen substituent directly bound to the carbene center in **I**, the carbene center is even more electron-rich then in carbenes with only one nitrogen atom in α-position, and these carbenes are often referred to as remote carbenes (rNHCs). Taken to the extreme, this concept has lead to the development of carbenes like pyridine-4-ylidene, which feature only one nitrogen atom in the cycle, separated by three bonds from the carbene carbon.[43]

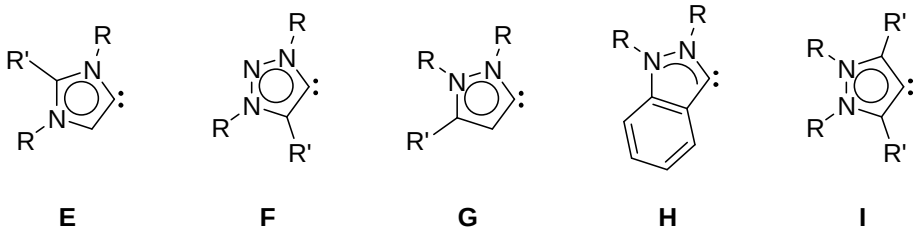

Fig. 1.5. NHCs with reduced heteroatom stabilization.

For imidazolin-4-ylidene, no canonical structure can be drawn without charge separation. (Fig. 1.6). The same is true for 1,2,3-triazolin-5-ylidenes and pyrazolin-4-ylidenes. As a consequence, these carbenes are often regarded as a distinct subclass of NHCs, and they are either referred to as abnormal carbenes (aNHCs) or mesoionic carbenes (MICs).[44,45]

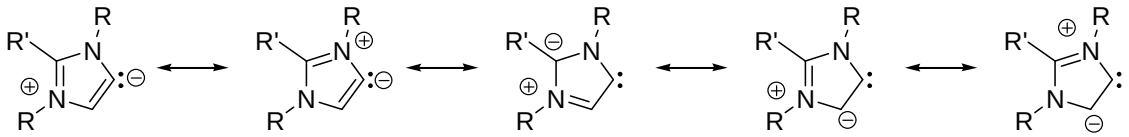

Fig. 1.6. Resonance structures of imidazolin-4-ylidene, a mesoionic carbene.

Several methods have been proposed for the quantification of ligand donor strengths. A method for probing the donor strength of Werner-type ligand has been devised by Lever, and is based on the E_0 value of a Ru(II)/Ru(III) redox couple of complexes incorporating the ligands of interest.[46] The electron density of the metal center, which depends on the amount of electron density

transferred from the ligands to ruthenium, determines the ease of oxidation, allowing for a qualitative estimate of ligand donor strength. However, this method is mostly employed for classical coordination compounds, and plays only a minor role in organometallic chemistry. The main methods commonly used for donor strength determinations in this field are either based on the observation of carbonyl stretch frequencies by IR spectroscopy (Tolman electronic parameter),[47] or by NMR spectroscopy using a suitable probe nucleus.[48]

The Tolman parameter was originally determined by determining the wavenumber of the CO A_1 band in IR spectra of $[Ni(CO)_3L]$ (L = ligand to be characterized) complexes. Metal-to-ligand π-backdonation populates the π* orbital of the CO ligand and weakens the CO bond, thus a smaller wavenumber indicates a more electron-rich metal center caused by a more strongly donating ligand L. The wide availability of IR spectrometers has contributed to the popularity of this method, but there are several drawbacks. The probe complexes have to be synthesized from highly toxic and gaseous $[Ni(CO)_4]$, and while phosphine complexes are readily available, complexes with other ligand classes can be difficult to obtain. To mitigate toxicity issues, alternative methods base on Rh(I) and Ir(I) complexes of the general formula $[MX(CO)_2L]$ (M = Rh, Ir; X = halide) have been proposed, yet the synthesis of these complexes still requires the use of toxic carbon monoxide.[49] Besides the toxicity of the required reagents, the Tolman electronic parameter is limited in its ability to distinguish small changes in donor strength by the broadness of IR bands, which allows an accurate measurement only with an error margin of at least 2 cm^{-1}.[50] Additionally, competition for π-backdonation between the ligand to be characterized and carbonyl ligands generally poses a problem in all CO-based methodologies, and occasionally leads to inaccurate results.

An approach that provides higher accuracy is a method based on the ^{13}C NMR chemical shift of the carbene carbon in NHC complexes of the general formula *trans*-$[PdBr_2(^iPr_2\text{-bimy})L]$ ($^iPr_2$-bimy = 1,3-diisopropylbenzimidazolin-2-ylidene).[48] Such complexes can be readily obtained both with organometallics and Werner-type ligands in excellent yields and without the need for toxic reagents, and their characterization by NMR spectroscopy is straightforward (Scheme 1.8).

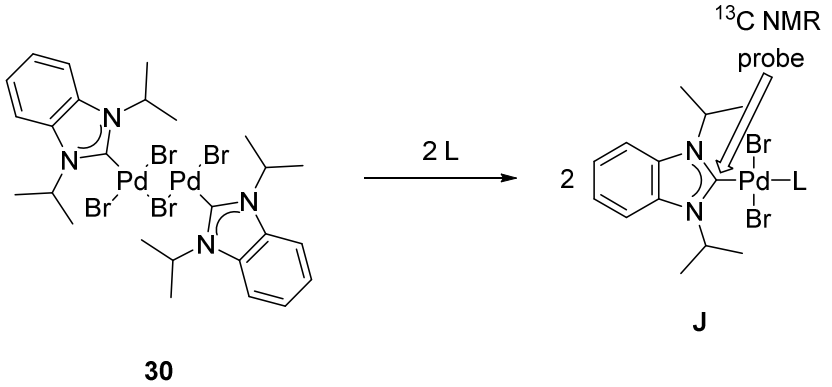

Scheme 1.8. Synthesis of probe complexes *trans*-[$PdBr_2$(^{i}Pr_2-bimy)L].

In these complexes, transoid ligands with high donor strength lead to a reduction in the Lewis acidity of the metal center, which induces a downfield shift of the carbene carbon signal.[51] In contrast to IR spectroscopy, signals in ^{13}C NMR spectra are very sharp and allows the differentiation of even relatively minor changes in donating properties. As a result, a comprehensive and detailed donor-strength scale compromising both Werner-type and organometallic ligands can be easily constructed (Fig. 1.7).

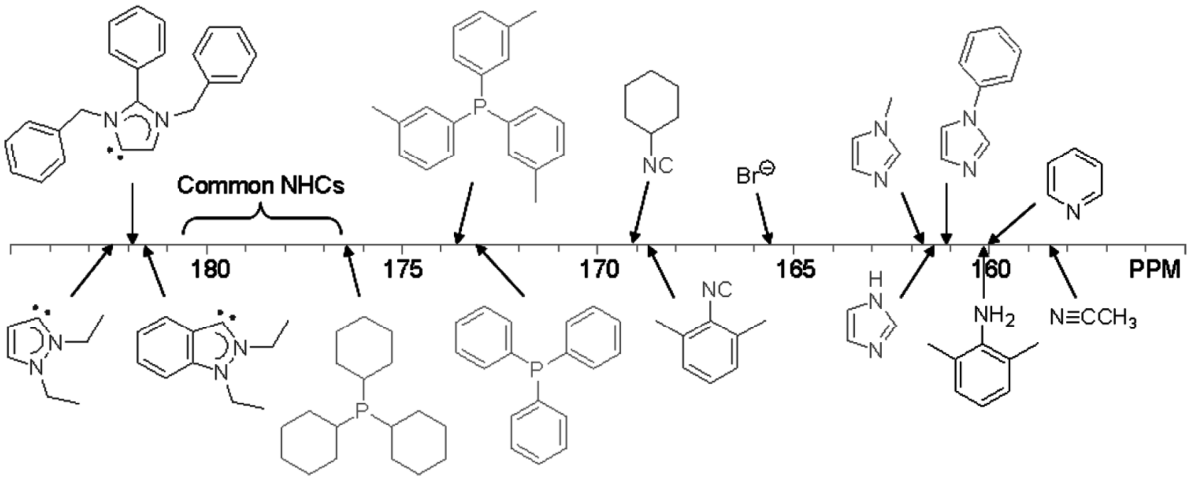

Fig. 1.7. Donor strength scale based on the Huynh electronic parameter.[48]

Besides electronic factors, the steric bulk of ligands can have a considerable impact on complex reactivities and their performance in catalysis. Besides protecting and stabilizing the metal-ligand bond, sterically bulky substituents can influence selectivities, and promote faster catalytic

turnover by favoring the dissociation of products or reductive elimination steps. For this reason, NHCs with particularly bulky wingtip substituents – which are the main contributor to steric bulk in these ligands - have been synthesized.[52] However, while high steric bulk might favor certain steps in a catalytic cycle, it also hinders the coordination of substrates to the metal or the occurrence of oxidative additions. Therefore, NHC ligands with flexible steric bulk have been proposed as well, in which different conformations of the wingtip substituents can accommodate the varying steric requirements of individual step in the catalytic cycle.[53]

Two distinct parameters are commonly employed to characterize the steric bulk of organometallic ligands. The cone angle θ was the first one of these parameters to be introduced.[47c] It is defined as the solid angle of a cone with the metal at the tip, and the ligand of interest bound to the metal center with a bond length of 2.28 Å, and touching the perimeter of the cone. This method is well suited to describe ligands such as teriary phosphines, which occupy a cone-shaped segment of space, and cone angles can be determined based on molecular structures obtained by X-ray crystallography. However, this method fails to accurately describe the steric ligands which are not cone-shaped, such as NHCs. To overcome this limitation, the "percentage of buried volume" parameter $\%V_{bur}$ was proposed.[54] In this approach, the ligand is placed at at fixed distance from a metal center. Then, it is calculated what percentage of a virtual sphere of a fixed radius around the metal center is occupied by the ligand, and the value is expressed as a percentage of the total volume of this sphere. The resulting values are independent of ligand shape, and can be used as an indication of the steric shielding a ligand provides.

The wingtip substituents allow the adjustment of the steric bulk of the ligand, but they also open up the possibility of incorporating additional donor sites into the NHC ligands. This can lead to chelating and pincer-type NHC ligands based on additional C-, N-, O-, P-, and S-donors,[55] and even more complex structures such as tripodal ligands.[56] Multidentate ligand architectures can be used to impose a desired geometry on the complex, increase ligand binding and consequently complex stability through the chelate effect, or to create distinct reactivities by pairing the soft NHC donor with a harder donor moiety.

Donor functionalities that bind only weakly to the metal center are also of interest. If the bond between the additional donor site and the metal center is weak, the donor moiety can easily dissociate and open up a coordination site, but due to the linkage to the tightly bound NHC, they are forced to remain in the vincinity of the metal, and can coordinate to the metal center again

easily. This hemilabile behaviour allows for the easy coordination of incoming substrates to the metal center, thus enhancing catalytic turnover, while being able to revert to a more stabilized chelating resting state, which prolongs catalyst lifetime.[57] Especially sulfur-functionalities were found to exhibit hemilabile behavior in late transition metal complexes, and the synthesis of group 10 complexes with NHCs bearing hemilabile thioether functionalities is presented in chapter 5.

Most commonly, donor functionalities are introduced during the synthesis of carbene precursors, prior to the metalation step. While a wide range of functionalities can be installed in this way, in rare cases the additional donor moieties are incompatible with the subsequent complex formation.[58] Additionally, if a library of NHC complexes with a wide array of different donor functionalities is desired, each carbene precursor has to be synthesized individually, followed by individual complexation steps. The introduction of functional groups into a metal-bound NHC ligand avoids such functional group incompatibilities, and allows for the generation of structural diversity with less synthetic effort.[59]

Corresponding to the plethora of reported NHC structures, a number of diverse synthetic protocols have been developed to obtain NHC complexes.[24] The most straightforward approach is the deprotonation of an azolium salt to yield the free carbene, which then adds to a metal center, or displaces a ligand in a suitable precursor complex (Scheme 1.9).[60]

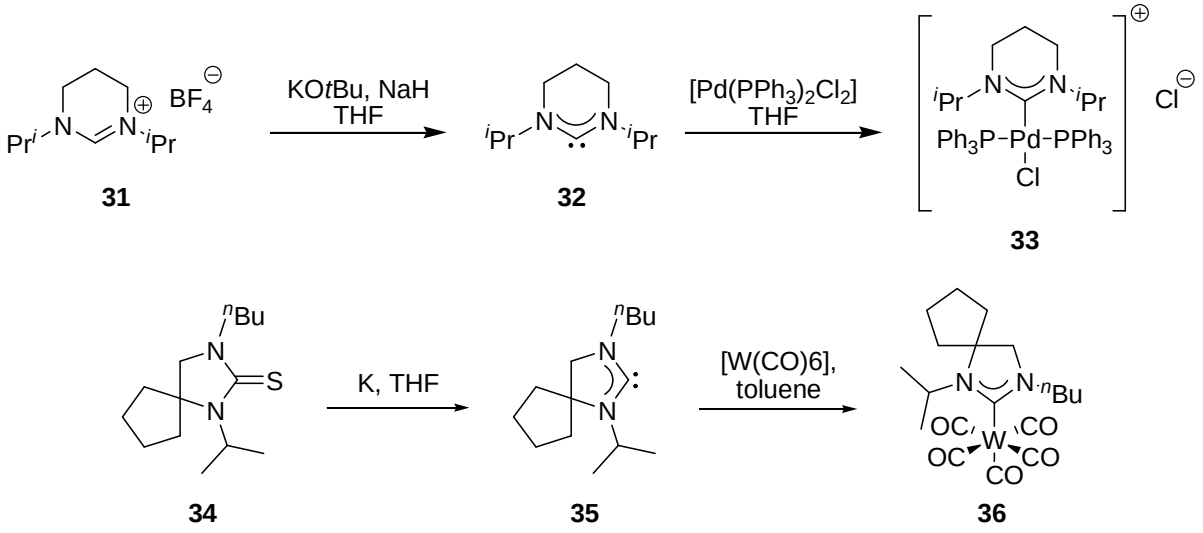

Scheme 1.9. Syntheses of NHC complexes using free carbenes.

Typically, bulky alkoxides, sometimes in catalytic amounts and in combination with sodium hydride, are used as base in anhydrous THF at low temperatures, but a variety of other bases and solvents has been employed as well. Free carbenes can also be obtained by other means than deprotonation, for example by reduction of a cyclic thiourea by potassium, but such reactions play only a minor role in modern NHC chemistry.[61] While the metalation step is usually easy using free NHCs as reagent, the sensitivity of these compounds to moisture requires strictly anhydrous reaction conditions, and complexes of NHCs with a propensity to dimerize can usually not be obtained following this route.

Insufficient stability of the free carbenes or overcomplexation reactions owing to the high reactivity of these species sometimes make it desirable to use labile NHC adducts instead of the free carbenes as reagents. Typical reagents for this reaction are zwitterionic imidazolium carboxylates, which are stable to air and water, NHC-borane adducts, or NHC adducts with alcohols or amines.[62] While the preparation of these reagents is less straightforward than the synthesis of simple azolium salts, the handling of free NHCs can be avoided, since the carbene is only liberated from the adduct *in situ* and immediately prior to the metalation (Scheme 1.10). Related to this approach are NHC complex syntheses using electron-rich olefins such as enetetramines and tetraazafulvalenes,[21] which are also synthetic equivalents for free NHCs.

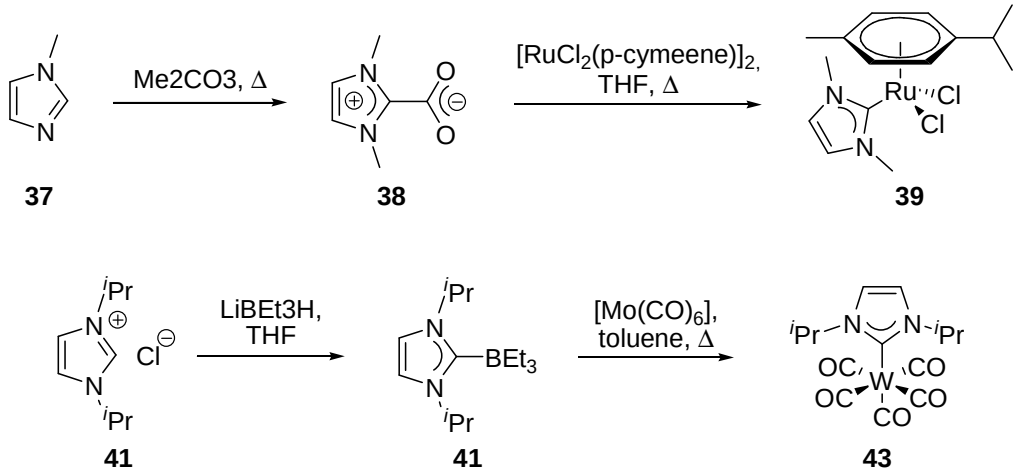

Scheme 1.10. Complex syntheses using azolium carboxylates and NHC-borane adducts.

Direct metalations are possible by reacting sufficiently acidic azolium salts with basic metal precursors, e.g. metal acetates.[20] This approach avoids the handling of free carbenes, and requires

less basic conditions than the preparation of free carbenes. Due to the presence of metal ions, which remove free carbene from the protonation/deprotonation equilibrium, even a relatively weak base such as acetate can still give good yields of NHC complex. Coinage metal oxides are particularly useful basic metal sources.[63] As a byproduct of the deprotonation, only water is formed. In the case of silver(I), the Ag-C bond is labile and the NHC ligand is readily transferred to other metals. The precipitation of insoluble silver(I) halides from the reaction mixture provides additional driving force for this reaction (Scheme 1.11).

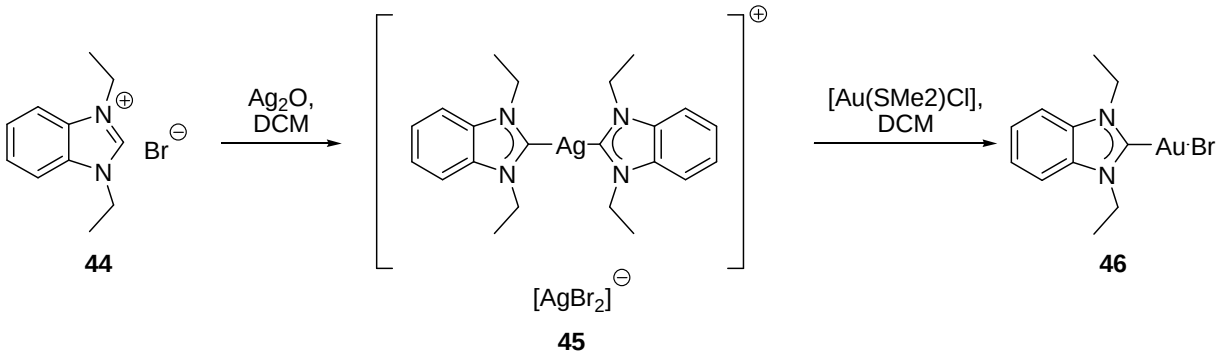

Scheme 1.11. Silver carbene transfer reaction.

The azolium salt precursors leading to carbenes with reduced heteroatom stabilization and rNHCs are only very weakly acidic. In this case, synthetic methodologies involving deprotonation reactions, whether by external base or by basic metal salts, can be hampered, and other approaches are required (Scheme 1.12).

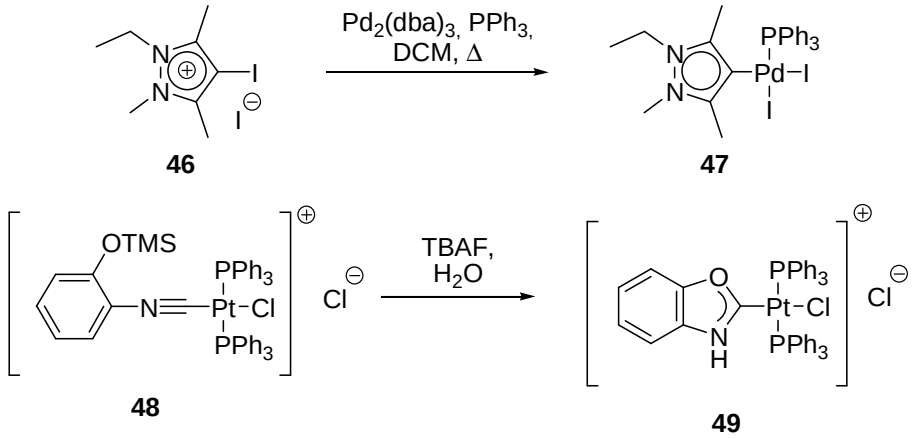

Scheme 1.12. Alternative approaches to NHC complexes.

A method to avoid *in situ* deprotonation or the handling of free NHCs altogether is the use of azolium halides, triflates, mesylates or tosylates. Such species can add oxidatively to low-valent metal precursors, yielding directly the desired carbene complexes.[42a] Alternatively, certain NHCs and acyclic diaminocarbenes (ADCs) can be generated by metal-templated reactions, where an already coordinated substrate is converted to an NHC.[16] An example for this approach is the synthesis of benzoxazolin-2-ylidene complexes by Hahn *et al.*[64] The phenylisocyanide ligand in platinum(II) complex **X** bears a silyl-protected hydroxyl group. Upon deprotection, the ligand rearranges to a protic N,O-carbene, which would be difficult to obtain otherwise.

In their free form, NHCs are powerful nucleophiles, making them useful organocatalysts, especiall in reaction involving carbonyls such as esters or aldehydes (Fig. 1.8).[65] Transesterifications can be catalysed by nucleophilic attack of a NHCs on esters yielding acyl azolium cations after elimination of alcoholate. These are good electrophiles, and readily react with alcohols, affording either transesterification products, or in the case of lactones, polyesters by ring-opening polymerization.[66] The reaction of NHCs and aldehydes gives rise to an enamine-like structure called Breslow intermediate.[67] In this species, the former carbonyl carbon is rendered nucleophilic in reversal of its normal reactivity, and such 'umpolung' products can react with electrophiles such as Michael acceptors (Stetter reaction) or aldehydes (Benzoin condensation), or be oxidized to acyl azolium cations and react with various nucleophiles.[68]

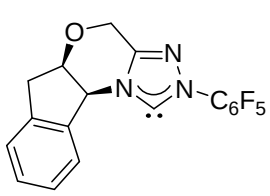

50

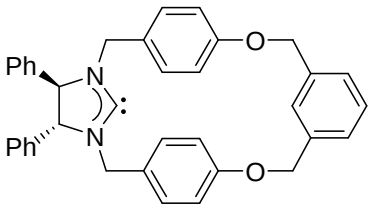

51

Fig. 1.8. Chiral organocatalysts based on free NHCs.

In transition metal catalysis, NHCs have established themselves as an important class of ligands, rivalling the position of phosphines.[69] Both phosphines and NHCs are powerful σ-donors and weak π-acceptors, but in contrast to phosphines, NHCs can be tuned sterically and electronically much easier, and are less prone to ligand dissociation resulting in more stable complexes.[70]

Replacement of phosphines by NHCs can dramatically improve a catalyst, as illustrated by the development of methathesis catalysts (Fig. 1.9).[71]

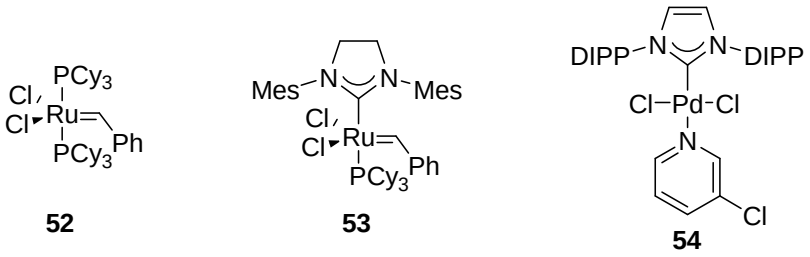

52 **53** **54**

Fig. 1.9. 1st and 2nd generation Grubbs' catalysts, and Pd-PEPPSI-IPr catalyst.

While the Grubbs' first generation catalyst bears two tricyclohexylphosphine ligands, in the second generation, one of these was replaced by an 1,3-dimesitylimidazolidin-2-ylidene (SIMes) ligand. As a result of this modification, the catalytic performance was significantly improved. Besides in olefin metathesis, NHC complexes are being used as catalysts for C–C cross-couplings such as the Suzuki–Miyaura and Mizoroki–Heck reactions,[72] but also for a many other reactions such as olefin polymerizations, Hartwig-Buchwald aminations, the α-arylation of ketones, hydroamination and hydrosilylation reactions, to name just a few.[22,73] Especially for cross-coupling reactions, the so-called PEPPSI catalysts (PEPPSI = pyridine enhanced precatalyst preparation, stabilization, and initiation) have emerged as a commercially successful palladium(II) NHC complex, benefiting from the combination of electron-rich, tightly bound, and comparatively bulky NHC ligands and a labile 3-chloropyridine ligand in *trans*-position which will readily dissociate to allow substrate coordination.[74]

The unique properties of NHCs, their facile tuning of steric and electronic properties independently from each other, the stability of their complexes, and the excellent performance of NHCs as ligands and as organocatalysts, will continue to attract research interest to this field of study for many years to come.

2. N-heterocyclic Carbenes with Varying Number of Nitrogen Atoms

2.1. Electronic Structure Trends in N-heterocyclic Carbenes

NHCs derived from five-membered heterocycles can either contain two, three or four nitrogen atoms in the ring. Within these series, three types of isomerism are possible. The arrangement of the heteroatoms relative to each other can vary, leading to NHCs derived from different parent azoles. The position of the nitrogen atoms relative to the carbene center can vary, leading to NHCs with varying degrees of heteroatom stabilization. If there are more than two nitrogen atoms present in the cycle, the substitution pattern on these can vary as well (Fig. 1.2).

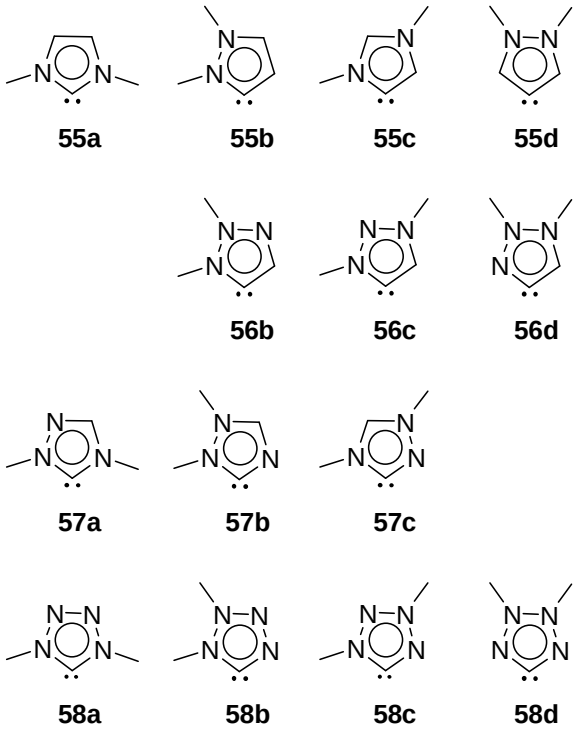

Fig. 2.1. NHCs with two to four nitrogen atoms in the heterocycle.

NHCs with two nitrogen atoms are the most commonly found NHCs. The heteroatoms in the cycle can be located adjacent to each other, leading to pyrazolin-ylidenes, or be separated by a carbon atom, leading to imidazolin-ylidenes. The carbene carbon can either be located between two heteroatoms (imdazolin-2-ylidene **55a**), next to one nitrogen atom (pyrazolin-3-ylidene **55b**

or imidazolin-4-ylidene **55c**), or be completely substituted by carbon (pyrazolin-4-ylidene **55d**). Due to the presence of only two nitrogen atoms in the heterocyle, the position of substituents cannot be modified independently of the heteroatom pattern.

Nitrogen and methine are isolobal fragements, and the formal replacement of one methine unit in **55a-d** gives rise to triazolin-ylidenes. With three contiguous nitrogen atoms, 1,2,3-triazolin-ylidenes **56** are obtained. In these, the carbene carbon is always located adjacent to a single nitrogen atom, and variations are only possible on the level of substitution pattern, giving rise to three distinct isomers with either a 1,2-dimethyl pattern and one methyl substituent on the α-nitrogen (**56b**), a 1,3-dimethyl pattern and one methyl substituent on the α-nitrogen (**56c**), or a 1,2-dimethyl pattern with both methyl groups bound to β-nitrogen (**56d**). In 1,2,4-triazolin-ylidenes, the carbene carbon is always flanked by two nitrogen atoms in α-position, and again, isomerism is only possible with respect to the substitution pattern, wich allows for 1,4-dimethyl, 1,2-dimethyl and 1,3-dimethyl patterns (**57a-c**, respectively).

A second isolobal exchange leads to tetrazolin-ylidenes **58a-d**. In these compounds, the four heteroatoms are necessarily arranged as a contiguous chain, and the carbene carbon is always substituted by nitrogen. Only substitution isomerism is possible for these compounds. Three of the possible isomers have at least one substituent on the α-nitrogen (**58a-c**), while one isomer is exclusively **b**-substituted (**58d**).

Not all of these NHCs are known, due to the difficulty to selectively generate each substitution pattern, and the inherent instability of some of these compounds. While all possible isomers of imidazole- and pyrazole-derived NHCs are well studied,[13,36,40,42] not all possible triazole-derived NHCs have been reported. Only derivatives of **56a**,**b** and **57a** are known, while the other species remain elusive, no doubt because of the difficulty to obtain suitable precursor salts regioselectively.[39,75] For tetrazolin-ylidenes, the situation is similar. **58b** or derivatives thereof have never been prepared, and a structure similar to **58d** has only been observed at 173 K as an unstable lithium adduct.[34a,b,e,76]

The selection of NHCs presented in figure 2.1 allows to systematically study the effects of varying numbers of heteroatoms in the azole, different substitution patterns and varying degrees of heteroatom stabilization.[77] Since half of these carbenes are normal NHCs and half of them are mesoionic, a comparison between their respective electronic structures can be made as well. This

is especially interesting for **58a**-**d**, in which the change between normal and mesoionic carbenes is brought about exclusively by a change of substitution pattern.

2.1.1 Optimised Geometries and Relative Stabilities

The geometry optimisation for free carbenes in their singlet ground states and their excited triplet states, and for the azolium cations as well as the doubly protonated dications was done using the Gaussian 09 software package at the B3LYP/aug-cc-pVTZ level of theory (Fig. 2.2).[78,79,80]

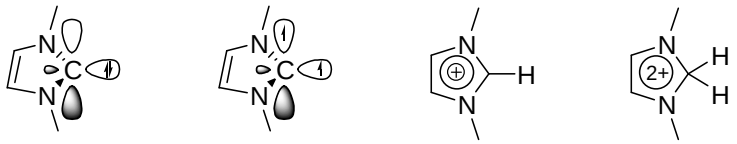

Fig. 2.2. Imidazolin-2-ylidene and related structures under scrutiny.

The singlet states of all NHCs were found to be perfectly planar structures, and bond lengths and angles were in good agreement with published molecular structures,[13a,36d] with deviations from experimental values generally below 1%. For the mono- and diprotonated forms of these carbenes, planar ring structures were obtained as well. However, during the optimisation of **58bHH** and **58dHH**, a rupture of the bond between N2 and N3 was observed, indicating a relatively low stability of these dicationic species. To prevent this problem, the bond length was constrained to the fixed value of 1.420 Å, close to the optimized value for this bond in the other tetrazolium dications.

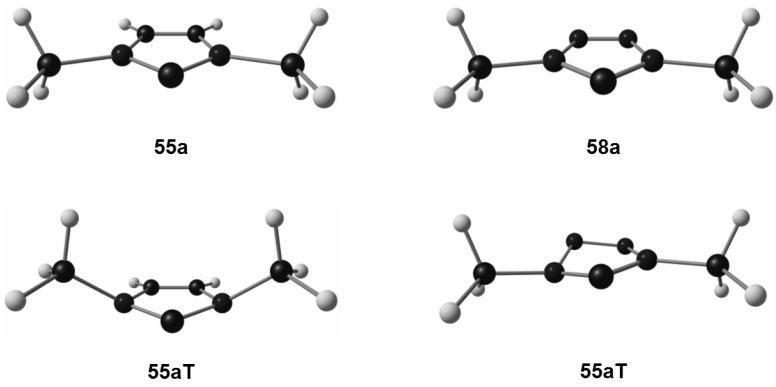

Fig. 2.3. Optimized geometries of singlet and triplet states.

In contrast to the other species, the triplet states showed a distortion of the NHC ring plane and pyramidalization at nitrogen, indication a disruption of π-delocalisation upon promotion of an electron into the p_π orbital at $C_{carbene}$. (Fig. 2.3).

The optimized bond lengths in the singlet carbenes as well as in the azolium cations fall – with rare exceptions – within the typical range for aromatic C-C, C-N and N-N bonds.[81] This underlines the notion that there is full delocalisation within the planar 6 π-electron system. The introduction of a second proton, which removes electron density from the π-system, or the promotion of an electron from the σ to the p_π orbital disrupts this delocalisation, however, and the bond lengths should be more typical for a system of alternating single and double bonds. Indeed, this is observed in the optimized structures for the dications and the triplet states.

Table 2.1. Relative stabilities of singlet and triplet states, mono- and dications.[a]

NHC	Singlet state [b]	Triplet state [b]	$[NHC + H]^{+}$ [b]	$[NHC + 2H]^{2+}$ [b]
55a	0	26	0	6
55b	136	29	82	153
55c	77	0	0	0
55d	202	36	82	81
56b	31	8	46	75
56c	0	16	0	0
56d	119	0	46	31
57a	0	34	0	4
57b	111	0	37	80
57c	78	13	0	0
58a	0	66	9	31
58b	130	21	66	80
58c	69	0	0	0
58d	195	13	51	30

[a] Differences of zero-point corrected energies at the B3LYP/aug-cc-pVTZ level within each series. [b] Values in kJ/mol.

A comparison of the relative stabilities within each series of NHCs shows a striking similarity in the trends for the mono- and dications forms (Table 2.1 and Fig. 2.4). Species with spatially separated methyl groups are considerably more stable than those with adjacent substituents. To a lesser extent, the same trend is discernible for the singlet states as well, even though **55a**, **57a** and **58a** are clearly lower in energy than **55c**, **57c** and **58c**, respectively. The reason for this energy difference can clearly be attributed to the sterical repulsion between vicinal methyl groups present in the less stable structures. When comparing the relative energies of the triplet states, no general trend can be found. The pyramidalization at the substituted nitrogen atoms allows the methyl wingtips to move away from each other, adopting a less encumbered arrangement and avoiding destabilisation caused by steric repulsion.

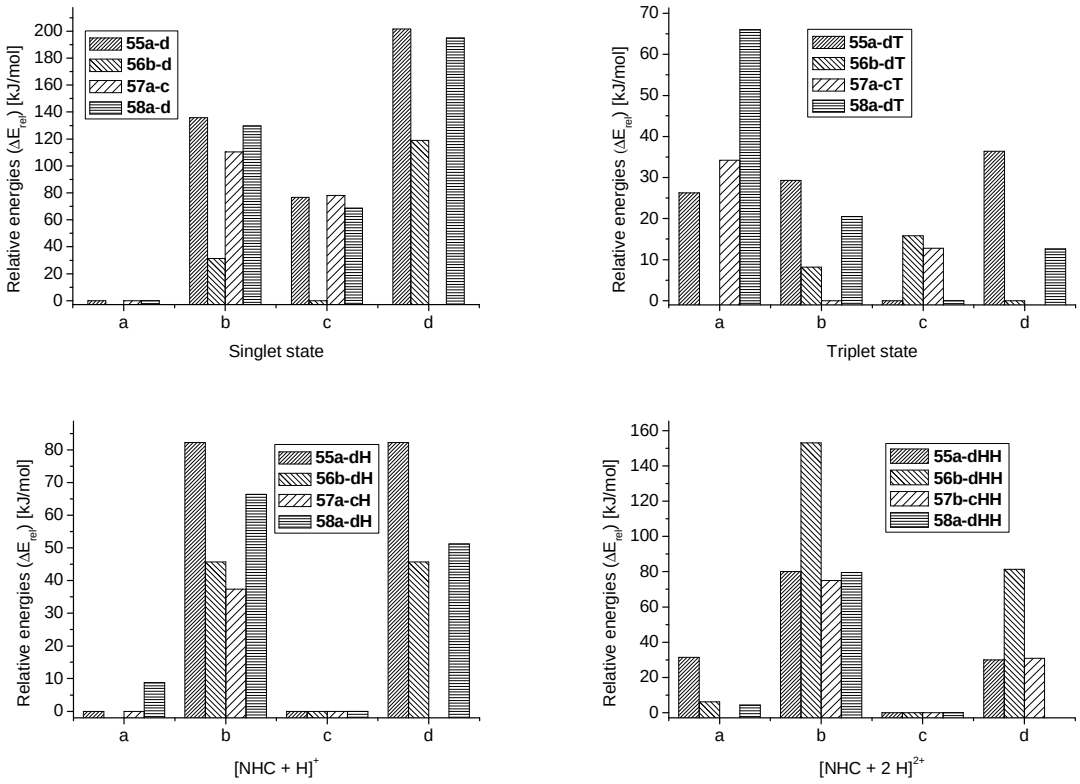

Fig. 2.4. Relative stabilities of singlet and triplet states, mono- and dications.

2.1.2 Singlet-Triplet Gap, Aromaticity, and Stability Towards Dimerization

The singlet state with spin-paired electrons in the σ orbital at $C_{carbene}$ is the ground state for NHCs. The energy required to promote an electron into the p_π orbital, followed by structural

relaxation, is the singlet-triplet energy gap $\Delta E_{S\rightarrow T}$. This energy difference is an important parameter in assessing the tendency of NHCs to dimerize to electron-rich olefins in the Wanzlick equilibrium.[2b,10,37b] Steric and electronic factors contribute to this dimerization tendency, and an empirical formula to estimate the enthalpy of dimerization taking into account these factors has been proposed.[15b] In this formula, the steric shielding of $C_{carbene}$ is estimated based on the percentage buried volume $\%V_{bur}$,[54] while the electronic contribution is based on the singlet-triplet energy gap. Larger $\Delta E_{S\rightarrow T}$ and $\%V_{bur}$ values favour monomeric carbenes, while small singlet-triplet energy gaps and low steric encumbrance shift the Wanzlick equilibrium to the dimer.

Table 2.2. HOMO-LUMO gap, vertical singlet-triplet energy gap and singlet-triplet energy gap.[a]

NHC	$\Delta E_{H\text{-}L}$ [eV] [b]	$\Delta E^{vert}_{S\rightarrow T}$ [kJ/mol] [c]	$\Delta E_{S\rightarrow T}$ [kJ/mol] [d]
55a	5.58	409	355
55b	4.57	314	222
55c	4.59	386	252
55d	3.73	270	164
56b	4.81	305	210
56c	4.55	317	249
56d	3.56	220	114
57a	6.10	415	355
57b	4.62	312	210
57c	4.60	354	256
58a	5.98	465	370
58b	4.77	310	195
58c	4.58	330	236
58d	3.54	226	122

[a] All energies calculated at the B3LYP/aug-cc-pVTZ level. [b] Energy difference of the Kohn-Sham frontier orbitals in the singlet state. [c] Zero-point corrected energy without structural relaxation. [d] Zero-point corrected energy with structural relaxation.

Since all carbenes in series **55-58** are sterically only minimally shielded, the electronic parameter is the main factor in determining dimerization tendencies. The energy differences for the vertical singlet-triplet transition, without taking into account the geometry relaxation of the triplet state

($\Delta E^{vert}_{S\rightarrow T}$) was obtained from single-point calculations at the B3LYP/aug-cc-pVTZ level using molecular geometries optimized for the singlet state, and the singlet-triplet energy gap which accounts for geometry relaxation ($\Delta E^{vert}_{S\rightarrow T}$) was obtained after full geometry optimization of the open-shell system.[79,80] For all NHCs, these energies were found to be decisively in favour of the singlet state (Table 2.2). The largest vertical singlet-triplet gap of 465kJ/mol was found for **58a**, while **56d** has the lowest vertical gap with a value of 220 kJ/mol. Relaxation energies after the vertical transition range from 54 kJ/mol in **55a** to 134 kJ/mol in **55c**, but despite these considerable differences in relaxation energy, $\Delta E_{S\rightarrow T}$ shows a good correlation to $\Delta E^{vert}_{S\rightarrow T}$. Again, **58a** has the largest singlet-triplet energy gap of 370 kJ/mol and **56d** shows the smallest gap of 114 kJ/mol.

Because the singlet and triplet states are related to each other by promotion of an electron from the σ to the p_π orbital, the HOMO-LUMO gap $\Delta E_{H\text{-}L}$ is closely related to the singlet-triplet transition of NHCs. Values for this gap were taken from the Kohn-Sham orbitals of the optimized singlet state, calculated at the B3LYP/aug-cc-pVTZ level.[79,80] The separation between the frontier orbitals ranges from 3.54 eV in **58d** to 6.10 eV in **57a**. Again, these values are sufficiently high to establish beyond any doubt that all NHCs under scrutiny are singlet species.[2a]

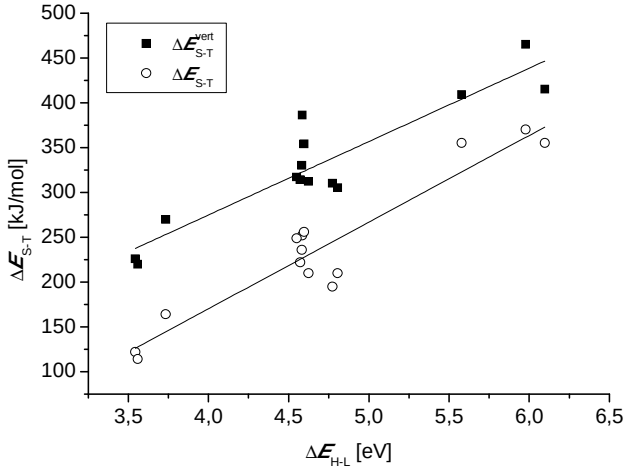

Fig. 2.5. Correlation between singlet-triplet and HOMO-LUMO energy gaps.

A weak correlation exists indeed between $\Delta E^{vert}_{S\rightarrow T}$ or $\Delta E_{S\rightarrow T}$ and $\Delta E_{H\text{-}L}$ (R^2 = 0.8326 for the vertical transition and R^2 = 0.8892 when accounting for relaxation) (Fig. 2.5). The imperfections

in the correlation between $\Delta E^{vert}_{S\rightarrow T}$ or $\Delta E_{S\rightarrow T}$ and $\Delta E_{H\text{-}L}$ can in all likelihood be attributed to inaccuracies of the latter values, since an electronic transition is always accompanied by a change in orbital energies, and the relatively high error margin associated with LUMO energies obtained by DFT calculations.

Based on their singlet-triplet energy gaps, the NHC can be sorted into three distinct groups. **55a**, **57a** and **58a** have exceptionally high $\Delta E_{S\rightarrow T}$ values above 350 kJ/mol. **55d**, **56d** and **58d** have particularly low $\Delta E_{S\rightarrow T}$ values below 170 kJ/mol, and the remaining NHCs have $\Delta E_{S\rightarrow T}$ values ranging from 195 kJ/mol to 256 kJ/mol, and occupy the middle ground. Based on these values, only for **55a**, **57a** and **58a** can dimerization be ruled out on purely electronic grounds, while additional stabilization from steric shielding might be required in all other cases.[82]

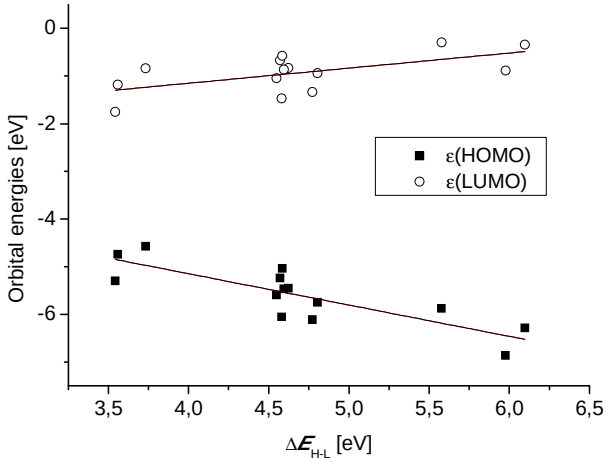

Fig. 2.6. Dependance of HOMO-LUMO gap on frontier orbital energies.

Interestingly, the number of nitrogen atoms in the heterocycle is largely irrelevant for the magnitude of the energy gaps, but a clear relationship exists between them and the carbene structure. Both the most stable group and the most unstable groups of NHCs are related to each other by isolobal exchange of methine groups for nitrogen atoms. This can be understood when considering the immediate impact of such an exchange on orbital energies. A nitrogen atom is more electronegative than a methine group, leading to lower energies for all orbitals. The conversion of **56d** to **58d** leads to a decrease in HOMO energy of 0.56 eV, but the LUMO is stabilized by an almost equal amount of 0.58 eV as well. Consequently, the absolute energies of

the frontier orbital changes upon isolobal exchange, but the relative orbital energy gap remains the same. Upon closer examination, increases in $\Delta E_{H\text{-}L}$ are due to a stabilization of the HOMO orbital, and a less marked destabilization of the LUMO orbital in the same compounds (Fig. 2.6). NHCs with stabilized σ orbitals have more destabilized p_π orbitals, and vice versa.

Table 2.3. Nucleus-independent chemical shifts.[a]

NHC	Singlet state[b]	Triplet state[b]	$[NHC + H]^{+}$ [b]	$[NHC + 2H]^{2+}$ [b]
55a	-11.14	-6.39	-13.09	-3.39
55b	-11.04	-7.53	-13.56	-5.19
55c	-11.05	-7.19	-13.09	-4.16
55d	-12.44	-11.07	-13.56	-4.61
56b	-11.53	-7.72	-13.48	-3.89
56c	-11.65	-8.84	-13.43	-3.03
56d	-11.93	-9.82	-13.48	-5.87
57a	-11.22	-4.90	-12.61	-1.88
57b	-11.00	-5.27	-12.67	-6.51
57c	-11.34	-7.45	-12.61	-4.52
58a	-12.88	4.22	-13.00	-1.80
58b	-12.03	-7.20	-12.98	-4.52
58c	-12.25	-4.76	-13.26	-4.65
58d	-13.91	-10.17	-13.81	-7.11

[a] Values calculated at the B3LYP/aug-cc-PVTZ level. [b] Values in ppm.

The aromaticity of the singlet state and its loss upon transition to the triplet state with an associated disruption of π-delocalisation is often invoked to explain singlet-triplet energy gaps.[15] To test this notion, the aromaticity of all singlet and triplet states as well as the mono- and diprotonated derivatives was assessed at the B3LYP/aug-cc-pVTZ level using the nucleus-independent chemical shift (NICS) method in conjunction with gauge-invariant atomic orbitals (Table 2.3).[79,80,83,84] In line with the estimates based on bond lengths (*vide supra*), both the singlet NHCs and the azolium cations were found to be fully aromatic species. Due to a better p_π-p_π resonance in the azolium salts, these species show a slightly higher degree of aromaticity than their neutral derivatives. By contrast, the dicationic species and the triplet states have low NICS

values, confirming the low degree of aromatic delocalization in these species predicted by analysis of their bond lengths. However, while variations are small for the charged species and the singlet states, NICS values for the triplet states show no such uniform behaviour. It is noteworthy that **55aT**, **57aT** and **58aT** have comparatively low NICS values, while for **55dT**, **56dT** and **58dT**, the drop in NICS when compared to the singlet states is particularly low. The most stable singlet carbenes would lose an above average degree of aromatic stabilization, while for the least stable singlet carbenes, the triplet states retain a high degree of aromaticity and the loss of aromatic stabilization can be assumed to be small.

2.1.3 Measuring the σ-Basicity of the Carbene Lone Pair

One of the main appeals of NHCs as ligands in transition metal catalysis lies in their strongly σ-donating properties. Therefore, it is of interest to explore in detail the factors that influence the donating properties of the σ orbital at $C_{carbene}$. For all 14 NHCs that were studied, Kohn-Sham orbitals were calculated at the same level of theory the geometry optimization was done at, and the highest occupied Kohn-Sham orbitals were found to be of σ-symmetry with a major lobe at $C_{carbene}$ lying in the NHC ring plane. Visual inspection of these orbitals revealed no significant difference within or between the different series (Fig. 2.7).

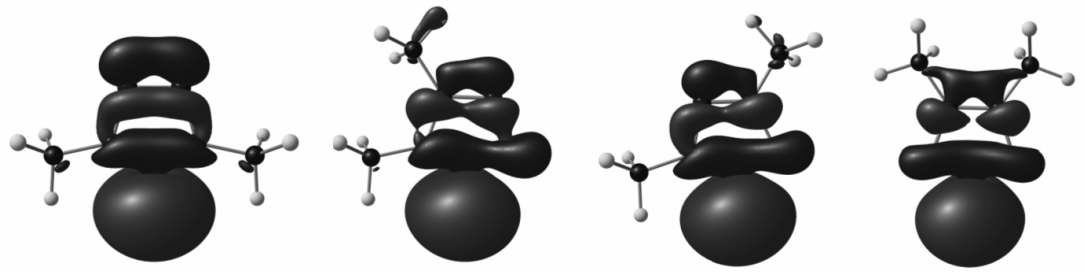

Fig. 2.7. Highest occupied molecular orbitals of **58a**-**d**.

It has been demonstrated that first proton affinities and the energy eigenvalues of the donor orbitals in strong carbon bases such as NHCS are in excellent agreement.[85] The C-H bond formed upon protonation of $C_{carbene}$ is covalent in nature. Differences in the enthalpy of this reaction, i. e. the first proton affinity, will be dependant on the energies of the involved orbitals – the 1s orbital on hydrogen and the σ orbital on $C_{carbene}$. While electrostatic interactions and changes in the

geometry of the carbene also contribute to the bonding interaction, the differences of these contributions between NHCs can be safely assumed to be negligible. A good correlation between the energy eigenvalue of the highest occupied Kohn-Sham orbital ε(σ-HOMO) and first proton affinity should exist (Table 2.4).

Table 2.4. Proton affinities and ε(σ-HOMO) of NHCs, and ε(π-HOMO) of $[NHC + H]^+$.[a]

NHC	1st PA [kJ/mol]	ε(σ-HOMO)[b] [eV]	2nd PA [kJ/mol]	ε(π-HOMO)[c] [eV]
55a	1088	-5.88	316	-12.04
55b	1140	-5.24	256	-12.33
55c	1164	-5.04	323	-12.04
55d	1206	-4.57	326	-12.33
56b	1093	-5.75	211	-12.98
56c	1109	-5.60	238	-13.12
56d	1179	-4.74	253	-12.98
57a	1039	-6.29	214	-13.23
57b	1111	-5.46	181	-13.38 [d]
57c	1116	-5.47	219	-13.23
58a	985	-6.87	123	-14.27 [d]
58b	1055	-6.11	135	-14.23 [d]
58c	1061	-6.06	147	-14.22
58d	1134	-5.30	168	-13.96

[a] Values calculated at the B3LYP/aug-cc-pVTZ level. [b] Values for the singlet NHCs. [c] Values for $[NHC + H]^+$. [d] Values taken from HOMO-1.

As expected, the correlation between first proton affinity and ε(σ-HOMO) was excellent ($R^2 = 0.9936$, cf. Fig. 2.8). Additionally, the values obtained are in excellent agreement obtained either experimentally or by calculations at high levels of theory, ascertaining the accuracy of the calculations presented here.[32,86]

The proton can be thought of as the simplest possible Lewis acid, interacting with the NHCs and acting exclusively as σ-acceptor. Due to the correlation between the two parameters, both ε(σ-

HOMO) and the first proton affinity can therefore be seen as a measure for the σ-donating properties of the NHC ligands, allowing to rank them by ligand donor strength.

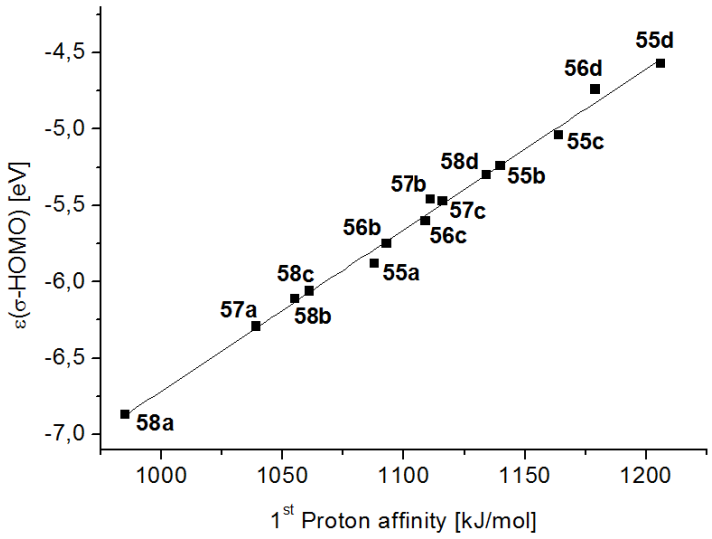

Fig. 2.8. Correlation between first proton affinity and ε(σ-HOMO).

Tetrazolin-5-ylidenes **58a-c** make up the group of weakest donors, along with 1,2,4-triazolin-5-ylidene **57a**. Among these, **58a** is by far the weakest donor, with a very low-lying HOMO orbital and the only first proton affinity to fall under 1000 kJ/mol. After these four nitrogen-rich NHCs, imidazolin-2-ylidene **55a** follows, then two 1,2,3-triazolin-5-ylidenes are next (**56b** and **56c**). Slightly more donating are the remaining 1,2,4-triazolin-5-ylidenes **57b** and **57c**. For these two compounds, the orbital eigenvalues ε(σ-HOMO) and first proton affinities differ only by a marginal amount, making a ranking difficult. By orbital energies, **57b** is a marginally better donor, while the proton affinity of **57c** is slightly higher. Within the computational margin of error, these differences can be discarded, and the donor strength should be considered to be equal. Following these compounds, **58d** is the most strongly donating tetrazolin-ylidene. The series is completed by imidazolin-4-ylidene **55b**, pyrazolin-3-ylidene **55c**, the remaining 1,2,3-triazolin-ylidene **56d**, and finally pyrazolin-4-ylidene **55d** as the strongest donor in this series.

Separating the data into four series with distinct NHC backbone allows for a detailed analysis of the factors governing their donor strength (Fig. 2.9).

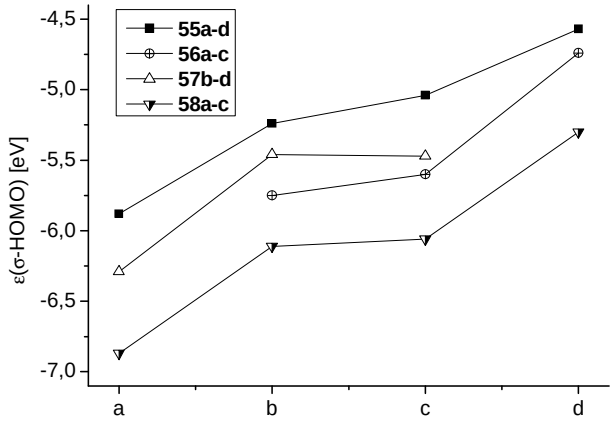

Fig. 2.9. Donor strength trends within and between NHC series.

A clear order of the series becomes apparent, based on the number of nitrogen atoms present in the heterocycle. Imidazolin- and pyrazolin-ylidenes lie above triazolin-ylidenes in terms of orbital energy, and these lie above tetrazolin-ylidenes. The NHCs can be broken down into a carbene carbon, substituted by a X_α-X_β-X_β-X_α system, consisting of a variable number of methine groups and nitrogen atoms. The group electronegativity of this system depends on the electronegativity of its constituents, and the gradual introduction of an increasing number of nitrogen atoms will lead to an increase in group electronegativity. With more electronegative substituents, the bonds between $C_{carbene}$ and the flanking groups will become more polarized, and the increased p character in these bonds leads to a corresponding increase in s character of the σ lone pair orbital. The s orbital becomes more stabilized, ε(σ-HOMO) and first proton affinity decrease, and the NHCs are becoming weaker donors. In extension of this argument, NHCs with only one nitrogen atom present in the heterocycle, such as cyclic alkyl amino carbenes (CAACs), are exceedingly strong σ-donors.[87]

The introduction of additional nitrogen atoms can have a substantial impact on ε(σ-HOMO) of the NHCs, and a drop of 1.02 eV can be found when introducing two additional nitrogen atoms into **55c** to give **58c**. However, the change within series **55a-d** itself is far more striking. The σ orbital of **55d** is 1.31 eV higher in energy than the same orbital in **55a**. The reason is not the removal of nitrogen atoms from the backbone per se, but rather the change of nitrogen atoms

from the α-position to the β-position within the heterocycle. While two nitrogen atoms are adjacent to $C_{carbene}$ in **55a**, there is only one in **55b** and **55c**, and in **55d**, both nitrogen atoms are located in β-positions. Placing the more electronegative nitrogen atoms further away from the carbene center, the inductive effects that stabilize the σ orbital are weakened, resulting in higher orbital energies. The slightly better orbital stabilization in **55b** when compared to **55c** can be explained by a higher group electronegativity of the N_α-N_β substituent when compared to two isolated nitrogen atoms.

Following the same argument, ε(σ-HOMO) in the 1,2,3-triazolin-5-ylidenes **56b** and **56c** should be higher than the same orbital energy eigenvalue in the 1,2,4-triazolin-5-ylidene isomers **57b** and **57c**, since only one nitrogen atom is adjacent to $C_{carbene}$ in the former, while there are two nitrogen substituents in the latter. However, the opposite trend is observed, and the 1,2,4-triazolin-5-ylidenes are found to be the stronger donors. This seemingly contradictory observation can be resolved when taking into account the exact nature of the moiety in α-position. In series **55a-d**, the nitrogen atoms always bear methyl groups. In **57b** and **57c**, the nitrogen atom in α-position is not methylated, however, but has a lone pair in an sp^2 orbital lying in the NHC ring plane. The two molecular orbitals containing the adjacent lone pairs at the α-nitrogen and at $C_{carbene}$ can interact in an in-phase and out-of-phase interaction, stabilizing the energetically slightly lower nitrogen lone pair, and destabilizing the energetically higher carbene lone pair even further. The presence of small lobes at the other center in the molecular orbitals containing both lone pairs is a clear indication of such an interaction (Fig. 2.10)

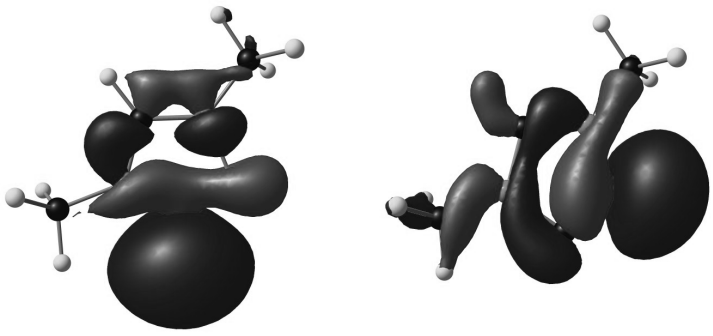

Fig. 2.10. $C_{carbene}$ and α-nitrogen lone pair orbitals in **57c**.

No such destabilizing influence is exerted by the methine groups in **56b** and **56c**, hence, the 1,2,4-triazolin-5-ylidenes are stronger donors than their 1,2,3-triazolin-5-ylidene congeners despite being better stabilized by inductive effects from α-nitrogen substituents.

The phenomenon of lone pair destabilization is taken to the extreme in series **58a-d**. Within this series of NHCs, the ε(σ-HOMO) eigenvalues differ by a staggering 1.57 eV between the weakest and the strongest donor, yet all of them contain an N_α-N_β-N_β-N_α system, and varying inductive effects cannot be invoked to explain this variation. The only structural change within this series is the position of the methyl groups, and by consequence, the lone pairs at the unsubstituted nitrogen atoms. In the weakest donor **58a**, no unsubstituted nitrogen atom is in α-position. The considerably stronger donors **58b** and **58c** have one nitrogen lone pair adjacent to $C_{carbene}$, and two pairs are found in this position in **58d**, which is by far the strongest donor in this series. Since no changes in inductive effects occur within this series, it can be determined that a nitrogen lone pair adjacent to the carbene center destabilizes the carbene lone pair orbital by an approximate 0.8 eV.

In summary, three independent factors influence first proton affinity, ε(σ-HOMO) and ligand donor strength in the NHCs under scrutiny:

- the number of nitrogen atoms present in the heterocycle
- their location in the ring with respect to $C_{carbene}$
- the presence or absence of nitrogen atoms with an in-plane lone pair in α-position.

2.1.4 The Electronic Structure of the π-System

The orbital interacting with an incoming proton in the free NHCs is the σ orbital at $C_{carbene}$, but for the second protonation step, no lone pair with σ symmetry at $C_{carbene}$ is available anymore, and consequently, an orbital of π symmetry has to be used. Examples of such doubly protonated salts exist in the literature.[88] The first proton affinity and the associated ε(σ-HOMO) eigenvalues provide insights into the σ-donor properties of NHCs. Similarly, the addition of a second proton to the resulting azolium salts can provide insights into the π-electronic structure in general, and π-basicity of NHCs in particular. It has been shown that there exists a correlation between ε(π-HOMO) of azolium salts, and the second proton affinity of NHCs.[85]

When determining ε(π-HOMO) of the azolium salts, caution has to be exerted, since the HOMO often has σ symmetry in these compounds and corresponds to lone pairs at the non-alkylated nitrogen atoms, particularly in the tetrazolin-ylidenes. Compared to the correlation found between first proton affinities and ε(σ-HOMO), the correlation between second proton affinities and ε(π-HOMO) was not as strong (R^2 = 0.9188, cf. Fig. 2.11).

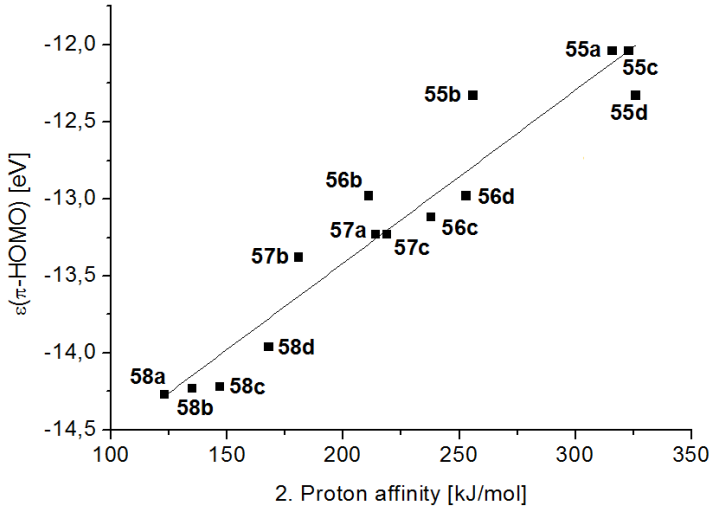

Fig. 2.11. Correlation between second proton affinity and ε(π-HOMO).

Partly, this less than perfect correlation arises from pairs of NHCs which are derived from the same azolium salt by deprotonation at different positions. The ε(π-HOMO) values in these azolium cations are identical, while the second protonation takes place at different carbon atoms in the ring, leading to vastly different second proton affinities. As an example, **55b** and **55d** are both derived from the 1,2-dimethylpyrazolium cation, which has an ε(π-HOMO) of -12.33 eV. Depending whether this cation is protonated either on C3- or C4-position, the second proton affinities are 256 kJ/mol or 326 kJ/mol, respectively. This difference of 70 kJ/mol arises from different orbital coefficients at the carbon atoms, the likely participation of other orbitals with suitable shape, and to a minor extent from differences in geometry relaxation, but neither of these factors is reflected in the orbital energy eigenvalue. Similar cases are **55a**/**55c**, **56b**/**56d** and **57a**/**57c**. Attempts to refine the picture, such as taking orbital coefficients into account, were met with failure, as no improvement in the correlation was observed.

Despite the simplifications implicated in the approach, and the obvious problem of using ε(π-HOMO) as indicator for π-basicity, it is nevertheless valid to analyze the underlying trends in the dataset. The NHCs can be divided into three groups based on their second proton affinity. The first group compromises tetrazolin-ylidenes with second proton affinities ranging from 123 kJ/mol to 168 kJ/mol, the second group consist of triazolin-ylidenes with second proton affinities that fall between 181 kJ/mol and 253 kJ/mol, and the last group contains imidazolin-ylidenes and pyrazolin-ylidenes with second proton affinities between 256 kJ/mol and 326 kJ/mol. While these separations might seem arbitrary due to the small separations between the cut-off values, the boundaries are clearer when considering ε(π-HOMO). In the first group, orbital energies fall between 14.27 – 13.96 eV, in the second, 12.98 – 13.38 eV, and in the last, 12.04 – 12.93 eV.

The common theme in each group is the number of heteroatoms in the ring, regardless of their position relative to the carbene carbon. The presence of these more electronegative atoms leads to more stabilized π-HOMO orbitals, and consequently the second proton affinities are lower. Tetrazolin-ylidenes are the weakest π-bases among the studied NHCs, followed by triazolin-ylidenes, and imidazol- and pyrazole-derived carbenes are the strongest π-donors.

2.1.5 Local Electronic Structure at $C_{carbene}$: p_π Population and Natural Charge

Even though NHCs are only weak π-bases, the fact that there is π-electron density at $C_{carbene}$ available for bonding demonstrates that their description with the lone pair occupying the σ-HOMO and the p_π orbital being unoccupied is too simplistic and might be only applicable to simple singlet carbenes not substituted with π-donors. The extraordinary stability of NHCs can in part be attributed to the transfer of π-electron density from the flanking nitrogen substituents into the p_π orbital of $C_{carbene}$, which stabilizes this orbital and tempers the electrophilicity associated with it, and widens the singlet-triplet gap.

A detailed picture of the p_π population and natural charges can be obtained form natural population analysis, which was done at the same level of theory as previous calculations.[89] All NHCs were found to possess a considerable p_π population at the carbene center, ranging from 0.60 electrons located in this orbital in **57b** to 0.79 electrons in **55d** (Fig. 2.12 and Table 2.5).

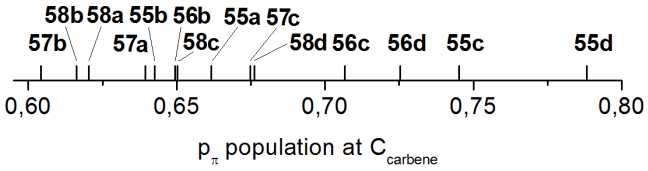

Fig. 2.12. The population of the p_π orbital at $C_{carbene}$.

Table 2.5. Natural charge and p_π population at $C_{carbene}$.[a]

NHC	Natural charge [e]	p_π population [electrons]
55a	0.09	0.66
55b	-0.08	0.64
55c	-0.18	0.75
55d	-0.41	0.79
56b	-0.11	0.65
56c	-0.16	0.71
56d	-0.20	0.73
57a	0.09	0.64
57b	0.10	0.60
57c	0.04	0.67
58a	0.09	0.62
58b	0.07	0.62
58c	0.03	0.65
58d	-0.02	0.68
CH_2	-0.12	0.00
Ph^-	-0.39	0.72

[a] Values calculated at the B3LYP/aug-cc-pVTZ level.

Abnormal or mesoionic carbenes have attracted considerable research interest, sparked by their oftentimes superior performance in catalysis.[38] These NHCS, which cannot be described by a canonical structure without charges, are occasionally treated as a class of NHCs distinct from their classical or normal congeners. Among carbenes **55** – **58**, half are normal carbenes, while the

other half is mesoionic. This allows for a detailed comparison of their electronic structures. For normal carbenes, p_π populations of 0.66 electrons or less were found, while mesoionic carbenes had p_π populations in excess of 0.65 electrons. However, the local electronic structure of the π system at $C_{carbene}$ does not allow for a clear distinction between normal and mesoionic carbenes. While p_π populations below 0.65 electrons are indicative for normal NHCs, and values above 0.66 electrons were found for mesoionic species, there is an overlap between these two zones. The p_π population in the normal NHC **55a** was found to be higher than the population in the MIC **58c**. The transition from normal NHCs to MICs is gradual in nature, without a sharp change in electronic structure, illustrating that the distinction made between these two classes of compounds is rather based on the inadequate representation of electronic structures by drawing canonical structures than by real properties of the carbenes themselves.

The observed trend in p_π population can be understood in terms of π orbital energies, and the absence or presence of π-donors in α-position. As mentioned above, the replacement of methine groups by nitrogen atoms leads to lower orbital energies, and more π-electron density will be located at the nitrogen atoms, depleting the remainder of the π-system. Therefore, **55a** as an NHC with only two nitrogen atoms in the heterocycle, has a relatively high p_π population for a normal carbene, while **58c** has a particularly low p_π population due to the presence of four nitrogen atoms. This explains the overlap of mesoionic and normal zones.

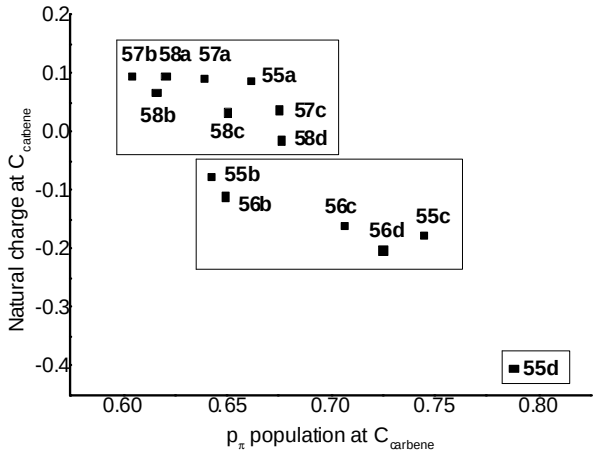

Fig. 2.13. Natural charges and p_π population at $C_{carbene}$.

The natural charges at $C_{carbene}$ are related superficially to p_π populations (Fig. 2.13), but it is clear that no linear interdependence exists between these two variables. The electron density in the p_π orbital is only a part of the total electron density of the carbene center, and an isolated consideration of the π-system neglects the significant changes inductive effects can make in the σ-system. These inductive effects area dominated by the electronegativity of the substituents directly adjacent to $C_{carbene}$, and to a lesser extent, the amount of heteroatoms in the ring (*vide supra*). This becomes apparent when ranking the NHCs by the natural charge of $C_{carbene}$. Species that have the same number of α-heteroatoms are very similar in charge to each other, regardless of differences in p_π population. If two nitrogen atoms are present in α-position, $C_{carbene}$ has a slightly positive to neutral charge, ranging from 0.10 e in **57b** to -0.20 e in **58d**. NHCs with only one nitrogen flanking the carbene center are consistently negatively charged, and natural charge values range from -0.08 e in **55b** to -0.20 e in **56d**. The pyrazolin-4-ylidene **55d** occupies a special position, as it is the only species with no α-nitrogen. It is distinctly negatively charged, with a value of -0.41 e.

Based on natural charges and p_π populations, NHCs can be described as a continuum ranging from species like **57b**, with a p_π orbital that contains a small fraction of the π-electron density of the heterocycle, to species like **55d** at the other extreme, in which a positive partial charge is delocalised over the ring and a negative partial charge is localised at the carbene center. While normal carbenes are closer to the electronic structure of **57b** and mesoionic carbenes have electronic structures more similar to **55d**, the transition is gradual. In this context, it is also noteworthy that the electronic structure of **55d**, at least as far as the carbene carbon is concerned, bears semblance to the local electronic structure of aromatic carbanions, which have almost identical p_π populations and natural charges (cf. Table 2.5). However, this similarity does not extend to the chemical behavior of the molecule as a whole.

2.2. The Interaction of N-heterocyclic Carbenes and Transition Metals

Since NHCs are widely used as ligands in transition metal chemistry, a detailed understanding of the interaction between the carbene ligand and transition metal fragments is required. In-depth studies into the bond properties between imdazole-derived NHCs and a wide variety of transition metals have been conducted,[69e,90] but computational analyses focusing on a larger selection of

NHCs are lacking. To gain a systematic insight into the bonding between NHCs **55**-**58** with transition metals, the bonding of these carbenes to titanium(IV) tetrachloride and gold(I) chloride fragments were studied. Ti(IV) is an early transition metal with a d^0 configuration, while gold has a completely filled d subshell and is a late transition metal. By choosing these two extreme ends of the spectrum, a fuller picture of NHC-metal bonds can be obtained than by focusing on a single metal only. Chlorido coligands were chosen for these model systems for the sake of computational simplicity.

2.2.1 Geometries of Gold(I) and Titanium(IV) NHC Complexes

The geometries of NHC-AuCl and NHC-$TiCl_4$ (NHC = **55** – **58**) were optimized using the B3LYP functional used for all previous calculations,[79] but with the smaller basis set cc-pVDZ for the lighter atoms and cc-pVDZ-PP for the description of gold.[80,91,92] During optimisation, C_S symmetry was imposed, with the NHC ring and the carbon-metal bond lying in the mirror plane.

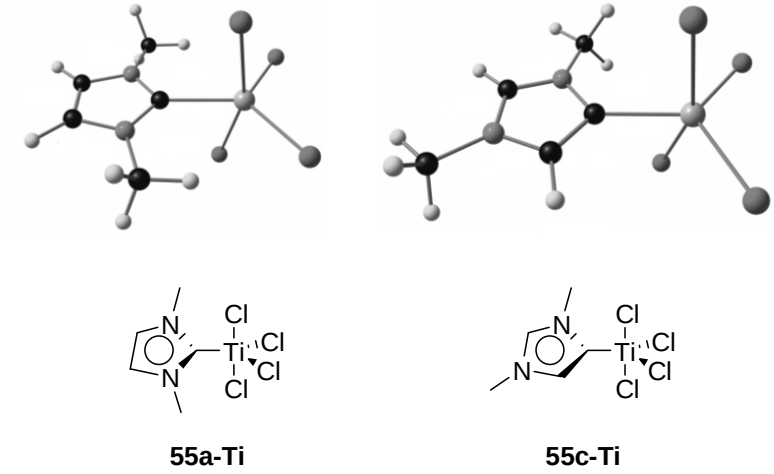

Fig. 2.14. Structures and optimized geometries of titanium(IV) tetrachlorido complexes incorporating **58a** and **55c**.

The titanium complexes adopt a distorted trigonal-bipyramidal coordination geometry, with the NHC ligand occupying a position in the equatorial plane.[69e] Under the constraints of C_S symmetry, the NHC ring can either lie in the equatorial plane, or in the plane defined by titanium and the two axial chlorido ligands. For most of the titanium complexes, the alignment of the NHC plane with the equatorial plane of the complex was found to be energetically more

favourable. By adopting this conformation, unfavourable steric interactions between the wingtip methyl groups of the NHCs and the axially bound chlorido ligands can be avoided, especially since the latter are tilted slightly towards $C_{carbene}$. Exceptions were complexes **55b-Ti**, **55d-Ti**, and **56b-Ti**, which did not converge to a true energetic minimum in this conformation, but instead reached transition states only. For the sake of comparison, these geometries were used nevertheless for all further studies.

Table 2.6. Selected bond lengths in Ti(IV) and Au(I) complexes.[a]

	NHC-$TiCl_4$	NHC-AuCl	
	C-Ti [Å]	C-Au [Å]	Au-Cl [Å]
55a	2.203	2.010	2.302
55b	2.169	2.007	2.308
55c	2.166	2.008	2.312
55d	2.153	2.014	2.319
56b	2.174	2.001	2.302
56c	2.177	2.003	2.305
56d	2.165	2.004	2.314
57a	2.198	2.002	2.297
57b	2.172	1.997	2.304
57c	2.179	2.003	2.305
58a	2.197	1.996	2.291
58b	2.182	1.993	2.297
58c	2.187	1.997	2.298
58d	2.177	1.996	2.307

[a] Values calculated at the B3LYP/cc-pVDZ(-PP) level.

The C-Ti bond lengths show a significant degree of variation and range from 2.153 Å in **55d-Ti** to 2.197 Å in **58a-Ti**. A clear correlation between the ε(σ-HOMO) values of the NHC ligand and the associated C-Ti bond lengths was found, with shorter bonds resulting from higher-lying σ-donor orbitals (Fig. 2.16 and Table 2.6, R^2 = 0.7334). The electron-poor nature of the titanium(IV) center makes it prone to bind tighly to more strongly donating NHC ligands, resulting in the observed shorter bond lengths.

NHC complexes incorporating titanium(IV) fragments are very sensitive to hydrolysis, hence molecular structures of these compounds are rare.[93] However, comparison of the optimized structures with the molecular structure of a complex featuring a benzimidazolin-2-ylidene ligand bearing sterically bulky neopentyl wingtip substituents revealed good structural agreement despite the obvious steric and electronic differences of this ligand to the NHCs **55**-**58**. For the most closely related compled **55a-Ti**, the C-Ti bond lengths was found to be only marginally shorter in the calculated complex when compared to the experimental structure, and the associated relative difference lies well within the usually accepted error range for DFT calculations.

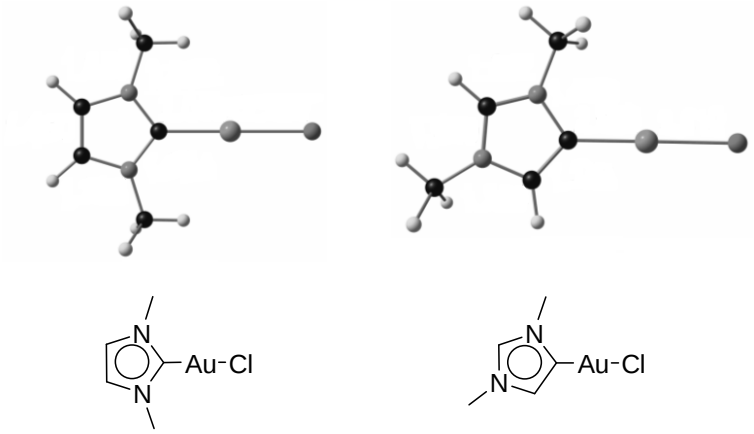

Fig. 2.15. Structures and optimized geometries of gold(I) chlorido complexes incorporating **58a** and **55c**.

The gold(I) complexes adopt the linear coordination geometry typical for coinage metal complexes in this oxidation stage. The C-Au bond lengths range from 1.993 Å in **58b-Au** to 2.014 Å in **55d-Au**. Longer bonds are found in the case of more strongly donating NHC ligands, but there is linear correlation between ligand donor strengths and C-Au bond lengths, in contrast to the titanium(IV) complexes. However, the Au-Cl bond lengths are dependant on ε(σ-HOMO), which provides a measure of the *trans*-influence exerted by the NHC ligand (Fig. 2.16, $R^2 = 0.9685$). Longer bond distances are found with more strongly donating NHC ligands (Fig. 2.16). The shortest Au-Cl bond was found for **58a-Au** with a distance of 2.291 Å and the longest bond was 2.319 Å long and found in complex **55d-Au**.

Similarly to the titanium(IV) complexes, the comparison of calculated structural parameters to those obtained experimentally showed only minor deviations.[94] For example, the C-Au and Au-Cl bond lengths in **55a-Au**, were elongated by 1.5% and 0.6%, respectively, which is well within the acceptable error margin for DFT calculations.

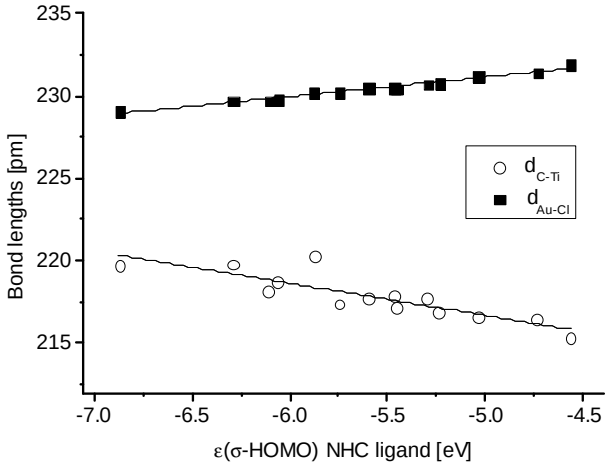

Fig. 2.16. Variation of C-Au and C-Ti bond lengths with ε(σ-HOMO).

2.2.2 Energy Decomposition Analyses of the C-Au and C-Ti Bonds

The energy decomposition analysis is a computational approach to analyzing chemical bonds by breaking the interaction down into three distinct contributions.[95] The instantaneous interaction energy ΔE_{int} between two fragments A and B in the frozen geometry of a molecule AB is decomposed into $\Delta E_{int} = \Delta E_{elstat} + \Delta E_{Pauli} + \Delta E_{orb}$. In this equation, ΔE_{elstat} is the electrostatic interaction between the two fragments, i.e. Coloumbic attraction and repulsion of partial charges. The Pauli interaction ΔE_{Pauli} corresponds to the repulsion of electrons on both fragments having the same spin. Occasionally, the combination of electrostatic interaction and Pauli repulsion is summarized into a steric interaction term $\Delta E^0 = \Delta E_{elstat} + \Delta E_{Pauli}$, which reflects the overall interaction between the fragments without allowing for orbital mixing and charge transfer. This term should not be confused with the commonly used concept of steric repulsion, which corresponds more closely to the Pauli repulsion ΔE_{Pauli}. ΔE^0 includes attractive Coloumbic interactions in addition to Pauli repulsion, and may thus become attractive in certain cases.

Lastly, the orbital interaction term ΔE_{orb} accounts for energetic contributions from orbital mixing between the two fragments, orbital relaxation, charge transfer, and polarization. It can be decomposed further into contributions of orbitals with different symmetry. In the case of molecules with C_S symmetry, these individual contributions are either of σ or π symmetry: $\Delta E_{orb} = \Delta E_\sigma + \Delta E_\pi$. By removing virtual, i.e. unoccupied orbitals, from either fragment, it is possible to assess the contributions of π-donation $\Delta E_{\pi(LM)}$ and π-backdonation $\Delta E_{\pi(ML)}$ to the ΔE_π term.[69e,90,96] However, the removal of virtual orbitals from a fragment has an effect on all other orbitals within this fragment, so the sum of $\Delta E_{\pi(L\rightarrow M)}$ and $\Delta E_{\pi(M\rightarrow L)}$ differs slightly from ΔE_π.
Energy decomposition analyses of all complexes were performed using the ADF2012.01 program at the BP86/TZ2P level of theory (Tables 2.7 and 2.8).[79a,97,98,99]

Table 2.7. Energy decomposition analysis results for the C-Ti bond in NHC-$TiCl_4$.[a]

	ΔE_{int}	ΔE_{Pauli}	ΔE_{elstat}	ΔE_{orb}	ΔE_σ	ΔE_π	$\Delta E_{\pi(LM)}$	$\Delta E_{\pi(ML)}$
55a-Ti	-206.8	551.6	-497.8	-260.6	-227.2	-33.4	-8.9	-24.9
55b-Ti	-229.9	579.9	-532.1	-277.7	-244.6	-33.1	-9.2	-24.1
55c-Ti	-240.4	580.7	-544.7	-276.4	-242.3	-34.0	-11.2	-22.8
55d-Ti	-264.7	574.6	-557.7	-281.6	-249.4	-32.2	-11.3	-20.4
56b-Ti	-211.2	562.4	-507.6	-266.0	-233.2	-32.8	-8.1	-25.1
56c-Ti	-215.7	554.1	-509.4	-260.3	-228.1	-32.2	-8.7	-23.9
56d-Ti	-243.3	563.9	-534.7	-272.6	-241.1	-31.5	-9.3	-22.1
57a-Ti	-185.1	531.8	-467.6	-249.4	-218.0	-31.4	-7.2	-25.1
57b-Ti	-215.9	570.6	-513.3	-273.2	-239.1	-34.1	-8.3	-26.4
57c-Ti	-216.0	553.7	-504.3	-265.5	-232.4	-33.0	-8.9	-24.6
58a-Ti	-166.3	512.0	-438.0	-240.3	-207.6	-32.8	-6.3	-27.6
58b-Ti	-192.5	538.4	-473.8	-257.0	-223.2	-33.8	-7.2	-27.4
58c-Ti	-193.4	528.6	-471.6	-250.5	-217.7	-32.8	-7.3	-26.3
58d-Ti	-215.5	529.7	-489.2	-256.0	-224.5	-31.4	-7.39	-24.2

[a] Values calculated at the B3LYP/cc-PVDZ//BP86/TZ2P level, all values given in kJ/mol.

The detailed energy decomposition analyses done by Frenking *et al.* on the carbene-metal bonds between variety of transition metal fragement, including AuCl and $TiCl_4$, and NH,NH-

imidazolin-2-ylidene as well as NH,NH-imidazolin-4-ylidene can serve as a benchmark for the results obtained from the analyses reported here.[69e] Despite the presence of methyl groups as wingtip substituents in carbenes **55-58** in place of the protons in Frenking's study, there is good agreement in terms of ΔE_{int} as well as the individual contributing energy terms for the NHC-AuCl complexes. However, the interaction energies ΔE_{int}, the Pauli repulsion term ΔE_{Pauli}, and especially the orbital interaction term corresponding to π-interactions, ΔE_{π}, differ considerable in the NHC-$TiCl_4$ complexes. The reason for these deviations can be found in the complex geometries. While the most stable conformations for the $TiCl_4$ adducts of **55-58** were those with the NHC ring lying in the equatorial coordination plane, in the titanium(IV) complexes analyzed by Frenking, the NHC plane lies in the plane defined by titanium and the axial chlorido ligands. It is presumably the presence of substituents on nitrogen, which would interact unfavourably with the axial ligands in the geometry described by Frenking, which leads to the preference for a different geometry, and hence for differences in orbital interactions and Pauli repulsion.

Table 2.8. Energy decomposition analysis results for the C-Au bond in NHC-AuCl.[a]

	ΔE_{int}	ΔE_{Pauli}	ΔE_{elstat}	ΔE_{orb}	ΔE_{σ}	ΔE_{π}	$\Delta E_{\pi(LM)}$	$\Delta E_{\pi(ML)}$
55a-Au	-333.2	834.4	-874.2	-293.4	-244.3	-49.1	-6.1	-45.6
55b-Au	-349.4	853.0	-904.8	-297.6	-248.3	-49.3	-5.8	-45.9
55c-Au	-354.3	849.0	-910.2	-293.1	-246.9	-46.2	-6.0	-42.3
55d-Au	-358.9	833.9	-904.4	-288.4	-247.0	-41.4	-5.4	-37.6
56b-Au	-336.1	837.1	-878.3	-295.0	-243.3	-51.6	-5.6	-48.5
56c-Au	-338.0	830.5	-878.7	-289.8	-240.7	-49.1	-5.6	-45.9
56d-Au	-352.0	841.6	-901.0	-292.6	-246.3	-46.3	-5.2	-43.0
57a-Au	-319.9	818.5	-847.0	-291.3	-238.9	-52.5	-5.9	-49.4
57b-Au	-341.7	858.6	-898.0	-302.3	-247.8	-54.5	-5.8	-51.4
57c-Au	-338.2	833.6	-875.6	-296.1	-246.7	-49.4	-5.5	-46.3
58a-Au	-303.5	788.6	-802.0	-290.1	-233.9	-56.2	-5.9	-53.4
58b-Au	-325.1	823.5	-848.8	-299.7	-243.0	-56.7	-5.7	-53.8
58c-Au	-322.7	813.8	-843.1	-293.4	-240.1	-53.3	-5.5	-50.5
58d-Au	-336.7	821.1	-862.7	-295.1	-243.6	-51.50	-4.97	-48.8

[a] Values calculated at the B3LYP/cc-PVDZ//BP86/TZ2P level, all values given in kJ/mol.

Energy decomposition analyses revealed both differences and similarities in the carbon-metal bond properties between titanium(IV) and gold(I) NHC complexes. In all complexes, the Pauli repulsion term is positive, while ΔE_{elstat} and ΔE_{orb} were negative, thus corresponding to an attractive interaction. For both metals, the major attractive contribution is electrostatic in nature. In the titanium(IV) complexes, ΔE_{elstat} accounts for 66% of attractive interactions on average, while this percentage rises to 75% in the case of NHC-AuCl complexes. The remaining 34% and 25%, respectively, are due to the orbital interaction term. The nature of the bonded NHC has little impact on this distribution.

The C-Au bonds were found to be considerably stronger than the C-Ti bonds in terms of total interaction energy ΔE_{int}. For titanium(IV), the largest value for ΔE_{int} is -265 kJ/mol in **55d-Ti**, while the smallest is -166 kJ/mol in **58a-Ti**. By contrast, the largest value in NHC-AuCl complexes was a ΔE_{int} of -358 kJ/mol in **55d-Au** and the smallest 303 kJ/mol in **58a-Au**. It is no coincidence that both the largest and the smallest interaction energies were found with the same ligands in both the gold(I) and the titanium(IV) complexes, because ΔE_{int} in both series shows a high degree of correlation (R^2 = 0.9729 (NHC-$TiCl_4$) and 0.9514 (NHC-AuCl)). This observation suggests that NHCs will have the same trends in overall bond strength, which is related to the ΔE_{int}. Metal-NHC bonds are stronger for more strongly donating NHC ligands independently of the transition metal they are binding to (Fig. 2.17).

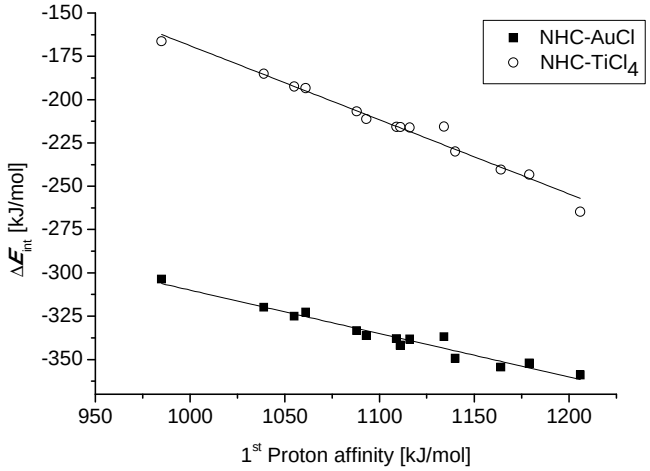

Fig. 2.17. Correlation of ligand donor strength and interaction energy.

A detailed explanation for this behaviour can be found by analyzing the trends for the individual contributions to the interaction energy term. First proton affinities are used as measure of donor strength, as they are an equally good measure for this property than ε(σ-HOMO), but give slightly better correlation coefficients, presumably due to better capturing minor contributions to σ-bonding made by other orbitals than the NHCs' σ-HOMO.

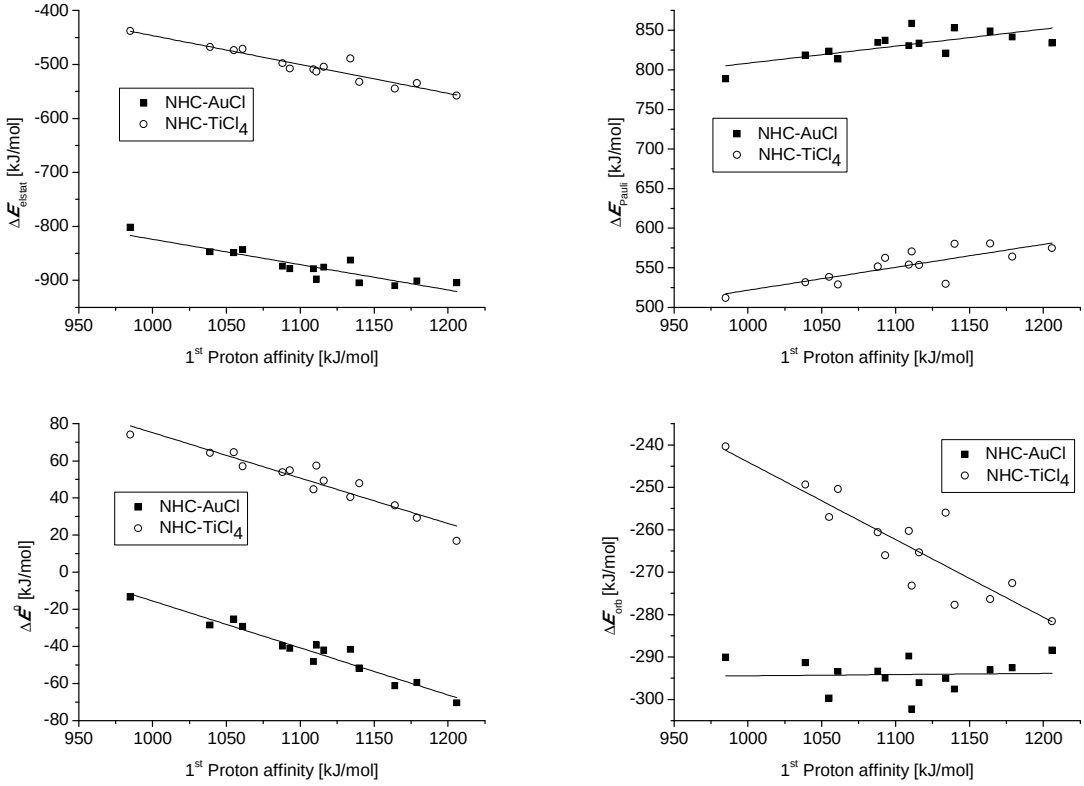

Fig. 2.18. Variation of electrostatic interaction, Pauli repulsion, steric interaction and orbital interaction with first proton affinity in titanium(IV) and gold(I) NHC complexes.

Both the electrostatic interaction and the Pauli repulsion terms vary widely with the ligands in both the titanium(IV) and gold(I) complexes (Fig. 2.18). ΔE_{elstat} shows a moderately strong correlation to the first proton affinity (R^2 = 0.8920 (NHC-$TiCl_4$) and 0.8000 (NHC-AuCl)), and the attractive interaction is stronger with more strongly donating NHCs. By contrast, the ΔE_{Pauli} term gets gradually more repulsive with increasing donor strengths in both series of complexes, albeit the correlations are only weak (R^2 = 0.6044 (NHC-$TiCl_4$) and 0.4652 (NHC-AuCl)). In

both cases, the observed trend can be traced back to the gradually increasing electron density at $C_{carbene}$, albeit in the case of ΔE_{Pauli}, the difference in α-substitution patterns between NHCs might be a major confounding factor due to their contribution to steric repulsion, leading to the observed irregularities. Both ΔE_{elstat} and ΔE_{Pauli} are smaller in the titanium(IV)complexes.

The combination of these two terms into a steric interaction term ΔE^0 reflects the interaction between the NHCs and the transition metal fragments without orbital mixing and electron transfer. For the titanium(IV) complexes, this steric interaction term remains positive, that is, a small repulsive force exists between the NHCs and the transition metal fragments, while for the gold(I) complexes, this term is negative and therefore attractive. Despite ΔE_{elstat} and ΔE_{Pauli} increase and decrease with ligand donor strengths, respectively, a clear trend for ΔE^0 can be observed, and correlations to ligand donor strengths are good for both metals (R^2 = 0.8996 (NHC-$TiCl_4$) and 0.9362 (NHC-AuCl)). Electrostatic interaction outcompetes Pauli repulsion, and ΔE^0 becomes less repulsive for more strongly donating NHCs in the case of the titanium(IV) complexes, and more attractive for gold(I) complexes with increasing ligand donor strengths of the NHCs.

In contrast to the steric interaction term, which shows a range of 57 kJ/mol between the smallest and the largest value for both titanium(IV) and gold(I) NHC complexes, the orbital interaction term varies very little. The strongest orbital interaction with -302 kJ/mol in **57b-Au** is only 14 kJ/mol more exothermic than the weakest with -288 kJ/mol in **55d-Au**. For the titanium complexes, this difference is more pronounced, but with 41 kJ/mol lying between the orbital interactions of -240 kJ/mol in **58a-Ti** and -281 kJ/mol **55d-Ti**, the variations of ΔE^0 are still more important.

The behaviour of the orbital interaction term differs between the metal fragments. While for titanium(IV) complexes, stronger orbital interactions are found for more strongly donating NHCs (R^2 = 0.7737), this is not true for gold(I) complexes, in which the orbital interactions are wholly uncorrelated to ligand donor strengths. ΔE_{orb} includes both σ- and π- contributions to the orbital interaction, but only the former can be accurately described by first proton affinities. Therefore, further decomposition of the ΔE_{orb} term into ΔE_{σ} and ΔE_{π} contributions is required. The energy decomposition approach allows the separation of orbital interactions into individual contributions corresponding to the irreducible representations of the point group the molecule belongs to. Since C_S symmetry was imposed during geometry optimisation of the complexes, these are A' and A'',

which translate into orbital interactions which are symmetric with respect to the mirror plane, in which the NHC ring lies (σ-interactions), and interactions which are antisymmetric to it (π-interactions. However, this formalism does not provide information about the direction of electron density flow, nor is it able to distinguish σ-interactions from in-plane π-interactions, which might be minor contributions in certain cases. An estimation of the contributions of π-donation $\Delta E_{\pi(\mathrm{LM})}$ and π-backdonation $\Delta E_{\pi(\mathrm{ML})}$ to the ΔE_{π} term is possible by removing virtual orbitals from either fragements to restrict the flow of electron density to one direction exclusively, as described above.

Using this approach, for the titanium(IV) complexes, an average of 88% σ-contribution is found, and the remaining 12% of π-contribution to ΔE_{orb} can be further broken down into 75% of π-backbonding and 25 % of π-donation. Given that NHCs are considered to be almost exclusively σ-donors, the observation of π-donation can be puzzling, but it should be noted that it only accounts for 3% of the total orbital interaction energy term, and not more than 11 kJ/mol of the total interaction energy. Equally puzzling is the somewhat larger contribution due to π-backbonding, which should not occur at all because of the absence of filled d orbitals on titanium(IV). An explanation to this behaviour requires an even more detailed analysis of the bonding situation than what energy decomposition analysis can provide (*vide infra*).

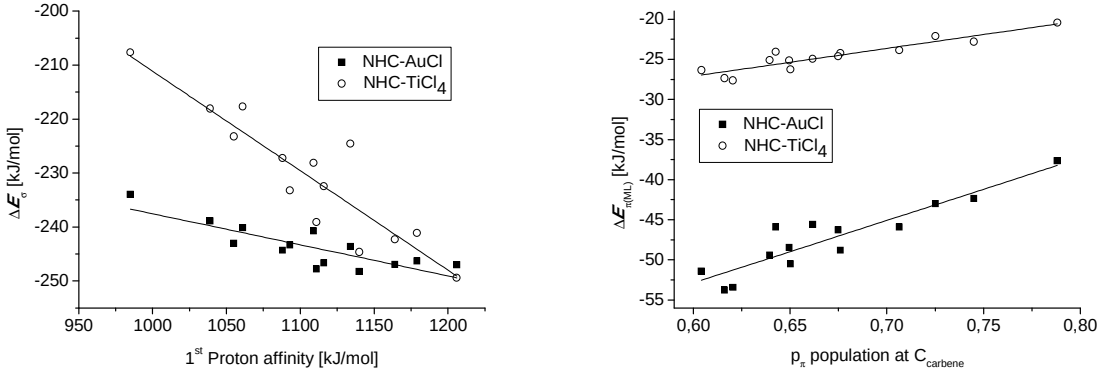

Fig. 2.19. Correlation of ΔE_{σ} and ΔE_{π} terms and NHC electronic parameters.

For the gold(I) complexes, σ-contributions to ΔE_{orb} drop to an average of 83% and π-contributions rise to 17%. As one would expect for a metal center with fully occupied d orbitals,

these π-interactions are almost exlusively due to π-backdonation. Interestingly, the changes in σ-donation and π-backdonation balance each other out for gold(I), explaining the absence of correlation between first proton affinities and ΔE_{orb}.

For both metals, the ΔE_{σ} values are correlated moderately well to first proton affinities and ligand donor strength (Fig.2.19, R^2 = 0.8156 (NHC-$TiCl_4$) and 0.6680 (NHC-AuCl)). The imperfections in these correlations are possibly caused by other contributions to the ΔE_{σ} term, in which the σ-HOMO orbital of the ligand is not directly involved, such as in-plane π-interactions or internal reorganizations of the electronic structure. The π-donation term $\Delta E_{\pi(LM)}$ is small for both metals, and seemingly uncorrelated to a single descriptor. This mirrors the problems in analyzing the π-basicities of NHC ligands discussed above. By contrast, the π-backdonation term $\Delta E_{\pi(LM)}$ is correlated to the p_{π} population at $C_{carbene}$ (R^2 = 0.8397 (NHC-$TiCl_4$) and 0.8349 (NHC-AuCl)), which provides a more accurate measure of the NHCs' π-accepting ability than error-prone metrics like ε(π-LUMO).

2.2.3 Extended Transition State – Natural Orbitals for Chemical Valence

The extended transition state – natural orbitals for chemical valence (ETS-NOCV) formalism allows a more detailed decomposition.[100] Within this framework, the orbital interactions between the NHCs and the transition metal fragment can be separated into individual contributions associated with the deformation density within the orbitals of each fragment, each of which is associated with an energy contribution towards ΔE_{orb}. Complementary NOCVs with identical absolute energy eigenvalues and opposing signs can be grouped together into NOCV pairs (NP) and used to describe charge-transfer channels between the molecular fragments. Their visualization allows to determine the direction of charge transfer upon fragment interaction, thus allowing to distinguish donating and back-donating processes. In some cases, the shape of NPs allows to identify the fragment orbitals involved in these interactions as well.

The ETS-NOCV analyses for all NHCs **55-58** were carried out using ADF2012.01.[97] The same molecular geometries as in the energy decomposition analysis were used, and their electronic structure was described using the BP86/TZ2P level of theory again.[79a,98,99] Similarly shaped NOCVs and NPs were obtained for all NHCs. While a considerable number of NPs is derived from the ETS-NOCV approach, only a small number makes relevant contributions towards ΔE_{orb}, and these are the ones which will be analyzed more in detail. Only contributions which contribute

more than 5 kJ/mol towards ΔE_{orb} in at least some of the NHCs were selected for closer study. For the titanium(IV) complexes, this criterion was met by six NOCV pairs, which accounted for an average of 92% of ΔE_{orb} (Fig. 2.20). The dark grey areas represent loss of electron density, light grey areas represent gain of electron density and the isosurface values are 0.004 for $NP_{\sigma\text{-d}}$ and $NP_{\pi\text{-bd}}$, and 0.001 for $NP_{\sigma\text{-bd}}$, $NP_{\pi//\text{-bd}}$, $NP_{\pi\text{-d}}$ and $NP_{\pi//\text{–TiCl4}}$.

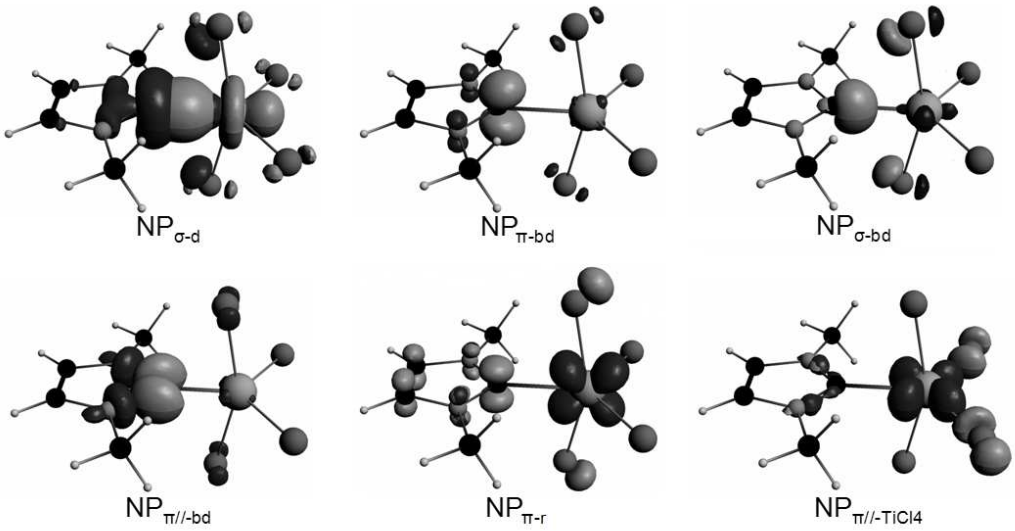

Fig. 2.20. Relevant NOCV pairs in **55a-Ti**.

As expected, the first NOCV pair for the titanium(IV) NHC complexes corresponds to the σ-donation from the carbene to the metal fragment ($NP_{\sigma\text{-d}}$). Electron density is depleted in the area corresponding to the lobe of ε(σ-HOMO) located at $C_{carbene}$, i.e. the carbene lone pair, and transferred predominantly into the d_{z^2} orbital of titanium, and to a lesser extend it is redistributed to nonbonding orbitals of the chlorido ligands. The second NOCV pair ($NP_{\pi\text{-bd}}$) is of π symmetry with respect to the NHC plane, and corresponds to a transfer of electron density from the p orbitals of the axial chlorido ligands into the p_π orbital at $C_{carbene}$. This observation explains the seemingly paradox observation of π-backbonding in a titanium(IV) complex, despite the absence of filled d orbitals at the metal. Instead of a real π-backdonation from the metal to the NHC, this interaction is a pseudo-backdonation involving the coligands. Despite the relative scarcity of NHC complexes of early transition metals in high oxidation states bearing coligands with

available lone pairs, such interactions have been observed experimentally, and examined superficially by means of DFT calculations.[101]

Four more, much weaker interactions were taken into account. These are an σ-backbondation ($NP_{\sigma\text{-bd}}$) involving a transfer of electron density from the d_{z^2} orbital of titanium back to the NHC ligand and into the p orbitals on the axial chlorido ligands involved in the π-backbonding interaction, an in-plane π-backdonation involving antibonding σ-orbitals of the NHC ring and a different set of p orbitals on the axial chlorido ligands ($NP_{\pi//\text{-bd}}$), a redistribution of electron densitiy involvig the metal center and the NHC ring system ($NP_{\pi\text{-r}}$), and finally an electronic reorganisation predominantly within the $TiCl_4$ fragment involving a transfer of electron density from the metal d orbital to p orbitals on the equatorial chlorido ligands ($NP_{\pi//\text{-TiCl4}}$). Of these interactions, $NP_{\sigma\text{-d}}$, $NP_{\sigma\text{-bd}}$, $NP_{\pi//\text{-bd}}$ and $NP_{\pi//\text{-TiCl4}}$ are of A' symmetry, thus contribution to ΔE_σ in the energy decomposition analysis. This explains the poor agreement between first proton affinities and ΔE_σ, since only the first two NOCV pairs are related to σ-HOMO of the NHCs. By contrast, $NP_{\pi\text{-bd}}$ and $NP_{\pi\text{-r}}$ are of A''symmetry and contribute to ΔE_π.

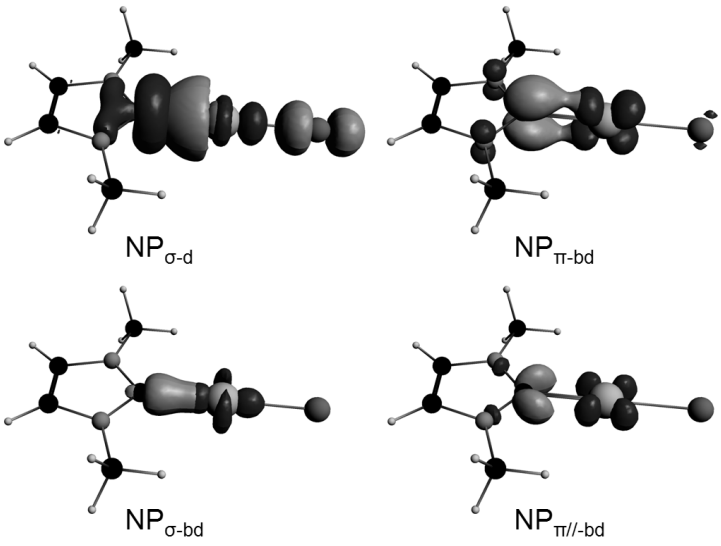

Fig. 2.21. Relevant NOCV pairs in **55a-Au**.

For the gold(I) complexes, four NOCV pairs were above 5 kJ/mol, and accounted for a total of 95% of ΔE_{orb} on average (Fig. 2.21). Again,the dark grey areas represent loss of electron density and light grey areas represent gain of electron density. All isosurface values are 0.004.

The NOCV pairs for gold(I) NHC complexes differ from those for titanium(IV) NHC complexes, especially since involvement of the coligand is not possible due to the distance to $C_{carbene}$, and reorganisations within the transition metal fragment does not occur. The NOCV pair with the highest energetic contribution can be attributed to a transfer of electron density from the σ-lone pair at $C_{carbene}$ into the σ* orbital of the Au-Cl bond ($NP_{\sigma\text{-}d}$). The electron densities in the area of the lone pair and in the space between chlorine and gold is depleted, and redistributed to the area between $C_{carbene}$ and gold, and into the p_z orbital of the chlorido ligand. This interaction should weaken the Au-Cl bond, and indeed, longer bond lengths are observed with stronger σ-donors due to the carbenes' *trans*-influence (cf. Fig. 2.16).

The second interaction is a π-backdonation from a d orbital on gold to the p_π orbital on $C_{carbene}$, which is accompanied by a minor reorganisation of the π-system within the NHC ring ($NP_{\pi\text{-}bd}$). The remaining two pairs correspond to a σ-backdonation ($NP_{\sigma\text{-}bd}$), with electron density being withdrawn from the d_{z^2} orbital of gold, and finally an in-plane p-backdonation from a metal d orbital into the σ* orbitals of the $C_{carbene}$-X (X = X or N) bonds ($NP_{\pi//\text{-}bd}$). In NHCs in which the carbene carbon is flanked by different substituents, the third and fourth NOCV pairs are superpositions of the $NP_{\sigma\text{-}bd}$ and $NP_{\pi//\text{-}bd}$ interactions. Again, multiple NOCV pairs are of A' symmetry and contribute to ΔE_σ in the energy decomposition analysis. Of these, the σ-HOMO of the NHC ligands is only involved in $NP_{\sigma\text{-}d}$ and $NP_{\sigma\text{-}bd}$, while $NP_{\pi//\text{-}bd}$ is independent of the NHCs' ligand donor strengths. The only NOCV pair for gold having A'' symmetry is $NP_{\pi\text{-}bd}$, which is correctly assigned to ΔE_π in the energy decomposition analysis.

In contrast to the titanium(IV) complexes, in which the electron density for $NP_{\pi\text{-}bd}$ and $NP_{\pi//\text{-}bd}$ stems from the chlorido coligands and only the very weak $NP_{\pi\text{-}r}$ and $NP_{\sigma\text{-}bd}$ interactions involve loss of electron-density in metal-centered orbitals, the corresponding $NP_{\pi\text{-}bd}$, $NP_{\sigma\text{-}bd}$, and $NP_{\pi//\text{-}bd}$ interactions in the gold(I) complexes involve only gold-centered orbitals.

For both metals, σ-donation as expressed by $NP_{\sigma\text{-}d}$ is the largest term. In the titanium(IV) NHC complexes, it accounts for an average of 74% of ΔE_{orb} (Table 2.9). In the gold(I) analogues, the

percentage drops, but remains by far the most important single contribution towards ΔE_{orb} with an average of 61% (Table 2.10).

Table 2.9. ETS-NOCV results for the orbital interactions between NHCs and $TiCl_4$.[a]

	ΔE_{orb}	$NP_{\sigma\text{-}d}$	$NP_{\pi\text{-}bd}$	$NP_{\sigma\text{-}bd}$	$NP_{\pi//\text{-}bd}$	$NP_{\pi\text{-}r}$	$NP_{\pi//\text{-}TiCl4}$	Sum	% of ΔE_{orb}
55a-Ti	-260.6	-191.1	-22.1	-8.7	-6.5	-4.6	-4.0	-237.0	90.9
55b-Ti	-277.7	-205.9	-22.0	-8.1	-8.9	-5.0	-5.5	-255.5	92.0
55c-Ti	-276.4	-206.0	-20.7	-6.3	-9.1	-6.8	-6.5	-255.3	92.4
55d-Ti	-281.6	-213.9	-19.1	-8.6	-9.7	-7.1	-6.06	-264.4	93.9
56b-Ti	-266.0	-195.7	-23.0	-9.0	-8.0	-4.2	-4.9	-244.8	92.0
56c-Ti	-260.3	-193.2	-21.4	-8.5	-6.7	-4.8	-5.4	-240.1	92.2
56d-Ti	-272.6	-206.6	-20.1	-9.5	-6.0	-5.3	-6.1	-253.5	93.0
57a-Ti	-249.4	-181.0	-22.5	-8.6	-6.3	-3.3	-4.5	-226.3	90.8
57b-Ti	-273.2	-200.2	-24.2	-9.9	-5.8	-3.8	-4.8	-248.7	91.0
57c-Ti	-265.4	-196.7	-21.6	-9.3	-6.1	-4.8	-4.3	-242.8	91.5
58a-Ti	-240.3	-172.7	-24.8	-8.7	-7.0	-2.6	-3.7	-219.5	91.3
58b-Ti	-257.0	-185.8	-25.0	-9.7	-6.2	-3.1	-4.1	-233.8	91.0
58c-Ti	-250.5	-183.7	-23.5	-8.8	-6.6	-3.5	-3.3	-229.3	91.6
58d-Ti	-256.0	-191.6	-22.1	-9.5	-5.9	-3.7	-3.4	-236.1	92.2

[a] Values calculated at the B3LYP/cc-PVDZ//BP86/TZ2P level, all values given in kJ/mol.

Independently of NHC donor strength, $NP_{\sigma\text{-}d}$ is always stronger in the titantium(IV) complexes than in the corresponding gold(I) analogues, and variations of the energy associated with this NOCV pair are twice as large for titanium than for gold (Fig. 2.22). The electron-poor d^0 titanium(IV) center has a higher ability to accommodate electron density than the electronically saturated d^{10} gold(I) center. The strong σ-donation component in the C-Ti bonds might also explain why the lengths of these bonds depends on ε(σ-HOMO), while no such dependence exists in the case of the C-Au bonds.

Other contributions with A' symmetry, that is, either σ- or in-plane π-symmetric contributions, are much smaller than $NP_{\sigma\text{-}d}$, and correspond to backdonation from the metal center to the NHC ligand, or to electronic reorganization within a fragment. In the case of titanium(IV), $NP_{\sigma\text{-}bd}$,

$NP_{\pi//\text{-bd}}$ and $NP_{\pi//\text{-TiCl4}}$ make up almost negligible 9% of ΔE_σ from the energy decomposition analysis. This is not surprising, given the electron-poor nature of this metal center. For the more electron-rich gold(I) center, $NP_{\sigma\text{-bd}}$ and $NP_{\pi//\text{-bd}}$ account for an average of 23% of ΔE_σ. This explains why the σ-part of the orbital interaction term is larger for the NHC-AuCl complexes than for their titanium(IV) counterparts, despite the higher $NP_{\sigma\text{-d}}$ values for the latter.

Table 2.10. ETS-NOCV results for the orbital interactions between NHCs and AuCl.[a]

	ΔE_{orb}	$NP_{\sigma\text{-d}}$	$NP_{\pi\text{-bd}}$	$NP_{\sigma\text{-bd}}$	$NP_{\pi//\text{-bd}}$	Sum	% of ΔE_{orb}
55a-Au	-293.4	-174.7	-43.5	-32.8	-22.8	-273.8	93.3
55b-Au	-297.6	-183.1	-43.7	-32.9	-20.8	-280.5	94.3
55c-Au	-293.1	-183.3	-40.3	-33.1	-21.0	-277.8	94.8
55d-Au	-288.4	-188.1	-35.9	-34.6	-16.8	-275.4	95.5
56b-Au	-295.0	-177.9	-46.3	-32.5	-22.4	-279.1	94.6
56c-Au	-289.8	-177.2	-43.8	-32.4	-22.0	-275.4	95.0
56d-Au	-292.6	-185.8	-40.9	-33.7	-19.3	-279.7	95.6
57a-Au	-291.3	-171.3	-47.5	-31.5	-24.7	-275.1	94.4
57b-Au	-302.3	-180.0	-49.2	-33.6	-22.6	-285.3	94.4
57c-Au	-296.1	-178.2	-44.1	-32.8	-24.0	-279.1	94.2
58a-Au	-290.1	-167.0	-51.6	-33.3	-24.0	-275.9	95.1
58b-Au	-299.7	-174.9	-51.5	-32.7	-24.8	-283.9	94.7
58c-Au	-293.4	-173.0	-48.5	-31.1	-25.8	-278.3	94.9
58d-Au	-295.1	-181.3	-46.7	-33.3	-21.5	-282.8	95.8

[a] Values calculated at the B3LYP/cc-PVDZ//BP86/TZ2P level, all values given in kJ/mol.

Separating $NP_{\sigma\text{-d}}$, which depends on the σ-donating abilities of the ligand, from the other orbital interaction terms with A' symmetry, which are unrelated to this property, should lead to an improved correlation to the first proton affinity. And indeed, while ΔE_{orb} was only weakly correlated to first proton affinities for titanium(IV) NHC complexes, and completely uncorrelated for gold(I) NHC complexes, and ΔE_σ showed only moderate correlation to this parameter, the correlation between $NP_{\sigma\text{-d}}$ and first proton affinities (and by extension, ε(σ-HOMO)) was excellent (cf. Fig. 2.22, R^2 = 0.9087 (NHC-$TiCl_4$) and 0.9626 (NHC-AuCl)).

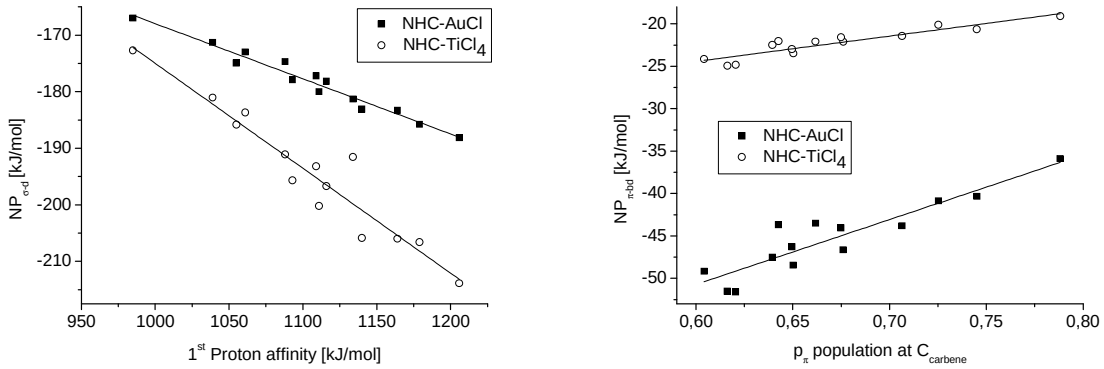

Fig. 2.22. Correlation of $NP_{\sigma\text{-d}}$ and $NP_{\pi\text{-bd}}$ and NHC electronic parameters.

Purely σ-donation accounts for roughly one third of the orbital interaction term in both the titanium(IV) and the gold(I) complexes. The exact percentage varies slightly with ligand donor strengths, and with ligands having lower-lying σ-HOMO orbitals, the fraction decreases slightly. Nevertheless, π-interactions should not be overlooked for NHCs.[69e,90,102]

Energy decomposition analysis places the percentage of π-interactions contributing to the orbital interaction term at an average of 12% for the titanium(IV) complexes, with a average breakdown of about three to one between π-backdonation and π-donation. With more π-basic carbenes such as **55d**, the percentage of the later can rise up to 35% of ΔE_π, however. This reinforces the notion that NHCs don't act as purely σ-donors, but that other interactions have to be taken into account to fully understand the bonding situation. Two NOCV pairs have π symmetry in the case of the titanium(IV) complexes: $NP_{\pi\text{-bd}}$ and $NP_{\pi\text{-r}}$. These correspond well to the $\Delta E_{\pi(\text{ML})}$ and $\Delta E_{\pi(\text{LM})}$ terms (R^2 = 0.9618 and 0.9790, respectively). However, it should be noted that the former interaction is largely due to the transfer of electron density from the axial chlorido coligands to p_π on $C_{carbene}$, while the latter involves a significant amount of electronic reorganization within the fragments, especially the NHC ring. Therefore, describing them as classical metal-to-ligand backdonation and ligand-to-metal π-donation would be oversimplifications.

For the gold(I) complexes, ΔE_π accounts for a larger percentage of the orbital interaction term. Since the $\Delta E_{\pi(\text{LM})}$ term is smaller with this already electron-rich d^{10} metal, and makes up less than one tenth of ΔE_π according to energy decomposition analysis, the bulk of this interaction can be

attributed to π-backdonation. Indeed, no NOCV pair corresponding to an A' symmetric π-donation was observed among the non-negligible NOCV pairs. $\Delta E_{\pi(ML)}$ is almost perfectly correlated to $NP_{\pi\text{-}bd}$ (R^2 = 0.9987), showing a good agreement between energy decomposition analysis and ETS-NOCV decomposition in this case. It should be noted that similarly to the case of the titanium(IV) complexes, a reorganization of the electronic structure within the NHC ring fragment accompanies the transfer of electron density from the transition metal fragment.

Both for titanium(IV) and gold(I) NHC complexes, $NP_{\pi\text{-}bd}$ corresponded nicely to the population at $C_{carbene}$, which was already found to be a useful descriptor for $\Delta E_{\pi(ML)}$ (R^2 = 0.8410 (NHC-$TiCl_4$) and 0.8226 (NHC-AuCl)). The fact that no such correlation between π-donation and electronic parameters for the NHCs can be found becomes easier to understand in the light of the ETS-NOCV results. For gold(I), π-donation plays only a negligible role in the orbital interaction, and for titanium(IV), it is complicated by a substantial amount of internal electronic reorganization within the fragments, which makes a description by a single electronic parameter very difficult.

3. Palladium(II) Complexes bearing Pyrazole-derived Ligands

3.1. Donor Strengths and Nucleophilicity of Differently Substituted Pyrazoles

In contrast to the ubiquitous imidazolin-2-ylidene complexes, NHCs with reduced heteroatom stabilization are less well studied, and the majority of research in this area focused on imidazolin-4-ylidenes.[36] However, their isomers, pyrazolin-3-ylidenes are equally strong donors, and pyrazolin-4-ylidenes,[42,81] which are remote NHCs, are even more strongly donating.[2b,37b]

Reports of the coordination chemistry of pyrazolin-4-ylidenes are rare, and focused often exclusively on palladium complexes.[42] However, pyrazolin-4-ylidenes incorporating exocyclic donor substituents have sparked a vigorous debate about the nature of their electronic structure, and adequate ways to describe them.[42d, 103] To date, only symmetrically 3,5-disubstituted pyrazolin-4-ylidenes have been described, bearing either two alkyl or aryl substituents (**I**),[81] or two exocyclic π-donor substituents (**K**).[104] To obtain a fuller picture of the electronic structure of these compounds, it would be desirable to study pyrazolin-4-ylidenes with an unsymmetric 3,5-disubstitution pattern, combining alkyl and aryl substituents of different sizes and electronic properties (**L**), or alkyl and aryl substituents in one position, and nitrogen- or oxygen-based π-donor substitutents in the other position (**M**, Fig. 3.1).

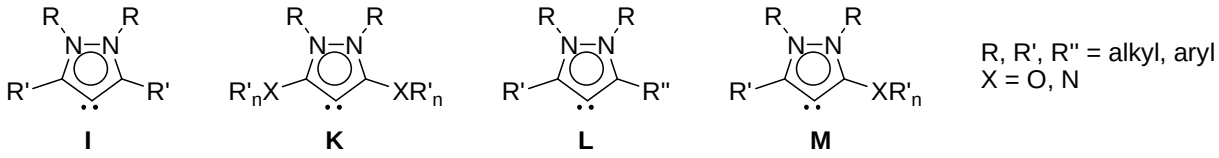

Fig. 3.1. Types of reported pyrazolin-4-ylidenes and potentially interesting new subclasses.

Based on previous work, the most promising approach to these compounds is the synthesis of pyrazoles with the desired substitution patterns and a halogen substituent in 4-position, followed by quarternization of the second nitrogen atom to yield pyrazolium salts, and finally oxidative addition to a suitable palladium(0) precursor.[42a,b] This avoids the preparation and handling of very basic and highly water sensitive free carbenes.

3.1.1. Synthesis of Substituted Pyrazoles and Attempted Synthesis of Pyrazolium Salts

Pyrazoles are commonly found in pharmaceutically active substances, and used as ligands in coordination chemistry. Thus it is hardly surprising that several procedures for the construction of this heterocycle have been developed since the discovery of the Knorr pyrazole synthesis.[105] However, the synthesis of donor-substituted pyrazoles by condensation of β-ketoesters and β-ketoamides with phenylhydrazone, which works well for 1,3-diketones (*vide infra*), yielded only minor amounts of the desired ether-functionalized pyrazole **60**, and no amine-functionalized product **63** could be isolated at all. Along with unidentified side products, considerable amounts of 1-phenyl-3-methyl-1*H*-pyrazol-5-one (**61**) were isolated in each case as well (Scheme 3.1).

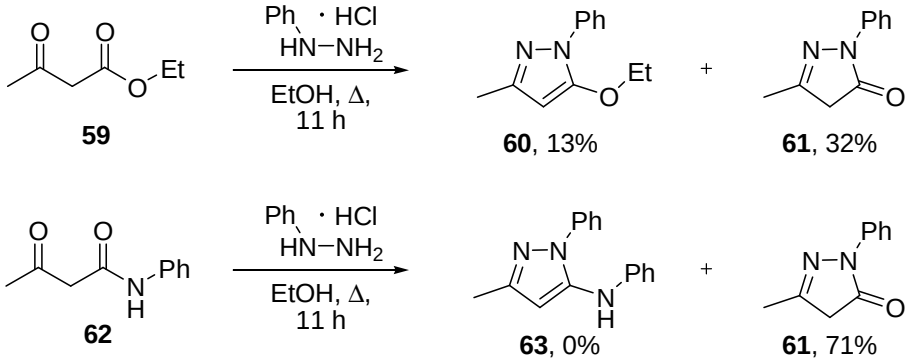

Scheme 3.1. Attempted condensations of β-ketoesters and β-ketoamides with phenylhydrazine·HCl.

Despite literature reports of successful condensation reactions of this type,[106] the reason for this failure lies in the mechanism of the reaction. When starting from 1,3-diketones, the intermediate is a hemiaminal, which eliminates water to form the pyrazole. However, when starting from β-ketoesters or β-ketoamides, an alcohol or amine can be eliminated instead, both of which are better leaving groups. The resulting hydroxypyrazole then tautomerizes to the observed pyrazolone. This side reaction is suppressed when instead of the β-ketoesters or β-ketoamides the corresponding β-ketothionoesters or β-ketothioamides are used as starting materials. Because the preparation and isolation of these compounds would add an additional step to the synthesis, it is preferable to prepare them *in situ*, directly prior to cyclization. This can be achieved by Lawesson's reagent, using a procedure described by Dodd and Martinez for β-ketoamides.[107]

However, this methodology failed to give the desired product, yielding intractable mixtures of predominantly oligomeric materials instead. Attempts to extend the approach to β-ketoesters yielded similar results.

Since the construction of the heterocycle by condensation reactions was fraught with difficulties, functional group interconversion starting from the commercially available 1-phenyl-3-methyl-pyrazolin-5-one (**61**), which was also obtained as byproduct in the previous attempts, provided an alternative synthetic strategy (Scheme 3.2).·

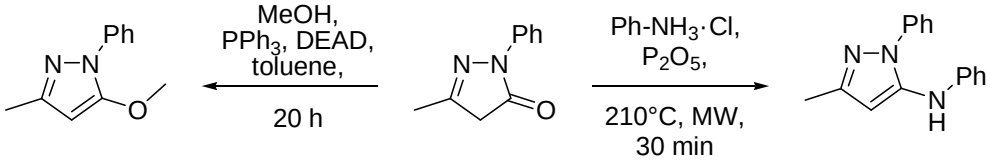

Scheme 3.2. Successful syntheses of ester- and amine-functionalized pyrazoles.

Under Mitsunobu conditions, the pyrazolone **61** could be converted into the 5-methoxy-substituted pyrazole **64** via the enol ether tautomer in moderate yields.[108] Since this reaction is not limited to methanol as substrate, other ether side chains can potentially be introduced by this route as well. The introduction of an amine can be achieved by heating a mixture of pyrazolone, anilinium chloride and phosphorous pentoxide as dehydrating agent to 200 °C and above.[109] However, this transformation requires long reaction times at very high temperatures. To improve the procedure, advantage was taken of the know acceleration effects associated with microwave heating. This allowed the isolation of **63** in acceptable yields after only 30 min reaction time.

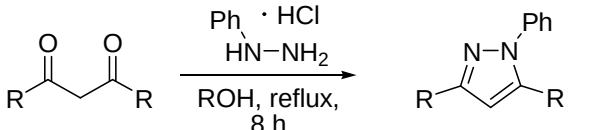

Scheme 3.3. Pyrazole syntheses starting from 1,3-diketones.

Pyrazoles with symmetric 3,5-dialkyl- and diaryl substitution patterns are easier to obtain.[42d,110] The condensation of commercially available 1,3-diketones **65**-**67** gives such compounds in good to excellent yields. When required, they could be purified either by recrystallization in the case of 3,5-diaryl pyrazole **68**, or by distillation in the case of the 3,5-dialkyl pyrazole **69**.

To set the scene for oxidative additions, a halogen substituent in 4-position is required. Selective iodination in 4-position can be achieved by treating the pyrazoles with elemental iodine, but harsh reaction conditions and reaction times of multiple days are required to achieve complete halogenation of the starting materials, or the addition of an external oxidant.[111] A milder, faster and more convenient method has been developed by Pereira *et al.*, who discovered that the by ultrasound irradiation, N-halosuccinimides react with pyrazoles at ambient temperature.[112] This procedure allows the introduction of chlorine, bromine and iodine substituents in 4-position without the need to handle highly reactive, elemental halogens, and gave the desired compounds in excellent yields (Scheme 3.4). The notable exception was the reaction between 1-phenyl-3,5-dimethyl-1*H*-pyrazole. Instead of the selective chlorination in 4-position on the pyrazole ring, a mixture of products arising from chlorination of the methyl side chains was observed. This is in contrast with the findings of Pereira, but the reason for this divergent behavior could not be elucidated.

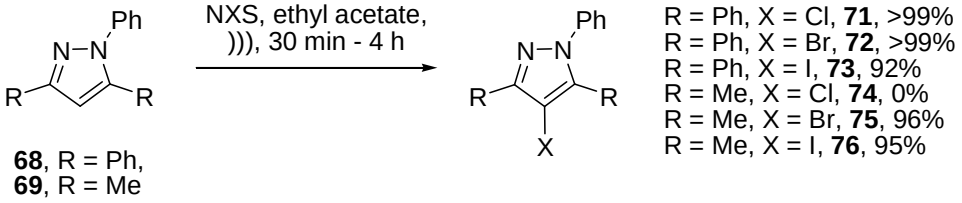

Scheme. 3.4. Selective halogenation of pyrazoles in 4-position using N-halosuccinimides.

The transformation of pyrazoles into the pyrazolium salts required for complex synthesis can be achieved by quarternization of nitrogen by reaction with a strong nucleophile. For the 4-halidopyrazoles **75** and **76**, this transformation has been achieved by heating them to reflux in neat ethyl iodide for several days, but the yields were moderate to low.[42b] Attempting to use this method for the alkylation of the 1,3,5-triphenylpyrazoles **72** and **73** were unsuccessful, although the reaction with trimethyloxonium tetrafluoroborate showed that these compounds can be alkylated by strong electrophiles (Scheme 3.5). Oxonium salts are considerably more

electrophilic than iodoalkanes and capable of alkylating even weak nucleophiles, while iodoalkanes should be able to distinguish between stronger and weaker nucleophiles. The low yields reported for the alkylation of **75** and **76** with ethyl iodide might indicate that their respective nucleophilicities are close to the threshold required to react with this electrophile, while the additional electron-withdrawing substituents on the pyrazole core in **72** and **73** reduce their nucleophilicities even further, rendering them effectively unreactive.

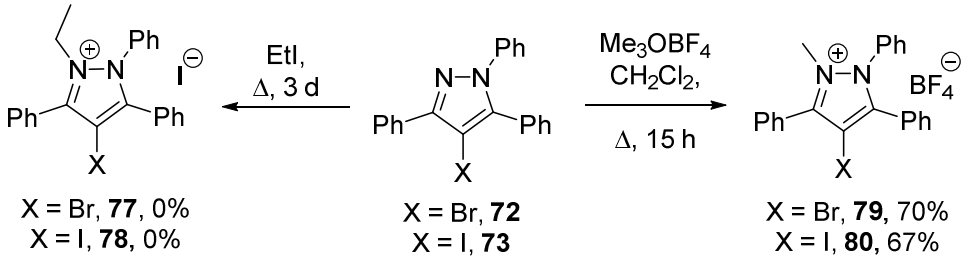

Scheme 3.5. Reaction of **72** and **73** with electrophiles of differing reactivity.

The question arises whether it is possible to establish a semi-quantitative relationship between the electron density at the nucleophilic nitrogen and their reactivity towards electrophiles with different alkylating strengths.[113]

3.1.2. Donor Strength Determinations by ^{13}C NMR Spectroscopy

As described in chapter 1, the ^{13}C NMR chemical shift of $C_{carbene}$ in complexes of the type *trans*-[$PdBr_2$(^{i}Pr_2-bimy)L] is highly sensitive to the ligand donor strength of the transoid ligand L.[48,114] The sharp signals typical for ^{13}C NMR spectroscopy allow exceptionally precise measurements. Stronger donors, which have a higher electron density at the donor site and which are stronger nucleophiles, decrease the Lewis acidity of the metal center. This induces a downfield shift of the $C_{carbene}$ resonance in the ^{13}C NMR spectrum. By consequence, less nucleophilic pyrazoles should lead to more upfield chemical shifts, while better nucleophiles should lead to more downfield shifts.

The synthesis of probe complexes is straightforward. It can be achieved by reacting suitable donor ligands with the dimeric species [$PdBr_2$(^{i}Pr_2-bimy)]$_2$ (**30**) in dichloromethane at ambient temperature (cf. Scheme 1.8). Similar to other neutral N-donor species, pyrazoles react cleanly

and rapidly with dimer **30**, giving excellent yields of the probe complexes after short reaction times of only 30 min (Scheme 3.6 and Table 3.1)

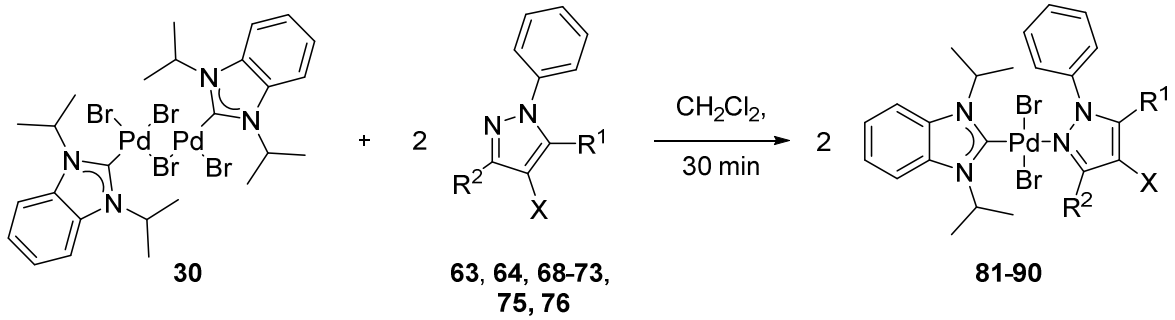

30 **63**, **64**, **68-73**, **75, 76** **81-90**

Scheme 3.6. Preparation of probe complexes **81**-**90** for ligand donor strength determination.

Table 3.1. Yields of pyrazole complexes **81**-**90** and ^{13}C NMR chemical shift of $C_{carbene}$.

Entry	R^1	R^2	X	Product	Yield	δ $C_{Carbene}$ (ppm)[a]
1	NHPh	Me	H	**81**	>99%	162.8
2	OMe	Me	H	**82**	>99%	162.6
3	Ph	Ph	H	**83**	95%	161.6
4	Me	Me	H	**84**	87%	163.0
5	iPr	iPr	H	**85**	>99%	163.1
6	Ph	Ph	Cl	**86**	>99%	160.9
7	Ph	Ph	Br	**87**	>99%	160.8
8	Ph	Ph	I	**88**	98%	160.9
9	Me	Me	Br	**89**	97%	161.8
10	Me	Me	I	**90**	>99%	161.8

[a] in $CDCl_3$, relative to the solvent signal at 77.7 ppm.

The crude complexes **81**-**90** were obtained as pale yellow to orange solids, which were analytically clean without the need for any additional purification steps. The complexes are readily soluble in chlorinated solvents, polar aprotic solvents such as acetonitrile, but insoluble in ethereal solvents, alkanes, and very polar protic solvents. This allowed to obtain single crystals suitable for X-ray diffraction studies for a selection of complexes by slow diffusion of diethyl ether into saturated chloroform solutions. These include complex **82**, in which the pyrazole bears

a π-donor functionality, and the complexes **84**, **89**·$CHCl_3$ and **90**·$CHCl_3$, which bear 3,5-dimethyl substituted pyrazoles with 4-H, 4-Br and 4-I substituents, respectively (Fig. 3.2, Fig. 3.3, and Table 3.2).

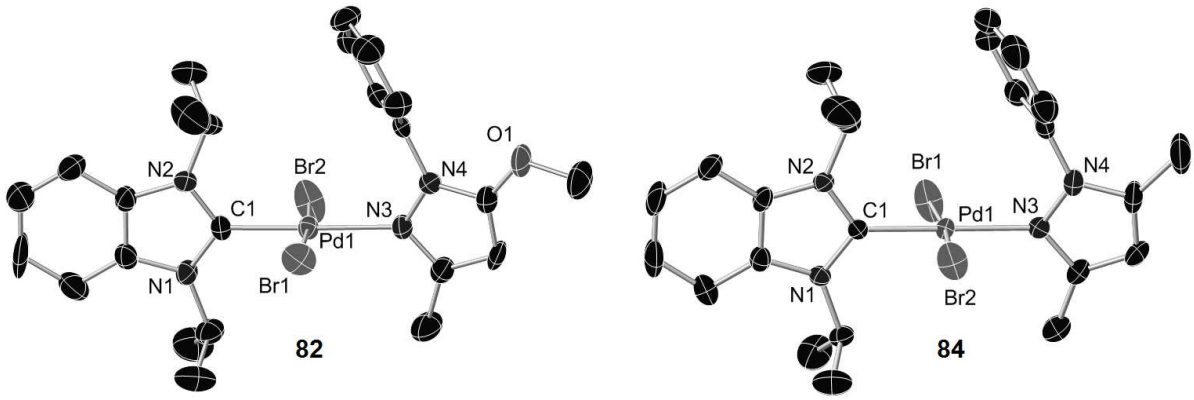

Fig. 3.2. Molecular structures of **82** and **84** (hydrogen atoms have been omitted for clarity, thermal ellipsoids are drawn at 50% probability).

In all molecular structures, palladium adopts a distorted square-planar coordination geometry. In all cases, the pyrazole is coordinated *trans* to the $^{i}Pr_2$-bimy ligand. This *trans*-coordination is common for nitrogen-donors and favored electronically,[48] but this arrangement also avoids steric crowding. The planes defined by the pyrazole core and the NHC ligand are aligned almost parallel, with dihedral angles not exceeding 14°. The methyl groups of the isopropyl substituents point away from the metal center, and the phenyl substituent on N4 is twisted out of the pyrazole ring plane by 50 – 64°, to minimize steric repulsion between these moieties.

The Pd-C and Pd-N bond lengths show little variation and fall between 1.943(5) Å for the Pd-C and 2.090(4) Å for the Pd-N bond in **84**, and 1.953(6) Å for the Pd-C bond and 2.108(5) for the Pd-N bond in **82**. These values are comparable to those reported previously for related complexes with pyridine, imidazole, and methylimidazole in trans-position to the $^{i}Pr_2$-bimy ligand.[48,115]

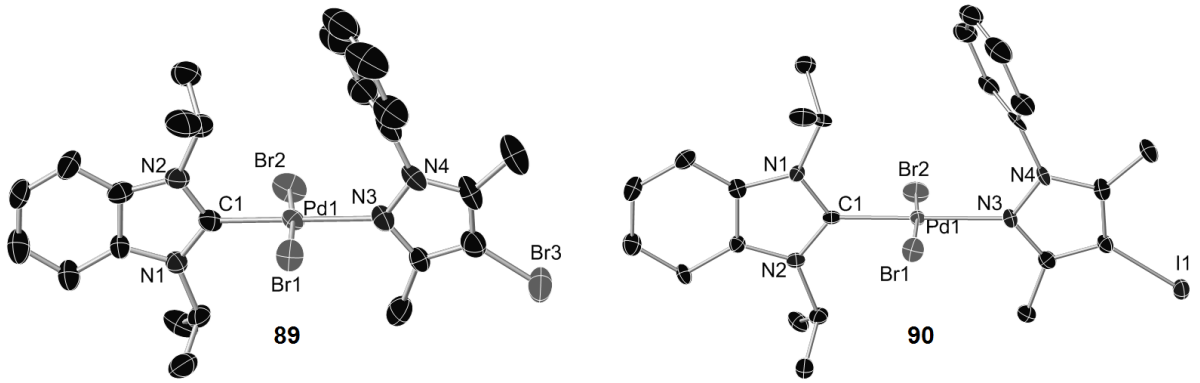

Fig. 3.3. Molecular structures of **89**·$CHCl_3$ and **90**·$CHCl_3$ (hydrogen atoms and solvent molecules have been omitted for clarity, thermal ellipsoids are drawn at 50% probability).

Table 3.2. Selected bond lengths [Å] and angles [deg] in **82**, **84**, **89**·$CHCl_3$, and **84**·$CHCl_3$.

	82	**84**	**89**·$CHCl_3$	**90**·$CHCl_3$
Pd(1)-C(1)	1.953(6)	1.943(5)	1.950(8)	1.947(5)
Pd(1)-Br(1)	2.4346(10)	2.4277(7)	2.4159(12)	2.4066(8)
Pd(1)-Br(2)	2.4251(10)	2.4266(7)	2.4164(12)	2.4063(8)
Pd(1)-N(3)	2.108(5)	2.090(4)	2.107(6)	2.097(4)
C(1)-Pd(1)-Br(1)	87.79(19)	87.97(14)	88.4(2)	88.21(15)
C(1)-Pd(1)-Br(2)	87.76(19)	87.33(14)	87.6(2)	88.52(16)
Br(1)-Pd(1)-N(3)	91.36(17)	92.95(13)	90.97(17)	91.35(12)
Br(2)-Pd(1)-N(3)	93.13(17)	91.76(13)	93.09(17)	91.94(13)
C(1)-Pd(1)-N(3)	178.5(3)	178.93(19)	179.3(3)	179.5(2)
Br(1)-Pd(1)-Br(2)	174.94(4)	174.75(3)	175.40(4)	175.25(3)

In the ^{1}H NMR spectra of complexes **81**-**90**, the chemical shifts of the resonances attributable to the ^{i}Pr$_2$-bimy ligand differ pronouncedly from those in **30**. Steric crowding around the metal center restricts rotation around the C-Pd and N-Pd bonds, generating magnetically inequivalent environments for the isopropyl wingtip substituents in the bimy ligand. Consequently, two sets of signals are observed. Both of these resonances are shifted upfield when compared to the starting material. In **30**, the methine protons resonate at 6.54 ppm, while the corresponding two sets of resonances in **81**-**90** are found between 5.07 ppm and 6.26 ppm. In all complexes, one of the methine protons is significantly more upfield than the other, due to a shielding effect exerted by

the N-phenyl moiety in the pyrazole ligands. Such shielding effects of phenyl groups in transoid ligands on the wingtip substituents of NHC ligands have been documented before.[116] The methyl moieties of the isopropyl wingtips are further removed from the phenyl ring in the pyrazole, thus upfield shifts are smaller in their case. Minor changes were observed for the resonances of the protons on the pyrazole core as well. For the pyrazoles **68**-**70**, the drop in electron density caused by coordination to the metal center caused a minor downfield shift of the proton in 4-position. By contrast, in **81** and **82**, the resonance of the same proton was shifted upfield when compared to the uncoordinated pyrazoles **63** and **64**. In these pyrazoles bearing π-donor substituents, the coordination might have cause a stronger mesomeric effect, increasing the ring electron density and improving the shielding of the proton in 4-position.

In the ^{13}C NMR spectra, chemical shifts of $C_{carbene}$ are of primary interest. For complexes **81**-**90**, $C_{carbene}$ of the $^{i}Pr_2$-bimy ligand resonates in a relatively narrow range from 160.8 ppm **87** to 163.1 ppm in **85**. The difference between the most strongly and the most weakly donating pyrazole ligand translates to a difference in chemical shift of only 2.3 ppm.

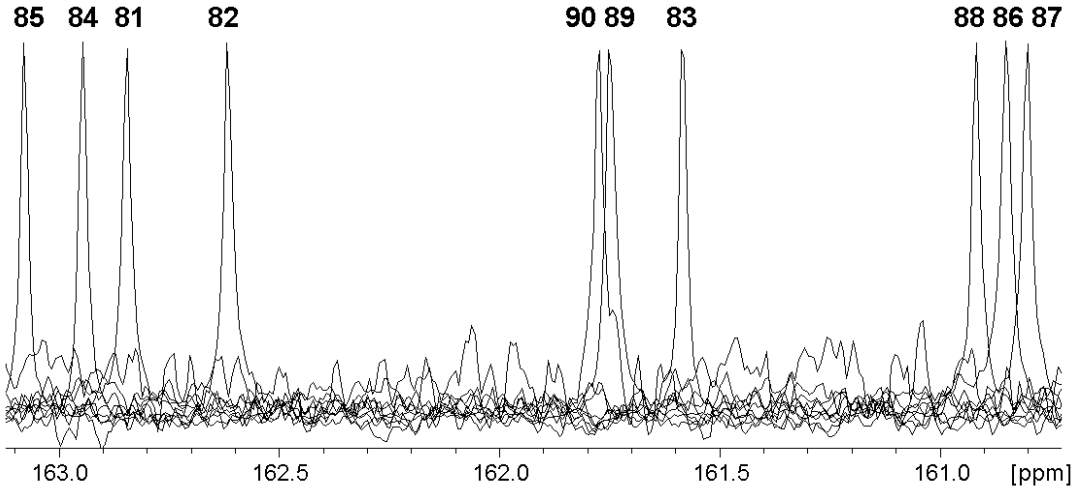

Fig. 3.4. ^{13}C NMR resonances of $C_{carbene}$ in complexes **81**-**90**.

Additionally, a closer inspection of the chemical shifts of all complexes reveals that **89** and **90** both have identical chemical shifts of 161.8 ppm for $C_{carbene}$, when given to the first decimal place. However, due to the sharpness of ^{13}C peaks, it is nevertheless possible to distinguish all complexes umambiguously (Fig. 3.4).

The $C_{carbene}$ resonances in **81**-**90** fall in the same range observed for comparable aromatic nitrogen donor ligands. In the [$PdBr_2$(^{i}Pr_2-bimy)(pyridine)] complex, $C_{carbene}$ resonates at 160.0 ppm, because pyridine is a weaker donor than pyrazoles. By contrast, imidazole is a stronger donor than pyrazoles, and gives rise to a $C_{carbene}$ resonance in [$PdBr_2$(^{i}Pr_2-bimy)(imidazole)] at 161.4 ppm.[48]

The observed chemical shifts, and by consequence the electron densities at N2, follow chemical intuition. When considering the pyrazoles without halogen substituents in 4-position, the pyrazoles in order of increasing donor strength are **68** < **64** < **63** < **69** < **70**. The most strongly donating ligand, **70**, bears two isopropyl substituents, which have a strong positive inductive effect. The two methyl groups in **69**, which is a weaker donor, provide less electron density to the pyrazole core than the isopropyl groups in **70**. In **63** and **64**, the negative inductive effects of the electronegative heteroatom substituents are compensated by their positive mesomeric effects. However, the donor strength of **64**, which contains the more electronegative oxygen, is a weaker donor than the amine-substituted pyrazole **63**. The weakest donor in this series is **68**, due to the electron-withdrawing nature of three phenyl substituents.

For the two series bearing different substituents in 4-position, the same trends can be observed. In the 3,5-dimethyl substituted series, the order of increasing donor strengths is **75** < **76** < **69**. Bromine is more electronegative than iodine, which in turn is considerably more electronegative than hydrogen. Consequently, the bromo-substituted pyrazole **75** is a weaker donor than the iodo-substituted pyrazole **76**, and this one is a weaker donor than the unsubstituted pyrazole **69**. The fact that the difference in inductive effect exerted by the substituent in 4-position on the pyrazole ring – five chemical bonds removed from $C_{carbene}$ – can still be picked up by the ^{13}C NMR method illustrates the precision of this method.

The series bearing phenyl-substituents shows generally more upfield $C_{carbene}$ chemical shifts in their complexes, but it also follows the donor strength pattern Br (**72**) < I (**73**) < H (**68**). However, there is an anomaly within this series. The chloro-substituted pyrazole **71** leads to a $C_{carbene}$ resonance at 160.9 ppm in **86**, while this resonance in **87** is more upfield at 160.8 ppm, despite the less electronegative bromo-substituent in the pyrazole ligand **72** in this complex. Based on electronegativity arguments alone, **72** should be the stronger donor, not **71**. This neglects positive mesomeric effects of the lone pairs on the substituents, however. Chlorine is smaller than bromine, allowing its lone pairs to overlap more efficiently with the orbitals on the

pyrazole core, thus enhancing the mesomeric effect. This can overcompensate the difference in inductive effects between chloro- and bromo-substituents, similarly to the observations for the ether- and amine-substituted pyrazoles **63** and **64**. Taking this effect into consideration, a good agreement is found between the experimentally determined values, and predictions based on mesomeric and inductive effects of the substituents.

3.1.3. Estimation of Nucleophilicities by Alkylation Experiments

In order to rank the pyrazoles according to their relative nucleophilicities, they were tested for their reactivity with three electrophiles of increasing alkylating strength. Ethyl bromide is only a weak alkylating agent because of the poor leaving group. A stronger electrophile is ethyl iodide, since the more polarizable iodine can act as a better leaving group. The strongest alkylating agent tested was trimethyloxonium tetrafluoroborate. This compound, often referred to as Meerwein's salt, is an exceptionally strong electrophile, and it can be expected to react with all pyrazoles independently of their electron density at nitrogen.

Based on prior experiments, alkylations with ethyl halides were carried out by heating the pyrazoles to reflux in a large excess of alkylating agent, which also acted as the solvent, for 3 days shielded from light to prevent photodecomposition reactions. The lower boiling point of ethyl bromide means that besides being a weaker alkylating agent, the reactions also had to be carried out at lower temperatures when compared to ethyl iodide. Alkylations with trimethyloxonium tetrafluoroborate were carried out in refluxing, anhydrous dichloromethane under an inert atmosphere, with reaction times of 15 h. (cf. Scheme 3.5).

As a consequence of the high reactivity typical for Meerwein's salt, almost all pyrazoles were alkylated by trimethyloxonium tetrafluoroborate (Table 3.3). The notable exception was the amine-substituted pyrazole **63**, which yielded only a black oil of intractable decomposition products upon alkylation. A likely cause for this deviant behavior is the presence of the secondary amine functionality, which can be alkylated to both the tertiary amine and the quaternary ammonium salt, which then might undergo further decomposition steps. The yields for the other alkylation reactions fluctuated unsystematically and without apparent correlation to the ligand donor strengths. The steric shielding exerted by the substituent in 3-position differs between pyrazoles, which introduces another factor influencing the yields. More importantly, however, were difficulties associated with the workups. The alkylation reactions yielded crude,

oily mixtures, from which the pure product had to be isolated by repeated washing or precipitation steps. Slightly different properties of the pyrazolium salts made these workups unpredictable, and losses during workup cannot be estimated reliably. Therefore, differences in yields can not and should not be attributed solely to differences in donor strength of the nucleophile.

Table 3.3. Reactivities of pyrazoles with various electrophiles.

Entry	Pyrazole	Electrophile		
		EtBr	EtI	Me_3OBF_4
1	**72**	0%	0%	70%
2	**71**	0%	0%	37%
3	**73**	0%	0%	67%
4	**68**	0%	0%	55%
5	**89**	0%	24%[b]	51%
6	**90**	0%	50%[a]	80%
7	**64**	0%	Decomposition[c]	62%
8	**63**	0%	58%	Decomposition[d]
9	**69**	7%[b]	99%	77%
10	**70**	Trace[b]	75%	74%

[a] literature value[117]. [b] obtained as a mixture of product and starting material; yield determined by ^{1}H NMR spectroscopy. [c] methoxy moiety was replaced by ethoxy moiety, no alkylation product obtained. [d] intractable mixture of oily material.

The same confounding factors that obscure any putative relationship between yields of alkylation products and the ^{13}C NMR parameter were at play in the case of the alkylation with ethyl iodide. Albeit the more electron-rich pyrazoles gave higher yields, a linear relationship could not be established. For example, the alkylation of **69** proceeded in near-quantitative yield, while the more electron-rich pyrazole **70** was only alkylated in 70% yield. For the four most electron-poor pyrazoles **68** and **71**-**73**, no alkylation products could be obtained, despite the large excess of alkylating agent, the harsh reaction conditions, and the prolonged reaction times. This

demonstrates unambiguously that there exists a threshold for the alkylation with ethyl iodide. Pyrazole **89** is slightly more nucleophilic, resulting in a yield of alkylated product of 24% under these conditions. Interestingly, the methoxy-substituted pyrazole **64** did not undergo clean alkylation, but instead the methoxy group was cleaved and replaced by an ethoxy group. This reaction was potentially driven by the formation of the more volatile methyl iodide as side product.

With ethyl bromide, the weakest electrophile out of the three, no alkylation products were found for the majority of the pyrazoles. The only exceptions were the alkyl substituted pyrazoles **69** and **70**, which were converted to the pyrazolium salts in trace amounts, but yields were less than 10% even after reaction times of 3 days, and most of the starting material remained unchanged. Interestingly, for these two pyrazoles, the trends in yield were similar to the ones for the alkylation using ethyl iodide, with higher yields in the case of the less electron-rich, but sterically more accessible dimethyl substituted pyrazole **69** then with the more shielded diisopropyl pyrazole **70**. This reinforces the notion that the steric bulk of the substituents, especially the one in 3-position, has a clear impact on the reactivity.

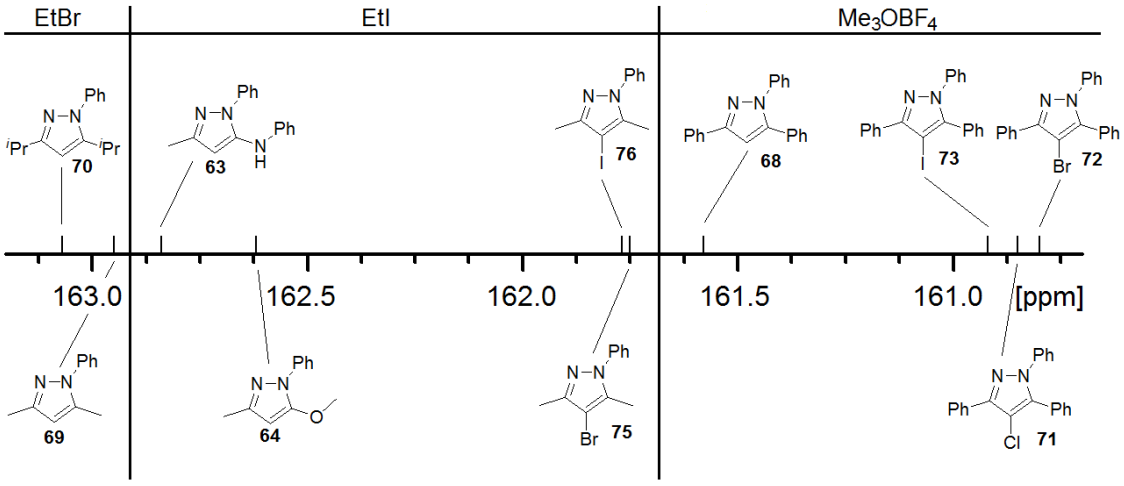

Fig. 3.5. The electronic parameters of pyrazoles and their reactivity towards electrophiles.

According to their reactivities with different electrophiles, the pyrazoles can be divided into three distinct groups (Fig. 3.5). The two compounds **69** and **70** with electronic parameters, i.e. $C_{carbene}$ resonances in *trans*-[$PdBr_2$($^iPr_2$-bimy)(pyrazole)], downfield of 162.9 ppm, show reactivity

towards even weak electrophiles such as ethyl bromide, and are readily alkylated by more reactive reagents. Pyrazoles with electronic parameters below this threshold, but above 161.7 ppm, are not reactive towards ethyl bromide anymore, but still undergo alkylation with ethyl iodide and trimethyloxonium tetrafluoroborate. The four 1,3,5-triphenylpyrazoles **83** and **86**-**88**, which have electronic parameters upfield of 161.6 ppm, are the weakest nucleophiles and can only be alkylated by Meerwein's salt.

The agreement between chemical shift and reactivity is consistent throughout. This suggests that the ^{13}C NMR parameter can be used to gauge the electron density at N2 of pyrazoles – and by extension of the argument, presumably other aromatic N-donor ligands as well – and predict their reactivity in alkylation reactions.

3.2. Pyrazolin-5-ylidene Complexes of Palladium(II)

A small number of pyrazolin-3-ylidene (or pyrazolin-5-ylidenes, in which the N-substituent with higher priority is adjacent to $C_{carbene,}$ pyry) complexes have been reported,[40,118] usually with late transition metals, although chromium complexes have been reported as well.[119] However, the structural diversity of these complexes is limited, and their preparation relies either on the use of not readily available metal alkoxides as basic metal precursors, oxidative additions to low-valent metal complexes, or metal-templated NHC syntheses on chromium followed by transmetallation steps. The silver carbene transfer reaction, a convenient method for the preparation of NHC complexes, has been less expored for pyry ligands, and only one report exists in the literature. [40d]

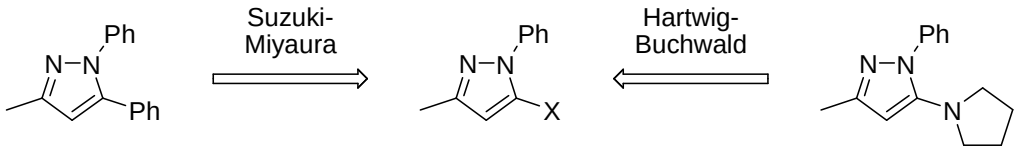

104 **N** **105**

Scheme 3.7. Retrosynthetic approach to unsummetrically substituted pyrazoles.

While exploring the possibility of preparing pyrazoles with an unsymmetric 3,5-disubstitution pattern by means of Suzuki-Miyaura or Hartwig-Buchwald cross-coupling reactions to introduce aryl or cyclic tertiary amine substituents in 5-position (Scheme 3.7), the potential applications of

the required pyrazole coupling partners as precursor materials for the preparation of pyrazolin-5-ylidenes by oxidative addition to palladium(0) precursors was realized.[120]

3.2.1. Ligand Precursor Synthesis

Similar to the syntheses of donor-functionalized pyrazoles **63** and **64**, the introduction of functionalities which can undergo oxidative addition reactions to low-valent metal precursors (e.g. halogens, triflates, mesylates, tosylates) can be achieved by exploiting the enol-tautomer of 1-phenyl-3-methyl-1*H*-pyrazol-5-one (**61**). The introduction of halogens can be achieved by reaction with phosphorus trihalides, or the more toxic phosphorus oxyhalides.[121] To shorten the long reaction times required to obtain 5-chloropyrazole **104**, the reaction was carried out using microwave heating, and indeed, after two hours, the desired product was formed together with red phosphorus (Scheme 3.8).

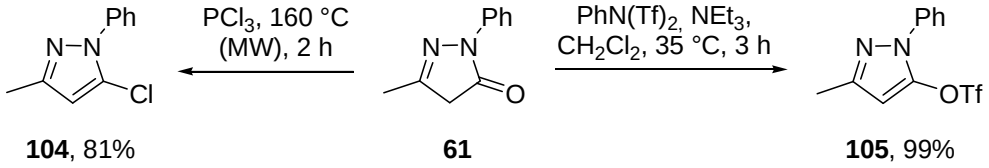

104, 81% **61** **105**, 99%

Scheme 3.8. Introduction of reactive functionalities into pyrazol-5-one **61**.

The 5-trifluoromethanesulfonylpyrazole **105** could be obtained using a slightly modified reported procedure.[122] The reaction of **61** with N-Phenylbis(trifluoromethanesulfoneimide) in the presence of triethylamine yielded **105** in quantitative yield.

Given the electron-poor nature of **104** and **105**, a strong alkylating agent is required to convert them into the pyrazolium salts.[113] Therefore, trimethyloxonium tetrafluoroborate was the reagent of choice. In line with previous observations, the reactivity of these two compounds was low, despite the relatively low steric bulk of the methyl substitutent in 3-position, and only moderate yields were obtained (Scheme 3.9). By contrast, the considerably more electron-rich pyrazole **106** yielded pyrazolium salt **109** in quantitative yield. The latter salt cannot undergo oxidative additions, but the acidic proton in 5-position allows the generation of carbenes by (*in situ*) deprotonation. An alternative route to pyrazolin-5-ylidene complexes can thus be explored and compared to the oxidative addition protocol.

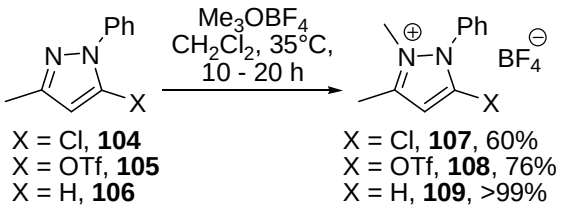

Scheme 3.9. Alkylation of pyrazoles **104**-**105**.

The pyrazolium salts **107**-**109** were obtained as colorless solids after precipitation and washing with diethyl ether. When exposed to the atmosphere, they were found to be slightly hygroscopic. All three compounds are readily soluble in chlorinated solvents, as well as alcohols, acetonitrile and DMSO, but their solubility in ethereal solvents and hydrocarbons are low.

3.2.2. Synthesis of a Cationic Palladium(II) Complex by Oxidative Addition

During the synthesis of six-membered ring rNHC complexes of group 10 metals, Raubenheimer *at al.* noticed that in certain cases, the oxidative addition of chloroquinolinium and chloropyridinium salts did not yield the expected complexes, but instead lead to decomposition to palladium black. In these cases, the oxidative addition to chloroquinolines or chloropyridines furnished complexes bearing a chlorido and an aryl ligand, which was subsequently alkylated to give an NHC.[43d] Both approaches, i.e. the oxidative addition of **104** and **105** to [Pd(PPh$_3$)$_4$] followed by methylation and the direct oxidative addition of **107** and **108**, were explored.

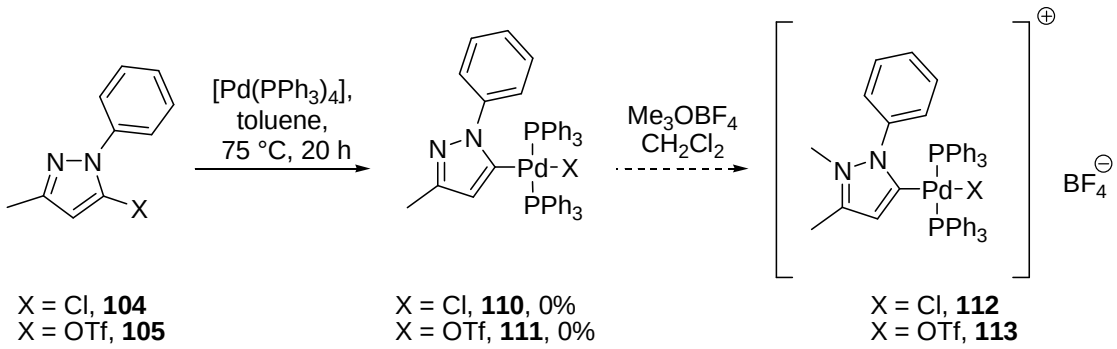

Scheme 3.10. Attempted oxidative addition of pyrazoles **104** and **105** to [Pd(PPh$_3$)$_4$].

The attempts at oxidative additions of neutral pyrazoles **104** and **105** to tetrakis-(triphenylphosphine)palladium(0) were not successful. In the case of 5-chloropyrazole **104**, the

rapid formation of palladium black was observed, and no identifiable material could be isolated from the reaction mixture. With **105**, the formation of palladium black was less pronounced, and a white solid could be isolated. Spectroscopic and ESI-MS data were inconsistent with the desired pyrazolyl complex **111**. However, the ^{1}H NMR spectrum showed peaks corresponding to 21 aromatic protons as well as a singlet corresponding to three protons in the region typical for the methyl substituents in 3-position on the pyrazole ring. A single peak in the ^{19}F spectrum at -2.10 ppm indicated the presence of a triflate anion, and a singlet at 9.88 ppm in the ^{31}P NMR confirmed the presence of at least one phosphorus atom, although the chemical shift of the latter signal ruled out a metal-bound phosphine ligand. Instead, it is more consistent with phosphonium salt **114** (Fig. 3.6).[123] The cationic unit of this salt was indeed observed as the only peak in ESI-MS at 419 *m*/*z*, thus confirming the formation of this species in 54% yield.

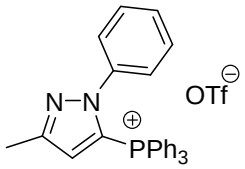

114

Fig. 3.6. Side product in the oxidative addition of **105** to [Pd(PPh_3)$_4$].

Due to apparent instability of pyrazolyl complexes **110** and **111**, the step-wise approach was not pursued any longer, and attention focused on the oxidative addition on the pyrazolium salts **107** and **108** instead (Scheme 3.11). The 5-chloropyrazolium salt **107** failed to react, and only intractable mixtures of decomposition product were obtained. By contrast, reaction of **108** gave a material with spectroscopic properties consistent with the desired NHC complex. However, ESI-MS spectroscopy showed a cationic peak with the distinct isotopic pattern of a palladium complex at 837 *m*/*z*. In this coordination unit, a chlorido coligand is bound to the palladium(II) center besides the pyrazolin-5-ylidene and two triphenylphosphine ligands, despite the absence of chlorine in the starting material. Since dichloromethane was used for this reaction, the solvent is the most probable source of this additional ligand. The weakly coordination triflate anion, which can still be observed in the ^{19}F spectra of the final product as counteranion besides tetrafluoroborate, is unable to displace the chlorido ligands.

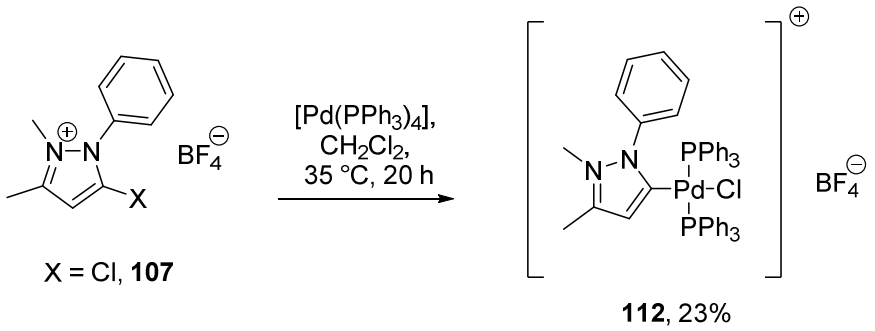

Scheme 3.11. Oxidative addition of pyrazolium salt **107** to $[Pd(PPh_3)_4]$.

Since the initial yield of **112** was a disappointingly low 23%, TBACl was added to the reaction mixture as an external chlorine source, in the hope that this would be more efficient at providing stabilizing chlorido ligands than the traces of hydrochloric acid naturally present in dichloromethane. Indeed, **112** could be isolated in 52% yield using a slightly modified protocol (Scheme 3.12).

The complex was obtained as a microcrystalline, off-white solid. Its solubility in chlorinated solvents and polar aprotic organic solvents was good, and it was insoluble in ethereal solvents and hydrocarbons. In the 1H NMR spectrum, pronounced changes in the chemical shifts of the methyl groups on the pyrazole ring were observed, when compared to the starting material. The resonance of the nitrogen-bound methyl group shifted upfield, from 3.77 ppm in **108** to 3.35 ppm in **112**. The changes for the methyl group in 3-position were even more pronounced, with a change from 2.67 ppm in the starting material to 2.05 ppm in the product. Remarkably, no significant changes in the chemical shift of H-4 were observed, despite being directly adjacent to $C_{carbene}$ in the product.

In the ^{13}C NMR spectrum, the $C_{carbene}$ resonance was observed at 165.6 ppm. For a structurally related pyrazolin-3-ylidene complex of palladium(II), Herrmann *et al.* reported a chemical shift of 161.1 ppm, which falls into the same range as the value found for **112**.[40a] The ^{31}P spectrum showed a single resonance at 22.9 ppm. This shift is virtually identical to the 22.7 ppm reported for Herrmann's compound, and a clear indication for the *trans*-arrangement of the phosphine ligands. In the ^{19}F spectrum, the typical signals for both the tetrafluoroborate and the triflate anions were observed, and elemental analysis confirmed the presence of these two anions. Two-thirds of the counteranions in **112** are BF_4^-, and the remainder consists of OTf^-.

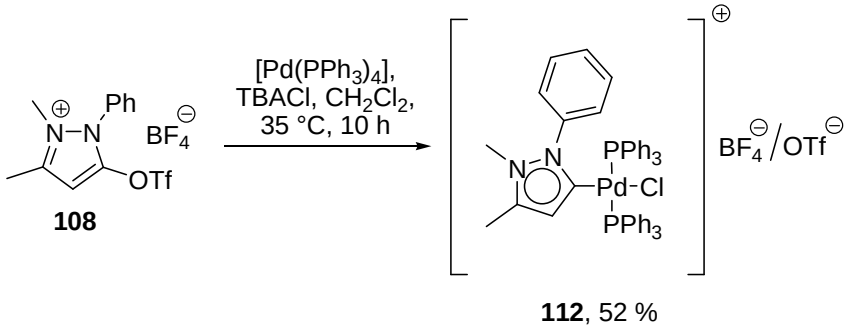

Scheme 3.12. Improved synthesis of the cationic pyrazolin-5-ylidene complex **112**.

Single crystals suitable for X-ray diffraction analysis were obtained by slow evaporation of a concentrated dichloromethane/hexane solution of **112**. The molecular structure of the cationic coordination unit confirmed the *trans*-arrangement of the phosphine ligands, based on NMR spectroscopy (Fig. 3.7).

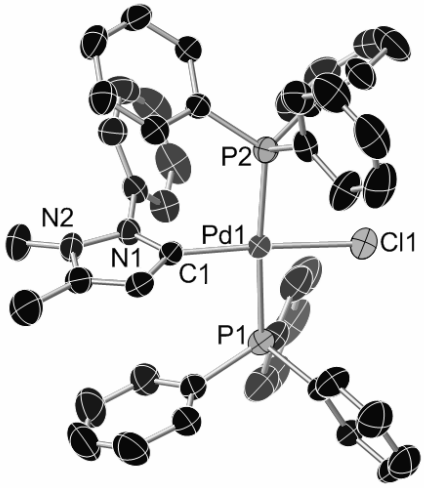

Fig. 3.7. Molecular structure of the cationic coordination unit in **112** (hydrogen atoms and counteranions have been omitted for clarity, thermal ellipsoids are drawn at 50% probability). Selected bond lengths [Å] and angles [°]: Pd1-C1 1.987(3), Pd1-P1 2.333(1), Pd1-P2 2.33(1), Pd1-Cl1 2.346(1); C1-Pd1-P1 90.2(1), C1-Pd1-P2 94.8(1), P1-Pd1-Cl1 86.80(4), P2-Pd1-Cl1 88.23(4), C1-Pd1-Cl(1) 176.9(1), P1-Pd1-P2 174.97(4).

The square-planar coordination geometry of palladium is slightly distorted, with C1-Pd1-P1/2 angles exceeding 90°. Due to their steric bulk, especially of triphenylphosphine, these ligands

bend away from each other. The Pd-C bond is 1.987(3) Å long, the Pd-Cl bond measures 2.346(1) Å, and the Pd-P bonds are on average 2.33 Å long. These values are similar to those reported for related compounds.[40a]

3.2.3. Synthesis of Neutral Palladium(II) Complexes by Silver Carbene Transfer

While oxidative addition of **108** to palladium(0) gave a pyrazolin-5-ylidene complex in moderate yield, this approach is limited by the need for additional donor ligands in order to prevent decomposition of the metal source under the reaction conditions. A more versatile and milder approach would be the silver carbene transfer method.[63a] The acidity of H-5 pyrazolium salt **109** was high enough to react with silver oxide, if TBAB as an external bromide source to facilitate the formation of silver(I) complex **115**, was added to the reaction mixture (Scheme 3.13). This silver(I) complex was found to be photo- and thermolabile, and its low stability foiled every attempt at isolation an characterization. The only evidence for its formation was indirect, by observation of the $[Ag(NHC)_2]^+$ cation at 451 *m*/*z*, which results from ligand redistribution processes commonly observed in silver(I) NHC complexes.

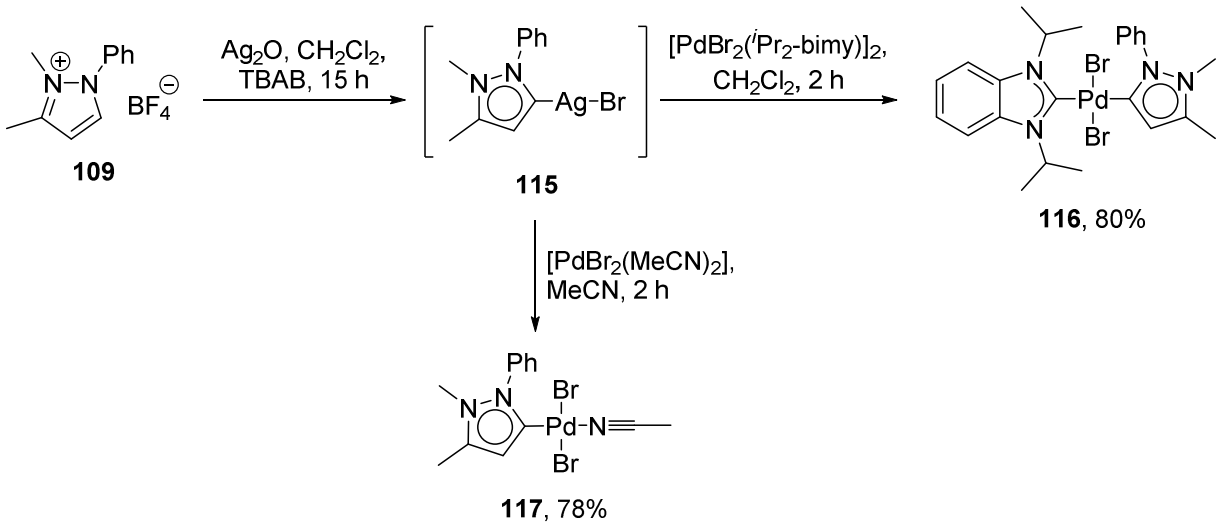

Scheme 3.13. Synthesis of a silver(I) pyry complex and transmetallation to palladium(II).

Despite hampering the isolation of **115**, the exceptional lability of the Ag-C bond in in silver(I) NHC complexes enabled the transmetallation to palladium(II), a reaction which gains additional driving force from the precipitation of insoluble silver(I) bromide. In the reaction of **115** with

dimeric $[PdBr_2(^iPr_2\text{-bimy})]_2$ (**30**),[29] the μ-bromido bridges in the latter were cleaved and a hetero-bis(NHC) palladium(II) complex **116** was obtained in good yield. As described above, the chemical shift of $C_{carbene}$ in the bimy ligand provides a measure for ligand donor strength of the transoid ligand, allowing the characterization of the electron-donating properties of the pyry ligand.[48] Equally efficient was the transmetallation to $[PdBr_2(acetonitrile)_2]$, which was freshly prepared prior to the reaction by dissolving palladium(II) bromide in hot acetonitrile. With a stochiometric ration of **115** to palladium(II) of 1:1, complex **117** was isolated in good yield. Stochiometric ratios of 2:1 did not lead to the expected formation of the corresponding homo-bis(NHC) palladium(II) complex, but gave rise to highly insoluble, off-white materials, which resisted attempts at structure elucidation.

While both complexes were obtained as yellow solids, their solubilities are vastly different. Both complexes are insoluble in hydrocarbons and ethereal solvents. The hetero-bis(NHC) complex **116** is very soluble in aprotic polar organic solvents and chlorinated solvents, while the acetonitrile adduct **117** could only be dissolved in coordinating solvents. In the latter, the acetonitrile ligand is weakly bound, and if it dissociates off, highly insoluble aggregates are formed.

The formation of complexes **116** and **117** is unambiguously confirmed by the absence of the doublet at 7.91 ppm in their spectra, which can be attributed to H-5 in the ^{1}H NMR spectrum of **109**. The ^{1}H NMR chemical shift of the neighbouring proton H-4 is shifted upfield by 0.2-0.3 ppm upon complexation, and due to the loss of a coupling partner, shows a singlet instead of the doublet found in the spectrum of the starting material. Similar to the changes observed in spectral characteristics upon the oxidative addition which yielded **112**, the resonances due to the methyl groups of the pyry ligand also experience slight upfield shifts.

The ^{13}C NMR spectrum of **116** showed two $C_{carbene}$ resonances, one at 182.8 ppm and one at 175.4 ppm. By comparison to structurally related complexes, the former can be assigned to the $^iPr_2$-bimy ligand, while the later is the carbene carbon resonance in the pyrazolin-5-ylidene ligand.[48] Based on the $C_{carbene}$ chemical shift of the $^iPr_2$-bimy ligand in **116**, the donor strength of the pyrazolin-5-ylidene ligand can be estimated. In line with the results from theoretical chemistry presented in chapter 2, this pyrazole-derived NHC gives rise to an exceptionally far downfield $C_{carbene}$ resonance, placing it among the strongest donors analyzed by the ^{13}C NMR method so far due to its reduced heteroatom stabilization.

For **117**, the $C_{carbene}$ signal in its ^{13}C NMR spectrum is observed at 150.0 ppm. Compared to the chemical shift of 175.4 ppm found for the carbene carbon in the pyry ligand in **116**, this considerably more upfield resonance reflects the poor electron-donating capabilities of the acetonitrile ligand, and the weakness of the Pd-N bond in this complex.

This weak metal-ligand bond made complex **117** a versatile intermediate for the synthesis of other pyrazolin-5-ylidene compexes, since the acetonitrile ligand can be readily replaced by a wide variety of other ligands (Scheme 3.14).

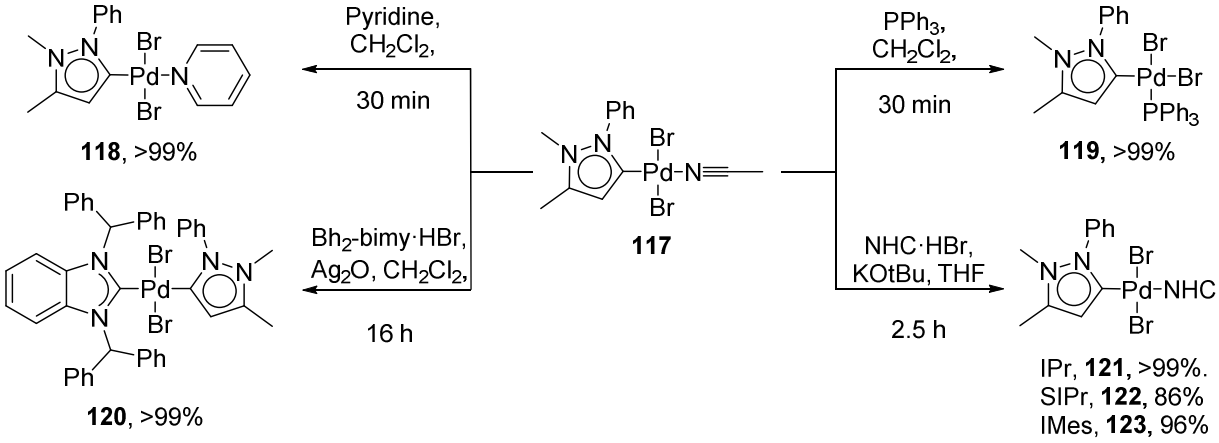

Scheme 3.14. Structural diversity by ligand substitution reactions starting from complex **115**.

The addition of pyridine or triphenylphosphine to a suspension of **117** in dichloromethane lead to the rapid formation of the pyridine complex **118** or the triphenylphosphine complex **119**, respectively. The reaction could be monitored by observing the colour change from orange-yellow to pale yellow, and the disappearance of undissolved material. Both *trans*-[$PdBr_2$(pyridine)(pyry)] and *cis*-[$PdBr_2(PPh_3)$(pyry)] were obtained after short reaction times of only 30 min at ambient temperature in quantitative yields.

The introduction of the sterically demanding 1,3-dibenzhydrylbenzimidazolin-2-ylidene (Bh_2-bimy) ligand was possible via a second silver carbene transfer step. A solution of the silver(I) Bh_2-bimy was prepared freshly by reaction of the benzimidazolium salt with silver(I) oxide,[124] followed by a rapid transmetallation to **117**, which was completed within one hour. The hetero-bis(NHC) complex **120** was obtained quantitatively.

Similar silver carbene transfer reactions failed for imidazolin-2-ylidenes and imidazolidin-2-ylidenes. The reaction between freshly prepared silver(I) NHC complexes incorporating 1,3-

diisopropylphenylimidazolin-2-ylidene (IPr), 1,3-dimesitylimidazolin-2-ylidene (IMes) as well as their unsaturated congeners 1,3-diisopropylphenylimidazolindin-2-ylidene (SIPr) and 1,3-dimesitylimidazolidin-2-ylidene (SIMes) failed to give the desired hetero-bis(NHC) complexes by transmetallation to the metal center in **117**. No precipitation of silver(I) bromide was observed, and the known silver(I) complexes of these four NHCs could be isolated from the reaction mixture.[125] Even forcing reaction conditions, such as heating a mixture of **117** and the respective silver(I) NHC complexes for a prolonged period to reflux in acetonitrile did not lead to the desired results. It seems that the relatively high stability of these silver(I) NHC complexes prevents the transmetallation reaction from occurring.

However, imidazolin-2-ylidenes are not prone to dimerization as free carbenes, and the steric bulk of the wingtip substituents in the imidazolidin-2-ylidene ligands of interest also prevents dimerization. Therefore, solutions of free NHCs could be generated *in sit*u by deprotonation of the respective azolium salts by potassium *tert*-butoxide in anhydrous THF. Addition of **117** to these solutions yielded complexes **121**-**123**. For the two imidazolin-2-ylidene ligands IPr and IMes, near-quantitative yields were obtained (**121** and **123**), while the unsaturated carbene SIPr, only 86% of the hetero-bis(NHC) complex **122** could be isolated. For SIMes, only complex mixtures were obtained under identical reaction conditions. This might reflect the lower electronic and steric stabilization of this free carbene. Complexes **120**-**123**, along with **116**, are the first examples of hetero-bis(NHC) complexes incorporating a pyrazolin-5-ylidene ligand.

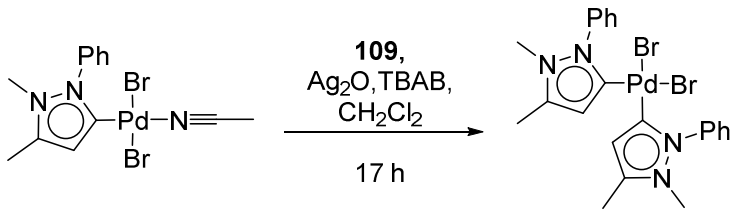

117 **124**, 93%

Scheme 3.15. Preparation of bis(pyry) palladium(II) complex **122**.

Starting from complex **117**, the homo-bis(NHC) complex **124** could be prepared as well by means of a second silver transfer reaction involving pyrazolium salt **109** (Scheme 3.15). This complex had proven to be elusive, when the introduction of both pyry ligands was attempted by a

single-step reaction using two equivalents of silver(I) NHC complex **115** and [$PdBr_2$(acetonitrile)$_2$].

Complexes **119**-**124** were all isolated as yellow solids, with solubilities comparable to the hetero-bis(NHC) complex **116**. The notable exceptions were **119** and **124**, which showed reduced solubilities in most solvents when compared to the other complexes, with the exception of DMSO. These complexes were found to adopt a *cis*-geometry (*vide infra*), in contrast to the *trans*-geometry prevailing for the other complexes. The higher dipole moment associated with *cis*-geometries renders them less soluble in relatively non-polar solvents such as dichloromethane, which readily dissolves *trans*-hetero-bis(NHC) complexes of palladium(II).

In the ^{1}H NMR spectra of **118**-**120** and **124**, the signals attributable to the pyry ligand are very similar to the ones observed in **116**, and chemicals shifts differ by less than 0.1 ppm. The incorporation of the relatively bulky IPr, SIPr and IMes ligands changes this, however. In the spectra of complexes **121**-**123**, the protons in the pyrazolin-5-ylidene ligand resonate at 0.2 – 0.3 ppm more upfield chemical shifts due to the shielding effect of the aryl wingtip groups in the additional NHC ligand. Additionally, signal broadening occurs due to steric congestion., which effects the isopropyl and methyl moieties on the aryl wingtip substituents of the imidazolin-2-ylidene and imidazolidin-2-ylidene ligands.

The changes in the ^{13}C NMR spectra were highly systematic (Table 3.4). The replacement of the weakly donating NHC ligand by stronger donors consistently lead to a downfield shift of the $C_{carbene}$ resonance in the pyry ligand. The underlying mechanism is identical to the one at work in the *trans*-[$PdBr_2$(^{i}Pr$_2$-bimy)(L)] used for the determination of ligand donor strengths.[39e,48,51,115]

The $C_{carbene}$ chemical shift of 150.0 ppm in **117** changes to a more downfield resonance of 154.1 ppm in complex **118**, which includes the more strongly donating pyridine ligand. The five hetero-bis(NHC) palladium(II) complexes show $C_{carbene}$ resonances attributable to the pyry ligand in the range from 172.6 ppm to 175.4 ppm. Despite this relatively narrow range of 2.8 ppm, the NHC ligands in *trans*-position to pyry can be unambiguously distinguished from each other, and ranked according to their respective ligand donor strengths. Increasingly more downfield $C_{carbene}$ resonances are found for stronger donors, starting from the weakest donor IMes, followed by IPr, SIPr, Bh$_2$-bimy, and finally the strongest donor ^{i}Pr$_2$-bimy.

Complexes **119** and **124** differ from their counterparts mentioned before in their coordination geometry, and due to their low solubilities in chloroform, the NMR spectra for these compounds

were recorded in different solvents. Despite these systematic errors, the pyry $C_{carbene}$ resonances in these complexes still fit within the general trend. The triphenylphosphine complex **119** has a $C_{carbene}$ resonance at 166.5 ppm, and triphenylphosphine is a stronger donor than pyridine, but weaker than NHCs. For complex **124**, the $C_{carbene}$ resonance is found at 181.8 ppm, which reflects the highly electron-rich nature of the pyrazolin-5-ylidene ligand.

Table 3.4. $C_{carbene}$ chemical shifts [ppm] in complexes **112** and **116**-**124**.[a]

Complex	Pyry	NHC
112	165.6	-
116	175.4	182.8 ($^{i}Pr_2$-bimy)
117	150.0	-
118	153.0[b]	-
119	166.5	-
120	174.3	189.7 (Bh_2-bimy)
121	173.2	179.4 (IPr)
122	173.4	207.6 (SIPr)
123	172.6	176.6 (IMes)
124	181.8[c]	-

[a] recorded in CDCl3. [b] recorded in CD_2Cl_2. [c] recorded in DMSO-d_6.

The $C_{carbene}$ resonances of the other NHC ligand in complexes **116** and **120**-**123** differ considerably depending on their respective backbones. The imidazolin-2-ylidene $C_{carbene}$ resonances in **121** and **123** are found at 179.4 ppm and 176.6 ppm, respectively, the imidazolidin-2-ylidene in complex **122** shows a chemical shift of 207.6 ppm for $C_{carbene}$, and the $C_{carbene}$ chemical shifts for the benzimidazolin-2-ylidene are 182.8 ppm in **116** and 189.7 ppm in **120**.

Single crystals suitable for X-ray diffraction analysis of complexes **116**, **117**, **121**, **122**, and **124** were obtained by slow evaporation of concentrated dichloromethane/hexane or dichloromethane/actonitrile solutions, while the slow diffusion of diethyl ether into concentrated dichloromethane solutions yielded single crystals of complexes **118** and **119**.

With the exception of the mixed NHC-triphenylphosphine complex **119** and the homo-bis(NHC) complex **124**, all complexes adopted a *trans*-arrangement. In mixed NHC-phosphine complexes,

it is usually observed that the phosphine ligand avoids the position *trans* to the carbene, an observation termed transphobia and rooted in the electronic structure of these complexes.[42d,126] In the case of **124**, the *trans*-influence of the strongly donating NHCs, combined with the low steric bulk of the ligands, also favors the *cis*-arrangement (*vide infra*).

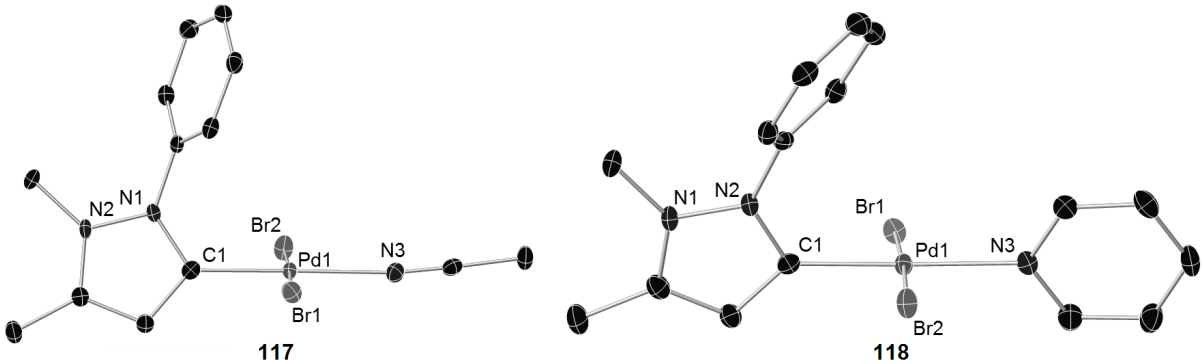

Fig. 3.8. Molecular structures of the solvent adducts **117** and **118**·CH_2Cl_2 (hydrogen atoms and solvent molecules have been omitted for clarity, thermal ellipsoids are drawn at 50% probability).

Table 3.5. Selected bond lengths [Å] and angles [deg] in **117** and **118**·CH_2Cl_2.

	117	**118**·CH_2Cl_2
Pd1-C1	1.950(2)	1.962(2)
Pd1-N3	2.083(3)	2.104(4)
Pd1-Br1	2.4289(3)	2.4376(4)
Pd1-Br2	2.4279(3)	2.4294(4)
C1-Pd1-Br1	89.08(7)	89.12(6)
C1-Pd1-Br2	88.88(7)	88.65(6)
Br1-Pd1-N3	92.18(6)	92.39(5)
Br2-Pd1-N3	89.86(6)	89.91(5)
C1-Pd1-N3	178.50(9)	177.88(8)
Br1-Pd1-Br2	177.80(1)	176.83(1)

For the solvent adducts, which incorporate the sterically unassuming nitrogen donors acetonitrile and pyridine, only marginally distorted square-planar coordination geometries were found (Fig. 3.8). In each case, the nitrogen donor is located in the position *trans* to the pyrazolin-5-ylidene

ligand. The palladium(II) center is less electron-rich than in the cationic bis(triphenylphosphine) complex **112**, and the higher Lewis acidity of the metal translates into shorter Pd-C bond lengths of 1.950(2) Å in **117** and 1.962(2) Å in **118**. In the latter complex, a dihedral angle of 6.5(2)° is found between the planes defined by the pyrazolin-5-ylidene and the pyridine ring systems. Selected bond distances and angles for **117** and **118** are given in table 3.5.

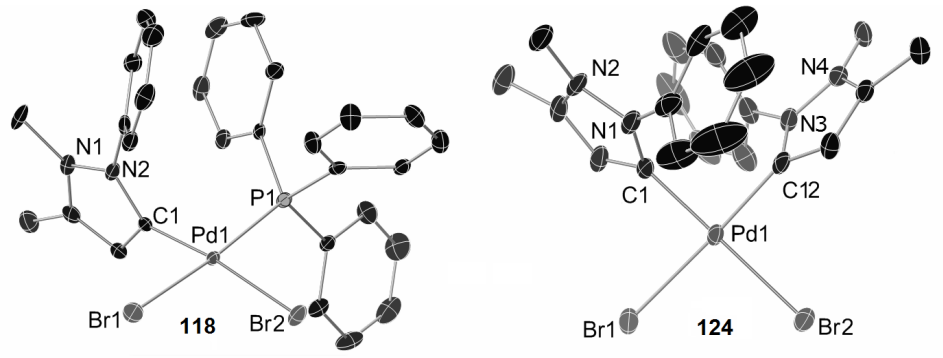

Fig. 3.9. Molecular structures of the *cis*-complexes **119**·CH_2Cl_2 and **124**·CH_2Cl_2 (hydrogen atoms and solvent molecules have been omitted for clarity, thermal ellipsoids are drawn at 50% probability).

Complexes **119** and **124** were equally found to be square-planar, but with a *cis*-arrangement of the ligands because of transphobia (Fig. 3.9). Since the pyry ligands are located *trans* to bromido coligands in these complexes, they experience comparable degrees of *trans*-influence and by consequence, the Pd-C bonds in these complexes are very similar in lengths. In **119**, a Pd-C distance of 1.977(5) Å was found, while in the slightly more electron-rich complex **124**, the average Pd-C bond length was 1.979 Å. The bulky triphenylphosphine ligand does not distort the coordination geometry significantly due to the small size of the pyry ligand. The angle between the NHC and the phosphine was found to be only marginally enlarged from the ideal geometry, with a value of 92.0(2)°, and the NHC plane has an almost perpendicular angle to the coordination plane defined by palladium and the bromido coligands, with a dihedral angle of 87.6(5)°. In **124**, the C1-Pd1-C12 angle between the NHC ligands is closer to the ideal 90°, reflecting the smaller size of the pyry ligands, which allows them to get closer to each other. However, to avoid unfavourable steric interactions between the phenyl wingtip substituents, the

NHCs adopt an *anti*-arrangement, and are tilted by 52.3(4)° abd 57.0(4)° with respect to the coordination plane. More detailed data is given in table 3.6.

Table 3.6. Selected bond lengths [Å] and angles [deg] in **119**·CH_2Cl_2 and **124**·CH_2Cl_2.

	119·CH_2Cl_2	**124**·CH_2Cl_2
Pd1-C1	1.977(5)	1.978(4)
Pd1-P1/C12	2.255(2)	1.980(4)
Pd1-Br1	2.4971(8)	2.4935(6)
Pd1-Br2	2.4878(6)	2.5191(5)
C1-Pd1-P1/C12	92.0(2)	89.3(2)
C1-Pd1-Br1	88.0(2)	87.9(1)
Br1-Pd1-Br2	91.06(2)	82.23(2)
Br2-Pd1-P1/C12	89.91(4)	90.7(1)
C1-Pd1-Br2	171.1(2)	173.8(1)
P1/C12-Pd1-Br1	173.47(4)	176.6(1)

Similar to the complexes with nitrogen donors, the hetero-bis(NHC) complexes **116**, **121**, and **122** are *trans*-complexes (Fig. 3.10). However, the additional NHC ligands are stronger donors and exert more *trans*-influence, which results in longer Pd-C_{pyry} bonds than found in **117** and **118**. These bonds range from 1.989(5) Å in the IPr complex **121** to 2.030(5) Å in the $^{i}Pr_2$-bimy complex **116**, and follow the order in NHC ligand donor strength established by the chemical shift of $C_{carbene}$ in the pyrazolin-5-ylidene ligand (*vide supra*).

The Pd-C bond to the other NHC ligands were less varied in lengths than the Pd-C_{pyry} bonds. The shortest bond is found with the $^{i}Pr_2$-bimy ligand in complex **116**, with a Pd-C distance of 2.031(5) Å, and the longest bond exists in the SIPr complex **122** and measures 2.049(4) Å. No obvious connection exists between steric or electronic parameters of the ligands and these bond lengths.

The planes defined by the NHC rings are at acute angles to the coordination planes of the complexes, and twisted with respect to each other to minimize steric congestion. The bulky IPr and SIPr ligands in **121** and **122** enforce larger dihedral angles of 30.9(6)° and 43.2(4)°, respectively, while the less bulky $^{i}Pr_2$-bimy ligand in leads to a smaller twist of only 17.8(5)°.

The latter complex bears a close resemblance to the pyrazole complex **84**, to which it is isomeric, and the other pyrazole complexes **82**, **89**, and **90** described above.

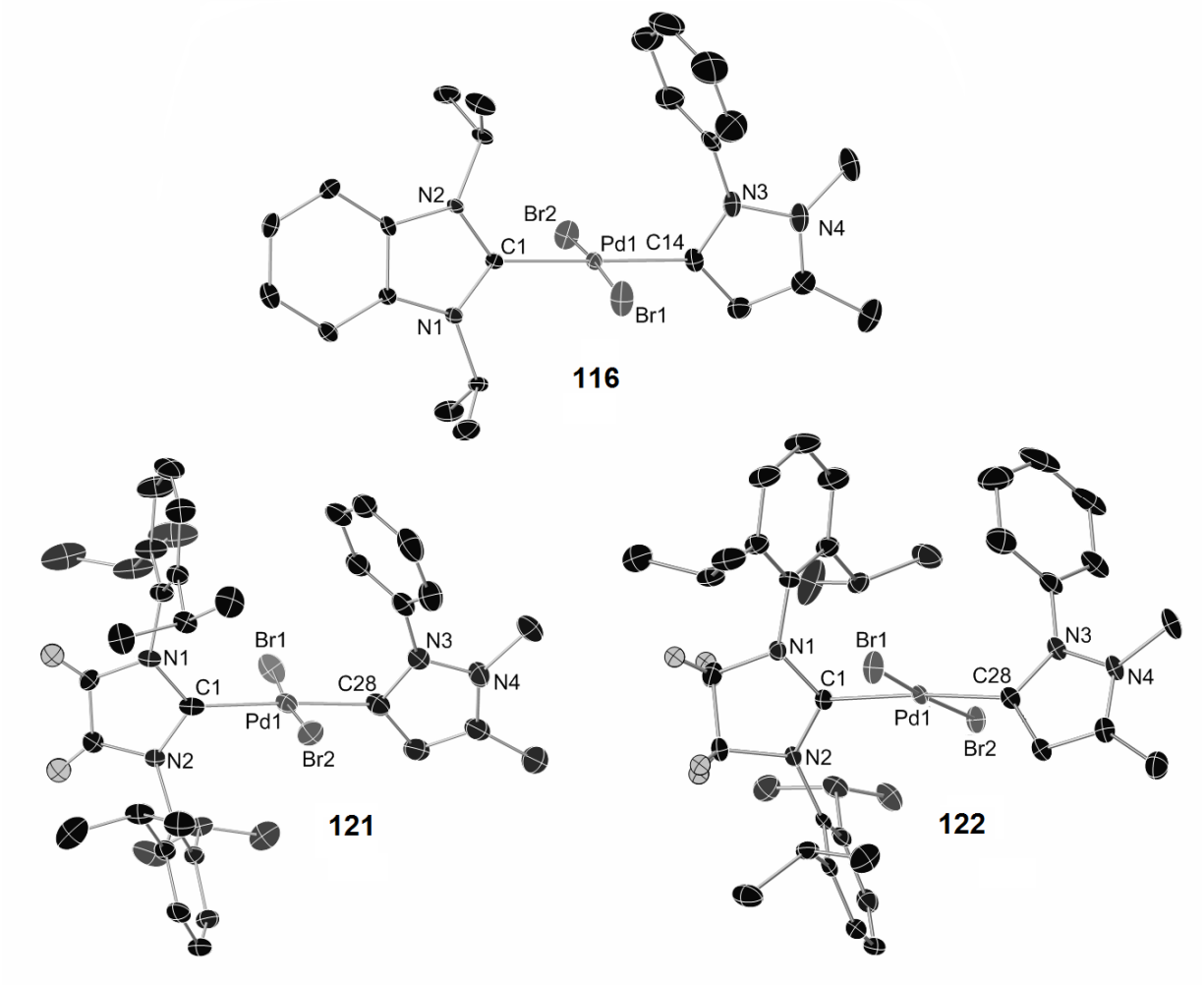

Fig. 3.10. Molecular structures of the hetero-bis(NHC) complexes **116**, **121**, and **122** (Hydrogen atoms, with the exception of those on C-4 and C-5 in **121** and **122**, have been omitted for clarity. Thermal ellipsoids are drawn at 50% probability. **122** was obtained as a cocrystal with $[PdBr_2(SIPr)]_2$, the structure of which is not shown here).

Table 3.7. Selected bond lengths [Å] and angles [deg] in **116**, **121**, and **122**.

	116	**121**	**122** (cocrystal)
Pd1-C1	2.031(5)	2.040(4)	2.049(4)
Pd1-C_{pyry}	2.030(5)	1.989(5)	2.007(4)
Pd1-Br1	2.4325(7)	2.4343(9)	2.4267(5)
Pd1-Br2	2.4339(7)	2.4430(9)	2.4289(4)
C1-Pd1-Br1	91.2(1)	95.5(1)	88.59(9)
C1-Pd1-Br2	89.4(1)	89.2(1)	96.68(9)
Br1-Pd1-C_{pyry}	88.3(1)	87.2(2)	88.3(1)
Br2-Pd1-C_{pyry}	91.2(1)	88.2(2)	86.54(9)
C1-Pd1-Cp_{yry}	179.0(2)	1175.4(2)	173.8(1)
Br1-Pd1-Br2	174.55(2)	174.85(3)	174.66(2)

3.2.4. Applications as Catalysts for the Direct Arylation of Pentafluorobenzene

Direct arylations of acidic C-H bonds in fluorinated arenes or heteroarenes are a convenient way to synthesize biaryls by means of C-C cross-coupling, without the need for an organometallic cross-coupling reagent. Additionally, the byproducts associated with classical cross-coupling methods are avoided in this approach.[127] Following the recent discovery that hetero-bis(NHC) complexes of palladium(II) can catalyze this reaction,[39e] the question arose whether the pyrazolin-5-ylidene complexes are also able to act as catalysts for this transformation.

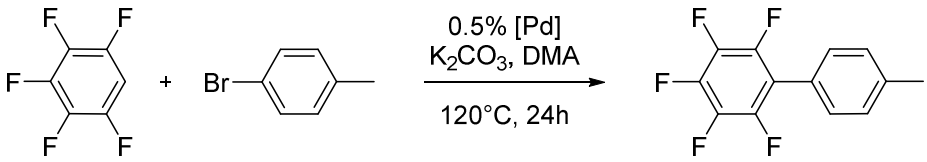

125 **126** **127**

Scheme 3.16. Direct arylation of pentafluorobenzene.

As a benchmark reaction, the coupling between pentafluorobenzene (**125**) and 4-bromotoluene (**126**) was chosen, and the same reaction conditions and reagents as in previous reports were used. The substrates were coupled at 120 °C, using a precatalyst loading of 0.5 mol%, K_2CO_3 as base, and 0.2 mL DMA per 1.0 mmol substrate as a solvent. It became quickly apparent that the

degradation of the catalyst into catalytically inactive colloidal palladium species was the main factor hampering the reaction. To suppress this catalyst deactivation pathway, the reaction mixtures were diluted in order to slow aggregation reactions. As a result, the yields increased from the initially observed 37% to 57% for complex **112**, and all further reactions were carried out at this higher dilution (Table 3.8)

Table 3.8. Precatalyst screening for the direct arylation of pentafluorobenzene.[a]

Entry	Precatalyst	Yield (%)[b]
1	-	0
2[c]	**112**	39
3	**112**	57
4	**116**	68
5	**117**	45
6	**118**	55
7	**119**	71
8	**120**	44
9	**121**	69
10	**122**	80
11	**123**	54
12	**124**	42

[a] Reaction conditions: 0.5 mol% precatalyst, K_2CO_3 (1.1 equiv.), pentafluorobenzene (1.1 equiv.), 4-bromotoluene (0.6 mmol), DMA (2 mL), 120°C, 24 h. [b] Isolated yields, average of two runs. [c] 200 µL DMA, 0.3 mmol 4-bromotoluene.

The initial screening showed catalytic activity for all complexes, while no product could be detected in the absence of a precatalyst. The precatalysts are structurally very diverse, making it difficult to understand the structure-activity relationships at work in this reaction. However, it is apparent that only moderate yields were obtained with the nitrogen donor complexes **117** and **118** as well as the cationic complex **112**. While the former two complexes were presumable insufficiently stabilized by the weakly coordinated acetonitrile or pyridine ligands, the steric bulk and coordinative saturation of the latter complex might have lead to reduced reactivity. Among the bis(NHC) complexes **116** and **120**-**124**, as well as the mixed NHC-phosphine complex **119**,

complexes with a coligand of moderate steric bulk performed best. Complex **120**, incorporating the very bulky Bh_2-bimy ligand, and complexes **123** and **124**, with the sterically somewhat less bulky IMes ligand and the very slender pyry ligand, respectively, performed less well than **116**, **119**, **121** and **122**. Due to the presence of the sterically bulky and relatively electron-rich SIPr ligand in **122**, this complex gave the highest yield of 80%, similar to other reported catalysts.[39e]

Table 3.9. Optimization of reaction conditions for the direct arylation.[a]

Entry	Catalyst	Solvent	Base	T (°C)	Yield (%)[b]
1	**122**	DMA	K_2CO_3	120	80
2	**122**	DMA	K_2CO_3	80	36
3	**122**	DMA	K_2CO_3	100	51
4	**122**	DMA	K_2CO_3	130	65
5	**122**	DMA	K_2CO_3	140	58
6	**122**	DMA	Cs_2CO_3	120	61
7	**122**	DMA	$KHCO_3$	120	42
8	**122**	DMA	KOH	120	49
9	**122**	DMA	NEt_3	120	0
10	**122**	DMA	DBU	120	1
11	**122**	DMSO	K_2CO_3	120	0
12	**122**	Toluene	K_2CO_3	120	2
13	**122**	1,4-Dioxane	K_2CO_3	120	0
14[c]	**122**	DMA	K_2CO_3	120	3

[a] Reaction conditions: 0.5 mol% precatalyst, base (1.1 equiv.), pentafluorobenzene (1.1 equiv.), 4-bromotoluene (0.6 mmol), solvent (2 mL), 24 h. [b] Isolated yields, average of two runs. [c] 1.5 h, microwave heating.

Attempts at optimizing the reaction conditions further, using the best-performing complex **122** as precatalyst, focused initially on the temperature (Table 3.9, entries 2-5 and 14). However, temperatures both above and below the initially used 120 °C lead to a drop in yield. At lower temperatures, the reaction rates are reduced, leading to lower turnover frequencies and consequently to the observed lower yields. By contrast, temperatures exceeding 120 °C accelerate the decomposition of the catalytically active species into inactive aggregates, thus reducing

catalyst turnover. This faster decomposition is not outbalanced by faster reaction rates, and lower yields are the result. Microwave heating, in combination with a shorter reaction time, was also explored as an alternative to conventional heating. In contrast to the microwave reactions described above, no acceleration was observed, and only trace amounts of product could be isolated after 1.5 h.

The next parameter that was varied was the nature of base (entries 6-10). When the use of potassium carbonate yielded 80% of biaryl **127** in the initial screening, other inorganic bases such as cesium carbonate, potassium bicarbonate, and potassium hydroxide gave only moderate yields. Organic bases such as triethylamine and diazabicycloundecen (DBU) performed even worse, and only trace amounts of product were observed, if at all. These results can be understood by considering the proposed mechanism, in which a carbonate anion plays a crucial role as metal-bound base, which deprotonates the pentafluorobenzene.[128]

A small number of other high-boiling solvents, i.e. DMSO, toluene, and 1,4-dioxane were screened as alternatives to DMA (entries 11-13). Neither of these three solvents was as efficient as DMA at stabilizing the catalytically active species, and the rapid formation of palladium black under reaction conditions forshadowed the low yields which were obtained after workup.

It is evident that the initial reaction conditions were already the optimum for this transformation, and no further attempts were made to improve them. Instead, the substrate scope of the direct arylation was explored with respect to the bromoarene coupling partner (Table 3.10).

Electron-rich bromoarenes, such as the initially used 4-bromotoluene, gave good yields of biaryl. This was true for both methoxy- and phenyl-substituted bromoarenes, as long as the donating substituent was located in *para*- or *meta*-position. If it was located in *ortho*-position, steric repulsion hindered the oxidative addition despite the electron-rich nature of the bromoarene, and consequently, no biaryl formation was observed with 2-bromotoluene and 2-methoxybromobenzene (entries 1-6).

Only moderate yields were observed with electronically neutral (entry 7) or electron-poor bromoarenes (entries 8-13), confirming that the oxidative addition is most likely the rate-determining step in this reaction. Interstingly, the electron-poor 4-chlorobromobenzene yielded exlusively chlorinated biaryl instead of the *para*-terphenyl resulting from double cross-coupling (entry 13). Despite an increase of electron density in the arene upon replacement of bromine with phenyl, no reaction occurred with the chloro-substituent. This demonstarates that arylation of

chloroarenes is not possible with precatalyst **122**. By contrast, when the almost equally electron-poor 1,3-dibromobenzene was used as a substrate, only *meta*-terphenyl was isolated, despite a slightly higher steric hindrance in the intermediate 3-phenylbromobenzene (entry 4). Finally, heteroarenes, which are not only electron-poor substrates but also potential catalyst poisons, could not be cross-coupled at all.

Table 3.10. Substrate scope of the direct arylation catalyzed by **122**.[a]

Entry	Aryl halide	Yield (%)[b]	Entry	Aryl halide	Yield (%)[b]
1	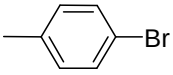	80	9	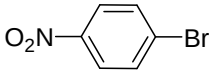	54
2	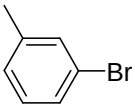	72	10	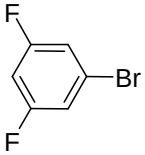	20
3	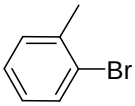	0	11	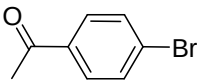	39
4	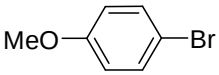	75	12	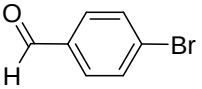	41
5	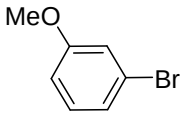	75	13[c]	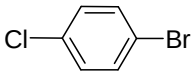	48[d]
6	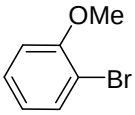	0	14[c]	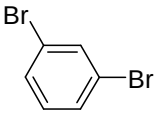	46[e]
7	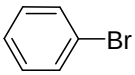	45	15	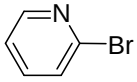	0
8	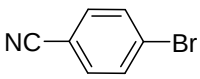	56	16	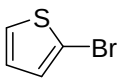	0

[a] Reaction conditions: 0.5 mol% **122**, K_2CO_3 (1.1 equiv.), pentafluorobenzene (1.1 equiv.), 4-bromotoluene (0.6 mmol), DMA (2 mL), 120°C, 24 h. [b] Isolated yields, average of two runs. [c] K_2CO_3 (2.2 equiv.), pentafluorobenzene (2.2 equiv.). [d] Mono-coupled product. [e] Doubly-coupled product.

4. Indazolin-3-ylidene Complexes of Palladium(II)

Indazole formally derives from pyrazole by benzannelation. Similar to benzimidazolin-2-ylidenes, which are less electron-rich than their non-benzannelated analogues imidazolin-2-ylidenes, the NHCs derived from indazole – indazolin-3-ylidenes – are a weaker donor than pyrazolin-3-ylidenes.[48] However, indazolin-3-ylidenes (indy) possess only one nitrogen atom adjacent to $C_{carbene}$, making them considerably stronger donors than NHCs with two stabilizing heteroatoms.

The earliest work done in the field of indy chemistry was focused on the physical organic chemistry of these compounds, theoretical studies, and the reactivities of free indazolin-3-ylidenes generated by thermal decomposition of carboxylate adducts.[41d,129] Such free NHCs can for example be used as reagents for the synthesis of amidines from thiolactames, in which the carbene acts as a desulfurization agent.[130] Other applications of *in situ* generated indazolin-3-ylidenes include organocatalytic transformations such as the redox esterification of aromatic aldehydes, although there is evidence for mechanistic differences compared to the organocatalytic mode of action of commonly employed NHCs.[131]

The first study focused on the coordination chemistry of these ligands with late transition metals was published in 2010, with the description of gold, palladium, and rhodium complexes.[41a] Only the description of a hetero-bis(NHC) complex of palladium(II), where one of the NHCs was an indy ligand, predates this report.[48]

Since these initial reports, the majority of published results focused on gold complexes, with extensive studies concerning the coordination chemistry, ligand redistribution reactions, ligand electronic parameters, and cyctotoxic properties of the resulting complexes having been conducted.[41b,c,132] Reports on complexes with other metals are more scarce, but a small number of complexes of palladium, rhodium, and copper have been reported as well.[41c,133]

In only two instances has the usefulness of these complexes for catalytic applications been studied. A cationic hetero-bis(NHC) copper(I) complex bearing an indy ligand has been used as catalyst for an azide-alkyne Huisgen cycloaddition reaction with *in situ* generated azides,[133b] and the ability of [AuCl(indy)] complexes to catalyze the hydration of alkynes to ketones has been studied to some extent.[41c]

The paucity of reports on the coordination chemistry of indy with palladium(II) is deplorable, given the superior ligand donor strength of these ligands. The synthesis of novel indy ligands and their palladium(II) complexes merits attention due to their potential applications in catalytic transformations.

4.1. Indazolin-3-ylidene Complexes of Palladium(II) with Phosphine Coligands

4.1.1. Synthesis and Characterization of Indazolin-3-ylidene Complexes

Simple, fused-ring indazolin-3-ylidene precursor salts can be obtained by alkylation of deprotonated indazole with a dibromoalkane, followed by ring closure to give the indazolium salt.[132a] The absence of regioselectivity in the first alkylation step, which is a major problem in the synthesis of N,N'-dialkylindazolium salts with different substituents at the nitrogen atoms, is irrelevant for fused-ring salts, since the same product is obtained from both regioisomeric intermediates (Scheme 4.1).

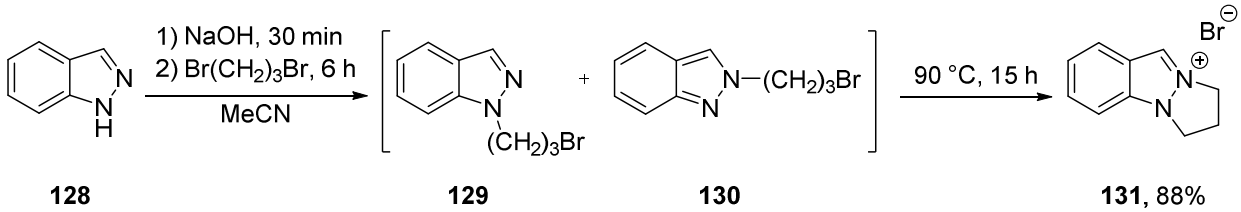

Scheme 4.1. Synthesis of fused-ring indazolium bromide **131**.

In contrast to other methods for the synthesis of such salts,[134] this synthetic protocol has the advantage of using commonly available starting materials, and all involved species are of sufficiently robust, so no inert reaction conditions are required. After 6 h at ambient temperature for the first alkylation step, and 15 h at 90 °C for the ring closure, 2,3-dihydro-1*H*-pyrazolo[1,2-*a*]indazolium bromide (indy-5·HBr, **131**) was obtained in good yield as an off-white, hygroscopic solid.[135]

Exploratory attempts at obtaining homo-bis(NHC) complexes of group 10 metals incorporating the indy-5 ligand were met with failure. The palladium(II) complex $[PdBr_2(\text{indy-5})_2]$ remained elusive, similar to the initial attempts at synthesizing complex **124** bearing chemically similar pyry ligands. The synthesis of nickel(II) complexes of the tye $[NiBr_2(\text{indy-5})_2]$ was equally fruitless (Scheme 4.2 and Table 4.1).

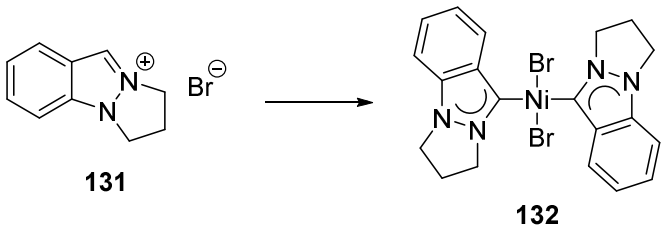

Scheme 4.2. Attempts at obtaining nickel(II) homo-bis(indy-5) complexes.

Table 4.1. Reaction conditions tested for the synthesis of **132**. [a]

Entry	Reaction conditions	Outcome
1	1) Ag_2O, DCM, 15 h. 2) $[NiBr_2(PPh_3)_2]$.	Intractable mixture of multiple species, no evidence of product.
2	$[NiBr_2(PPh_3)_2]$, KOtBu, THF, 0 °C, 2 h.	Starting material and paramagnetic impurities.
3	$[NiBr_2(PPh_3)_2]$, K_2CO_3, acetone, 15 h.	Starting material only.

[a] Reaction mixtures were analyzed by TLC, ESI-MS and ^{1}H NMR spectroscopy.

However, it was possible to obtain a dimeric complex of the formula $[PdBr_2(indy\text{-}5)]_2$ using either the protocol optimized for the synthesis of $[PdBr_2(^iPr_2\text{-}bimy)]_2$ by reacting palladium(II) acetate with the azolium salt in the presence of an external bromide source,[29] or by using the silver carbene transfer protocol.[63a] While only moderate yields of dimer **133** were obtained with the latter method, quantitative yields were obtained with the former (Scheme 4.3).[136]

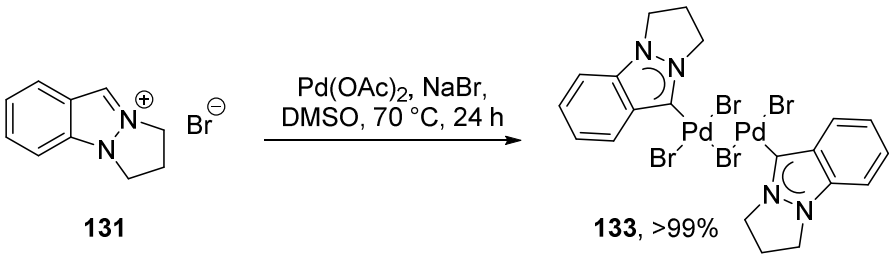

Scheme 4.3. Palladium(II) acetate route to $[PdBr_2(indy\text{-}5)]_2$.

Dimer **133** was isolated as an orange solid.[135] It did not dissolve in ethereal solvents, ethy acetate and hydrocarbons such as hexane, and solubilities in chlorinated solvents was low. However, the complex readily dissolved in coordinating, polar organic solvents such as acetonitrile and DMSO. Successfull complex formation was confirmed by the absence of the resonance of the acid proton on C-3 in the ^{1}H NMR spectrum of **133**, which was observed at 9.55 ppm in the starting material **131**. Since the dimer's low solubility in chloroform prevented to obtain NMR spectra in $CDCl_3$, and MeCN-d_3 was used instead, a direct comparison between the chemical shifts of **131** and **133** is not very meaningful. However, it should be noted that the aliphatic resonances of the saturated five-membered ring were shifted slightly upfield. The ^{13}C NMR spectrum of **131** showed the $C_{carbene}$ resonance at 141.0 ppm. This is only slightly more upfield than the resonances found for the carbene carbon in closely related complexes.[41a,120]

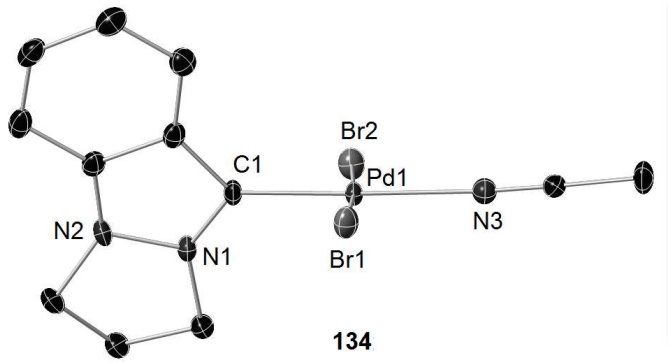

Fig. 4.1. Molecular structure of the acetonitrile adduct **134** derived from dimer **133** (hydrogen atoms have been omitted for clarity, thermal ellipsoids are drawn at 50% probability). Selected bond lengths [Å] and angles [°]: Pd1-C1 1.945(3), Pd1-Br1 2.4341(5), Pd1-Br2 2.4394(5), Pd1-N3 2.095(3); C1-Pd1-Br1 88.53(8), C1-Pd1-Br2 87.51(8), Br1-Pd1-N3 90.43(7), Br2-Pd1-N3 93.52(7), C1-Pd1-N3 177.9(1), Br1-Pd1-Br2 176.02(1).

Since acetonitrile can coordinate to the metal center, it is reasonable to assume that in the NMR samples in MeCN-d_3, the prevalent species is not dimer **133**, but the acetonitrile adduct [$PdBr_2$(acetonitrile)(indy-5)] (**134**) instead. In other solvents and in the solid state, the description as dimeric species is nevertheless correct. The ESI-MS spectrum showed peaks corresponding to

$[M - Br + CH_3CN]^+$, $[M + NH_4]^+$, and $[M + Na]^+$, which are indicative of an undissociated dimer, and elemental analysis results corresponded to a dimeric species as well, not a solvent adduct.

By contrast, the slow evaporation of a concentrated acetonitrile solution of **133** yielded single crystals suitable for X-ray diffraction of the acetonitrile adduct **134** instead (Fig. 4.1). In this adduct, the coordination geometry at palladium is square-planar, and the bromido coligands adopt a *trans*-arrangement. The NHC ring plane is twisted out of the coordination plane by ~68° to minimize steric repulsion. The slightly flexible five-membered aliphatic ring in the indy-5 ligand adopts a distorted envelope conformation. All bond distances between the central metal atom and the ligands fall within the expected range and are in good agreement with values published for a structurally related pyrazolin-5-ylidene complex.[120]

The facile interconversion between the dimeric form **133** and the acetonitrile adduct **134** demonstrates the lability of the μ-bromido bridges and the coordinated solvent molecule, respectively. This suggests that **133** can serve as an equally versatile starting material as **117**, to explore the coordination chemistry of indy-5 complexes of palladium(II) with a host of coligands. Indeed, reactions similar to the the formation of **118** and **119** were observed when **133** was exposed to pyridine and triphenylphosphine, albeit the time required to reach complete conversion was longer, both for **135** and **136**, and yields were marginally lower, but still excellent (Scheme 4.4).

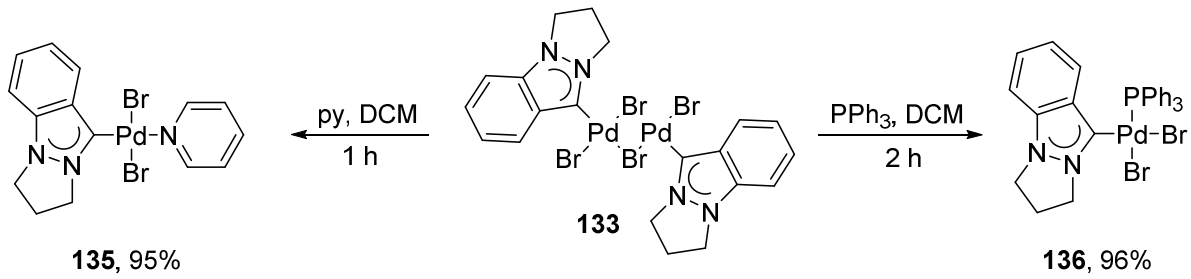

Scheme 4.4. Synthesis of indy-5 complexes incorporation an N- or P-donor ligand.

When a suspension of **133** in dichloromethane was treated with a two or more equivalents of pyridine, a rapid colour change from orange to yellow occurred, and the suspension slowly turned into a clear solution. This indicated the successful coordination of the pyridine ligand and the formation of the desired adduct *trans*-[$PdBr_2$(indy-5)(pyridine)] (**135**), which was isolated as a pale yellow solid. The required reaction times depended on the amount of pyridine used - with a

large excess of pyridine, the reaction was rapidly completed, while stochiometric amounts required reaction times of up to one hour.

The solubility of the product was markedly higher in most organic solvents when compared to the dimeric starting material. Polar organic solvents and chlorinated solvents readily dissolve **135**, while it is insoluble in hydrocarbons, ethereal solvents and esters. However, solutions showed a tendency to precipitate an orange solid upon prolonged standing, and the presence of free pyridine in these solutions was detected by ^{1}H NMR spectroscopy. This points towards ligand dissociation and subsequent formation of the insoluble dimer **133**.This process is favored by two factors - the strong *trans*-effect of the very good σ-donor indy-5, which leads to a weaker coordination of the pyridine ligand, and the poor solubility of the dimeric species **133**. Interestingly, similar ligand dissociations were not observed for **118**, albeit the pyry ligand in the latter is the stronger donor. The low solubility of the precipitating dimer seems thus to be the major driving force. This ligand dissociation process also explains the comparatively longer reaction times, and the excess of pyridine required for the formation of **135**.

Spectroscopically, complex **135** is inconspicious. In the ^{1}H NMR spectrum, an additional set of five aromatic protons is observed, which can be attributed to the pyridine ligand. The chemical shifts of the indy-5 resonances change marginally when compared to **134**, but since the spectra are recorded in $CDCl_3$ and MeCN-d_3, respectively, these should not be overinterpreted. In the ^{13}C NMR spectrum, the $C_{carbene}$ resonates at 145.7 ppm, which is slightly more downfield than the corresponding resonance in **134** at 141.0 ppm. This reflects the higher ligand donor strength of pyridine when compared to acetonitrile.[48]

Single crystals for X-ray diffraction studies were grown from concentrated dichloromethane/acetonitrile solutions of the pyridine adduct **135**. Similar to the structure of the acetonitrile adduct **134**, the coordination geometry around palladium is square-planar, and the pyridine ligand binds *trans* to the NHC (Fig. 4.2). The indazolin-3-ylidene ring plane is twisted by 74° out of the coordination plane, and almost parallel to the plane defined by the pyridine ring. The five-membered ring in the indy-5 ligand adopts the same distorted envelope conformation as observed before. In this complex, the Pd-C and Pd-N bonds are slightly longer than the corresponding bonds in the acetonitrile complex **134**, reflecting the more electron-rich nature of the pyridine ligand, which translates into a more pronounced *trans*-influence. By contrast, the Pd-Br bonds in **135** are slightly shorter than in **134**.

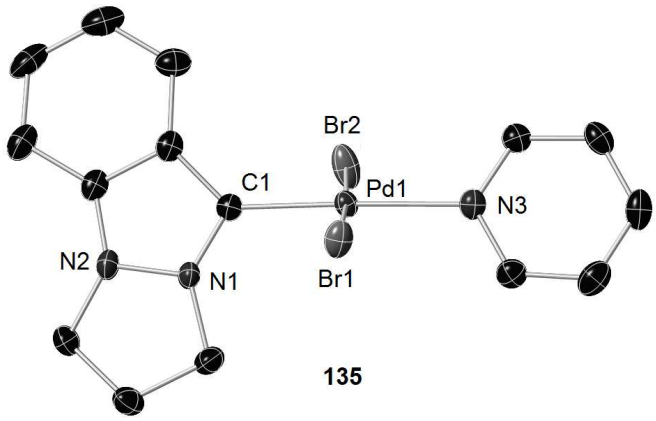

Fig. 4.2. Molecular structure of the pyridine complex **135**·MeCN (hydrogen atoms and solvent molecules have been omitted for clarity, thermal ellipsoids are drawn at 50% probability). Selected bond lengths [Å] and angles [°]: Pd1-C1 1.956(3), Pd1-Br1 2.4235(4), Pd1-Br2 2.4297(4), Pd1-N3 2.113(2); C1-Pd1-Br1 87.47(8), C1-Pd1-Br2 89.36(8), Br1-Pd1-N3 91.37(7), Br2-Pd1-N3 91.84(7), C1-Pd1-N3 177.5(1), Br1-Pd1-Br2 176.62(2).

The treatment of a suspension of **133** in dichloromethane with triphenylphosphine lead to a similar color change as the one observed for the reaction with pyridine. After 2 h, pale yellow to off-white solids could be isolated by evaporation of the solvent and subsequent washing with diethyl ether to remove unreacted material. ESI-MS and elemental analysis confirmed that this material was the desired *cis*-[$PdBr_2$(indy-5)(PPh_3)] (**136**), but the complex was found to be poorly soluble in all tested organic solvents. While the solubility of the corresponding pyry complex **119** was still sufficiently high in DMSO-d_6 to obtain NMR spectra, this was not the case for complex **136**, and no characterization by NMR spectroscopy was possible.

The replacement of bromido ligands with trifluoroacetato ligands has been shown to enhance the solubility of related complexes.[41a,137] This has the additional advantage of generating a potentially more catalytically active complex as well, since the weakly coordinating nature of the trifluoroacetato ligands in the resulting complex *cis*-[$Pd(O_2CCF_3)_2$(indy-5)(PPh_3)] (**137**)gives rise to two readily available coordination sites for incoming substrates.

The addition of 2.30 equivalents of silver(I) trifluoroacetate to a suspension of **136** in acetonitrile, and subsequent reaction for 15 h at ambient temperature, shielded from light in oder to prevent

photodecomposition of the silver reagent, gave complex **137** in an acceptable yield of 80% (Scheme 4.5).

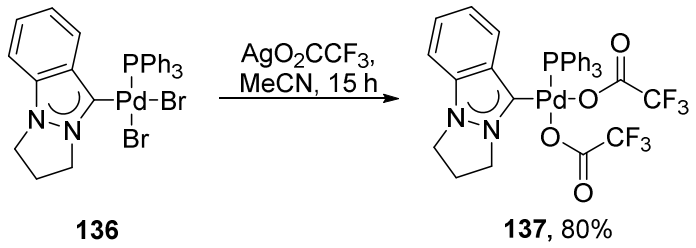

136 **137**, 80%

Scheme 4.5. Replacement of the bromido ligands by trifluoroacetato ligands.

The bis(trifluoroacetato) complex **137**, which was isolated as a pale yellow solid, was indeed better soluble in a variety of organic solvents, with the exceptions of ethereal solvents, hydrocarbons and esters, in which it remained insoluble. NMR spectra for **137** could be recorded in CD_2Cl_2, and confirmed the successful ligand exchange, in addition to ESI-MS and elemental analysis results.

The ^{1}H NMR spectrum of **137** differs significantly from those of **134** and **135**. The most obvious change is the presence of the additional aromatic signals attributable to the triphenylphosphine ligand. Other than that, peak patterns and chemical shifts of signals which can be assigned to the aliphatic ring in the indy-5 ligand also differ from those in the spectra of **134** and **135**. The NCH_2 groups no longer resonate as well resolved triplets, but instead give rise to four complicated multiplets, three of which are shifted upfield and one which is shifted downfield from their location in the spectra of the simple solvent adducts. Similarly, the resonance due to the methylene group is also split into two multiplets, which are found at more upfield chemical shifts than the single signal for this group in the spectra of **134** and **135**. All of these changes can be traced back to the magnetic anisotropy and steric congestion introduced into the complex by the aromatic rings of the triphenylphosphine ligand, which is in close proximity to the alicyclic protons.

In the ^{13}C NMR spectrum of **137**, the resonance of $C_{carbene}$ is found in the form of a doublet at 149.2 ppm, with a coupling constant of $^2J_{C\text{-}P}$ = 10 Hz. The chemical shift is more upfield than the corresponding resonance in a structurally related *cis*-[$PdBr_2(PPh_3)$(pyry)] complex, but this difference can be explained by the change in the nature of the coligands from bromido to

trifluoroacetato.[120] The comparatively small coupling constant is typical for the interaction in a *cis*-complex. In the spectra of other NMR-active heteroatoms, a single ^{31}P NMR resonance at 27.9 ppm indicates the presence of the triphenylphosphine ligand, and two ^{19}F resonances for the chemically inequivalent trifluoroacetato ligands are observed at 1.3 ppm and 0.5 ppm. The spectroscopy data strongly supports a cis-arrangement of the indy-5 and triphenylphosphine ligands, which is in line with the usually observed transphobia tendency in these systems.[41a,42d,81,126] The chemical shifts in the ^{13}C, ^{19}F and ^{31}P spectra of **137** are in good agreement with values reported for structurally related complexes.[41a]

Despite the low solubility of **136**, the slow evaporation of a concentrated dichloromethane/toluene solution yielded single crystals suitable for X-ray diffraction. Similarly, single crystals of **137** were otained by slow evaporation of a concentrated dichloromethane/diethyl ether solution. As can expected based on comparison to previously reported complexes and the spectroscopic evidence presented above, both compounds were found to be square-planar complexes with a cis-arrangement of indy-5 and triphenylphosphine (Fig. 4.3).

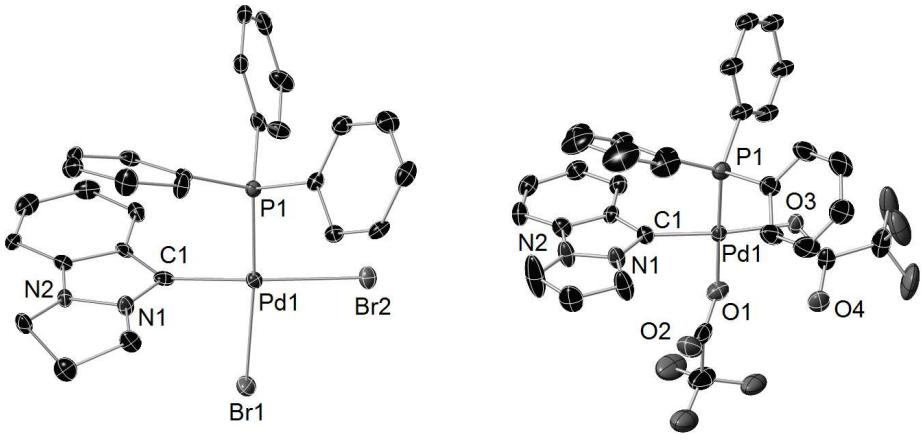

Fig. 4.3. Molecular structures of the mixed phosphine-NHC complexes **136** and **137** (hydrogen atoms and solvent molecules have been omitted for clarity, thermal ellipsoids are drawn at 50% probability).

Similar to the previous complexes, in **136** and **137**, the plane defined by the NHC ligand is twisted by ~76° out of the coordination plane, no doubt influenced by the steric bulk of the

triphenylphosphine ligand. The fused five-membered ring in the indy-5 ligand adopts the same distorted envelope conformation in **136**, while it is almost planar in the sterically more congested **137**.

Table 4.2. Selected bond lengths [Å] and angles [deg] in **136** and **137**.

	136	**137**
Pd1-C1	1.965(5)	1.949(4)
Pd1-P1	2.268(1)	2.230(1)
Pd1-Br1/O1	2.4808(6)	2.088(3)
Pd1-Br2/O3	2.4928(6)	2.087(3)
C1-Pd1-Br1/O1	86.3(1)	89.6(1)
C1-Pd1-P1	89.3(1)	91.4(1)
Br2/O3-Pd1-P1	93.25(3)	87.95(9)
Br2/O3-Pd1-Br1/O1	92.33(2)	91.0(1)
C1-Pd1-Br2/O3	170.4(1)	172.1(1)
P1-Pd1-Br1/O1	171.18(4)	178.90(9)

In complex **136**, the Pd-C bond was found to be 1.965(5) Å long, while bond distances of 2.268(1) Å were found for the Pd-P bond and the Pd-Br bonds were 2.4808(6) Å and 2.4928(6) Å long (Table 4.2). For the latter, the longer Pd-Br bond was found for the bromido ligand *trans* to indy-5 ligand, due to the stronger *trans*-influence of the NHC when compared to the phosphine. These values are in good agreement with the values found for the pyry analogue **119**.[120]

After exchanging the anionic ligands from bromido to trifluoroacetato, the Pd-C and Pd-P bonds were found to be 1.949(4) Å and 2.230(1) Å, respectively. The Pd-O bond distances were found to be 2.088(3) Å and 2.087(3) Å. All bond distances for **135** are in good agreement with previously reported values for a *cis*-[$PdBr_2$(indy)(PPh_3)] complex.[41a]

Occasionally, a side product was formed in the synthesis of monophosphine complex **136**, and identified by ESI-MS as the cationic bis(triphenylphosphine) complex **138**. Since these trace amounts were not enough for systematic study, reaction conditions were optimized to yield this species as the main product (Scheme 4.6).

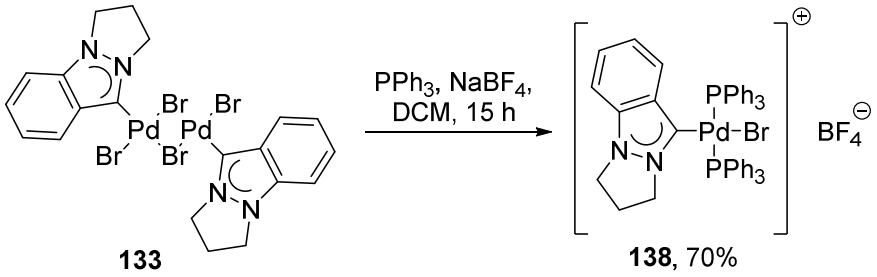

Scheme 4.6. Synthesis of the cationic bis(triphenylphosphine) complex **138**.

Adding sodium tetrafluoroborate to the reaction mixture, to provide a non-coordinating counteranion for the cationic coordinatinon unit, as well as increasing the amount of triphenylphosphine used to slightly more than the stochiometric amount required for the formation of *trans*-[PdBr(indy-5)(PPh_3)$_2$]BF_4 (**138**), moderate to good yields of this complex could be obtained as pale yellow solid.

This complex was readily soluble in polar organic solents such as acetonitrile or DMSO, while being less soluble in chlorinated and more unpolar organic solvents, and NMR spectra could be recorded in MeCN-d_3. In the ^{1}H NMR spectrum, 30 additional aromatic protons were observed, in addition to the four aromatic signals of the indy-5 ligand. Similarly to the spectrum of **137**, the resonances attributable to the aliphatic ring were found upfield from the corresponding signals in the starting material **133**, suggesting shielding by the abundant phenyl groups of the phosphine ligands. However, these signals were less complicated in the spectrum of **138** than those for **137**, due to the more uniform magnetic environment provided by the presence of two phosphine ligands.

In the ^{13}C NMR spectrum, the $C_{carbene}$ resonance was observed 156.4 ppm. This is more downfield than the chemical shift of the neutral indy-5 complexes described above, but upfield from the corresponding resonance in the structurally related pyry complex **112**.[120] Despite the presence of two phosphine ligands, the signal is observed as a doublet, which might be due to a slight magnetic inequivalence of the phosphine ligands due to hindered rotation in the sterically congested complex, and therefore nearly identical $^2J_{C\text{-}P}$ values of about 6 Hz, that cause a not resolved doublet of doublets. By contrast, only a single resonance at 23.2 ppm is found in the ^{31}P spectrum, which is at a typical chemical shift for a bis(triphenylphosphine) complex of palladium(II), and indicative of a *trans*-arrangement of these ligands.[120]

Attempts at crystallizing this complex for X-ray diffraction studies were met with failure. Only crystals of *trans*-[$PdBr_2(PPh_3)_2$] formed by ligand redistribution and decomposition processes, could be obtained. This hints at a lability of the indy-5 ligand in such sterically crowded and electron-rich complexes.

In contrast to two triphenylphosphine ligands, which adopt a *trans*-arrangement due to steric reasons, tethered bis(phosphine) ligands such as bis(diphenylphosphino)ethane (dppe) and bis(diphenylphosphino)propane (dppp) can be expected to impose *cis* geometries, as well as higher complex stabilities due to chelate effects. The synthesis of dppe and dppp analogues to **136** is straightforward, by replacing triphenylphosphine by the appropriate stochiometric amounts of the bidentate phosphine ligands (Scheme 4.7).

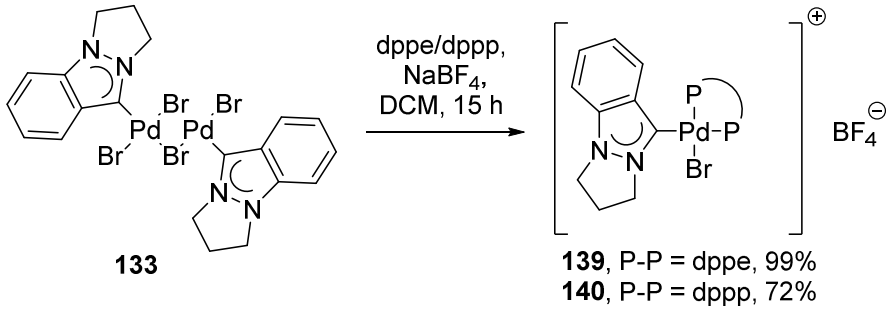

Scheme 4.7. Synthesis of cationic complexes featuring bidentate phosphine ligands.

Following this approach, *cis*-[PdBr(indy-5)(dppe)]BF_4 was isolated as yellow solid in quantitative yield, while a moderate yield of 72% of *cis*-[PdBr(indy-5)(dppp)]BF_4 was obtained as pale orange solid. Both compounds show solubilities similar to those of the other cationic complex **138**.

However, their ^{1}H NMR spectra differ considerably from that of **138**. In addition to the multiplet resonances of the 24 aromatic protons in the region from 8.02 ppm to 7.03 ppm, the NCH_2 groups as well as the other methylene units in both the indy-5 ligand and the aliphatic linkers of the bidentate phosphine ligands resonate as complicated set of multiplets. For the resonances of methylene groups bound directly to nitrogen, chemical shifts beween 4.48 ppm and 3.50 ppm were found, while the other methylene resonances were more upfield between 2.95 ppm and 1.67 ppm.

The ^{13}C NMR spectra are equally complex. Free rotation of most phenyl moieties in the diphosphine ligands is hindered, and C-P coupling additionally complicates the situation, leading to a myriad of signals especially in the aromatic region. The $C_{carbene}$ resonances for **139** and **140** are found at 163.5 ppm and 161.8 ppm, respectively. In **139**, only a doublet was observed, with a $^{2}J_{C\text{-}P}$ coupling constant of 145 Hz in line with a *trans*-coupling, while the *cis*-coupling was presumably not resolved. For **140**, the smaller *cis*-coupling with 4 Hz was observed besides the *trans*-coupling of 148 Hz, resulting in a doublet of doublets.

For the dppe ligand in **139**, the ^{31}P NMR resonances were observed as two doublets at 61.1 ppm and 50.7 ppm. For the dppp ligand in **138**, two doublets were observed at 13.3 ppm and -4.0 ppm, respectively. These shifts are close to those reported for other NHC complexes bearing diphosphine ligands.[138]

No single crystals suitable for X-ray diffraction could be obtained for complex **139** despite numerous attempts, but complex **140** could be crystallized by slow evaporation of a concentrated solution in acetonitrile/hexane (Fig. 4.4).

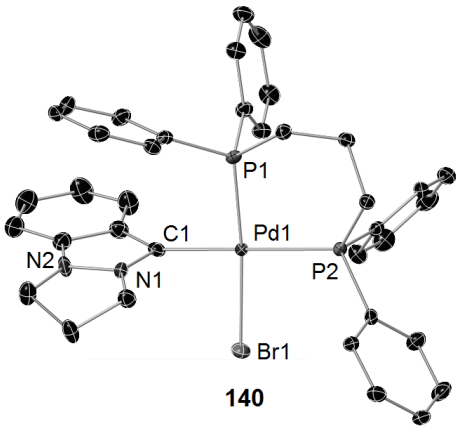

140

Fig. 4.4. Molecular structure of the cationic coordination unit of **140** (hydrogen atoms and counteranion have been omitted for clarity, thermal ellipsoids are drawn at 50% probability). Selected bond lengths [Å] and angles [°]: Pd1-C1 2.018(4), Pd1-Br1 2.4803(8), Pd1-P1 2.254(1), Pd1-P2 2.329(1); C1-Pd1-Br1 87.0(1), C1-Pd1-P1 87.6(1), Br1-Pd1-P2 92.64(4), P1-Pd1-P2 92.72(4), C1-Pd1-P2 179.1(1), Br1-Pd1-P1 176.64(4).

However, X-ray diffraction revealed that in the crystalline material, the tetrafluoroborate counteranions were replaced by bromide. This is not representative of the bulk of the material, since elemental analysis confirmed the presence of the tetrafluoroborate counteranion.

Mostly, the structural features of **140** are in line with the other indy-5 complexes described above. A distorted square-planar geometry around palladium is found, with the expected *cis*-coordination of the dppp ligand, which has a bite angle of 92.72(4)°. The NHC ring plane stands almost perpendicular to the coordination plane, at a torsion angle of ~80°, and the aliphatic ring in the indy-5 ligand adopts the distorted envelope shape absent only in **139**.

Notably, the Pd-C bond with a distance of 2.018(4) Å and the Pd-P bonds with distances of 2.254(1) Å and 2.329(1) Å are longer then in the neutral complexes **136** and **137**, due to the redistribution of electron density upon replacement of a bromido ligand with a more strongly donating phosphine moiety.[139] The Pd-P bond *trans* to the NHC ligand was found to be longer than the one *trans* to the bromido ligand, due to differences in *trans*-influence. All bond lengths and angles are within close proximity to values found for similar compounds.[138,140]

4.1.2. Applications in Catalysis

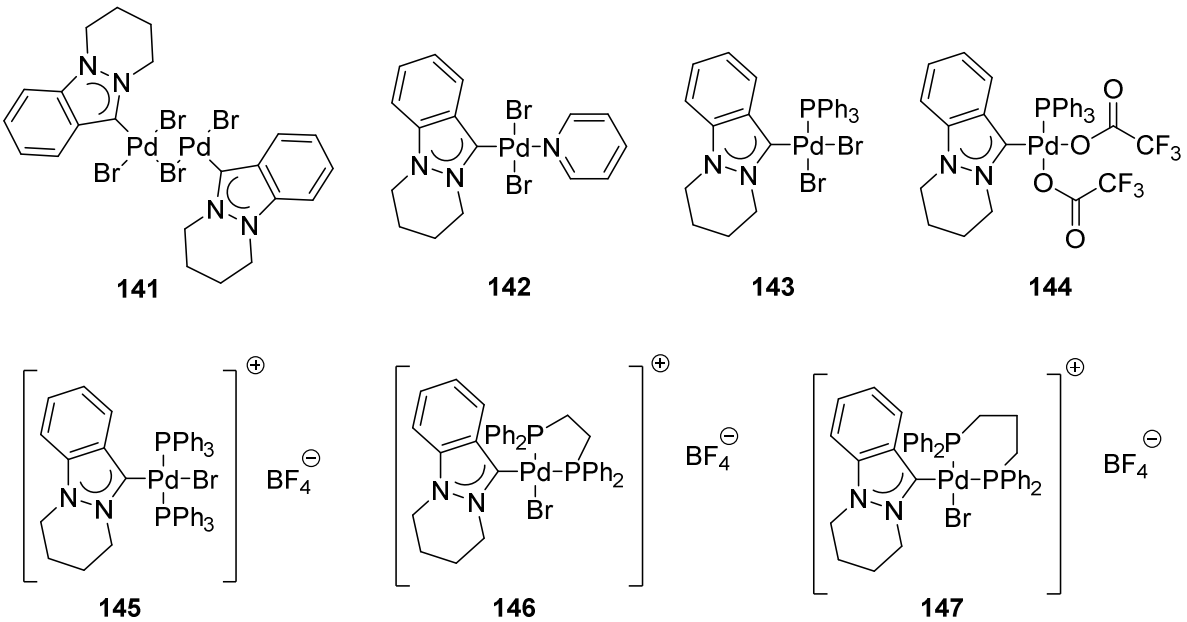

Fig. 4.5. Indy-6 analogues of complexes **133** and **135-140**.[136,141]

Palladium(II) NHC complexes have been shown to be active precatalysts for the hydroamination of carbon-carbon multiple bonds.[137b, 142] This important transformation, which allows the construction of carbon-nitrogen bonds with perfect atom economy by addition of primary or secondary amines to alkenes or alkynes, does not proceed without a catalyst despite being thermodynamically favorable. Hence, research interest into active catalysts for this reaction is considerable,[143] and as a contribution to this field, complexes **133**, **135**-**140**, and their congeners **141**-**147** bearing the 6,7,8,9-tetrahydropyridazino[1,2-*a*]indazolin-3-ylidene (indy-6) ligand (Fig. 4.5) were tested for their catalytic activities in the hydroamination of phenylacetylene (**148**) with 2,6-dimethylaniline (**149**) (Scheme 4.8 and Table 4.3).

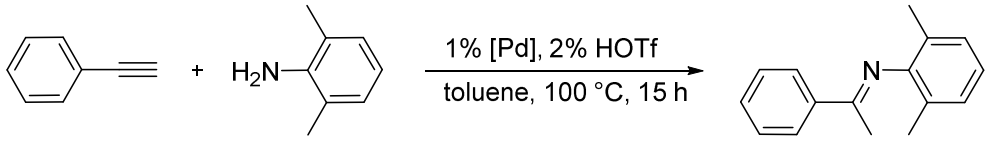

148 **149** **150**

Scheme 4.8. Hydroamination of phenylacetylene.

Table 4.3. Catalytic performance in the hydroamination of phenylacetylene.[a]

Entry	Precatalyst	Yield (%)[b]	Entry	Precatalyst	Yield (%)[b]
1	-	0			
2	**133**	37	9	**141**	30
3	**135**	44	10	**142**	43
4	**136**	43	11	**143**	17
5	**137**	56	12	**144**	50
6	**138**	13	13	**145**	6
7	**139**	>99	14	**146**	92
8	**140**	75	15	**147**	72

[a] Reaction conditions: Precatalyst (1 mol%), phenylacetylene (2.0 equiv), 2,6-dimethylaniline (1.0 mmol), toluene (3 ml), 100 °C, 15 h. [b] Yields determined by GC-MS with decane as internal standard; average of two runs.

With the exceptions of the cationic bis(triphenylphospine) complexes **138** and **145** (entries 6 and 13), which showed poor activity, all complexes were able to catalyse the hydroamination of

phenylacetylene in moderate to good yields, while in the absence of a precatalyst, no product was detected (entry 1). The enamine, which is initially obtained with perfect Markovnikov selectivity, rapidly tautomerizes to yield imine **150** as final product. In order to achieve good yields, the addition of a catalytic amount of triflic acid was required. This Brønsted acid is required to speed up the realease of the product in the final step of the catalytic cycle by protolytic cleavage of the Pd-C bond.[143b,144]

When comparing the series featuring different indy ligands, it becomes apparent that the indy-5 complexes (entries 2-8) consistently outperform the indy-6 complexes (entries 9-15), albeit the differences between related complexes are sometimes very small. The two ligands are relatively similar with respect to their electronic and steric properties, with both properties being subtly influenced by the presence or absence of an additional methylene unit in the fused aliphatic ring. Therefore, it is not possible to determine whether the observed differences in catalytic performance are due to differences in steric bulk, in ligand donor strength, or another electronic factor.

Classifying the complexes as either neutral or cationic allows to systematize the observed catalytic performances. The first class of complexes gave only moderate yields of **150**, with the best performance observed for **137** and **144** (entries 2-5 and 9-12). In these two complexes, the relatively tightly bound bromido ligands are replaced by trifluoroacetato ligands, and the catalytic performance clearly benefits from the availability of more accessible coordinations sites for substrates. Similar observations have been made for NHC complexes bearing carboxylato ligands before.[137b]

Among the cationic complexes, the bis(triphenylphosphine) species **138** and **145** perform extremely poor, while the diphosphine complexes were generally the best precatalysts for this reaction (entries 6-7 and 13-15). During attempts to crystallize **138**, it became obvious that this complex has a high propensity to decompose into other species, which might have been a factor in the low catalytic turnover of **138** and the related **145**. Other factors that might have hampered catalytic activity is the very saturated coordination sphere, containing two sterically bulky triphenylphosphine ligands, and the relatively low solubility of this complex in very unpolar organic solvents.

The better-performing complexes **139**, **140**, **146**, and **147** have a different coordination geometry (*cis* instead of *trans*) and benefit from the additional stability imparted by the chelating

diphosphines. However, for these complexes, the loss of the indy ligand is feasible under reaction conditions, and it is possible the the catalytically active species does not include an indy ligand at all. Palladium(II) complexes bearing a dppe ligand are known precatalysts for hydroaminations, giving further credence to the idea that diphosphine complexes without an NHC ligand are truly responsible for the good catalytic performances.[145] A comparison between dppe and dppe complexes (entries 7, 8, 14, and 15) showed that the best precatalysts **139** and **146**, which perform similar or better than reported precatalysts,[142c,d] incorporate the dppe ligand. This better performance can be explained by the difference in bite angles between dppe and dppp, the impact of which on catalytic performance has been documented before.[140,146]

Another useful transformation is the Sonogashira cross-coupling between terminal alkynes and aryl halides, which allows the construction of C-C bonds.[147] Since palladium(II) NHC complexes have distinguished themselves as efficient catalysts for this transformation,[148] complexes **133** and **135-147** were tested for their ability to serve as precatalysts for the coupling of phenylacetylene with 4-bromoacetophenone (Scheme 4.9). This is of special interest due to the entirely different mechanism when compared to the hydroamination described above.

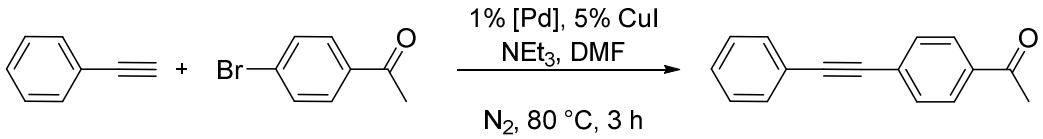

148 **151** **152**

Scheme 4.9. Sonogashira coupling of phenylacetylene and 4-bromoacetophenone.

No product was formed in the absence of a palladium(II) complex (Table 4.4, entry 1), but in contrast to the hydroamination described above, not all palladium(II) complexes were able to act as precatalysts either. To understand the results, this time it is useful to group the complexes not according to their charge (which is less relevant for Sonogashira couplings), but to the presence and the nature of the phosphine coligands. Entirely phosphine-free complexes (**133**, **135**, **141**, and **142**, entries 2, 3, 9, and 10) gave either no product at all, or only trace amounts of **152** close to the detection limit were formed. Since the reactions were carried out in DMF, which is a coordinating solvent and readily dissolves all complexes, solubility issues can be ruled out as root cause of this absence of activity. Instead, it is most likely that the lack of steric bulk of the indy-5 and indy-6 ligands disfavors the reductive elimination in the final step of the catalytic cycle. The

electron-rich nature of the NHC itself provides additional stability to this palladium(II) species, which thus forms the major bottleneck for catalytic turnover.[149] With no other bulky ligand bound to the metal center, product formation can thus not occur.

Table 4.4. Catalytic performance in the Sonogashira coupling.[a]

Entry	Catalyst	Yield (%)[b]	Entry	Catalyst	Yield (%)[b]
1	-	0			
2	**133**	2	9	**141**	0
3	**135**	3	10	**142**	2
4	**136**	84	11	**143**	93
5	**137**	82	12	**144**	96
6	**138**	>99	13	**145**	>99
7	**139**	18	14	**146**	17
8	**140**	30	15	**147**	17

[a] Reaction conditions: CuI (5 mol%), precatalyst (1 mol%), 4-bromoacetophenone (1.0 equiv), DMF (degassed, 2 mL), phenylacetylene (2.0 equiv), NEt_3 (1.2 equiv), 80 °C, 3 h.
[b] Yields determined by NMR spectroscopy; average of two runs.

Complexes **136**-**138** and **142**-**145** bear at least one monodentate phosphine ligand, and generally gave good to excellent yields (entries 4-6 and 10-12). The additional steric bulk of the triphenylphosphine ligand allows reductive elimination to occur efficiently, thus explaining the good catalytic turnover. When comparing the structure-activity relationship for these complexes to the trends observed in the hydroamination, three marked differences are obvious. The complexes including the indy-6 ligand are the more efficient catalysts, the trifluoroacetato groups do not lead to an increase in catalyst efficiency, and the cationic complexes bis(triphenylphosphine) complexes **138** and **145** are the best catalysts, and on par with other reported systems.[**Error! Bookmark not defined.**b]. While the root cause for the reactivity difference between indy-5 and indy-6 complexes remains elusive, the comparable performance of dibromido and ditrifluoroacetato complexes can be explained mechanistically. The catalytically active species in Sonogashira cross-couplings is a palladium(0) complex, hence the initiation step necessarily involves the reduction of the precatalyst, which entails the loss of the anionic

coligands. If the initiation step is sufficiently fast, the nature of anionic coligands therefore has little influence on catalyst performance.

It is plausible to assume that the same active species is formed from complexes **136**-**138** and **142**-**145**. This means that in the case of **138** and **145**, an additional equivalent of phosphine is present in the reaction mixture, which can either stabilize the precatalyst or the resting state of the catalytic cycle, thus increasing catalyst turnover. This explains the quantitative yields observed with these complexes as precatalysts.

The diphosphine complexes **139**, **140**, **146**, and **147** were not completely inactive as precatalysts, but showed a significantly poorer performance than the triphenylphosphine complexes (entries 7, 8, 14, and 15). In contrast to the bis(triphenylphosphine) complexes, dissociation of one phosphorus donor from the metal center is unlikely due to the chelate effect, thus two coordination sites are permanently blocked in these complexes, and the coordination sphere is relatively crowded. This hampers the catalytic turnover, leading to the observed low yields.[i]

4.2. Post-modification of Indazolin-3-ylidene Complexes of Palladium(II)

4.2.1. Precursor Complex and Post-Modification

The introduction of additional donor sites in the side chain of the NHCs allows a more nuanced modification of the coordination sphere, enhances complex stability, and in the case of hemilabile donors, allows for the rapid generation of free coordination sites when they are needed in the catalytic cycle.[57] For indazolin-3-ylidenes, no donor-functionalized systems have been described so far. Therefore, the preparation of such ligands and the study of the corresponding complexes with transition metals in catalytic transformations are of great interest. The preparation of suitable ligand precursor salts requires the introduction of a non-coordinating wingtip substituent on N-1, which is the distal nitrogen atom, and a coordinating side chain on the proximal nitrogen atom N-2. However, there is no regioselectivity in the alkylation of indazoles, leading to mixtures of 1- and 2-alkylated species being formed upon the introduction of the first side chain.[150] These need to be tediously separated, which entails a loss of approximately half of the starting material,

[i] Contributions to chapter 4.1 by Ramasamy Jothibasu (first synthesis and partial characterization of **131** and **133**), Binbin Zhou (first synthesis and partial characterization of **135**, **136**, **137**, and **138**) and Ning Xi Chong (synthesis and characterization of **141**-**147**, and contributions to precatalyst screenings) are gratefully acknowledged.

before the second side chain can be introduced. In order to prepare a diverse library of side chain functionalized indy complexes, it is therefore desirable to place the diversity-generating step late in the synthetic sequence, based on a common starting material.[151] This minimizes the synthetic effort associated with an already cumbersome ligand precursor preparation. It has been shown that the introduction of additional functionalities into the NHC is even possible after the coordination to the metal center, which allows the very rapid generation of diversity and avoids individual metalation steps for each ligand.[59,152] In the case of indazolin-3-ylidenes, this approach requires the preparation of a 2-bromoalkyl substituted indazolium salt and its subsequent metalation (Scheme 4.10).[153,154]

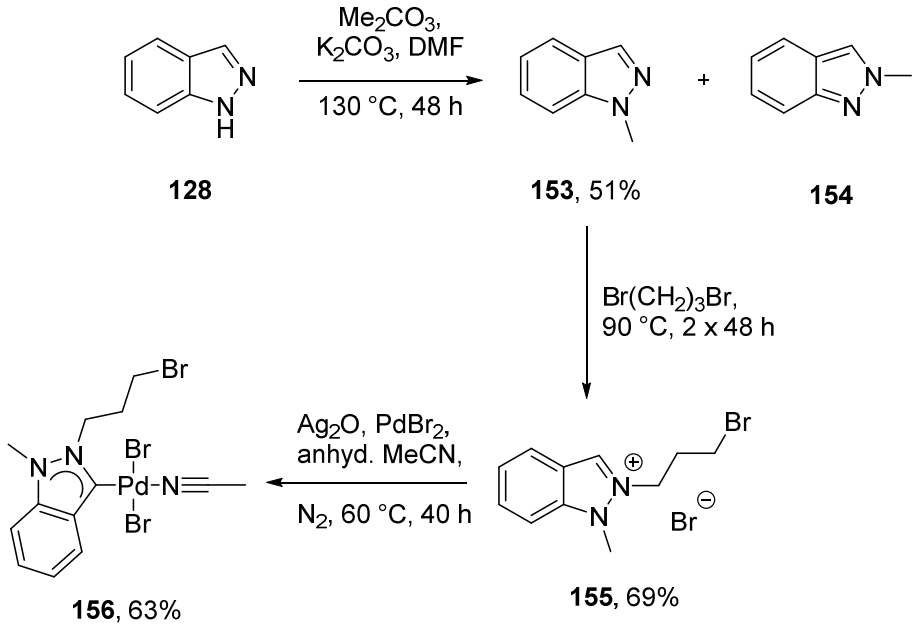

Scheme 4.10. Preparation of a palladium(II) indy complex as precursor for post-modification.

Indazole (**128**) could be conveniently alkylated using dimethyl carbonate as alkylating agent.[150b] The mixture of the desired 1-methylindazole (**153**) and the side product 2-methylindazole (**154**) could be separated by column chromatography. A second alkylation step using 1,3-dibromopropane as alkylating agent yielded the bromopropyl-functionalized imidazolium salt **155**, albeit long reaction times were required.[155] If the alkylation was carried out at higher temperatures, the fused-ring indazolium salt **131** − formed by intramolecular cyclization of **155** and elimination of methyl bromide − was isolated instead of **155**. A silver carbene transfer

reaction,[63a] carried out under anhydrous conditions to prevent solvolysis of the bromo functionality, yielded a *trans*-[$PdBr_2$(acetonitrile)(indy)] complex **156**. The overall yield of this three step sequence to this precursor for post-modification reactions, based on the starting material indazole, was 22%.

Complex **156**, which was an orange solid, was insoluble in esters, ethereal solvents, and hydrocarbons, poorly soluble in chlorinated solvents, and readily soluble in polar, coordinating organic solvents such as DMSO, acetone and acetonitrile. Its identity was confirmed by a full set of characterization data, and the ^{13}C NMR $C_{carbene}$ resonance, observed at 152.8 ppm, was close to the chemical shift for the carbene carbon in related complexes.[120,136]

As predicted, the introduction of functionalities by nucleophilic substitution of the bromo-moiety in the side chain of **156** was possible (Scheme 4.11).[154]

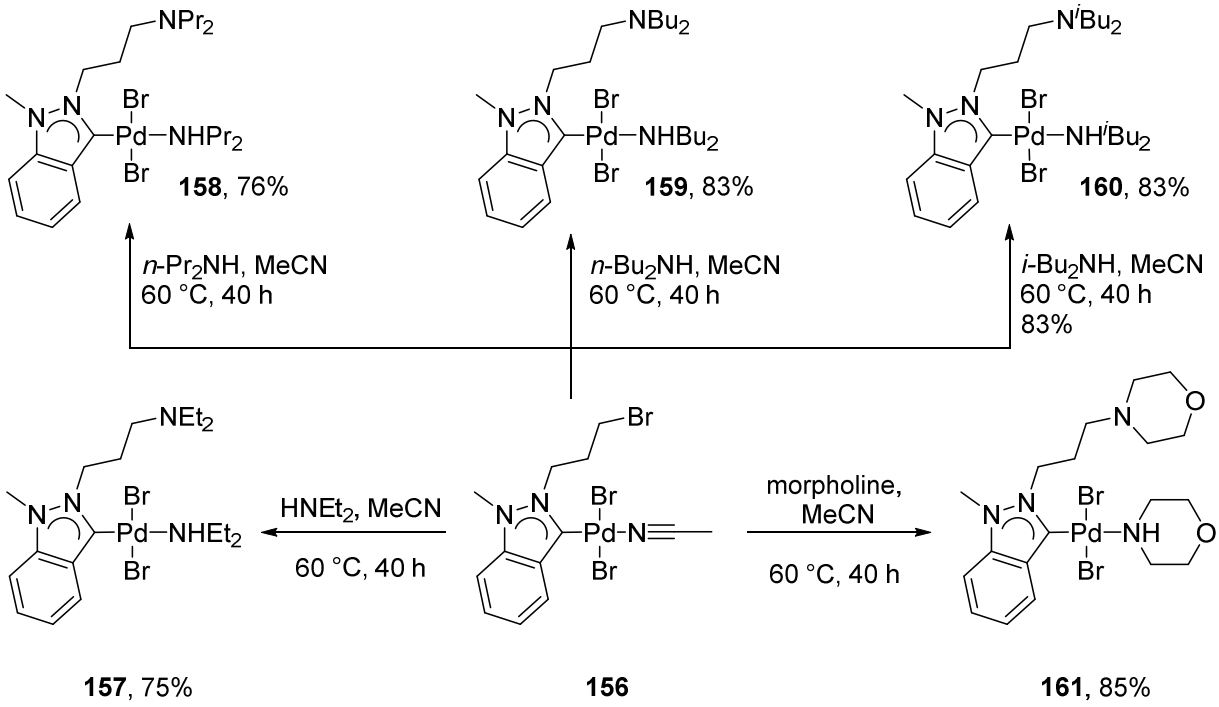

Scheme 4.11. Introduction of potentially coordinating groups by post-modification.

Using cyclic and acyclic secondary amines as nucleophiles, tertiarty amine functionalies could be introduced into the side chain in good yields.[ii] The amine, which was used in large excess, also performed the role of base in this reaction. Complexes **157-161**, which were obtained as yellow to orange solids, were readily soluble in chlorinated and polar organic solvents, and insoluble in hydrocarbons. In less polar organic solvents such as ethers and esters, the solubility depends on the lengths of the aliphatic side chains of the amine in the side chain.

Besides substituting the bromo-functionality in the side chain and neutralizing the side product hydrobromic acid, the secondary amines also displaced the acetonitrile ligand from the metal center. The identity of **157-161** as *trans*-[$PdBr_2$(amine)(indy)] complexes was confirmed by ESI-MS, elemental analysis, as well as ^1H and ^{13}C NMR data.

The ^{13}C NMR shifts of these complexes are particularly interesting. The $C_{carbene}$ resonances, are found ~8 ppm downfield from the corresponding resonance in **156** because of the more strongly donating nature of the secondary amine ligands,[48] and are close to values reported for the $C_{carbene}$ resonances of structurally related imidazolin-2-ylidene complexes with a secondary amine ligand in *trans*-position.[156] The $C_{carbene}$ chemical shift varies within series **157-161,** showing a dependence on the nature of the coordinated secondary amine (Table 4.5).

Table 4.5. ^{13}C chemical shifts of $C_{carbene}$ and pK_b values of the coordinated amines.

Complex	δ $C_{carbene}$ [ppm][a]	pK_b of the amine
157	161.0	3.02
158	160.9	3.00
159	161.2	2.75
160	160.6	3.50
161	158.9	5.64

[a] Recorded in $CDCl_3$.

Since the chemical shift of the carbene carbon in complexes of the formula *trans*-[PdX_2(NHC)(L)] (X = halide, L = any ligand of interest) shows a strong dependence on the ligand donor strengths of the ligand in *trans*-position, the observed variation in chemical shift can

[ii] Compounds **151-159** were synthesized and characterized by Harvenjit Singh. This includes the X-ray diffraction data for complexes **157-159**.

be assumed to be indicative for the ligand donor strength of the amines. Assuming a purely σ-donating interaction between the ligand and the metal center, ligand donor strength depends on the energy of the σ-HOMO orbital (*vide supra*), which in turn can be gauged by protonation reactions. Besides first proton affinities for carbon bases, which were used to this effect in chapter 2, basicities as described by pK_b values can be a useful measure of σ-electron density of the nitrogen lone pairs in the secondary amines, and a clear connection between this parameter and complex properties and reactivities has already been established.[157] And indeed, a strong correlation exists between the pK_b values of the metal-bound secondary amines[158] in **157**-**161** and the corresponding ^{13}C NMR $C_{carbene}$ shifts (R^2 = 0.9967, Fig. 4.6), which can not be explained by other factors such as an electronic influence of the different functionalities in the side chain.[59a]

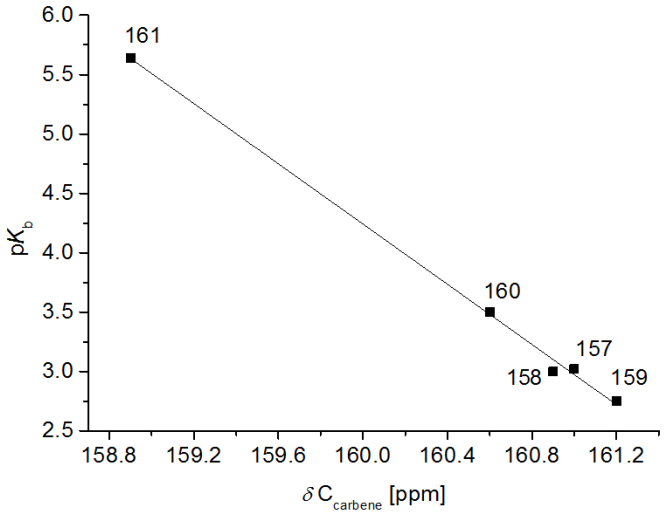

Fig. 4.6. Correlation of $C_{carbene}$ chemical shift and amine pK_b in *trans*-[$PdBr_2$(amine)(indy)] complexes.

Since the original aim was to study the influence of different chelating groups on complex properties and catalytic performance, the coordinated secondary amine ligand was an undesirable remnant of the functionalization reaction. However, attempts at removing it by stirring diluted solutions of the complexes, which is usually sufficient to cause weakly bound ligands to dissociate (cf. the dissociation of the pyridine ligand in **135**), did not lead to ligand dissociation and the formation of κ^2-*C*,*N*-chelated complexes. The apparent reason is a relatively strong bond between the amine ligand and the metal center. When studying catalyst iniation steps by

dissociation of nitrogen donors from palladium NHC complexes, Navarro *et al.* found that secondary amines form stronger bonds in *trans*-[$PdCl_2$(amine)(NHC)] complexes than tertiary analogues.[156b] Based on structural observations, it was concluded that intramolecular hydrogen bonds exist in these complexes between the nitrogen-bound proton in the secondary amine and one of the chlorido ligands. As a result, shorter Pd-N bond lengths as well as stronger than expected *trans*-influences and ligand donor strengths of the secondary amines are found.

For complexes **159**-**161**, molecular structures could be obtained by X-ray diffraction analysis performed on single crystals grown by slow evaporation of concentrated solutions in acetonitrile and chloroform (Fig. 4.7 and Table 4.6). However, it should be noted that instead of pure **159**, the hydrobromide **159**·HBr cocrystallized with two chloroform molecules. Since elemental analysis for **159** is consistend with a free amine complex, not the hydrobromide, the single crystal is not representative of the bulk of the material, and most likely formed by preferential crystallization of the protonated impurity.

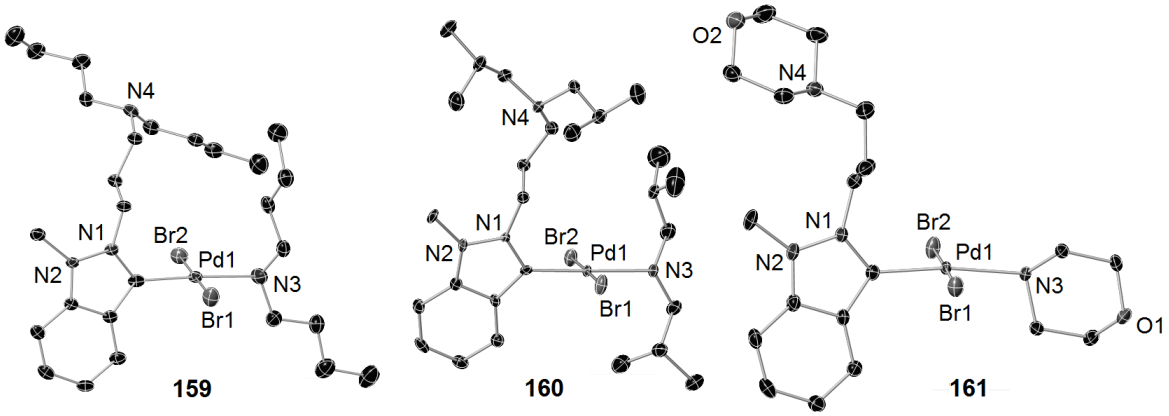

Fig. 4.7. Molecular structures of complexes **159**·HBr·2 $CHCl_3$, **160** and **161** (hydrogen atoms, solvent molecules, molecular disorder and counteranions have been omitted for clarity, thermal ellipsoids are drawn at 50% probability).

All three complexes have a square-planar coordination geometry, and the secondary amine ligands are positioned *trans* to the indy ligand. Similar to complexes **135**-**137** and **140**, which feature the indy-5 ligand, the indazolin-3-ylidene ring plane in **159**-**161** is close to perpendicular to the coordination plane. The aliphatic substituents on N-4 in **159** and **160** are almost perfectly aligned with the NHC ring plane, while the conformation of the propyl side chain in **161** prevents

such an alignment. In **159**, one of the butyl side chains of N-3 is crystallographically disordered. The Pd-C bond distances in these complexes range from 1.959(2) Å in **161** to 1.964(8) Å in **159**, while Pd-N bonds are between 2.128(8) Å in **159** 2.144(3) Å in **160** long. Interestingly, the Pd-C bond distance in *trans*-[$PdCl_2(NEt_2)$(SIPr)] is very similar to the values found for **159**-**161**, while the Pd-N bond in the imidazolidin-2-ylidene complex is shorter, due to the weaker *trans*-influence of the SIPr ligand.[156b] The Pd-Br bonds in **159**-**161** vary between 2.4186(5) Å and 2.4356(8) Å, which is in line with distances reported for structurally related complexes.[120,136]

Table 4.6. Selected bond lengths [Å] and angles [deg] in **159**·HBr·2 $CHCl_3$, **160** and **161**.

	159·HBr·2 $CHCl_3$	**160**	**161**
Pd1-C1	1.964(8)	1.961(4)	1.959(2)
Pd1-N3	2.128(8)	2.144(3)	2.142(2)
Pd1-Br1	2.4237(9)	2.4260(8)	2.4186(5)
Pd1-Br2	2.4249(9)	2.4356(8)	2.4225(5)
C1-Pd1-Br1	88.7(2)	87.1(1)	87.31(6)
C1-Pd1-Br2	90.8(2)	91.4(1)	90.74(6)
N3-Pd1-Br1	91.5(2)	92.23(8)	92.87(5)
N3-Pd1-Br2	89.0(2)	89.34(8)	89.25(5)
C1-Pd1-N3	176.8(3)	178.9(1)	172.44(8)
Br1-Pd1-Br2	178.87(4)	178.42(2)	177.65(2)

In line with the findings of Navarro *et al.*, the distances between the proton on N-3 and Br2 in complexes **160** and **161** are shorter than the sum of the van der Waals radii of the two atoms (3.05 Å)[159]. This is evidence for the existence of intramolecular hydrogen bonds in these complexes, which lead to a contraction of the Pd-N bonds and a tighter binding of the secondary amine to the metal center, thereby preventing ligand dissociation and formation of the κ^2-*C*,*N* chelates (Fig. 4.8). In complex **159**, the crystallographic disorder present in the secondary amine hampered the location of the nitrogen-bound hydrogen atom, thus making it impossible to prove or disprove the existence of a similar interaction in this complex. However, for all complexes **157**-**161**, the IR spectra exhibit the broad absorption bands typical for hydrogen bonding in the range from 3433 cm^{-1} to 3490 cm^{-1}, which is further evidence for the assumption that hydrogen bonding exists in all secondary amine complexes.

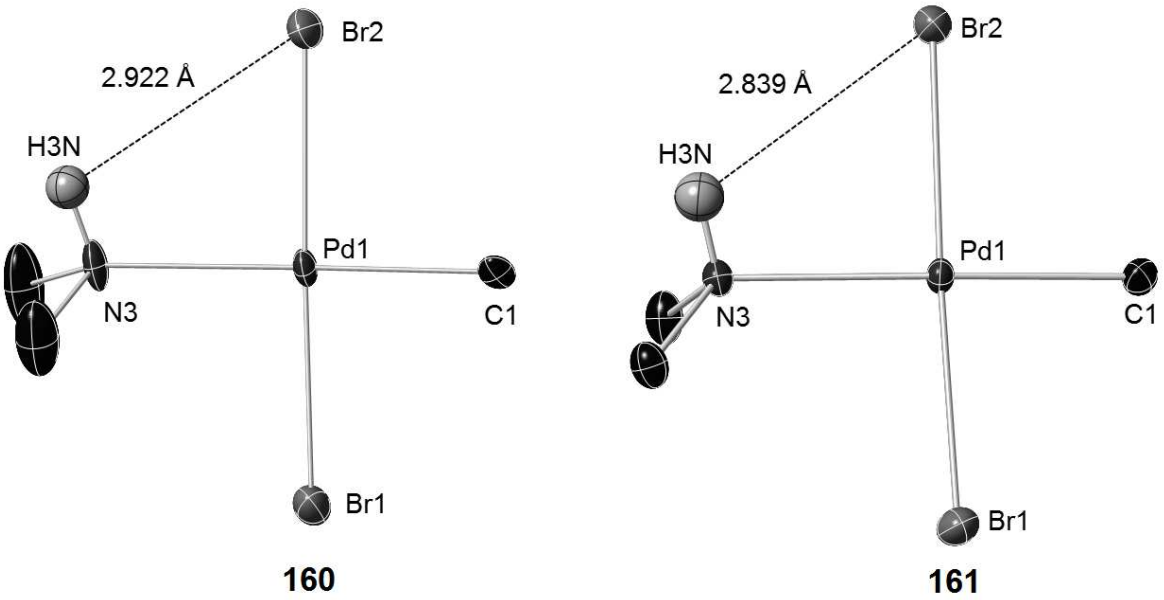

Fig. 4.8. Evidence for intramolecular hydrogen bonding in complexes **160** and **161**.

4.2.2. Application in the Direct Arylation of 1-Methylpyrrole

Similar to the direct arylation of pentafluorobenzene,[127] which avoids the use of difficult to handle and often troublesome to prepare organometallic reagents, and which avoids the formation of toxic heavy metal salts as byproducts, the direct arylation of electron-poor heteroaromatics is a greener and more efficient way to synthesize biaryl-derivatives by carbon-carbon cross-coupling. [160] The direct aylation of 1-methylpyrrole (**162**), which can be catalyzed by palladium(II) NHC complexes,[161] is an ideal benchmark to assess the catalytic activity of the unfunctionalized complex **156** and the amine-functionalized complexes **157**-**161** (Scheme 4.12).

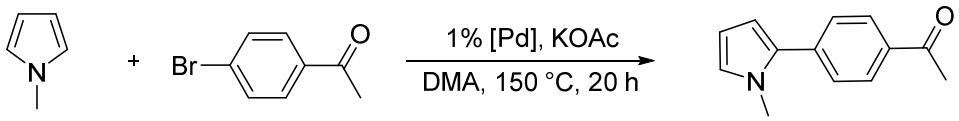

162 **151** **163**

Scheme 4.12. Direct arylation of 1-methylpyrrole with 4-bromoacetophenone.

When the reaction was run in the absence of a precatalyst, no product formation was detected (Table 4.7, entry 1). By contrast, when the reactions was run in the presence of 1 mol% of

catalyst under conditions previously used for the direct arrylation of pyrroles using NHC-based palladium(II) complexes as precatalysts, excellent yields in the range from 85% to 97% were obtained. Since complexes **156**-**161** are similar in terms of their electronic structure and the steric bulk of their ligands, similar levels of activity are found for all precatalysts. Yields are comparable to those obtained with previously reported precatalysts.[161b]

Table 4.7 Precatalyst screening for the direct arylation of 1-methylpyrrole.[a]

Entry	Precatalyst	Yield (%)[b]
1	-	0
2	**156**	85
3	**157**	97
4	**158**	88
5	**159**	87
6	**160**	84
7	**161**	88

[a] Reaction conditions: 1 mol-% precatalyst, 1-methylpyrrole (3.0 equiv.), 4-bromoacetophenone (1.0 mmol), KOAc (2.0 equiv.), DMA (3 ml), 150°C, 20 h. [b] Yields determined by GC-MS with decane as internal standard; average of two runs.

However, it is possible to discern a certain trend within the observed yields. The poorest precatalysts are complex **156** and **160**, which feature either a bromopropyl side chain or a tethered diisobutylamine functionality, while the most efficient precatalyst **157** has a diethylamine functionality in the side chain. The complexes only differ in terms of the secondary amine ligand, which is lost upon formation of the catalytically active species, and the nature (or absence) of the tertiary amine functionality in the side chain. Therefore, it is likely to assume that the coordination of the tertiary amine functinality, which can stabilize the catalytically active species, is the main factor which determines the yield of cross-coupled product **163**. In **157**, the relatively small ethyl groups allow for efficient coordination of the tertiary amine, thereby stabilizing the catalytically active species, while the absence of an amine functionality in **156**, or the steric shielding of it by the bulky isobutyl groups in **160**, doesn't allow this kind of stabilization. The other complexes occupy a middle ground between these extremes, and the

yields of **163** mirror the relative ease with which the tertiary amine can coordinate and prolong the catalyst lifetime under the harsh conditions required for the direct arylation to proceed.

4.3. Towards bulky indazolin-3-ylidene ligands

Despite the successful application of indy complexes of palladium(II) as precatalysts for Sonogashira couplings, hydroaminations, and the direct arylation of 1-methylpyrrole, their catalytic activities are severely limited in other reactions, which have been shown to be readily catalysed by palladium complexes featuring different types of NHC ligands.

Besides bulky phosphines, NHCs have been frequently used as ligands for Hartwig-Buchwald-type cross-couplings. [162] Indeed, the coupling between bromobenzene and pyrrolidine, a moderately reactive substrate for this type of reaction, proceeded in good yields when using the PEPPSI-type complex *trans*-[$PdCl_2$(IPr)(pyridine)] as precatalyst (Scheme 4.13).[74] However, under identical reaction conditions, not even traces of product could be detected when complexes **133** and **135**-**140** were used instead.

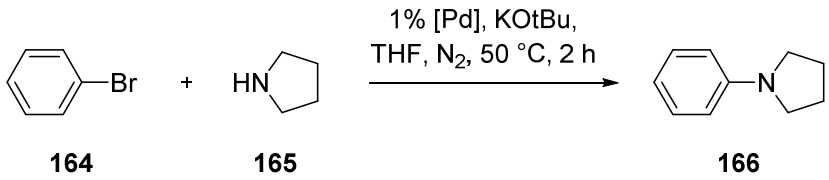

164 **165** **166**

Scheme 4.13. Hartwig-Buchwald cross-coupling using *trans*-[$PdCl_2$(IPr)(pyridine)] and indy complexes **133** and **135**-**140**.

Another useful reaction is the α-arylation of ketones. This reaction is mechanistically related to the cross-coupling between organometallic compounds and aryl halides, but instead of the former, *in situ* generated ketone enolates are used, and α-aryl ketones are obtained as the products. For this reaction to proceed, transition metal catalysts are required. Similar to the Hartwig-Buchwald coupling, complexes of late transition metals (typically group 10 metals) with bulky phosphine ligands have been used, but it has been demonstrated that palladium(II) NHC complexes are capable of acting as catalysts for this C-H functionalization reaction.[163] However, when the reaction between bromo- and chlorobenzene and propiophenone was examined under previously reported conditions was attempted, no product was found in the case of the reaction

with chlorobenzene, and only minor traces with bromobenzene (Scheme 4.14).[73b] Since these traces were close to the detection limit of GC-MS, attempts at reaction optimization were deemed to be futile.

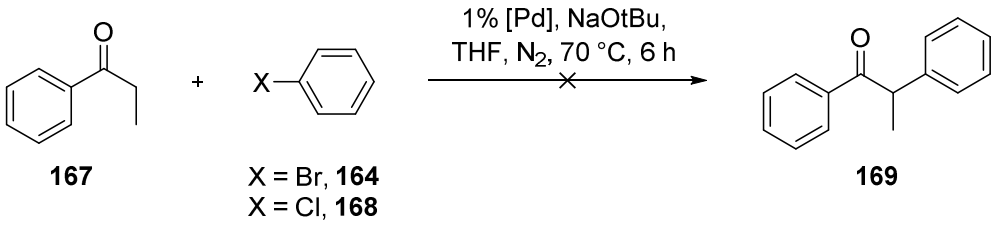

Scheme 4.14. Failed attempts at the α-arylation of propiophenone using indy complex **161** as precatalyst.

Due to the structural diversity of the indy complexes studied for their performance in the Hartwig-Buchwald amination and the direct arylation of propiophenone, it can be concluded that their poor performance must be traced back to the indy ligand itself. Possible shortcomings of this ligand could either be the inability to stabilize the catalytically active species under reaction conditions, or the undesired stabilization of an intermediate or resting state in the catalytic cycle to such an extent that no reaction can occur. The former possibility can be ruled out based on the performance of indy complexes in other types of reaction, which require even harsher reaction conditions than the ones used for the α-arylation and Hartwig-Buchwald cross-coupling.

When considering the catalytic cycles of both reactions, they both contain an oxidative addition step to an aryl halide as the first step, and the realese of the final product through reductive elimination. The introduction of the second substrate to the coordination sphere differs, however. In the Hartwig-Buchwald cross-coupling, the amine coordinates to the metal center, and is subsequently deprotonated by the base, while the ketone is first transformed into the enolate by the base, and subsequently transmetallated to palladium. Oxidative additions are favored by electron-rich, sterically readily accessible metal centers. It is reasonable to assume that the strongly σ-donating and sterically unassuming indy ligands are ideally suited to facilitate this step. The transmetallation step or the coordination of the amine and its subsequent deprotonation are equally favored by a sterically unencumbered metal center, although the reduced Lewis acidity of palladium(II) in the indy complexes might not be ideal for the coordination of the

amine. The reductive elimination is favored by an electron-poor metal center, and sterically bulky ligands.[52,149] Clearly, neither of these criteria are met in the indy complexes, and it can be assumed that the reductive elimination step is the main barrier that hinders both reactions.

In indazolin-3-ylidene ligands, only one nitrogen substituent is adjacent to $C_{carbene}$, and the other position at which sterically bulky moieties could be installed is C-7, wich is relatively remote to the carbene carbon, and modifications in this position are synthetically challenging.

The introduction of bulky substituents on N-2 is limited by the currently employed synthetic methodologies used for the preparation of indy ligand precursors. A survey of the literature reveals that with one exception, ligand precursor salts were prepared through alkylation reactions starting from indazole.[41] This approach is viable for the introduction of primary alky chains, but problems arise when different substituents at N-1 and N-2 are desired, because the first alkylation step proceeds without regioselectivity. No report has been made of the use of secondary or tertiary alkyl substituents in indazolium salts used as NHC precursors, although 2-isopropylindazole and 2-*tert*-butylindazole have been prepared by alkylation of indazole in moderate yields.[164]

A more flexible approach was chosen by Zhao and coworkers (Scheme 4.15).[41c] They reacted 2-nitrobenzaldehyde with different anilines, and subjugated the obtained imines to the Cadogan reaction, which produced the desired indazole by deoxygenation of the nitro group.[165]

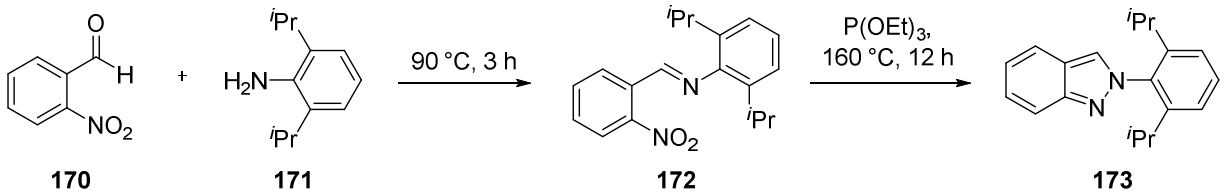

Scheme 4.15. 2-Arylindazole synthesized from 2-nitrobenzaldehyde.

Lee *at al.* have reported a different approach at constructing 2-substituted indazoles through a three-component condensation reaction. [166] Starting from commercially available 2-bromobenzaldehyde (**178**), the aldehyde functionality is converted into an imine *in situ* by reaction with either anilines or primary amines, and under copper catalysis, the bromide is converted into an azide. In a second catalytic step, the azide coordinates to copper, is activated

for an intramolecular attack by the imine nitrogen, and the heterocycle is formed, while dinitrogen is formed as a byproduct. In this reaction, a wide variety of anilines could be used as substrates, although sterically bulky anilines tend to give low yields. More interestingly, it has also been shown that functionalities such as esters and acetals can be present in the amine component, and that alkylamines such as cyclopropylamine and 1-adamantylamine are good substrates. This indicates that the introduction of the desired bulky substituents in 2-position is synthetically possible with this methodology, given the wide availability of primary amines and anilines.

In an initial assessment, the synthesis of four 2-functionalized indazoles was reproduced. (Scheme 4.16). Throughout, the yields were considerably lower than the reported yields, which is at least partially due to the unusually difficult workup procedures and the tedious separation of the product from byproducts and reagents by column chromatography.

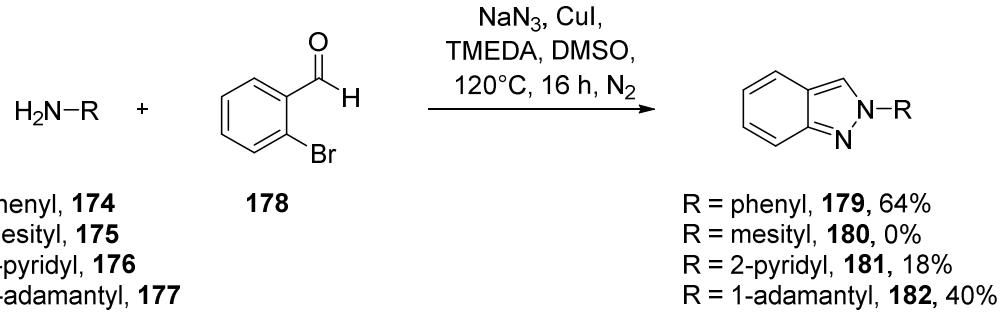

Scheme 4.16. Indazoles with aryl- and alkyl-substitution in 2-position made from 2-bromobenzaldehyde.

While no product could be isolated for the reaction mixture in the case of mesityl-subsituted indazole **180**, and yields were too low to be synthetically useful for 2-pyridyl-substituted indazole **181**, the phenyl- and 1-adamantyl-substituted indazoles **179** and **182** were isolated in moderate yields. When assessing these reactions for their usefulness, it should be kept in mind that alkylation reactions only yield ~50% of 2-substituted indazole. By comparison to this, the condensation route is a viable alternative. While the phenyl substituent in **179** is sterically unassuming, the 1-adamantyl moiety in **182** is very bulky, so this compound was the focus of further efforts. However, it was found to be impossible to convert **182** into an indazolium salt by alkylation in 1-position (Scheme 4.17). Neither the reaction with a large excess of ethyl iodide at

70 °C for 24 h, nor the attempted alkylation using an oxonium salt were successful, and the starting material was reisolated in both cases. Since oxonium salts were able to aklylate even very electron-poor pyrazoles under identical reaction conditions (*vide supra*), the reason **182** did not react is in all likelihood the steric shielding of N-1 by the bulky and unflexible 1-adamantyl group directly adjacent to it.

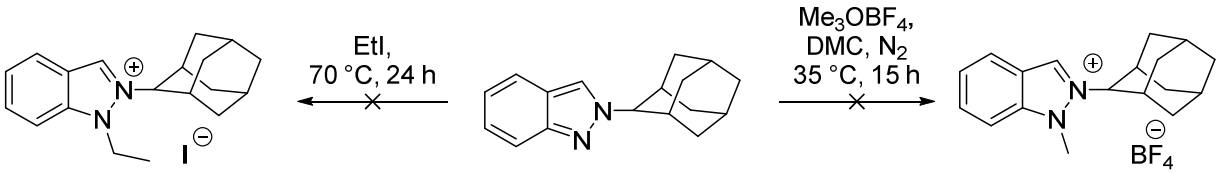

183 **182** **184**

Scheme 4.17. Attempted alkylation reactions with 1-adamantyl-substituted indazole **179**.

A reduction in steric bulk is possible by using changing the substituent in 2-position to a conformationally less rigid and less bulky group. Heartened by the fact that cyclopropylamine can undergo Sun *et al.*'s condensation reaction, cyclohexylamine was examined as substrate (Scheme 4.18). Indeed, 2-cyclohexylamineindazole (**186**) could be obtained in moderate yields, but the removal of trace impurities from the product was difficult even by column chromatography. Reasoning that the indazolium salt would be easier to purify, the still impure material was subjected to an alkylation reaction with methyl triflate. As expected, the low solubility of indazolium salt **184** in esters, ethereal solvents and hydrocarbons allowed to remove trace impurities, which were carried over from the condensation reactiong, by washing with diethyl ether, and an analytically pure product was obtained in a yield of 32% over two steps.

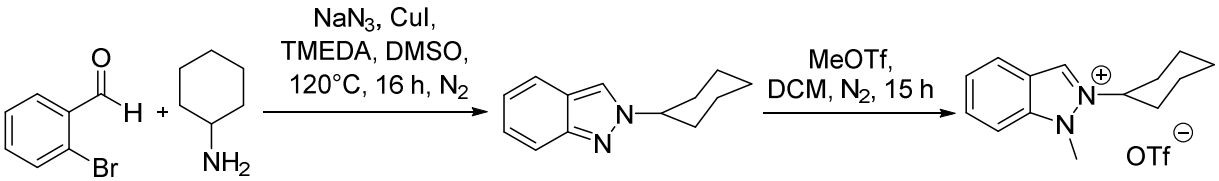

178 **185** **186** **187**
32% over 2 steps

Scheme 4.18. Synthesis of 1-methyl-2-cyclohexylindazolium triflate (**187**).

The relatively low yield of **187** is due to the low yield of the condensation product **186**, not because of the alkylation step which proceeded satisfactorily. In an attempt to suppress the formation of side products, the condensation of **178** and **185** to the imine was carried out as a separate step, followed by a separate reaction to exchange the bromide for an azide and condense these functionalities into the indazole ring. However, while the first reaction proceeded quantitatively, the second step gave yields that were equal to the one-pot procedure. Therefore, the additional experimental effort of carrying out two separate reactions did not pay off, and future efforts should be directed at optimizing the one-pot reaction instead by examining different copper(I) catalysts.

Having demonstrated the feasibility of preparing indazolium salts with bulky alkyl side chains in 2-position, the synthesis of palladium(II) complexes based on this ligand precursor was undertaken. Similar to salt **131**, the reaction with silver(I) oxide yielded a labile silver(I) NHC complex,[63a] which was directly used in transmetallation reactions to suitable palladium complexes. The reaction with $[PdBr_2(^iPr_2\text{-bimy}]_2$ (**30**) gave the hetero-bis(NHC) complex *trans*-$[PdBr_2(^iPr_2\text{-bimy})(\text{indy-Cy})]$ (**188**, indy-Cy = 1-methyl-2-cyclohexylindazolin-3-ylidene) in 78% yield, while transfer to *in situ* prepared $[PdBr_2(\text{acetonitrile})_2]$ yielded 71% of the dimeric species-$[PdBr_2(\text{indy-Cy})]_2$ (**189**), which is an analogous to **133** (Scheme 4.19).

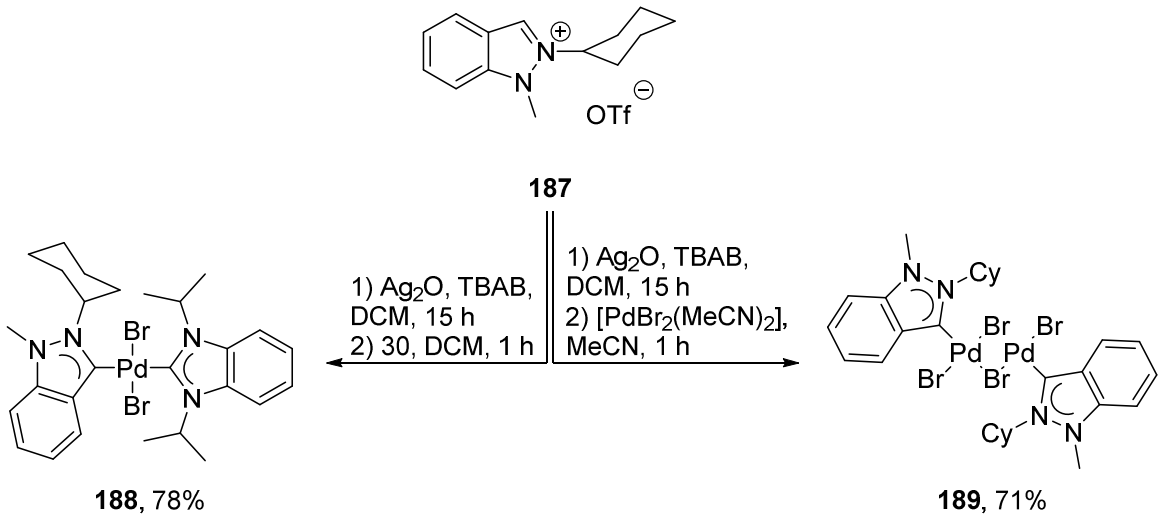

Scheme 4.19. Preparation of palladium(II) complexes bearing the indy-Cy ligand.

Both compounds were isolated as yellow solids. Their solubilities were comparable to those of structurally related complexes. Like hetero-bis(NHC) complex **116**, complex **188** is readily soluble in aprotic polar organic solvents and chlorinated solvents, while complex **189** behaves similar to acetonitrile adduct **117** and dimeric indy complex **133**, which are only soluble in polar organic solvents which can coordinate to the metal center, such as DMSO, acetonitrile, and DMF.[120,136]

The successful complex formation was corroborated by all characterization data. In the ^{1}H NMR spectra of **188** and **189**, the resonace attributable to the acidic proton on C-3 in **187** is not observed anymore, indicating deprotonation at this position and carbene formation. Upon complex formation, the most downfield resonance for the four aromatic protons of the indazole backbone was shifted further downfield by 0.2 − 0.5 ppm, while the remainder of the aromatic region was unchanged. The resonance assigned to the methine proton of the cyclohexyl ring experienced also a downfield shift by 0.2 − 0.3 ppm, while the nitrogen-bound methyl group resonated more upfield in the complexes than in the precursor salt.

For complex **188**, two $C_{carbene}$ resonances are present in the ^{13}C NMR spectrum. These are observed at 181.6 ppm and 177.8 ppm, respectively. By comparison to values reported for the related complex **116**, the former resonance can be assigned to the $^{i}Pr_2$-bimy ligand, while the latter belongs to the indy-Cy ligand. With a chemical shift for $^{i}Pr_2$-bimy above 180 ppm, indy-Cy is among the most strongly s-donating ligands placed on the ^{13}C NMR donor strength scale so far.[48]

The ^{13}C NMR spectrum of dimer **189** showed the $C_{carbene}$ peak at 157.0 ppm. This is downfield from the values found for the chemically similar complexes **117** and **133**.[120,136] It should be noted that the spectrum for this compound was recorded in DMSO-d_6, and instead of the acetonitrile adduct, which was the prevalent species in the NMR samples of **117** and **133**, a DMSO adduct of the formula *trans*-[$PdBr_2$(dmso)(indy-Cy)] was most likely the observed species in the case of complex **189**. This notion is supported by ESI-MS data, with peaks being assignable to mononuclear dmso adducts instead of a dimeric species. However, elemental analysis data for **189** is in agreement with the dimeric structure.

Single crystals suitable for X-ray diffraction experiments were grown from a concentrated dichloromethane/acetonitrile solution in the case of **188**, and a ternary mixture of

dichloromethane, DMSO and acetonitrile in the case of **189**, which crystallized as the acetonitrile adduct **190** (Fig. 4.9 and Table 4.8).

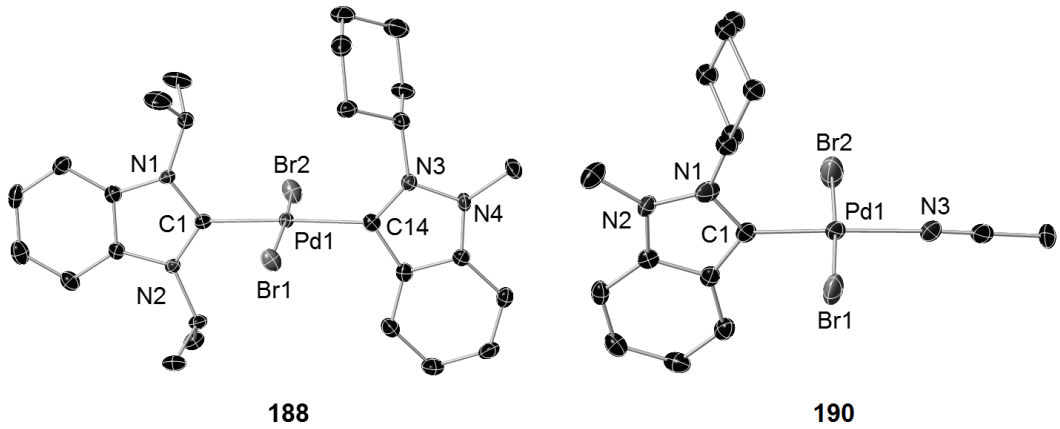

Fig. 4.9. Molecular structures of indy-Cy complexes **188** and **190** (hydrogen atoms and disordered in the cyclohexyl ring of **189** have been omitted for clarity, thermal ellipsoids are drawn at 50% probability).

Table 4.8. Selected bond lengths [Å] and angles [deg] in **188** and **190**.

	188	**190**
Pd1-C_{indy}	2.050(3)	1.949(4)
Pd1-C_{bimy}/N3	2.011(3)	2.077(4)
Pd1-Br1	2.4406(7)	2.4152(8)
Pd1-Br2	2.4373(6)	2.4277(8)
C_{indy}-Pd1-Br1	92.7(1)	87.1(1)
C_{indy}-Pd1-Br2	92.7(1)	89.8(1)
Br1-Pd1-C_{bimy}/N3	88.4(1)	90.6(1)
Br2-Pd1-C_{bimy}/N3	85.8(1)	92.5(1)
C_{indy}-Pd1-C_{bimy}/N3	176.4(2)	176.2(2)
Br1-Pd1-Br2	171.19(3)	176.89(2)

In both complexes, the palladium center adopts a slightly distorted square-planar coordination geometry with a *trans*-arrangement of the bromido ligands. The NHC ring planes are almost perpendicular to the coordination plane, and the bimy and indy ring planes in **188** are oriented

parallel to each other. This is different from the situation in the structurally related pyry complex **116**, where a torsion of ~18° was found between the ring planes. This indicates a lower level of steric congestion in complex **188**, possibly because of the greater conformational flexibility of the cyclohexyl ligand when compared to a phenyl group. In both **188** and **190**, the cyclohexyl moiety adopts a boat conformation.

The Pd-C bond distances in **188** are 2.031(5) Å for the Pd-C_{bimy} bond and 2.050(3) Å for the Pd-C_{indy} bond. While the former bond length is identical to the corresponding value in **116**, suggesting an equal level of *trans*-influence for the indy and pyry ligands, the Pd-C_{indy} bond in **188** is longer than the Pd-C_{pyry} bond in **116**.[120] By contrast, comparison of bond lengths between complex **190** and the indy and pyry congeners **134** and **117** reveals essentially identical Pd-C bond distances in all three compounds, and a slightly shorter Pd-N contact in **190**.[120,136] Nevertheless, bond distances and angles are in good agreement with the previously described structures.

The small acetonitrile ligand in **117**, **134** and **190** does not influence the conformation of the pyry and indy ligands in these complexes. Therefore, the molecular structures of these three compounds are ideally suited to calculate $\%V_{bur}$ values for the pyry, the indy-5 and the indy-Cy ligand (Fig. 4.10).[54]

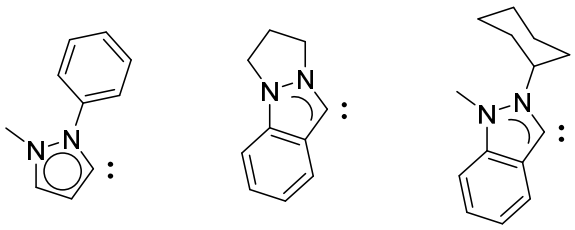

Fig. 4.10. Buried volume ($\%V_{bur}$) for the pyry, the indy-5 and the indy-Cy ligands.

With a buried volume of only 23.3%, the pyry ligand is the smallest among the three, followed by indy-5 with a buried volume of 25.1%. The indy-Cy ligand is the largest, with 27.5% of the coordination sphere shielded by it. However, it should be noted that despite the observed increase, the indy-Cy ligand is still less bulky than most commonly used NHC ligands.[54b]

Future work in this field should exploit the plethora of primary amines that are commercially available. This includes cycloalkylamines with varying ring-sizes and conformationally locked cycloalkylamines, and acyclic amines such as isopropylamine or *tert*-butylamine. However, a careful optimization of the three-component condensation reaction is required to pursue this approach further. An interesting alternative to the homogeneous catalyst used by Sun *et al.* is the application of copper nanoparticles as catalysts as described by Sarghi and Aberi, which has been demonstrated to give 2-*tert*-butylindazole in 79% yield.[166,167]

5. Thioether-functionalized NHC Complexes

Similar to the tethered tertiary amine functionalities in the side chain of NHC ligands, which were discussed in the previous chapter, it is also possible to include donor functionalities based on other elements. Donors based on nitrogen-, oxygen- and phosphorous are common, and κ^2-chelating as well as pincer-type complexes have been reported.[55,168] Usually, functionalities based on these elements form relatively strong bonds to transition metals. These complexes benefit from chelate effects, and especially in the case of pincer complexes, they can reach remarkable levels of stability. However, due to the irreversible binding of NHCs to metals and the strong coordination of the additional donor moiety, two coordination sites are inaccessible for substrates in the catalytic cycle. This is not true in the case of weakly coordinating functionalities, such as electron-poor donor sites, and in cases where hard donor is mismatched to a soft metal center or vice versa. In such situations, the tethered donor moieties exhibit hemilabile behavior, striking a balance between stabilizing the catalytically active species by chelation, and opening up coordination sites for incoming substrates.[57]

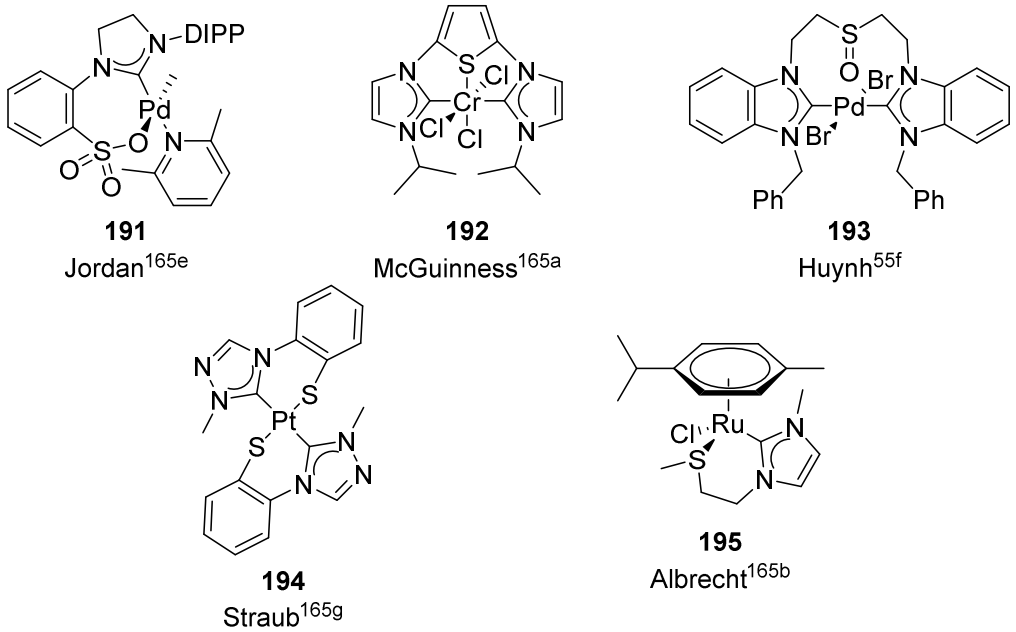

Fig. 5.1. Selected complexes bearing NHCs with sulfur-based functionalities in the side chain.

Sulfur-based functionalities in the side chains of NHC ligands have been less explored than donor-functionalities based on other elements.[169] Since sulfur can adopt a variety of oxidation states easily, a wide variety of sulfur-containing moieties can be introduced, which includes sulfonates, sulfoxides, thiolates, thioethers and thiophenes(Fig. 5.1).[55f, 170] Among these, especially thioethers exhibit pronounced hemilabile behavior, making them an excellent choice to be paired with strongly coordinating NHCs.[171]

5.1. Platinum(II) Complexes Bearing Thioether-functionalized Benzimidazolin-2-ylidene Ligands

5.1.1. Synthesis of Thioether-functionalized Benzimidazolium Salts

Benzimidazolium salts with an alkyl-alkyl thioether side chain can be prepared in three steps from benzimidazole (Scheme 5.1).[172]

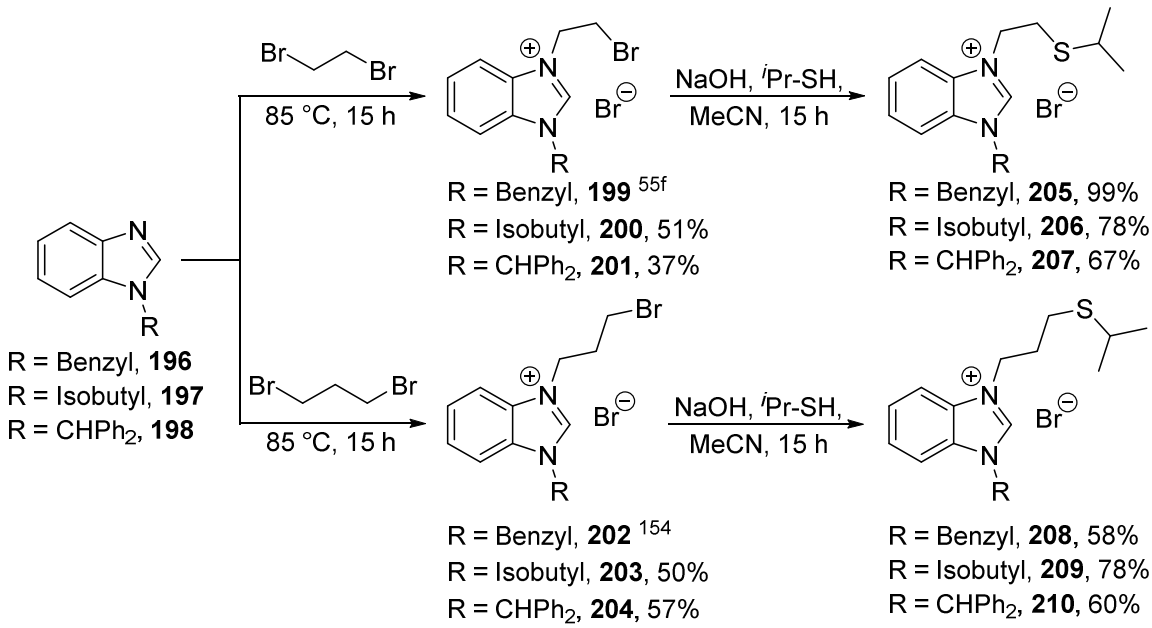

Scheme 5.1. Synthesis of thioether-functionalized benzimidazolium salts.

The preparation of benzimidazoles **196**-**198**, which bear substituents of varying steric bulk, can be done following established procedures.[124, 173] Deprotonation of benzimidazole by sodium hydroxide, followed by alkylation with alkyl bromides, yields **196**-**198** in good yields. The second side chain, which contains the thioether functionality, was built up in two steps.

Bromoethyl- and bromopropyl-substituted benzimidazolium salts were obtained by alkylation with 1,2-dibromoethane and 1,3-dibromopropane, respectively. The bifunctional reagents open up the possibility of side reactions. Since the products **199**-**204** contain a nucleophilic moiety themselves, they can react with another molecule of **196**-**198**, and form cross-linked, dicationic benzimidazolium salts. To mitigate this problem, a large excess of alkylation agent was used in a dual role as reagent and solvent.[55f,155] Unreacted 1,2-dibromoethane and 1,3-dibromopropane could be recycled by distillative removal from the reaction mixture, and used for subsequent batches. Nevertheless, considerable amounts of dicationic byproduct were formed, from which the products had to be isolated by extraction with dichloromethane. In this solvent, the desired, monocationic products are somewhat soluble, while the dicationic, cross-linked material did not dissolve. The products were obtained as colorless solids, and generally showed low solubilities in chlorinated and polar aprotic organic solvents, while being insoluble in ethereal solvents and hydrocarbons.

The bromoalkyl-substituted benzimidazolium salts **199**-**204** were then subjected to a nucleophilic substitution with propane-2-thiolate, which was generated in situ by deprotonation of the corresponding thiole with sodium hydroxide under an inert atmosphere to prevent the formation of disulfides. After 15 h, thioester-functionalized benzimidazolium salts could be isolated in moderate to excellent yields. With the exception of **209**, which was a highly viscous oil, all benzimidazolium salts were isolated as white or off-white solids. With the introduction of the thioether moiety into the molecule, solubilities in chlorinated solvents increased markedly, but the salts **205**-**210** remained insoluble in hydrocarbons and ethereal solvents.

5.1.2. Platinum(II) Complexes: Synthesis and Characterization

Three different pathways were explored for the preparation of κ^2-*C*,*S* platinum(II) complexes incorporating ligands **205**-**210**. Using platinum(II) acetylacetonate as a precursor complex with basic ligands, in the presence of potassium bromide as external bromide source, did not lead to the formation of a chelating complex when using benzimidazolium salt **205**, even after prolonged heating of the reaction mixture in acetonitrile.[174] In the case of platinum(II) bromide as metal source and sodium acetate as external base, the formation of small amounts of a platinum(II) complex was observed, but the reaction was accompanied by a severe amount of decomposition reactions which led to a very low yield, and the crude mixture was found to be hard to purify.

The silver carbene transfer protocol was found to be a higher yielding and more convenient route to platinum(II) NHC complexes.[63a] Unstable silver(I) NHC complexes were formed in the reactions of benzimidazolium salts **205-210** with silver(I) oxide. These species, which could not be isolate in substance but were observed by means of ESI-MS, were directly reacted with freshly prepared [$PtBr_2(dmso)_2$] solutions. In each case, the transmetallation proceeded rapidly, and platinum(II) NHC complexes were isolated in moderate to good yields (Scheme 5.2).

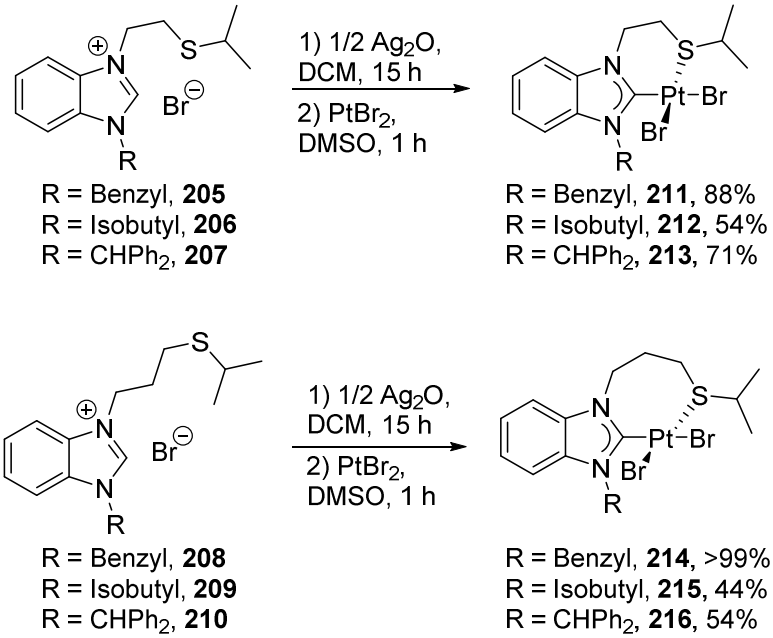

Scheme 5.2. Synthesis of κ^2-*C*,*S* platinum(II) NHC complexes **211-216**.

The platinum(II) complexes **211-216** were obtained was white to off-white, microcrystalline solids. Yields varied widely, from a mere 44% for complex **215** to a quantitative yield in the case of **214**. All six complexes showed unusually low solubilities. They were insoluble in most common organic solvents, and sparingly soluble in chlorinated solvents and DMSO.

For this reason, NMR samples were prepared using DMSO-d_6. The ^{1}H NMR spectra of **211-216** differed clearly from those of the precursor salts **205-210**. The resonance of the acidic proton on C-2 in the benzimidazolium salts was not observed anymore in the spectra of the complexes, indicating their successful deprotonation and conversion into benzimidazolin-2-ylidenes. While changes to the chemical shifts of the resonances in the aromatic region were only minor, differences in the aliphatic region were drastic. The signals attributable to the thioether side

chains changed dramatically, with a downfield shift of the resonances in the complexes, and a marked increase in the complexity of coupling patterns. Since the κ^2-*C*,*S* coordination mode renders the methylene protons in the newly formed metallacycle diastereotopic, such changes were to be expected, and confirm the assigned structures of complexes **211**-**216**. Interestingly, diasterotopic splitting of the NCH_2 protons of the isobutyl side chains in **212** and **215** is also observed.

The $C_{carbene}$ resonances in the ^{13}C NMR spectra of the platinum(II) complexes **211**-**216** had chemical shift in the range from 150.6 ppm to 156.0 ppm. These values agree well with previously reported chemical shifts for platinum(II) complexes with benzimidazolin-2-ylidene ligands.[175] The resonances did not show satellites caused by carbon-platinum coupling. This is not uncomon because of the low signal intensity of $C_{carbene}$ resonances, which together with the poor solubility of **211**-**216** made it impossible to observe these weak signals.

For complexes **214** and **216**, the NMR spectra showed the presence of multiple species. Attempts at separating them by means of crystallization or column chromatography failed. This suggests a dynamic equilibrium between these species, which is not uncommon for complexes of thioether-functionalized NHCs with group 10 metals.[57d,171b,c] While platinum(II), as the softer metal center, has a higher affinity for sulfur-based donor moieties then the comparatively harder palladium(II), it is not impossible that destabilizing factors in **214** and **216**, such as the ring strain in the seven-membered metallacylce, destabilize the κ^2-*C*,*S* chelate form sufficiently to induce conversion into other species (Fig. 5.2).

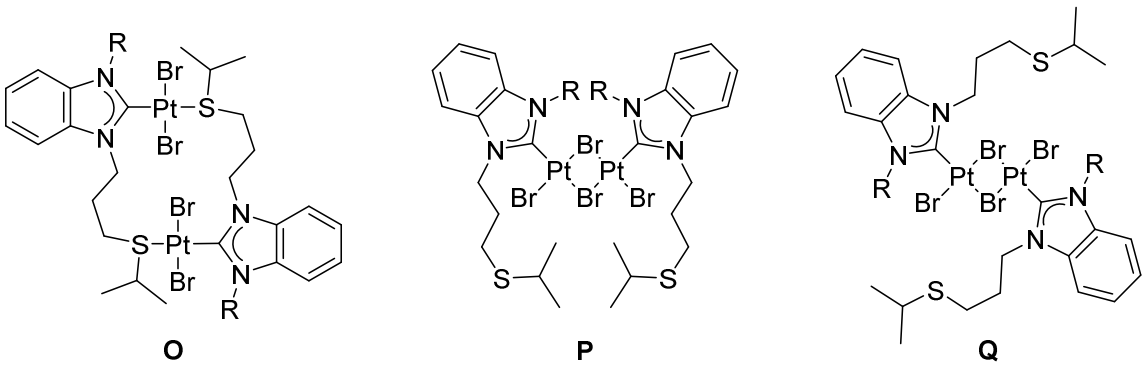

Fig. 5.2. Dimeric species potentially coexisting with the monomeric complexes **214** and **216**.

To confirm the assigned structures, single crystal X-ray diffraction experiments were carried out. The prerequisite single crystals of **211**-**216** were grown by slow evaporation of concentrated solutions(**212**, **214**, and **215** from dichloromethane, **211** from dichloromethane/THF, **213** from dichloromethane/hexane, and **216** from dichloromethane/toluene). As expected based on spectroscopic data, the chelating κ^2-*C*,*S* coordination mode was found for all complexes (Fig. 5.3, Fig. 5.4, and Fig. 5.5).

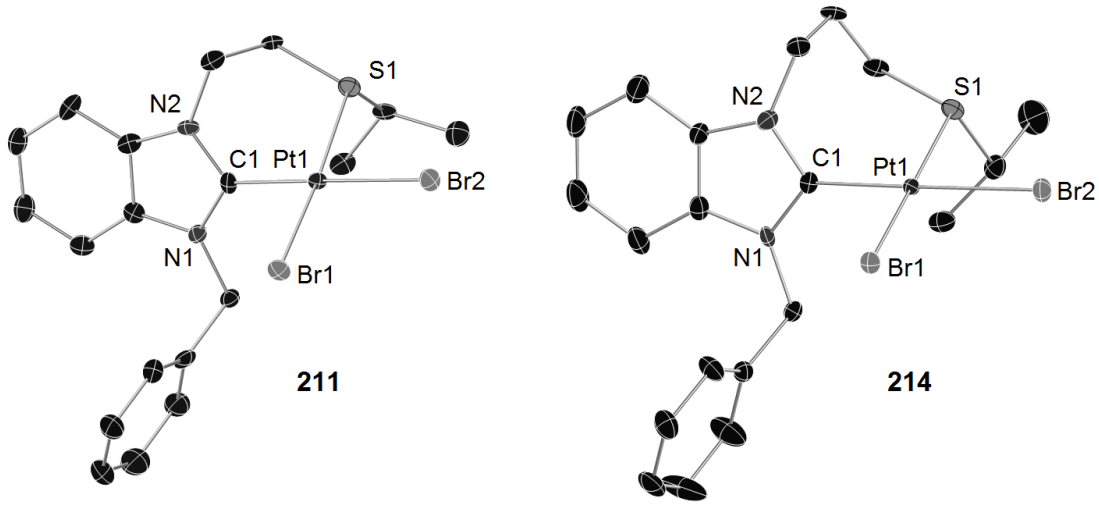

Fig. 5.3. Molecular structures of complexes **211** and **214** (hydrogen atoms have been omitted for clarity, thermal ellipsoids are drawn at 50% probability).

The coordination geometry at the platinum center is distorted square-planare in all cases, with a *cis*-arrangement of the bromido ligands. While a *trans*-geometry would be energetically more favorable purely on electronic grounds, it is not possible due to the constraints imposed by the tether between the thioether and NHC moieties. The six- and seven-membered metallacycles in the chelate complexes adopt slightly distorted boat conformations, irrespective of the number of atoms in the ring. The plane defined by the aromatic system of the benzimidazolin-2-ylidene ligand is twisted out of the coordination plane by 55.0(5)-71.5(5)°. Thes values are lower than the twist observed in the indy complexes described above. The most plausible reason for this different behavior is the constraint imposed by the tether between the two coordinating moieties, which severely restricts twist angles in the case of complexes **211**-**213** with ethylene-thethered thioethers. For the propylene-tethered complexes **214**-**216**, which possess a higher degree of

conformational freedom due to the longer linker, the twist angles are generally larger than in their ethylene-tethered analogues.

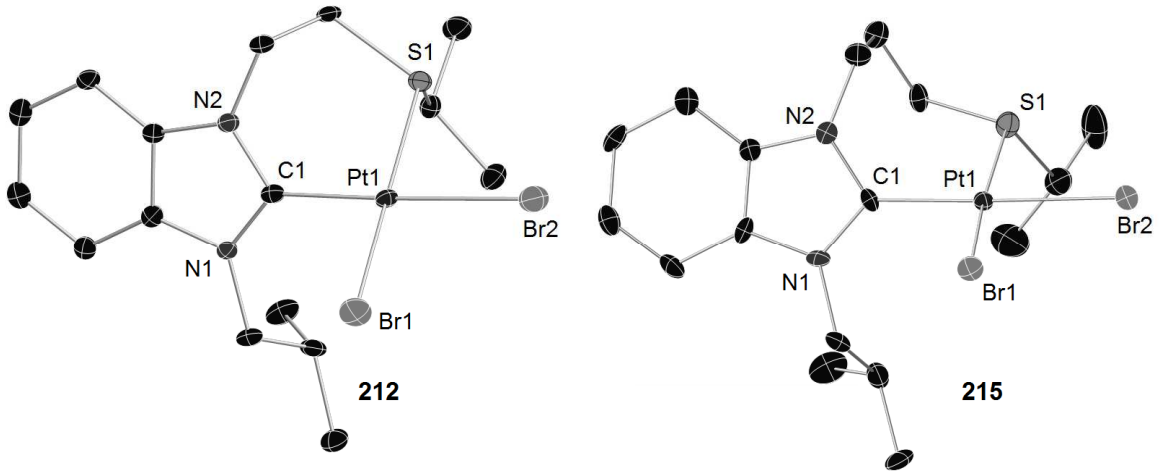

Fig. 5.4. Molecular structures of complexes **212** and **215**·0.5 CH_2Cl_2 (hydrogen atoms and solvent molecules have been omitted for clarity, thermal ellipsoids are drawn at 50% probability).

Table 5.1. Selected bond lengths [Å] and angles [deg] in complexes **211**-**216**.

	211	**212**	**213**·MeC	**214**	**215**·0.5CH_2Cl_2	**216**
Pt1-C1	1.972(8)	1.972(6)	1.972(5)	1.970(5)	1.975(9)	1.971(6)
Pt1-S1	2.267(2)	2.271(1)	2.279(2)	2.267(1)	2.277(3)	2.277(1)
Pt1-Br1	2.4478(9)	2.4410(7)	2.4546(7)	2.4580(6)	2.444(1)	2.4496(7)
Pt1-Br2	2.4819(9)	2.4765(7)	2.4845(5)	2.4824(6)	2.492(1)	2.4886(8)
C1-Pt1-S1	92.0(3)	90.6(2)	91.5(2)	93.1(2)	94.5(3)	94.2(4)
C1-Pt1-Br1	89.5(3)	93.3(2)	91.8(2)	89.4(1)	91.1(3)	91.4(2)
S1-Pt1-Br2	88.23(6)	84.99(4)	87.28(4)	84.83(4)	85.11(7)	83.21(4)
Br1-Pt1-Br2	90.48(3)	91.45(2)	89.90(2)	92.70(2)	89.00(4)	91.08(2)
C1-Pt1-Br2	179.0(3)	174.7(2)	176.7(2)	177.9(1)	178.0(3)	177.0(2)
S1-Pt1-Br1	171.21(6)	171.86(4)	169.18(4)	174.83(4)	171.44(7)	173.03(4)

The ligand-platinum bond distances varied only marginally between different complexes (Table 5.1). For the Pt-C bond, an average bond length of 1.972 Å was found, and the average Pd-S bond length was 2.273 Å. Since the NHC and the thioether moiety differ vastly in terms of

trans-influence, the average Pt-Br1 bond was shorter with an average length of 2.449 Å, while a longer average bond distance was found for the Pt-Br2 bond *trans* to the carbene with an average 2.484 Å. All observed bond lengths are comparable to previously reported for structurally related complexes.[175]

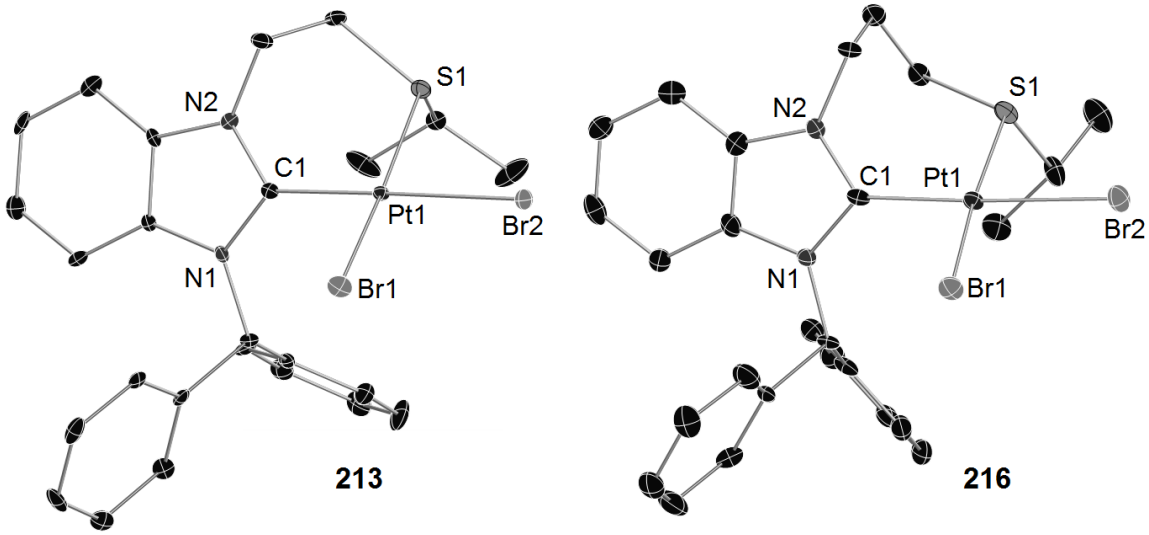

Fig. 5.5. Molecular structures of complexes **213**·MeCN and **216** (hydrogen atoms and solvent molecules have been omitted for clarity, thermal ellipsoids are drawn at 50% probability).

5.1.3. Applications in Catalysis

Hydroaminations of carbon-carbon multiple bonds are an important class of atom economic transformations.[143] Although they are thermodynamically favored, they require a catalyst to proceed. Besides palladium NHC complexes (*vide supra*),[136,137b,142] salts and complexes of group 9 to group 12 metals catalyze these reactions,[176] including NHC complexes of other metals such as zirconium, rhodium, iridium and gold.[94c,177] Platinum, whether as a simple salt or in more elaborate complexes, can also catalyze hydroaminations,[178] and a number of platinum NHC complexes have been reported as active catalysts.[73d,179] For this metal, detailed experimental and computational studies are also available.[180]

To assess the catalytic activities of complexes **211**-**216** for intermolecular hydroamination reactions, the same model reaction as in chapter 4 was chosen - the hydroamination of phenylacetylene with sterically hindered 2,6-dimethylaniline (Scheme 5.3, cf. also Scheme 4.8).

However, due to the higher activity of the platinum(II) complexes, milder conditions and shorter reaction times could be used (Table 5.2).

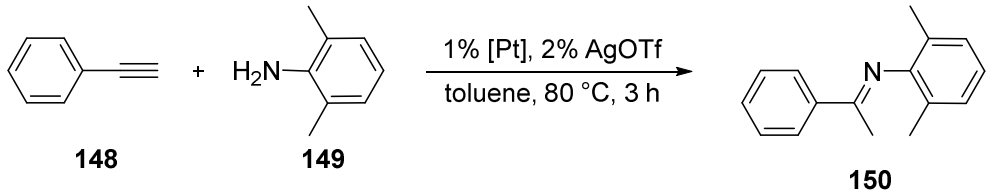

148 **149** **150**

Scheme 5.3. Hydroamination of phenylacetylene using platinum catalysts.

Table 5.2. Catalytic performance of platinum complexes for the intermolecular hydroamination.[a]

Entry	Precatalyst	Yield (%)[b]	
		No additive	+ 2% AgOTf
1	-	0	8
2	**211**	0	34
3	**212**	3	75
4	**213**	1	87
5	**214**	0	38
6	**215**	0	31
7	**216**	0	61

[a] Reaction conditions: 1 mol% precatalyst, phenylacetylene (2.0 eq), 2,6-dimethylaniline (1.0 mmol), toluene (3 mL), 80 °C, 3 h. [b] Yields determined by GC-MS with decane as internal standard, average of two runs.

At temperatures of 80°C, and reaction times of 3 h, all six complexes were able to catalyze the formation of imine **150** in moderate to good yields, and similar to the reaction catalyzed by palladium(II) NHC complexes, the Markovnikov product was exclusively observed. However, the presence of silver(I) triflate was required to enhance the catalytic activity, most likely by in situ removal of the bromido coligands and generating free coordination sites. In the absence of this additive, only trace amounts of **150** could be detected with complexes **212** and **213**, which were also the most active precatalysts when silver(I) triflate was added. Without the addition of a platinum precatalyst and silver salt, no product formation was observed, while a small amount of

150 was formed when only the silver(I) triflate was present. However, with a yield of only 8%, silver(I) triflate on its own is a poor catalyst.

The best-performing precatalysts were complexes **213** and **216**, which bear NHC ligands with the bulky benzhydryl side chain. While in the absence of silver(I) triflate, the reaction is limited by substrate coordination to platinum(II), with the additive the rate-limiting step is most likely the dissociation of the product from the metal center after the attack of the amine on the activated alkyne. The higher steric bulk of the NHC ligand in **213** and **216** favors this step, which explains the good yields. When comparing between the ethylene-tethered complexes **211**-**213** and the propylene-tethered complexes **214**-**216**, on average better results were obtained with precatalysts that have a six-membered metallacycle. It should be noted, however, that complex **214** with a seven-membered metallacycle slightly outperformed its six-membered metallacycle analogue **211**. The reason for the superior performance of **212** and **213** is the higher stability of the less strained six-membered ring, which enhances the stability of the catalytically active species and prolongs its lifetime.

In comparison to other catalysts described for this reaction, the best-performing precatalyst **213** allowed for shorter reaction times, lower catalyst loading, and milder reaction conditions.[181]

Since complexes **211**-**216** were active precatalysts for the intermolecular hydroamination of alkynes, the question arises whether they are able to catalyse other hydroelementation reactions and whether they show reactivity towards alkenes as well. Hydrosilylations are a convenient way to synthesize alkylsilanes and alkenylsilanes,[182] and the most commonly employed catalysts for this reaction, the Speier catalyst and the Karstedt catalyst, are based on platinum.[183] One of the major drawbacks of these commercially used systems is the rapid formation of platinum black during the reaction, which reduces the regioselectivity of the hydrosilylation. For platinum(0) and platinum(II) NHC complexes, higher complex stabilities are found and the problematic decomposition to platinum black does not occur as readily.[73a,184]

To study the activity of the platinum(II) complexes **211**-**216**, the reaction between styrene and bis(trimethylsilyloxy)methylsilane was chosen as benchmark, using reaction conditions which have been previously used for this reaction with platinum NHC complexes (Scheme 5.4).[184j] The catalytically active species is formed rapidly under reaction conditions, so in in contrast to the hydroamination, no additives were required for this reaction.[185]

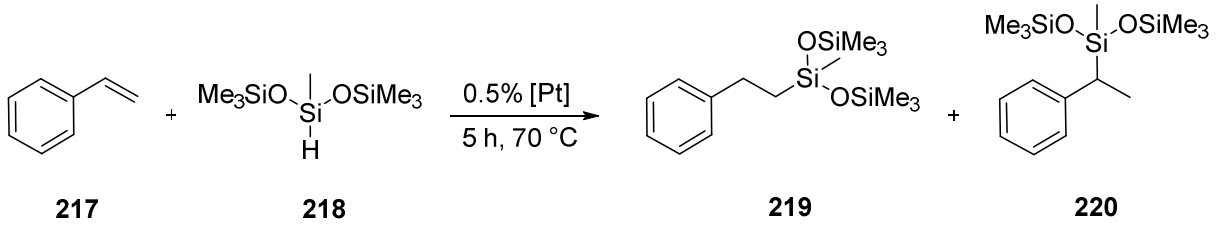

217 **218** **219** **220**

Scheme 5.4. Hydrosilylation of styrene catalyzed by platinum(II) NHC complexes.

Table 5.3. Precatalyst screening for the hydrosilylation of styrene.[a]

Entry	Precatalyst	Yield (%)[b]	**219**/**220**
1	-	0	-
2	**211**	79	87/13
3	**212**	75	87/13
4	**213**	86	88/12
5	**214**	>99	89/11
6	**215**	>99	88/12
7	**216**	>99	88/12

[a] Reaction conditions: 0.5 mol% precatalyst, styrene (4.0 mmol), silane **218** (1.1 eq), 70 °C, 5 h.
[b] Yields determined by GC-MC with decane as internal standard, average of two runs.

All tested complexes showed a high level of activity under very mild conditions, and no formation of platinum black was observed. After 5 h at 70°C, quantitative yields were obtained when complexes **214**-**216** were used as precatalysts, while lower yields were produced when using **211**-**213** (Table 5.3). During the reaction, it was observed that the complexes were only sparingly soluble in the reaction mixture, and differences in solubility are the most likely cause for the observed trends in catalytic activity. The longer aliphatic side chain in the best-performing complexes enhances the solubility in the relatively unpolar reaction mixture, thus increasing the concentration of the catalyst. This in in line with observations made in previous studies, which report that at temperatures lower than 50 °C, low reactivities were observed due to the poor solubilities of the precatalyst.[184j]

While for **214**-**216**, uniformely quantitative yields were observed, differences in reactivity were discernible for ethylene-tethered complexes **211**-**213**. Complex **212** with an isobutyl wingtip on the NHC ligand gave the lowest yields, followed by the complex **211** bearing a benzyl side chain

on the ligand, and complex **213** with the benzhydryl-substituted NHC gave the highest yield. However, it remains unclear whether this trend depends on complex solubilities or a beneficial influence of the increasing steric bulk.

In all cases, the linear regioisomer **219** was the major product, but in contrast to the hydroamination, the reaction also produced the regioisomeric, branched alkylsilane **220** as a minor product. The observed selectivities for **219** were similar for all complexes and slightly better than those observed in previous studies.[184j]

5.2. Palladium(II) Complexes Bearing Thioether-functionalized Benzimidazolin-2-ylidene Ligands

5.2.1. Complex Synthesis, Characterization, and Dynamic Behavior

While the silver carbene transfer reaction with benzimidazolium salts **205**-**210** to the $[PtBr_2(dmso)_2]$ complex gives platinum(II) NHC complexes **211**-**216**,[63a,172] by transfer to $[PdBr_2(acetonitrile)_2]$ instead, the palladium(II) analogues **221**-**226** can be obtained (Scheme 5.5).[186]

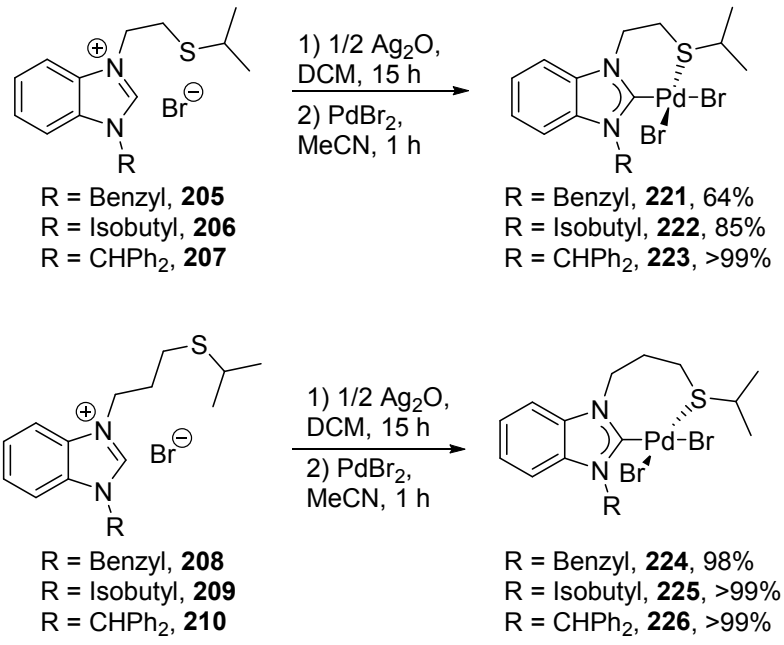

Scheme 5.5. Synthesis of κ^2-*C*,*S* palladium(II) NHC complexes **221**-**226**.

While complexes **221** and **222** were isolated in moderate to good yields, quantitative or near-quantitative yields were obtained for all other complexes. The complexes are microcrystalline, yellow solids with poor solubility in chlorinated solvents such as dichloromethane and polar organic solvents such as DMSO. In ethereal solvents, esters and hydrocarbons, they are completely insoluble. This is in line with the behavior for other *cis*-complexes of group 10 metals, which also showed poor solubility. However, in the presence of strongly coordinating solvents such as pyridine, the weakly bound thioether moiety can be displaced from the metal center, and more soluble *trans*-adducts are obtained.

While **221**-**226** could be characterized by ESI-MS, elemental analysis, and X-ray diffraction studies in some cases, NMR spectra of the chelating complexes could not be recorded because of their poor solubilities. The situation was further complicated by the fluxional behavior exhibited by these complexes, which resulted in signal broadening due to a coalescence temperature close to ambient temperature. Therefore, the signals of the methylene groups in the thioether side chains, which were particularly affected by this behavior, were not observable. Since solubilities were already low in DMSO-d_6 at ambient temperatures, measurements at low temperatures were impossible. However, the high boiling point of DMSO allowed to conduct measurements at elevated temperatures up to 368 K (Fig. 5.6).

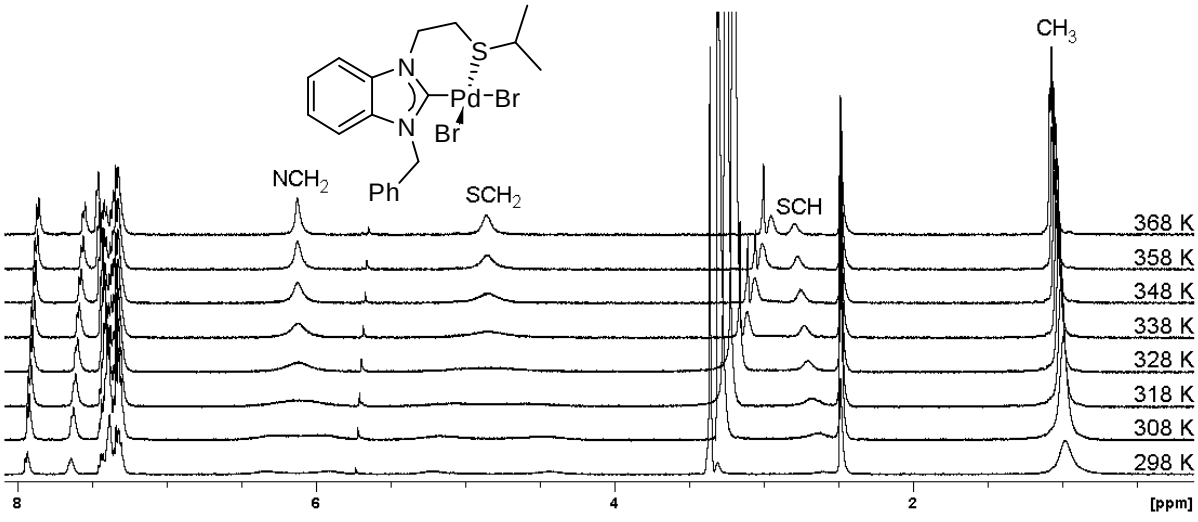

Fig. 5.6. Variable temperature ^{1}H NMR spectra of complex **221** in DMSO-d_6.

In the ^{1}H NMR spectrum of **221**, the resonances of the four protons in the ethylene liker were spread out into broad, barely detectable peaks, and the methine proton of the isopropyl moiety could not be observed at all at ambient temperature. As the temperature was increased, full coalescence occurred for these three singals, and by lowering the temperature again to 298 K, the initial spectrum could be fully restored. By contrast, the coalescence temperatures for complexes **222-226** are higher, and these complexes decomposed before it could be reached.

Since the low solubility of complexes **221-226** made their spectroscopic characterization difficult, and the fluxional behavior due to the weak coordination of the thioether moiety additionally muddled the situation, the complexes were converted into their pyridine adducts by reacting them with this ligand in dichloromethane. For complexes **221-223**, clean adducts were obtained quantitatively, while mixtures of the desired adducts and other species were found in the case of complexes **224-226** with the propylene tether in the side chain. Purification attempts failed for these complexes because of a rapid re-equilibration.

The pyridine adducts of **221-223** are readily soluble in polar organic solvents and chlorinated solvents, which made it possible to record their NMR spectra in deuterated chloroform. The ^{1}H NMR spectra confirm the successful formation of NHC complexes, by the absence of the resonance due to the acidic proton on C-2. As expected, the introduction of an additional donor ligand into the complex suppressed the dynamic behavior, and sharp multiplets were observed for the methylene and methine moieties in the thioether side chains. This indicates a change from the labile κ^2-*C*,*S* coordination mode to a more stable form with a pendant thioether side chain and a pyridine ligand completing the coordination sphere.

The multiplets for the NCH_2 moities' resonance are found between 5.13 ppm and 4.97 ppm, while the SCH_2 methylene groups resonate between 3.47 ppm and 3.33 ppm. The SCH methine groups are found as multiplets or septets between 3.26 ppm and 3.06 ppm, while the methyl groups of the isopropyl moieties resonate as doublets at ~1.40 ppm. All of these values are shifted slightly downfield when compared to the respective benzimidazolium salt precursors.

The $C_{carbene}$ resonances in their ^{13}C NMR spectra are found between 163.3 ppm in **222** to 166.6 ppm in **223**. These chemical shifts are in good agreement with the values found for the $C_{carbene}$ resonance in other *trans*-[$PdBr_2$(bimy)(pyrdine)] compexes.[59a,115]

Single crystals suuitable for X-ray diffraction studies could be obtained by slow evaporation of concentrated solutions (**222** in dichloromethane, **223** in dichloromethane/toluene, and **226** in

acetonitrile/hexane) and by slow diffusion of diethyl ether into a concentrated dichloromethane solution of **221**. Despite all efforts, no single crystals of **224** and **225** could be grown, presumably due to the presence of the long, flexible aliphatic side chains in these complexes, which prevent efficient crystal packing.

Only **221** and **226** show the expected κ^2-*C*,*S* packing, while **222** and **223** crystallized as dimers, with $C_{carbene}$ and the thioether moiety coordination to different metal centers, thus forming 12-membered metallacycles (Fig. 5.7 and Fig. 5.8).

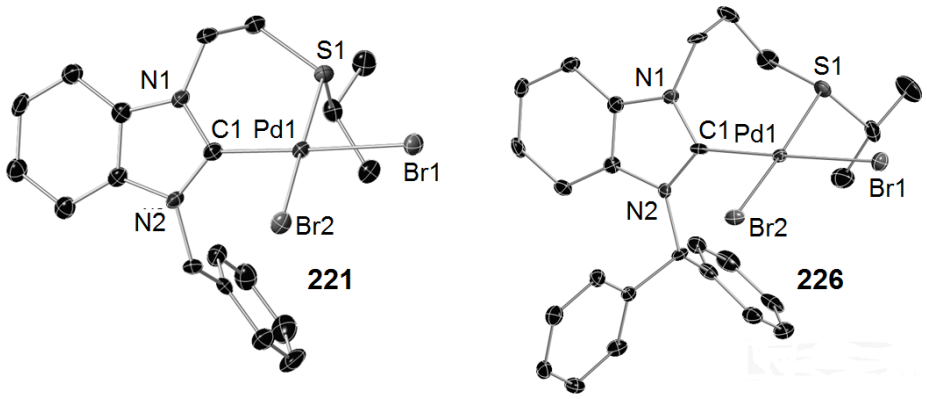

Fig. 5.7. Molecular structures of the κ^2-*C*,*S* complexes **221** and **226** (hydrogen atoms have been omitted for clarity, thermal ellipsoids are drawn at 50% probability).

The chelate complexes **221** and **226** resemble their platinum(II) analogues **211** and **216**. They have distorted square-planar coordination geometries around palladium, with a *cis*-arrangement of the bromido ligands. The six- and seven-membered metallacycles adopt slightly distorted boat conformations, and the NHC ring planes are twisted by 44.0(3)° out of the coordination plane in **221**, while the longer propylene tether in complex **226** allows a larger twist of 58.0(5)° due to a higher degree of conformational freedom. Nevertheless, these twist angles are smaller than in the platinum(II) complexes due to the smaller size of the palladium(II) center.

The Pd-C bond distance in **221** is 1.974(3) Å, and a slightly longer bond with a length of 1.993(5) Å is found in **226** (Table 5.4). For the Pd-S bond, distances of 2.2955(9) Å and 2.296(1) Å are found, respectively, and similarly to what was observed for the platinum(II) chelate complexes (*vide supra*), the Pd-Br bonds showed a clear difference in lengths due to the drastically different

trans-influences of the thioether moiety and the NHC. The bond lengths in complexes **221** and **226** are in good agreement with values found for structurally related chelate complexes.[57d,171c]

Table 5.4. Selected bond lengths [Å] and angles [deg] in the κ^2-*C,S* complexes **221** and **226**.

	221	**226**
Pd1-C1	1.974(3)	1.993(5)
Pd1-S1	2.2955(9)	2.296(1)
Pd1-Br1	2.4739(6)	2.4799(7)
Pd1-Br2	2.4392(5)	2.4431(7)
C1-Pd1-S1	90.9(1)	94.1(2)
C1-Pd1-Br2	92.39(9)	88.0(2)
S1-Pd1-Br1	85.57(2)	85.21(4)
Br1-Pd1-Br2	91.22(1)	92.61(2)
C1-Pd1-Br1	176.33(9)	178.9(2)
S1-Pd1-Br2	173.81(3)	172.93(4)

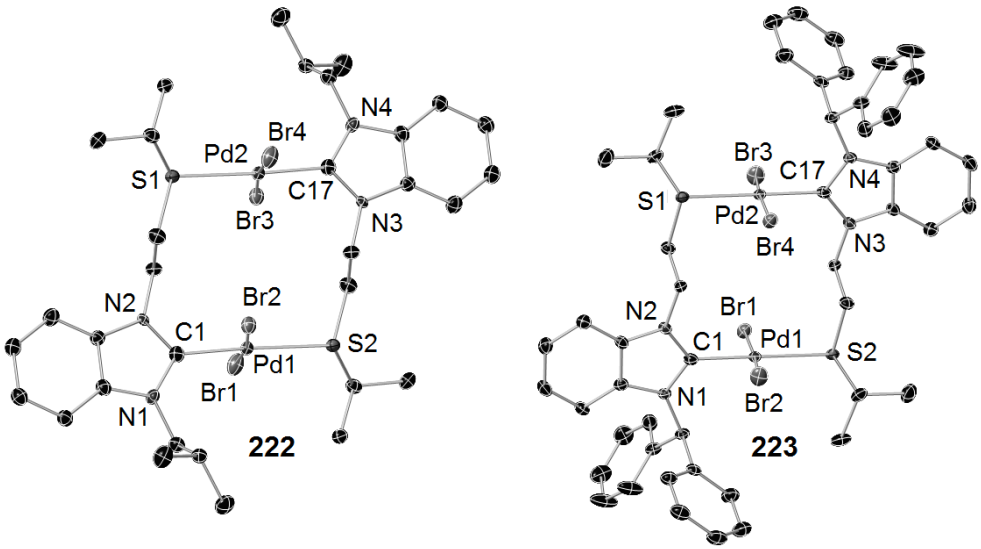

Fig. 5.8. Molecular structures of the dimeric complexes **222** and **223**·C_7H_8 (hydrogen atoms and solvent molecules have been omitted for clarity, thermal ellipsoids are drawn at 50% probability).

Complexes **222** and **223** did not show the κ^2-*C,S* coordination mode found in **221** and **226**. Instead, the coordination unit contains two palladium(II) centers, each one with a distorted square-planar coordination geometry and a *trans*-arrangement of the NHC moiety and the thioether unit of another ligand. Such species have been proposed to exist in solution for structurally related palladium (II) and platinum(II) complexes, but before they were never directly observed.[171c,172] However, is is common for sulfur-functionalized palladium(II) complexes to adopt multiple coordination modes.[57d,169b,171a,b,187]

The observed bond distances in **222** and **223** agree well with reported values for structurally related compounds (Table 5.5).[171a]

Table 5.5. Selected bond lengths [Å] and angles [deg] in complexes **222** and **223**·C_7H_8.

	222	**223**·C_7H_8
Pd1-C1	1.95(1)	1.964(2)
Pd1-S2	2.379(3)	2.3791(6)
Pd1-Br1	2.434(2)	2.4308(3)
Pd1-Br2	2.427(2)	2.4189(3)
C1-Pd1-Br1	89.6(3)	89.08(7)
C1-Pd1-Br2	85.0(3)	86.31(7)
S2-Pd1-Br1	86.80(9)	89.88(2)
S2-Pd1-Br2	98.93(9)	94.78(2)
C1-Pd1-S2	174.1(3)	178.77(7)
Br1-Pd1-Br2	173.27(6)	173.13(1)

Comparison between the chelate complexes **221** and **226** and the dimeric complexes **222** and **223** revealed shorter Pd-C bond distances in the latter. In **222**, the Pd-C bond is 1.95(1) Å long, and in **223** the bond distance is 1.964(2) Å. By contrast, the Pd-S bonds are longer in the dimeric complexes, with distances of 2.379(3) Å in **222** and 2.3791(6) Å in **223**. These changes can be traced back to the differences in *trans*-influence after changing from *cis*- to *trans*-geometries. By consequence, the Pd-Br bond distances in the dimeric complexes falls between the extremes defined by the Pd-Br bond lengths *trans* to the thioether and carbene moieties in the chelating complexes.

It should be noted that while the dimeric form is clearly preferred for these two complexes in the solid state, in solution only complex **223** seems to exist predominantly as a dimer. In ESI-MS, a peak corresponding to the dimeric form was observed for **223**, while for **222**, only the peak assignable to the monomeric chelate complex was found.

The weak sulfur-palladium bond can be cleaved easily by stronger carbon, nitrogen or phosphorus donors. To avoid problems with the low solubilities of cis-coordinated mixed NHC-phosphine complexes, and the sometimes unsatisfactory stabilities of pyridine adducts, the weak coordination of the thioether moiety was demonstrated instead by introduction of a second NHC ligand. Hetero-bis(NHC) complexes of palladium(II) with a pendant thioether side chain in one NHC can either be synthesized by transmetallation of a silver(I) NHC species to complexes **221**-**226**, thereby cleaving the Pd-S bond, or by transmetallation of the silver(I) NHC complexes derived from benzimidazolium salts **205**-**210** to a common palladium(II) mono-NHC complex (Scheme 5.6).

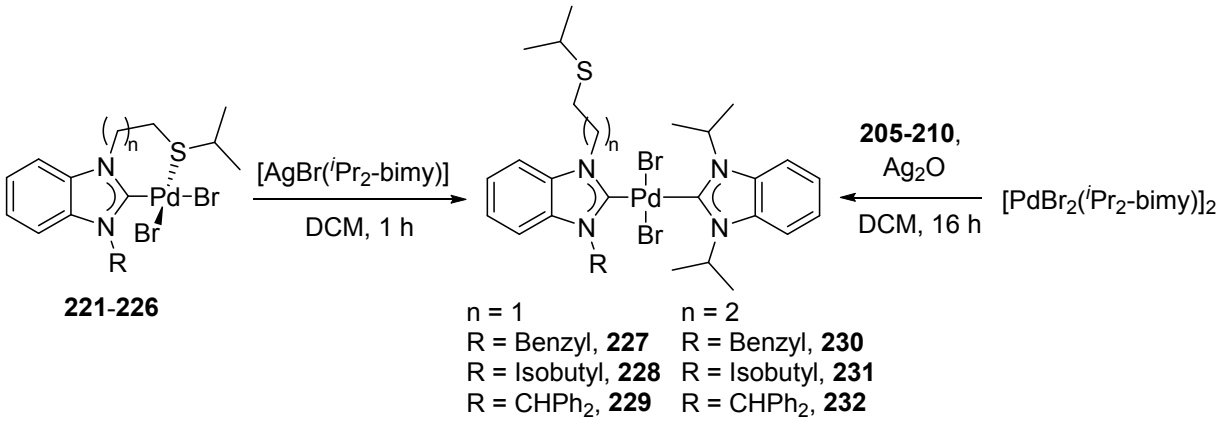

Scheme 5.6. Synthesis of hetero-bis(NHC) complexes with a pendant thioether side chain.

Both approaches were examined, and it was found that the reaction between [AgBr(^{i}Pr$_2$-bimy] and complexes **221**-**226** was rather sluggish, and subject to the formation of homo-bis(NHC) complexes through ligand scrambling. By contrast, the reaction between [AgBr(bimy)] complexes prepared from **205**-**210** and dimer [PdBr$_2$(^{i}Pr$_2$-bimy)] (**30**) was faster and yielded the same complexes **227**-**232** in higher purities. This demonstrates that while the thioether moiety is labile, it is less readily displaced in transmetallation reactions than a μ-bromido ligand. Besides faster and cleaner reactions, this approach requires less individual reactions to obtain **227**-**232**,

since it does not require the preparation of six individual precursor complexes **221**-**226**, but always uses dimer **30** as starting material for the second transmetallation step.

The hetero-bis(NHC) complexes **227**-**232** were obtained in yields ranging from 61 to 85% as yellow solids. They showed better solubilities than their mono-NHC counterparts **221**-**226**. Complexes **227**-**232** were fully soluble in chlorinated solvents and polar organic solvents, but insoluble in ethereal solvents, hydrocarbons and esters. This allowed their full characterization, including NMR spectra besides ESI-MS, elemental analysis and X-ray diffraction.

In their ^{1}H NMR spectra the absence of the resonance due to the acidic proton on C-2 in the benzimidazolium salts was an indication for the successful formation of NHC complexes. For complexes **227**-**229** with an ethylene tether in the side chain, the resonances due to the NCH_2 and SCH_2 moieties were very similar to those of the pyridine adducts of complexes **221**-**223**. The resonances for the thioether side chain in **228**-**232** were equally well-resolved, but were found more upfield in the case of the SCH_2 and SCH moieties. The additional methylene group in the tether resonates as multiplet at 2.71 ppm to 2.60 ppm. In all six hetero-bis(NHC) complexes, the asymmetry of the thioether-functionalized bimy ligand, together with the sterically crowded environment around the metal center which hinders the rotation along the Pd-C bonds, leads to magnetically different environments for the isopropyl wingtips of the $^{i}Pr_2$-bimy ligand, which consequently resonate as two distinct sets of signals.

In the ^{13}C NMR spectra of hetero-bis(NHC) complexes **227**-**232**, there are two $C_{carbene}$ resonances, one for each bimy ligand. The $^{i}Pr_2$-bimy $C_{carbene}$ resonances are found in the narrow range from 178.6 ppm to 179.6 ppm, and the thioether-functionalized bimy ligand has its $C_{carbene}$ resonance between 183.5 ppm and 186.3 ppm. The chemical shifts are in good agreement with previously reported values.[48,132b] When comparing the shifts between the different complexes, it becomes apparent that the variation of the non-functionalized side chain influences these chemical shifts more than the length of the thioether-functionalized side chain. The addition or removal of an additional methylene group to the linker has a negligible impact on the electronic properties of the complexes.

Single crystals of the hetero-bis(NHC) complexes for X-ray diffraction experiments were grown by slow evaporation of concentrated solutions (**227**, **228** and **232** in dichloromethane/acetonitrile, and **229** in dichloromethane/hexane) or by the slow diffusion of hexane into a concentrated dichloromethane solution in the case of **230**. No single crystals of **231** could be obtained, because

similarly to **224** and **225**, the long aliphatic wingtip substituents hindered the crystallization. All hetero-bis(NHC) complexes adopt a distorted square-planar geometry around the palladium center, with a trans-arrangement of the two bimy ligands (Fig. 5.9 and Fig. 5.10).

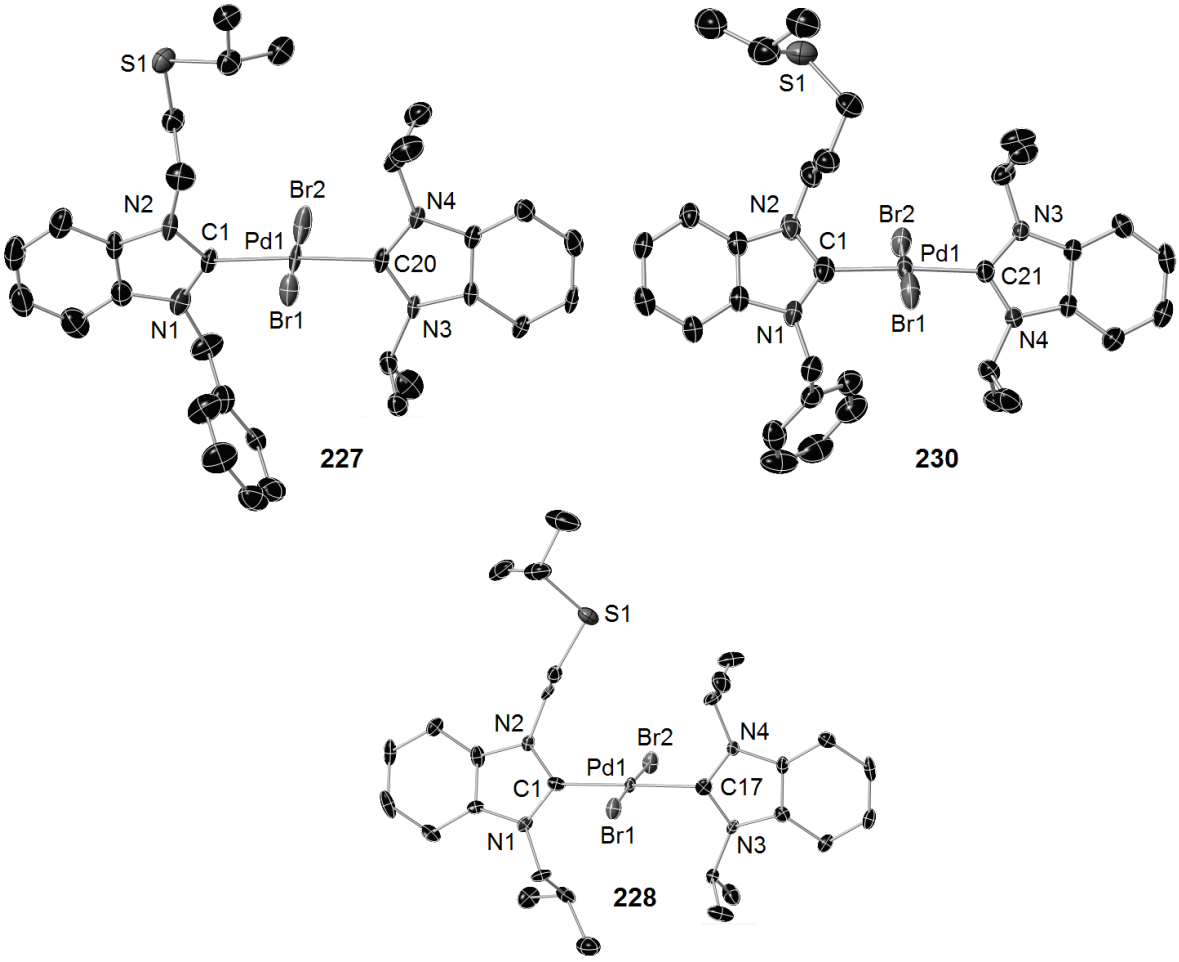

Fig. 5.9. Molecular structures of complexes **227**, **228**, and **230** (hydrogen atoms and molecular disorder have been omitted for clarity, thermal ellipsoids are drawn at 50% probability).

With the exception of complex **228**, crystallographic disorder was present in the long and flexible thioether side chains of all complexes. The bond distances between palladium and $C_{carbene}$ in the two different benzimidazolin-2-ylidene were comparable in all cases, and found to range from 2.011(5) Å in complex **229** to 2.040(4) Å in complex **232** (Table 5.6). The Pd-Br bonds fall in the range from 2.440(2) Å to 24567(9) Å, and are slightly longer than those in complexes **222** and **223** due to the reduced Lewis acidity of the palladium(II) center bearing two strongly donating

NHC ligands. The differences between the complexes are small, and all bond parameters are close to those reported for similar complexes.[48,188]

Table 5.6. Selected bond lengths [Å] and angles [deg] in complexes **227-229**·1.5 CH_2Cl_2, **230**, and **232**.

	13	**14**	**15**	**16**	**18**
Pd1-C1	2.031(7)	2.013(8)	2.029(5)	2.031(4)	2.040(4)
Pd1-$C_{carbene}$	2.027(7)	2.023(8)	2.011(5)	2.021(3)	2.01(2)
Pd1-Br1	2.443(2)	2.456(2)	2.443(1)	2.4567(9)	2.4451(5)
Pd1-Br2	2.440(2)	2.453(2)	2.447(1)	2.4383(9)	2.4262(6)
C1-Pd1-Br1	90.9(2)	90.2(3)	91.9(9)	92.0(1)	94.3(1)
C1-Pd1-Br2	89.9(2)	92.5(3)	91.0(1)	88.9(1)	89.4(1)
C-Pd1-Br1	89.1(2)	89.4(3)	89.5(1)	89.3(1)	89.7(1)
C-Pd1-Br2	90.1(2)	87.9(3)	87.6(1)	89.8(1)	86.5(1)
C1-Pd1-$C_{carbene}$	176.6(2)	179.5(4)	178.4(2)	176.8(2)	174.8(2)
Br1-Pd1-Br1	178.94(3)	177.17(5)	176.63(3)	177.78(2)	176.19(2)

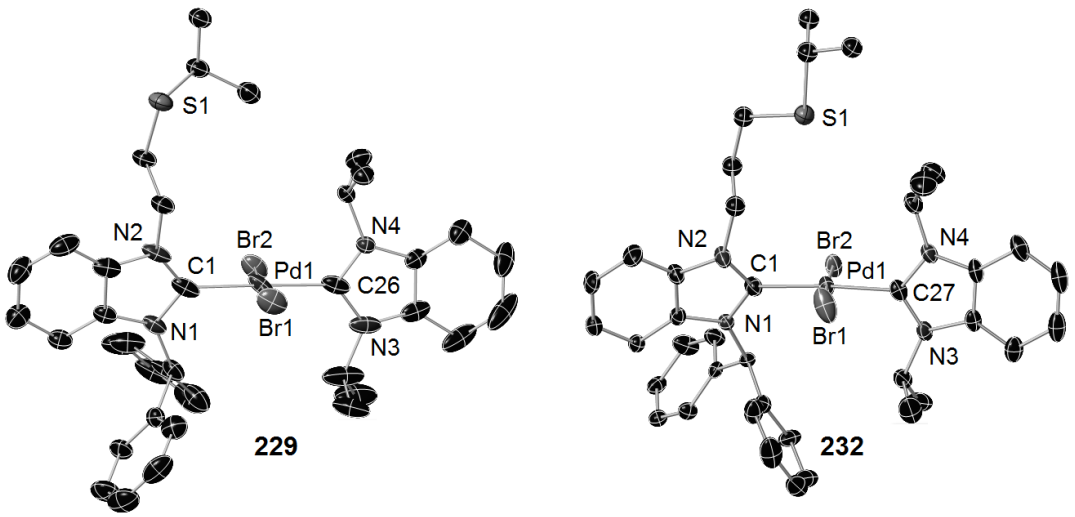

Fig. 5.10. Molecular structures of complexes **229**·1.5 CH_2Cl_2 and **232** (hydrogen atoms, solvent molecules, and molecular disorder have been omitted for clarity, thermal ellipsoids are drawn at 50% probability).

5.2.2. Applications in Catalysis

Given the good activities palladium(II) NHC complexes demonstrated for the hydroamination of carbon-carbon triple bonds,[136,137b,142] it is of interest to assess the activities of complexes **221-232** in this important reaction (Scheme 5.7).[143]

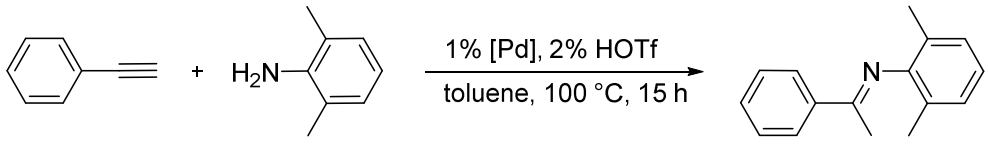

148 **149** **150**

Scheme 5.7. Hydroamination of phenylacetylene catalyzed by complexes **221-232**.

Table 5.7. Catalytic performance of **221-232** in the hydroamination of phenylacetylene.[a]

		Yield (%)[b]	
Entry	Catalyst	no additive	+ 2% HOTf
1	-	0	0
2	**221**	20	88
3	**222**	34	78
4	**223**	51	56
5	**224**	53	53
6	**225**	29	38
7	**226**	48	58
8	**227**	-	37
9	**228**	-	46
10	**229**	-	60
11	**230**	-	51
12	**231**	-	55
13	**232**	-	51

[a] Reaction conditions: 1 mol-% precatalyst, phenylacetylene (2.0 equiv.), 2,6-dimethylaniline (1.0 mmol), toluene (3 ml), 100°C, 15 h. [b] Yields determined by GC-MS with decane as internal standard; average of two runs.

Without a precatalyst, no product formation was detected (Table 5.7, entry 1). In line with previous observations, in the absence of catalytic amounts of triflic acid to facilitate the protolytic release of the product, only low to moderate yields of imine **150** were formed with the κ^2-C,S complexes **221**-**226**.[143b,144] Complex **224** gave the highest yield of 53% (entry 5), but no clear structure-activity relationship was discernible.

Upon addition of triflic acid to the reaction mixture, a clear increase in yield due to improved protolytic release of the product was noticable. Moderate to good yields were obtained with the chelating complexes **221**-**226** as precatalysts, and the hetero-bis(NHC) complexes **227**-**232** gave moderate yields. By far the best-performing precatalysts are the κ^2-*C,S* complexes **221** and **222**, with 88 % and 78%, respectively (entries 2 and 3)), although they perform less well than indy complexes **139** and **146**.[136] Complexes **221** and **222** feature a six-membered metallacycle, which is more stable than the seven-membered analogue, thus enhancing catalyst lifetime, leading to a higher turnover of the catalytically active species. No clear influence of the second wingtip substituent was observed.

By contrast to the chelating complexes, the hetero-bis(NHC) complexes **227**-**232** were in the majority of all cases less efficient precatalysts than their mono-NHC counterparts. A plausible explanation for this behavior is the slower formation of the catalytically active species, since an additional coordination site is blocked by the tightly bound $^{i}Pr_2$-bimy ligand.

As a mechanistically different reaction, the direct arylation of 1-methylpyrrole (**162**) with 4-bromoacetophenone (**151**) was chosen as a benchmark reaction (Scheme 5.8). Direct arylations of electron-poor heteroaromatics can be catalyzed by palladium(II) NHC catalysts,[161] and previous experiments have shown that hemilabile donor functionalities in the NHC side chain are beneficial for this transformation.[153]

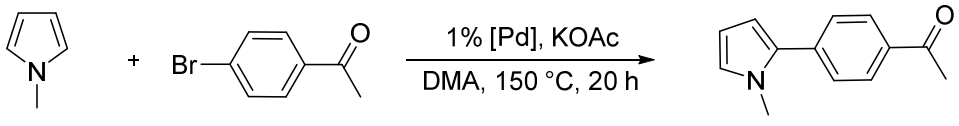

162 **151** **163**

Scheme 5.8. Direct arylation of 1-methylpyrrole catalyzed by complexes **221**-**232**.

All tested complexes were able to act as precatalysts for this reaction, with generally moderate to good yields of the cross-coupled product **163** (Table 5.8). The performance of complexes **221**-**232** showed only minor variations, with the lowest yield of 67% found for precatalyst **224** and the highest yield at 86% in the case of complex **232**. The reason for this is presumably partial decomposition to catalytically active colloidal palladium species, which show comparable activities irrespective of the ligand in the precatalyst. The activities of complexes **221**-**232** were also similar to those reported for other catalytic systems.[153,161]

Table 5.8. Catalytic performance of **221**-**232** in the direct arylation of 1-methylpyrrole.[a]

Entry	Catalyst	Yield (%)[b]
1	-	0
2	**221**	69
3	**222**	75
4	**223**	80
5	**224**	67
6	**225**	74
7	**226**	77
8	**227**	74
9	**228**	77
10	**229**	83
11	**230**	71
12	**231**	66
13	**232**	86

[a] Reaction conditions: 1 mol-% precatalyst, 1-methylpyrrole (4.0 equiv.), 4-bromoacetophenone (1.0 mmol), KOAc (2.0 equiv.), DMA (3 ml), 150°C, 20 h. [b] Yields determined by GC-MS with decane as internal standard; average of two runs.

No significant difference was found between the chelate complexes with different lengths of the linker in the thioether side chain, but a weak dependance of catalytic performance on the steric bulk of the non-coordinating side chain was discernible. The highest yields were found with

complexes **223** and **226** with the bulky benzhydryl side chain. The increased steric bulk in these complexes is favorable for the reductive elimination step.[189]

For the hetero-bis(NHC) complexes **227-232**, a similar reactivity pattern was found. Variations between complexes with different tether lengths in the thioether side chain were minor and unsystematic, while the steric bulk of the other side chain was found to show a better correlation with catalytic activities. When compared to the chelating complexes, the hetero-bis(NHC) complexes performed better than their counterparts. This is different from the behavior observed for the hydroamination (*vide supra*). While for the latter reaction, the additional tightly bound ligand slowed catalyst initiation, the additional stability imparted by the $^{i}Pr_2$-bimy ligand is beneficial for the survival of palladium species under the harsh conditions required for the direct arylation to proceed.

5.3. Nickel(II) Complexes Bearing Thioether-functionalized Benzimidazolin-2-ylidene Ligands

5.3.1. Complex Synthesis, Characterization, and Study of Rotamer Isomerism

Silver carbene transfer reactions are usually not the route of choice for the prepration of nickel(II) complexes, due to the often incomplete transmetallation. Instead, nickel(II) NHC complexes have been prepared by the reaction of free carbenes with suitable metal precursors or by the deprotonation of azolium salts *in situ* by basic nickel precursors, with transmetallation reactions being used only in rare cases.[190] However, benzimidazolin-2-ylidenes are very prone to dimerization in their free from, rendering most of these approaches useless for the preparation of their nickel complexes. A very convenient pathway to homo-bis(NHC) complexes of nickel(II) is the reaction of basic nickel(II) acetate with two equivalents of a suitable benzimidazolium salt in a large excess of molten tetrabutylammonium bromide under vacuum.[191] Acetate is only a weak base, and in the acid-base reaction with benzimidazolium salts, the equilibrium lies with the starting materials. However, under the reaction conditions, acetic acid is volatile and easily removed from the mixture, thus shifting the equilibrium towards the formation of free carbenes and subsequently the homo-bis(NHC) complexes *trans*-[$NiBr_2(NHC)_2$]. For this reason, a high vacuum was found to be crucial for the reaction to proceed in good yields. The thioether-functionalized benzimidazolium salts **205-210** were reacted under these conditions, and moderate to good yields of homo-bis(NHC) complexs were obtained when salts bearing a benzyl or a

isobutyl side chain were used (Scheme 5.9).[192] However, the reaction with benzhydryl-substituted benzimidazolium salts failed, and only intractable mixtures containing large amounts of paramagnetic impurities were obtained. The steric bulk of the azolium precursors is known to play a crucial role in this reaction, so it is unsurprising that the bulkiest benzimidazolium salts failed to react cleanly.

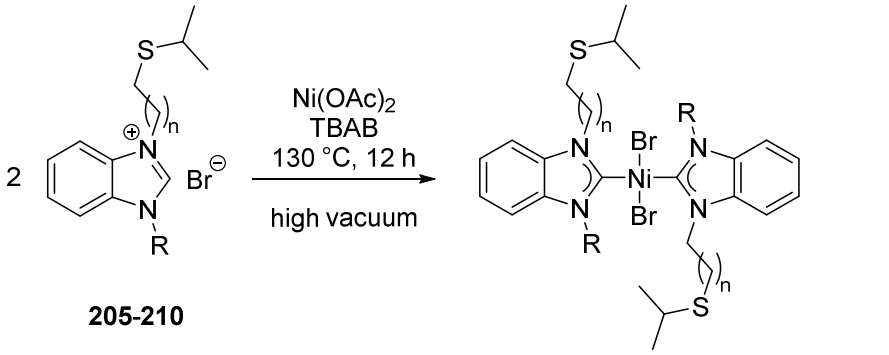

n = 1, R = Benzyl, **233**, 75% (3:2 *anti*/*syn*)
R = Isobutyl, **234**, 51% (1:1 *anti*/*syn*)
R = $CHPh_2$, **235**, 0%
n = 2, R = Benzyl, **236**, 57% (3:2 *anti*/*syn*)
R = Isobutyl, **237**, 81% (3:2*anti*/*syn*)
R = $CHPh_2$, **238**, 0%

Scheme 5.9. Synthesis of homo-bis(NHC) complexes of nickel(II).

Complexes **233**, **234**, **236** and **237** are readily soluble in common organic solvents, with the exception of very polar protic solvents such as alcohols, and in water. This allowed the easy removal of excess TBAB by triturating the solidified reaction mixture with water, and the isolation of the complexes by subsequent filtration of the resulting suspensions. Further purification, when required, can be done by column chromatography, altough the purity after aqueous workup was usually satisfactory.

In the ^{1}H NMR spectra of the purified complexes, the resonances for the acidic protons on C-2 in the benzimidazolium salts were absent. Deprotonation and NHC formation has taken place, and the desired homo-bis(NHC) complexes have been formed successfully. All four spectra showed two sets of signals, corresponding to inseparable mixtures of the *trans-syn* and *trans-anti* rotamers in a dynamic equilibrium. (Fig. 5.11).

No strong preference for one rotameric form over the other exists in complexes **233**, **234**, **236** and **237**. For complex **234**, in which the NHCs bear isobutyl and ethylene-tethered thioether side chains that are close in steric bulk, both rotamers were observed in roughly equal amounts. In the presence of the bulkier benzyl side chains in **233** and **236**, or in complex **237** with the longer (isopropylthio)propyl side chain, a slight preference for one rotamer with a ratio of 3:2 was observed instead. For complexes **234** and **237**, which contain only aliphatic wingtip substituents, it is difficult to assign the signal sets to the respective *trans-syn* and *trans-anti* rotamers.

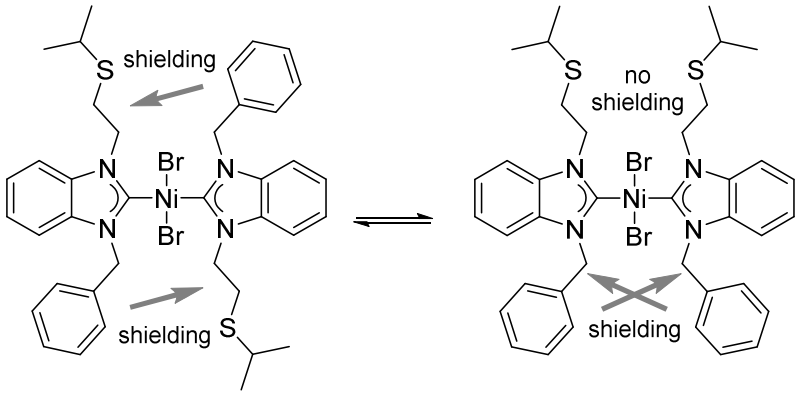

Fig. 5.11. Dynamic equilibrium between rotamers in **233**, and shielding effect of the benzyl groups.

In complexes **233** and **236**, the benzyl side chain introduced a magnetic anisotropy in the molecules, which can act as a built-in spectroscopic probe and allow to distinguish the rotamers. The ^{1}H NMR resonances of the side chains in the *trans-syn* and *trans-anti* rotamers of these complexes are well separated. In the major rotamer of complexes **233** and **236**, the methylene group of the benzyl side chain resonates more downfield, and the SCH and SCH2 groups in the other wingtip substituent are found more upfield than the corresponding signals in the minor rotamer. In the *trans-anti* rotamer, a shielding effect of the phenyl rings in the benzyl side chain should act on the thioether side chain, while in the trans-syn rotamer, the benzyl side chains are exposed to the shielding effects themselves. As a result, resonances of the thioether side chain should be shifted upfield in the trans-anti rotamer, while the methylene group of the benzyl side chain should resonate more upfield in the *trans-syn* isomer (cf. Fig. 5.11). Similar shielding

effects have been observed in other *trans*-[$MBr_2(NHC)_2$] complexes (M = Pd, Ni), in which aromatic rings are present in the NHC wingtip substituents.[116]

Therefore, it is apparent that the major rotameric form of **233** and **236** is the *trans-anti* rotamer. However, due to the lack of sufficiently clear spectroscopic differentiation between the rotamers of **237**, a similar assignment of the major isomer cannot be made. Since the preference for the trans-anti isomer in **233** and **236** stems from the difference in steric bulk of the side chains, it is likely to assume that the (isoproyplthio)propyl side chains in **237** should prefer to be arranged in an anti-fashion as well.

The ^{13}C NMR spectra of complexes **233**, **234**, **236** and **237** showed two sets of signals as well. All peaks could be assigned, and the $C_{carbene}$ resonances occur in the narrow range from 183.9 ppm to 185.5 ppm. These values are typical for *trans*-[$NiBr_2(bimy)_2$] complexes.[124,191,193]

To paint a fuller picture of the rotamer isomerism, the energetics of the rotamers were studied by computational chemistry. Since the flexibility of the long thioether side chains give rise to a dazzling number of energetically very similar conformers, it was shortened to ethyl side chains in the computational model. This has the added advantage of reducing the computational costs associated with geometry optimisations. For both the *trans-anti* and the *trans-syn* rotamers, molecular geometries were optimized at the B3LYP/cc-pVDZ level of theory, and free energies were calculated at the same level at 298 K(Fig. 5.12).[79,80,91b,c,194]

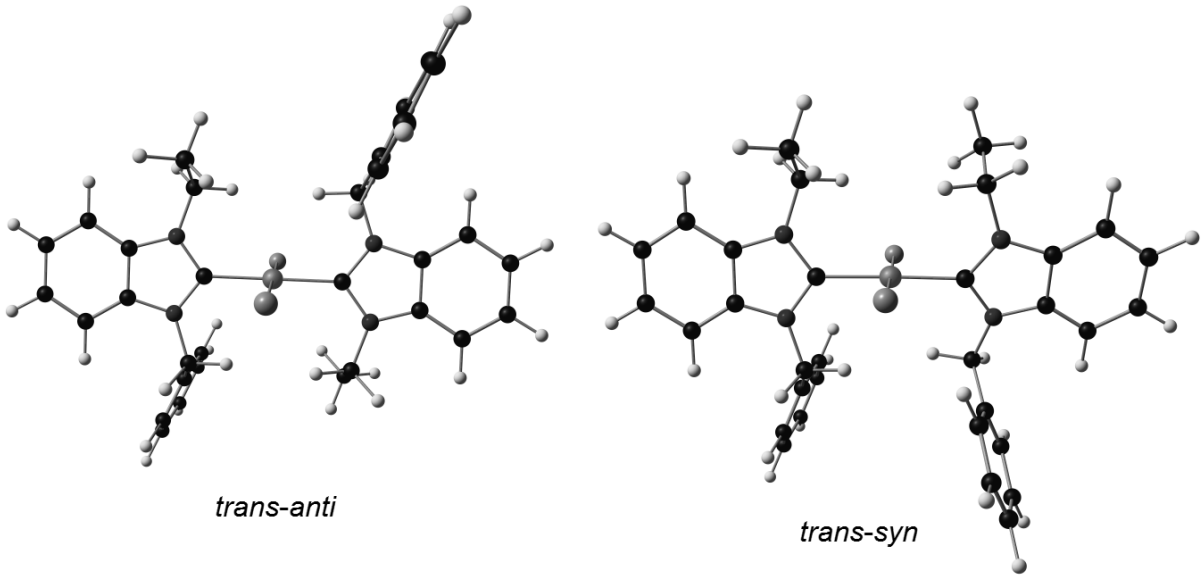

Fig. 5.12. Optimized geometries of simplified *trans-anti* and *trans-syn* rotamers.

The molecular structure of **233** is available (*vide infra*), and a comparison to the optimized geometry of the trans-anti rotamer showed good agreement. When comparing their relative energies of both rotamers, the Gibbs free energy of the *trans-anti* rotamer was found to be lower by 1.85 kJ/mol. This confirms the assignment based on the shielding effect of the phenyl ring. The experimental ratio of rotamers translates to an equilibrium constant of 1.5, while the calculated energy difference predicts an equilibrium constant of 2.1. These values are relatively close to each other, given the simplifications made in the model system such as the removal of the thioether moiety, and the negelect of solvent influences.

By slow evaporation of a concentrated solution of **233** in dichloromethane/toluene, single crystals of sufficient quality for X-ray diffraction experiments were grown. Despite all efforts, no crystals of the other three complexes could be obtained due to their unusually high solubility in many solvents as well as their tendency to form waxy, amorphous solids. However, the similarities in their spectra indicate that **233** is isostructural to the other three complexes.

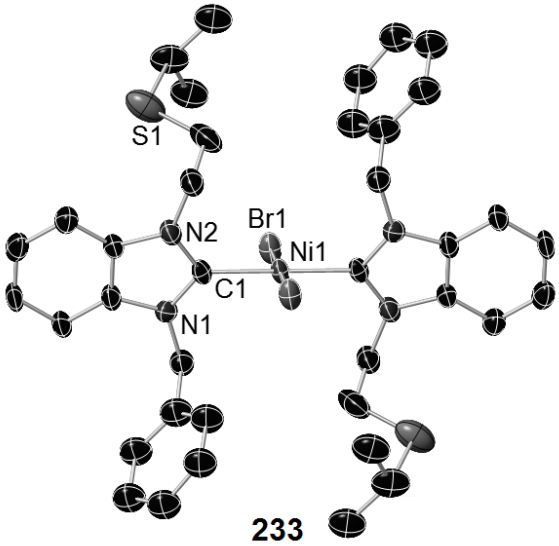

Fig. 5.13. Molecular structure of complex **233** (hydrogen atoms and molecular disorder have been omitted for clarity, thermal ellipsoids are drawn at 50% probability). Selected bond lengths [Å] and angles [°]: Ni1-C1 1.911(5), Ni1-Br1 2.3124(8), Br1-Ni1-C1 90.1(2)/89.9(2), Br1-Ni1-Br1' 180.0(2), C1-Ni1-C1' 180.0(2).

In line with spectrocsopic data and in good agreement with the calculated geometries, the nickel(II) center showed a square-planar coordination geometry with a *trans*-arrangement of the bimy ligands (Fig. 5.13). And as expected, the benzimidazolin-2-ylidene ligands are oriented in an *anti* manner, confirming the structural assignments. The NHC ring planes are twisted out of the coordination plane by 75.5(5)°. The Ni-C bond lengths of the symmetrical complex **233** are 1.911(5) Å, and the Pd-Br bond lengths are 2.3124(8) Å, respectively. These values are in good agreement with previously published data for related compounds.[124,191]

5.3.2. Application in the Suzuki-Miyaura Coupling

One of the most widely used carbon-carbon cross-coupling reactions is the Suzuki-Miyaura cross-coupling. The reaction is very reliable, a wide range of functional groups are tolerated, and reaction conditions are mild.[195] An additional advantage are the properties of the required organoboron reagents. These are more stable than the organometallic species used in other types of cross-couplings, can be handled in the presence of air and moisture, show no toxicity and are readily available.

Typically, palladium catalysts are used for Suzuki-Miyaura cross-couplings. However, the lower price of nickel has triggered an increasing research interest in using nickel-based catalysts as well.[196] Besides the obvious economic advantages, the smaller size of the nickel center, and the accessibility of the Ni(I) and Ni(III) oxidation states, which have no analogues in the chemistry of palladium, allow for alternative mechanisms and different reactivities when compared to the heavier homologues. This encompasses the possibility to cross-couple substrates, which don't undergo the Suzuki-Miyaura reaction easily with palladium-based catalysts.[196k,197]

To study the activity of complexes **233**, **234**, **236** and **237** in this reaction, the Suzuki-Miyaura cross-coupling between 4-bromoacetophenone (**151**) and phenylboronic acid (**239**) was chosen as a benchmark reaction (Scheme 5.10).

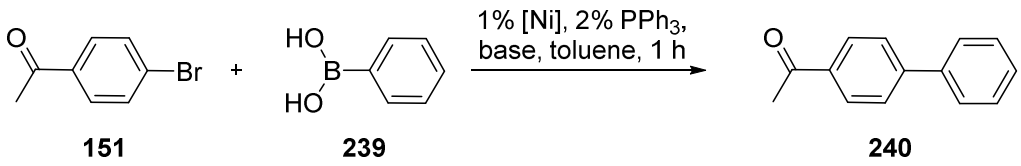

151 **239** **240**

Scheme 5.10. Nickel-catalyzed Suzuki-Miyaura coupling.

Using complex **233** as precatalyst, an initial screening of reaction conditions was performed. It has been noted that the presence of catalytic amounts of free phosphine is often required for nickel-catalysed Suzuki-Miyaura couplings to proceed in good yields.[196a,198] This effect was observed in the case of complex **233** as well, with a poor yield of 32% in the absence of a phosphine additive, and quantitative yields under identical conditions in the presence of 2% triphenylphospine (Table 5.9, entries 3 and 8). Under all reaction conditions examined, only trace amounts of biphenyl arising from the oxidative homocoupling of phenylboronic acid (**239**) were observed.

Table 5.9. Optimization of reaction conditions for the Suzuki-Miyaura cross-coupling.[a]

Entry	Base	Temperature (°C)	Yield (%)[b]
1	K_2CO_3	90	22
2	Cs_2CO_3	90	64
3	KOH	90	99
4	NaOAc	90	0
5	$NaOAc \cdot 3H_2O$	90	4
6	KOAc	90	0
7	$K_3PO_4 \cdot H_2O$	90	>99
8[c]	KOH	90	32
9	KOH	80	>99
10	KOH	70	>99
11	KOH	60	>99
12	KOH	50	54
13	KOH	40	6
14	KOH	30	0
15	KOH (2.0 equiv)	70	>99
16	KOH (1.5 equiv)	70	89
17	KOH (1.3 equiv)	70	72
18[d]	KOH (2.0 equiv)	70	0

[a] Reaction conditions: **233** (1 mol%), 4-bromoacetophenone (1.0 mmol), phenylboronic acid (1.3 equiv), PPh_3 (2 mol%), base (2.6 equiv), anhyd. toluene (3 mL), 1 h. [b] Yields determined by GC-MS with decane as internal standard, average of two runs. [c] reaction run without addition of PPh_3. [d] reaction run without exclusion of air and moisture.

The first parameter to be examined in the reaction optimization was the nature of the base. Several strong inorganic bases were tested (entries 1-7). Sodium and potassium acetates were poor bases, and only trace amounts of **240** were formed with sodium acetate trihydrate. Potassium carbonate gave poor yields, while the more soluble cesium carbonate gave a higher yield. The best-performing bases were potassium hydroxide and potassium phosphate hydrate. In the presence of these bases, the quantitative formation of **240** was observed. Both phosphate and hydroxide anions play an active role in the catalytic cycle by activating the boronic acid as an ate-complex for transmetallation, or by acting as a basic ligand to the catalytically active metal center, which explains this observation.[199]

Since both bases performed equally well, potassium hydroxide was chosen for the next optimization step. Reaction temperatures are an important factor, since they have a bearing on the survival of sensitive substrates and reagents under reaction conditions, an on the energy consumed by large-scale processes. Using complex **233** as precatalyst, it was possible to lower the temperature from 90 °C to 60 °C without compromising the quantitative yields obtained for this reaction, but at lower temperatures a drop in the formation of **240** was observed, and no product was formed at all at 30 °C (entries 9-14). Since 4-bromoacetophenone is an activated substrate for the Suzuki-Miyaura cross-coupling, further optimizations were carried out at 70 °C to allow for the expected lower reactivities of less activated aryl halides.

A large excess of base is usually used in this reaction, and as much as 2.6 equivalents with respect to **151** were used in the screening. This produced additional waste, rendering the reaction less economically viable, and a reduction in base would be desirable. Indeed, it was possible to lower the base loading to 2.0 equivalents without compromising the yield, and only a minor drop was observed upon lowering it even further to 1.5 equivalents (entries 15 and 16). However, at 1.3 equivalents, only 72% of **240** were formed (entry 17).

Running reactions under an inert atmosphere is a hassle, especially in in large-scale processes, so the possibility of running the reaction under air and in solvents which were not dried prior to use was examined (entry 18). Under these conditions, not even traces of product were observed. This can be rationalized by taking into account the sensitivity of the nickel(0) species formed by the reduction with phenylboronic acid in the initiation step.[196f] With this species being destroyed under atmospheric conditions, no coupling reaction takes place.

Using the improved conditions, i.e. 70 °C as reaction temperature and 2.0 equivalents of potassium hydroxide as base, the performance of all four nickel(II) complexes was explored. To allow for a better differentiation of their catalytic activities, a less reactive substrate was chosen. Instead of the electron-poor 4-bromoacetophenone (**151**), the more electron-rich 4-bromotoluene (**241**) was used as cross-coupling partner (Scheme 5.11 and Table 5.10).

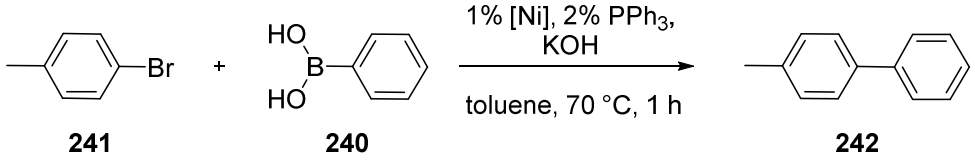

241 **240** **242**

Scheme 5.11. Precatalyst screening for the cross-coupling of 4-bromotoluene and phenylboronic acid.

Table 5.10. Screening of precatalysts and further optimization of the Suzuki-Miyaura reaction.[a]

Entry	Catalyst	Yield (%)[b]
1	-	0
2	**233**	23
3	**234**	19
4	**236**	16
5	**237**	22
6[c,d]	**233**	27
7[d,e]	**233**	33
8[d,f]	**233**	35
9[d,g]	**233**	43

[a] Reaction conditions: precatalyst (1 mol%), 4-bromotoluene (1.0 mmol), phenylboronic acid (1.3 equiv), PPh_3 (2 mol%), KOH (2.0 equiv), anhyd. toluene (3 mL), 70 °C, 1 h. [b] Yields determined by GC-MS with decane as internal standard, average of two runs. [c] 2 h. [d] Single run. [e] 3 h. [f] 6 h. [g] 2 h, $K_3PO_4 \cdot H_2O$ used instead of KOH.

In the absence of a nickel(II) complex as precatalyst, no product was detected in the reaction mixture. When 1 mol% of nickel complex was present, the cross-coupling product **242** was observed, but yields were generally poor and ranged from 16% with complex **236** as prectalyst, to

23% when complex **233** was used (Table 5.10, entries 2-5). However, the dearth of data points, and the small range in which the yields fluctuated between the four complexes, made it impossible to discern structure-activity relationships. Neither the length of the thioether side chain, nor the steric bulk imparted by the non-functionalized wingtip substituent had an obvious impact on reactivities. Complex **233**, which was also used in the initial optimization, was the best-performing precatalyst, and therefore used for all further reactions.

Since the low yields obtained with 4-bromotoluene as substrate were unsatisfactory, reaction times were increased successively, but only minor increases in yield were observed (entries 6-8). However, when the base was changed to potassium phosphate hydrate instead of potassium hydroxide, 43% of the product was isolated after 2 hours (entry 9).

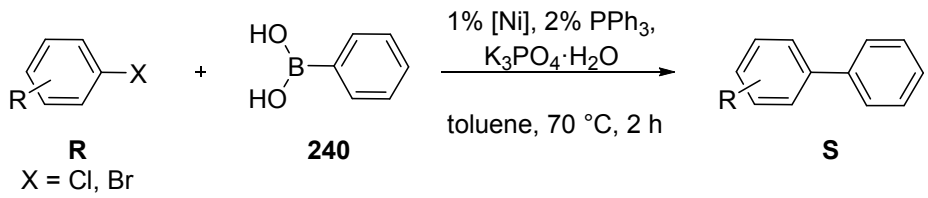

R **240** **S**

Scheme 5.12. Substrate scope of the Suzuki-Miyaura reaction catalyzed by complex **233**.

Using these improved conditions, the substrate scope of the cross-coupling was explored systematically (Scheme 5.12 and Table 5.11).

Electron-poor aryl bromides such as 4-bromoacetophenone, bromobenzaldehydes and 4-bromobenzonitrile gave good to quantitative yields of the corresponding biaryls (entries 1-4 and 6). However, 3,5-difluorobromobenzene gave only a moderate yield, and 4-nitrobromobenzene failed to react entirely (entries 7 and 8).

Similarly, 4-chloroacetophenone, 4-chlorobenzaldehyde, and 4-chlorobenzonitrile could be cross-coupled in good to quantitative yields, although longer reaction times of 24 h instead of 2 h as in the case or aryl bromides were required to achieve good yields. The turnover frequency of the catalyst is lower when aryl chlorides are used as substrate, but quantitative conversions can still be achieved. This demonstrateds that in the absence of moisture and oxygen, the catalytically active species is stable for extended periods of time under reaction conditions.

More electron-rich aryl bromides, such as bromotoluenes and bromobenzene, could be cross-coupled in acceptable yields, but it was necessary to extend the reaction times to 24 h to achieve

these yields as well. When chlorobenzene was used as a substrate, a low yield of 36% was obtained under these conditions.

Electronic factors are more important in determining the yield than steric repulsion. Bromobenzaldehydes were coupled in good yields even with the aldehyde moiety in ortho-position, although the yields for the ortho- and meta-substrates were lower than for the para-substrate (entries 2-4). The corresponding bromotoluenes, with the same substitution patterns, gave lower yields despite extended reaction times, and no correlation between steric hindrance and the obtained yields was apparent (entries 9-11).

Table 5.11. Nickel-catalyzed Suzuki-Miyaura cross-coupling of aryl halides.[a]

Entry	Substrate	Yield (%)[b]	
		Aryl bromide	Aryl chloride
1	4-$COCH_3$	100	100[c]
2	4-CHO	100	75[c]
3	3-CHO	75	-
4	2-CHO	72	-
5	4-H	76[c]	36[c]
6	4-CN	100	100[c]
7	4-NO_2	0	0
8	3,5-difluoro	44[c]	-
9	4-CH_3	60[c]	-
10	3-CH_3	77[c]	-
11	2-CH_3	72[c]	-
12	2-halopyridine	0	Traces
13	2-halothiophene	0	-
14[d]	1,3-dihalobenzene	38[e]	-
15[d]	4-Cl-bromobenzene	56[f]	-

[a] Reaction conditions: precatalyst (1 mol%), aryl halide (1.0 mmol), phenylboronic acid (1.3 equiv), PPh_3 (2 mol%), $K_3PO_4 \cdot H_2O$ (2.0 equiv), anhyd. toluene (3 mL), 70 °C, 2 h. [b] Yields determined by GC-MS with decane as internal standard, average of two runs. [c] 24 h. [d] phenylboronic acid (2.6 equiv), $K_3PO_4 \cdot H_2O$ (4.0 equiv), anhyd. Toluene (6 ml) used instead. [e] 1,3-terphenyl, trace amounts of biaryl. [f] biaryl, trace amounts of 1,4-terphenyl.

Nitrogen- and sulfur-containing heteroarenes were no good substrates for the reaction. Neither 2-bromopyridine nor 2-bromothiophene underwent cross-coupling, and only minor traces of the product were observed with 2-chloropyridine (entries 12 and 13).

The reactivity of difunctional aryl halides was explored as well. For 1,3-dibromobenzene, cross-coupling occurred twice, and m-terphenyl was found as the major product, with 3-bromobiphenyl only observed in trace amounts (entry 14). In the case of 4-chlorobromobenzene, the situation was different. 4-Chlorobiphenyl was found as the major product, and only traces of p-terphenyl were present in the reaction mixture (entry 15). This demonstrates that it is possible to discriminate between different reactive sides in aryl halides, and that the reaction of aryl bromides is substantially faster than the cross-coupling of aryl chlorides.

In the wider context of Suzuki-Miyaura cross-couplings catalyzed by nickel(II) NHC complexes, **233** and its three congeners are not the most efficient catalysts for this reaction.[196k, 200] Nevertheless, they represent the first examples of catalytically active nickel(II) complexes bearing sulfur-functionalized NHCs, thereby demonstrating the viability of these structures for further study.

5.4. Pincer-Pseudopincer Isomerism in Palladium(II) complexes with κ^3-*C,S,C* Ligands

While bidentate, chelating ligands impart an increased degree of stability to complexes, this effect is even more pronounced in the case of tridentate ligands. Especially pincer and pincer-type ligands have attracted considerable research interest due to the remarkable thermal stabilities and the robustness of their complexes, as well as the rigid κ^3-*mer* or κ^3-(pseudo)-*mer* coordination geometries these ligands impose. Complexes of such ligands have been used in catalysis as well as other fields with tremendous success.[201] Therefore, it is not surprising that a number of NHC pincer ligands have been reported as well.[55a-c,f,i,j,177c,202]

For pincer ligands composed of two NHC moieties, linked by a thioether which functions as the central donor site, it has been observed that when coordinating counteranions such as halides are present, their complexes with palladium(II) can exist either as the expected, cationic κ^3-*mer*-*C,S,C* pincer form, but also as a neutral, κ^2-*C,S* pseudopincer.[55f,142c] This observation is interesting, since the fine-tuning of ligand properties by modification of steric and electronic properties as well as chemical behavior is an important field of study, in order to tailor complexes

to their unique tasks.[203] In catalytic applications using pincer complexes, reactions typically take place at the coordination sites not blocked by the pincer ligand, but instances of partial decoordination are also know. Such decoordinations are similar to the behavior of hemilabile donor sites in κ^2-chelating ligands, by rapidly opening up coordination sites for incoming substrates, while the donor moiety remains in the vincinity of the metal center which allows for rapid recoordination and stabilization of a resting state.[57] Decoordinations can occur either in the peripheral positions of the pincer ligands,[204] but hemilabile behavior of the central donor site has also been observed.[205] To adjust this hemilability, a deeper understanding of the factors that govern it in *C,S,C* pincer complexes can be useful.[206]

The ligand donor strengths of the carbene moieties were suggested to have a strong influence on the pincer-pseudopincer isomerism. To study the electronic factors, *C,S,C*-pincer ligands with NHC moieties with vastly different ligand donor strengths were studied, and their preference for either the pincer or pseudopincer form was probed.[207] To avoid the confounding effects of changes in steric bulk, methyl groups were chosen as wingtip substituents for the NHC moieties. Besides being sterically small, they only contain four atoms and not many degrees of freedom, which helps limit computational costs. Electronic differences were introduced by modifications of the NHC backbones, including structures which have already been examined experimentally (Fig. 5.14).[55f,142c]

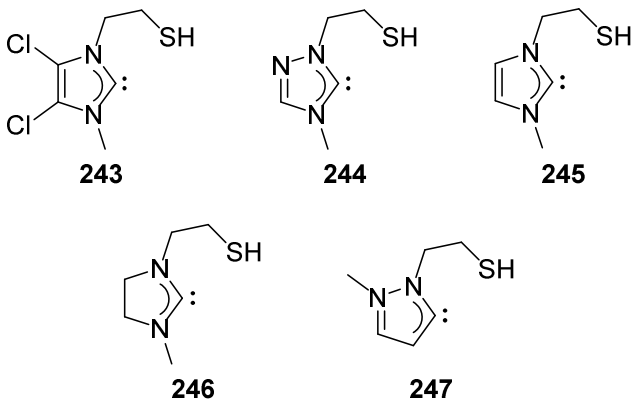

Fig. 5.14. Truncated ligands with NHCs having different backbones.

Since no experimental donor strength values are available for the five *C,S,C* ligands under examination, the energy eigenvalues of the Kohn-Sham orbitals containing the σ-lone pair, i.e.

ε(σ-HOMO), were used as a readily available and accurate estimate.[77] To limit computational cost, truncated ligands were used, in which the NHC moiety bears an ethylthiol side chain instead of a thioether linker to another, identical NHC moiety. This simplification reduces the computational effort significantly by almost halving the number of atoms, and considerably reducing the degrees of conformational freedom present in the ligands. However, since it can be assumed that inductive effects due to changes in the side chain do not impact the electron density of the carbene lone pair,[59a] and the orbitals of both NHC moieties are independent from each other, the loss in accuracy from this simplification is minor. Orbital energies for NHCs **243**-**247** were calculated at the B3LYP/aug-cc-pVTZ level after geometry optimization at the B3LYP/-cc-pVDZ level.[79,80,91a, 208] Four all five NHCs, the highest occypied orbital with σ-symmetry corresponds to the carbene lone pair (Fig. 5.15).

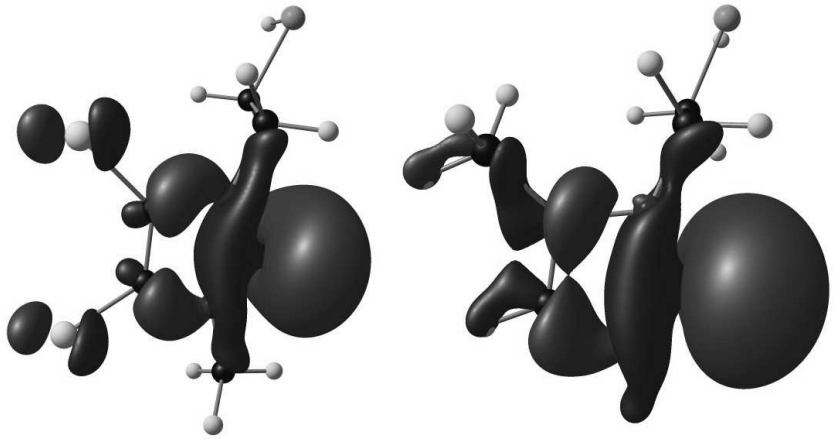

Fig. 5.15. σ-HOMOs of the most and least electron-rich NHCs.

The calculated orbital energies range from -6.56 eV in **243** to -5.52 eV in **247**, and confirm the increase in electron density at the carbene center in the order **243** < **244** < **245** < **246** < **246** (Table 5.12).

To gauge the preference of each ligand for the pincer or pseudopincer form, the homodesmotic reaction between a pincer and a pseudopincer was studied (Scheme 5.13).

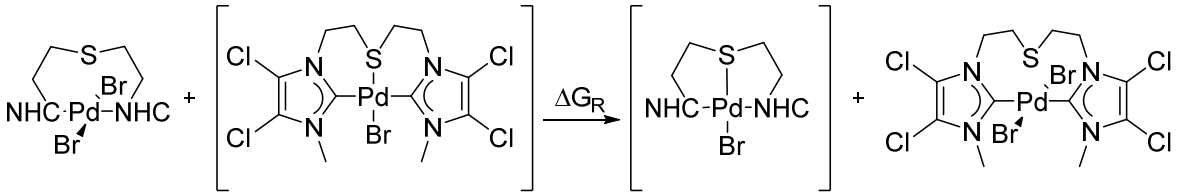

Scheme 5.13. Homodesmotic reaction between pincer and pseudopincer complexes.

This approach is preferable, since the relative Gibbs free energies ΔG of cationic pseudopincer complexes **T**, including the bromide counteranion, and their corresponding neutral pseudopincer complexes **U** are hard to obtain. Especially for the charged species, it is hard to acount correctly for ion pairing and solvatation. In the homodesmotic reaction, the number of ionic species remains constant throughout the reaction, and the Gibbs free energy of the bromide anion as well as solvatation effects can be neglected, as they are virtually identical for both the starting materials and the products.

As a reference system, the pincer complex incorporating the least electron-rich NHC moieties, 3,4-dichloroimidazolin-2-ylidene, was used. For this ligand, the preference for the pseudopincer form is known, and a relative scale of pincer preference energy ΔG_R with respect to this reference system can be obtained. Negative ΔG_R values signify a higher preference for the pincer form than the reference system, while positive ΔG_R values are indicative for a lower preference.

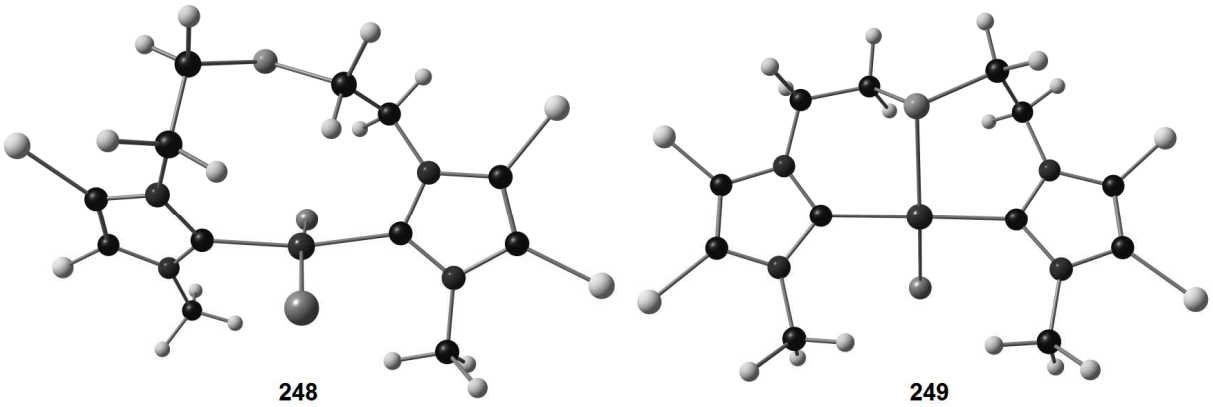

Fig. 5.16. Optimized geometries of pincer complex **248** and corresponding pseudopincer **249**.

For all complexes, the geometries of the pincer and pseudopincer forms were optimized at the B3LYP/cc-pVDZ level of theory, and their Gibbs free energies were calculated at the same level of theory.[79,80,91a,92b,209] The optimized geometries were in good agreement with the available molecular structures.[55f,142c] The coordination geometry at the metal center was distorted square-planar, and clear differences between the pincer and the pseudopincer geometries can be found (Fig. 5.16). In the pseudopincer, the NHC planes showed a twist of 26-43° with respect to each other, while they were almost coplanar in the pincer complexes. The metallacycles in the latter adopt distorted boat conformations.

The Gibbs free energies associated with these optimized geometries allow to calculate the change in Gibbs free energy of the homodesmotic reaction (cf. Scheme. 5.13) and obtain ΔG_R as a measure for pincer preference (Table 5.12).

Table 5.12. Pincer preference energy ΔG_R and ε(σ-HOMO) of the NHC moieties.

NHC moiety	ε(σ-HOMO) [eV]	ΔG_R [kJ/mol]
Cl_2-imidazole	-6.56	0.0
1,2,4-triazole	-6.52	-5.4
Imidazole	-6.12	-26.5
Imidazoline	-5.94	-32.8
Pyrazole	-5.52	-57.0

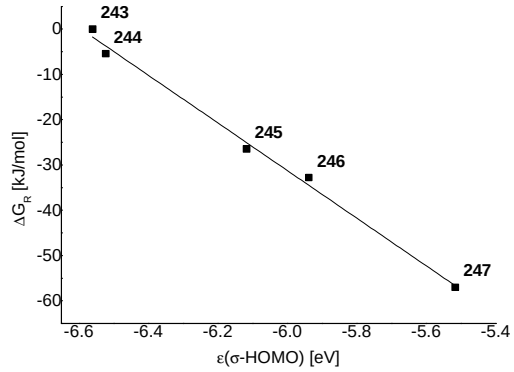

Fig. 5.17. Correlation of ε(σ-HOMO) and ΔG_R.

Indeed, the preference for the pincer form increased in the same order as the orbital energies of the σ-lone pair of the carbene moieties, and a strong correlation between the two parameters was found (Fig. 5.17, $R^2 = 0.9931$).

More strongly donating carbene moieties in the *C*,*S*,*C*-ligand favor the pincer isomer. The higher amount of electron density provided by more electron-rich donor sites allows to stabilize the cationic coordination unit of the pincer complex, and this stabilization obviously scales linearly with increases in ligand donor strengths. Since the pincer form is also entropically favored, and solvatation can be expected to provide additional stabilization especially in polar solvents, the ionic pincer form becomes more stable than the pseudopincers with electron-rich *C*,*S*,*C*-ligands. By contrast, if the carbene donors provide comparatively little electron density to the metal center, the pseudopincer form becomes more stable. The additional bromido ligand in the pseudopincer is a better donor ligand than the thioether moiety in the pincer, and thus better matched to the less electron-rich metal center.

A more formalistic way to describe the isomerism is to consider a $[PdBr(NHC)_2]^+$ fragment, wich can choose to interact in a Lewis acid/Lewis base reaction with either a bromide or a thioether. Upon coordination of the Lewis base, an internal charge redistribution occurs, which is more pronounced when the more strongly donating bromido ligand binds to the metal center.[210] Since the charge redistribution is more favorable with less electron-rich NHC moieties, the pseudopincer form is prefered with such ligands.

6. Conclusion

In this thesis, DFT studies concerning the electronic structure of N-heterocyclic carbenes (NHCs) and their bonding to early and late transition metal fragments, the preparation, characterization and application in catalysis of palladium(II) complexes of NHCs with reduced heteroatom stabilization, and the coordination chemistry of sulfur-functionalized NHCs with group 10 metals as well as the catalytic properties of the resulting complexes have been presented.

In chapter 2, fourteen isomerically or isolobally related, five-membered N-heterocyclic carbenes with two, three or four nitrogen atoms in the heterocycle have been studied computationally.

Relative stabilities within each series were established to depend on intramolecular steric repulsion of the substituents on the heteroatoms, and the singlet carbenes as well as the monocations were found to be aromatic species. Aromaticity was reduced in the diactions and the triplet states due to the disruption of the π system, and pyramidalization of the substituted nitrogen atoms was observed in the latter.

The electronic structures of NHCs **55**-**58** are characterized by the energy eigenvalues of the highest occupied Kohn-Sham orbitals with σ and π symmetry, and these values are cross-correlated to the first and second proton affinities of the free carbenes. Factors determining the σ-donor strengths of the free carbene were determined to be the number of heteroatoms in the cycle, their positions relative to $C_{carbene}$, and a destabilizing effect of σ-lone pairs on heteroatoms adjacent to the carbene carbon. By contrast, the π-basicity seems to be largely determined by the number of heteroatoms in the parent azole, with other structural influences playing a very minor role.

The singlet-triplet energy gaps were calculated, and they showed a weak correlation to the HOMO-LUMO energy gaps. All NHCs **55**-**58** are more stable in the singlet form, but only for a few NHCs, the singlet-triplet gaps are large enough to rule out dimerization to electron-rich olefins purely on electronic grounds. No correlation between the number or position of heteroatoms in the ring and the singlet-triplet gaps was observed. Instead, orbital shapes seem to play an important role, since isolobally related NHCs had similar singlet-triplet gaps. It is especially noteworthy that the smallest gaps were found for NHCs which retain a high degree of aromaticity in the triplet state.

The local electronic structure at $C_{carbene}$ was characterized by its p_π population and the natural charge. It was found that normal carbenes tend to have lower p_π populations than mesoionic carbenes, although the transition between the two is smooth and there is an area of overlap. Natural charges of $C_{carbene}$ are very loosely correlated to the p_π population, although the main determining factor is the number of nitrogen atoms in α-position. It is noteworthy that the most electron-rich NHC **55d**, which is a pyrazolin-4-ylidene, has a local electronic structure at $C_{carbene}$ that closely resembles an aromatic carbanion.

The bond between NHCs **55-58** and the transition metal fragments AuCl and $TiCl_4$ were exmined by means of energy decomposition analysis. The bonding between NHCs and both the early transition metal with d^0 configuration and the late transition metal with a d^{10} configuration was predominantely electrostatic, with orbital interactions contributing less than a third to the attractive interaction. The orbital interaction energy term ΔE_{orb} is mostly due to σ-interactions. However, π-interactions are not negligible. In the gold complexes, π-backdonation is the main orbital interaction with π symmetry, while in the bond between the NHCs and titanium, π-donation plays a minor role as well.

A more detailed analysis of ΔE_{orb} by the extended transition state - natural orbitals for chemical valence (ETS-NOCV) approach allowed the exact quantification of σ-donation, π-backdonation, σ-backdonation and in-plane π-backdonation, as well as internal orbital reorganization processes. The first proton affinity was found to be an excellent descriptor for σ-donation, while the π-backdonation processes could be correlated to the p_π population at $C_{carbene}$, which provides an measure of π-acidity. The donation of π-electron density to the metal centers was found to be negligible in all cases.

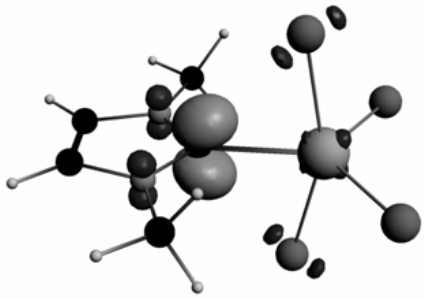

Fig. 6.1. Pseudo-backdonation in NHC-$TiCl_4$ complexes.

An interesting observation was the unexpectedly high π-backdonation from the $TiCl_4$ fragment to the NHCs, which can be explained by the involvement of the non-bonding electron pairs at the axial chlorido ligands (Fig. 6.1). This pseudo-backdonation is presumably present in many NHC complexes which feature coligands with free electron pairs and merits further investigation. Besides the study of this process, future work should focus on the study of additional NHCs, e.g. benzannelated systems, systems containing other heteroatoms than nitrogen, and more exotic carbenes such as CAACs and anti-bredt NHCs.

The first part of chapter 3 focuses on the determination of subtle variations in ligand donor strengths in pyrazoles **63**, **64**, **68**-**73**, **75**, and **76** by means of a previously developed electronic parameter based on the ^{13}C NMR chemical shift of the carbene carbon in *trans*-[$PdBr_2$($^i Pr_2$-bimy)L] complexes. For each of the ten pyrazoles, a corresponding probe complex was prepared in excellent yields and fully characterized, including the determination of molecular structures for the *trans*-[$PdBr_2$($^i Pr_2$-bimy)(pyrazole)] complexes **82**, **84**, **89**, and **90**. Despite falling within a narrow range of 2.3 ppm, all shifts could be clearly distinguished. Alkylation experiments with the weak electrophile ethyl bromide, the stronger electrophile ethyl iodide, and the very strong alklating agent trimethyloxonium tetrafluoroborate were carried out, and the pyrazoles were sorted into three groups of different nucleophilicity according to their reactivity with these reagents. A good correlation between the experimentally determined donor strength values and the nucleophilicity of the nitrogen donor atom in the pyrazoles was observed. This indicates that the ^{13}C NMR parameter is useful not only for donor strength determinations, but also for the prediction of the reactivity of nucleophiles. Given the simplicity of the method, it is a viable alternative to the determination of nucleophilicities by kinetic experiments in cases where only an estimate is required. Further investigations in this field should focus on nucleophiles other than pyrazoles, as well as incluce more electrophiles to paint a nuanced picture.

In the second part of this chapter, the synthesis of pyrazolin-5-ylidene (pyry) complexes of palladium(II) is reported. Oxidative addition of a triflato-functionalized pyrazolium salt to [$Pd(PPh_3)_4$] in the presence of an external chloride source yielded the cationic complex *trans*-[$PdCl(PPh_3)_2$(pyry)]OTf/BF_4 (**112**), while carbene silver transfer starting from azolium salt **109** gave the hetero-bis(NHC) complex *trans*-[$PdBr_2$($^i Pr_2$-bimy)(pyry)] (**116**) and the acetonitrile adduct *trans*-[$PdBr_2$(acetonitrile)(pyry)] (**117**). While the former complex allowed to characterize

the ligand donor strength of the pyry ligand by means of ^{13}C NMR spectroscopy, the latter complex was found to be a versatile starting material for the preparation of complexes incorporating carbon-, nitrogen-, and phosphorus-donors (Scheme 6.1)

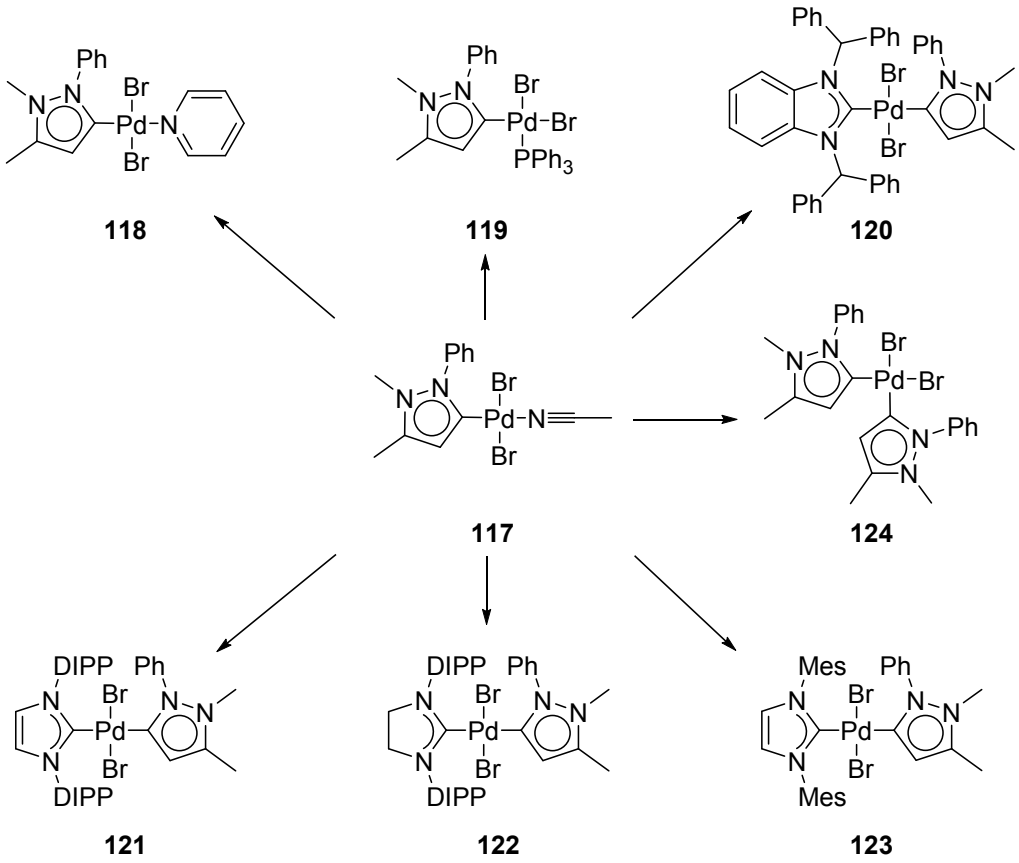

Scheme 6.1. Preparation of a selection of palladium(II) pyry complexes.

All complexes were fully characterized, and with the exception of *trans*-[$PdBr_2$(Bh_2-bimy)(pyry)] (**120**) and *trans*-[$PdBr_2$(IMes)(pyry)] (**122**), molecular structures were obtained. While the mixed phosphine-NHC complex **119** and the homo-bis(NHC) complex **124** were found to adopt a *cis*-configuration, the other complexes adopted a *trans*-arrangement.

All complexes were found to be catalytically active in the direct arylation of pentafluorobenzene. The best results were obtained with the mixed phosphine-NHC complex **119** and the hetero-bis(NHC) complexes **177**, **121** and **122**. An intermediate steric bulk of the coligand seems to be beneficial for this reaction. Given the higher acitivites of palladium(II) NHC complexes bearing carboxylato coligands, it might be of interest to exchange the bromido coligands in the most

active precatalysts for acetato or trifluoroacetato ligands in order to improve the catalytic activities.

In chapter 4, the preparation of indazolin-3-ylidene (indy) complexes of palladium(II), their characterization and their respective catalytic acitivies are discussed. The first section focuses on the 2,3-dihydro-1*H*-pyrazolo[1,2-*a*]indazolin-3-ylidene (indy-5) ligand. Starting from the indazolium salt **131**, reaction with palladium acetate in the presence of an external bromide source yielded the dimeric complex $[PdBr_2(indy\text{-}5)]_2$ (**131**). From this complex, neutral mononuclear complexes **135**-**137** incorporating pyridine or phosphine donor ligands could be prepared. It was also possible to either introduce two triphenylphosphine or one diphosphine ligand, giving rise to the cationic complexes **138**-**140**. All complexes, with the exception of the very insoluble *cis*-$[PdBr_2(PPh_3)(indy\text{-}5)]$ complex **136** were fully characterized. Molecular structures were obtained for all complexes except the cationic complexes **138** and **139**, which were prone to decomposition upon crystallization.

All complexes, along with their congeners featuring an 6,7,8,9-tetrahydropyridazino[1,2-*a*]indazolin-3-ylidene (indy-6) ligand, were tested as precatalysts for two mechanistically different reactions. In the intermolecular hydroamination of phenylacetylene with the sterically shielded 2,6-dimethylaniline, the neutral complexes gave moderate yields, and the *trans*-$[PdBr(PPh_3)_2(indy\text{-}5)]BF_4$ complex **138** and its indy-6 analogue were almost inactive. Good yields were obtained with the dppe and dppp complexes **139**, **140**, **146**, and **147**. However, when considering the instability of these complexes, the catalytic acitivity is most likely due to a decomposition product not containing an indy ligand. In the Sonogashira cross-coupling, the complexes **136**-**138** and **143**-**145** containing monodentate triphenylphosphine ligands performed generally best, while only low yields were observed with the other complexes as precatalysts. The cationic bis(triphenylphosphine) complexes **138** and **145** gave the highest yields, presumably due to the presence of an additional stabilizing phosphine ligand. In both reactions, differences between the catalytic activities of the indy-5 and indy-6 series were minor.

The second part of chapter 4 focuses on the preparation of donor-functionalized indy complexes by post-functionalization of a common precursor complex *trans*-$[PdBr_2(acetonitrile)(indy)]$ (**156**). The indy ligand in **156** bears a bromopropyl side chain. By reaction with secondary amines, the bromo moiety can be replaced by a tertiary amine functionality, and an additional equivalent of secondary amine displaces the acetonitrile ligand at the metal centers. The resulting

complexes *trans*-[$PdBr_2$(amine)(indy)] **157-161** were fully characterized, and molecular structures for complexes **159-161** were obtained. Interestingly, the molecular structures showed evidence for the presence of intramolecular hydrogen bonds between the proton on the secondary amine ligand and one of the bromido coligands, shortening and strengthening the Pd-N bond. Infrared spectroscopy furnished additional evidence for this, and suggested the presence of similar hydrogen bonds in the other complexes as well. The ^{13}C NMR shifts of the $C_{carbene}$ atom in **157-161** showed a linear correlation to the pK_b values of the secondary amine ligands, providing yet another example of the correlation of $C_{carbene}$ chemical shift and ligand donor strength of the transoid ligand in complexes of the type *trans*-[$PdBr_2$(NHC)L]. When complexes **156-161** were used as precatalysts for the direct arylation of 1-methylpyrrole, high yields of the cross-coupled product were obtained with all complexes. The variation between the different precatalysts was only minor, with 84% yield for the least active complex **160** and 97% for the most active complex **157**. However, the substituents of the tertiary amine functionality seem to have an impact on the yields, with the sterically least shielded amine in **157** giving also the best yield, and the sterically most shielded amine in **160** leading to a yield comparable to that of the unfunctionalized complex **156**.

Complex **156** is a useful precursor for the introduction of other donor functionalities as well, and the introduction of potentially coordinating moieties based on nitrogen, oxygen, phosphorus, and sulfur should be explored further.

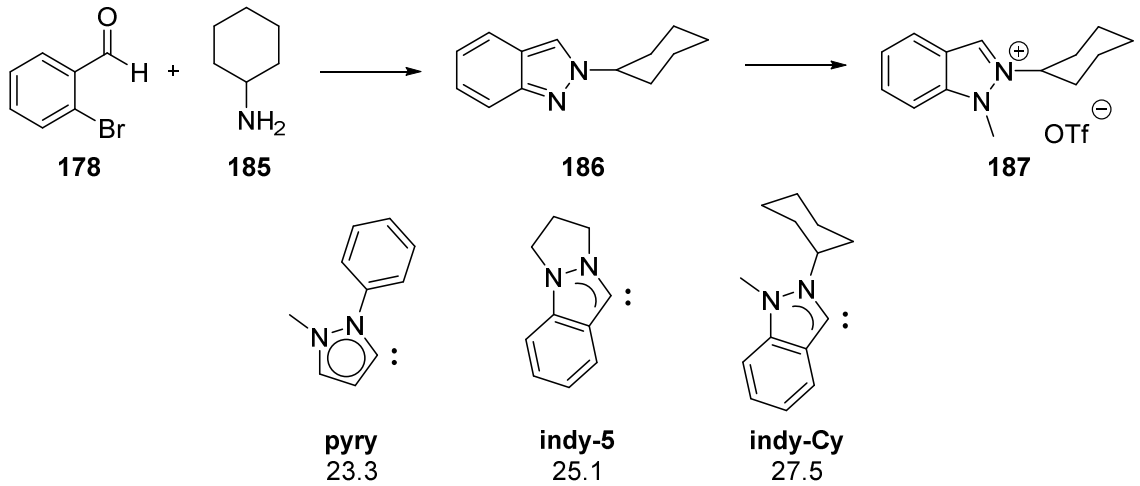

Scheme 6.2. Preparation of indazolium salt with a bulky side chain, and $\%V_{bur}$ values for pyry and indy ligands.

The last section of chapter 4 addresses some of the major shortcomings of the indazolin-3-ylidene chemistry. These are the difficulties associated with preparing a wide variety of ligand precursors, and the lack of steric bulk in most indy ligands reported to date. To address this issue, an alternative synthetic approach to indazolium salts featuring bulkier substituents on N-2 was explored (Scheme. 6.2). By condensation of 2-bromobenzaldehyde (**178**) with amines in the presence of sodium azide under copper(I) catalysis, 2-substituted indazoles could be obtained. In the case of indazole **186**, wich bears a cyclohexyl side chain, the feasibility of transforming these molecules into indazolium salts by alkylation with methyl triflate was demonstrated. The resulting indazolium salt **187** was used to prepare the hetero-bis(NHC) complex **188** and the dimeric complex **189** by means of silver carbene transfer reactions in good yields. Based on the molecular structure of the acetonitrile adduct *trans*-[$PdBr_2$(acetonitrile)(indy)], which was obtained by growing single crystals of dimer **189** in the presence of acetonitrile, the $\%V_{bur}$ value was calculated. Compared to the indy-5 and the pyry ligand in similar acetonitrile adducts, the indy-Cy ligand is sterically more bulky, albeit the $\%V_{bur}$ value falls still short of those found for imidazole-derived NHCs. Further optimization of the synthetic pathway, as well as attempts at including even bulkier or more rigid secondary and tertiary substituents on the amine, are efforts worth pursuing.

The final chapter describes the coordination chemistry of sulfur-functionalized benzimidazolin-2-ylidene ligands with group 10 metals. Two series of ligand precursor salts were prepared: The salts **205**-**207** with an ethylene linker between the NHC and the thioether moiety, and the salts **208**-**210** with a longer propylene linker. Mono-NHC complexes of palladium(II) and platinum(II) were prepared through silver carbene transfer reactions, while homo-bis(NHC) complexes of nickel(II) were synthesized by reaction the benzimidazolium salts with nickel(II) acetate in molten TBAB.

For the platinum(II) complexes **211**-**216**, the κ^2-*C*,*S* coordination mode was unequivocally confirmed as the predominant cordination mode, and all complexes were fully characterized, including their molecular structures. However, complexes **214** and **216**, both featuring a propylene linker between thioether and NHC moieties in the ligand, were found to coexist with other species in solution. Given the high reactivities of platinum-based catalysts in hydroelementation reaction, **211**-**216** were tested as precatalysts for the hydroamination of

phenylacetylene with 2,6-dimethylaniline, and for the hydrosilylation of styrene with bis(trimethylsilyloxy)methylsilane (Scheme 6.3).

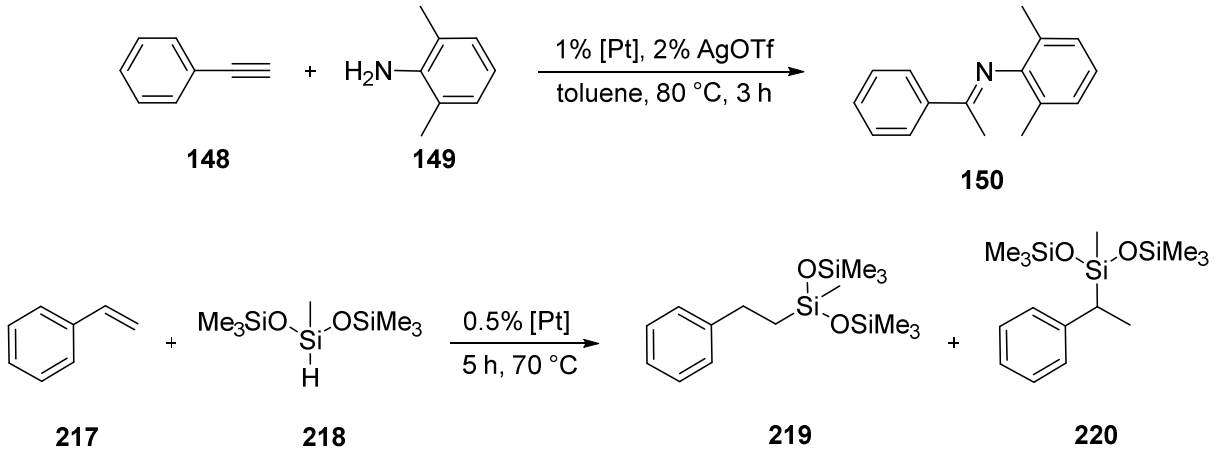

Scheme 6.3. Catalytic activities of platinum(II) complexes **211**-**216**.

The tested complexes were catalytically active for both reactions. In the hydroamination, activation of the precatalysts by addition of silver(I) triflate was required, and yields ranged from moderate to good. However, it should be noted that the reaction conditions were milder and reaction times were shorter than in comparable palladium(II) catalyzed reactions. The reaction, which proceeded with perfect Markovnikov selectivity in all cases, was favored by ethylene linkers between thioether and NHC, giving rise to more stable six-membered metallacycles, and by bulkier NHC wingtip substituents which favor dissociation of the product.

By contrast, in the hydrosilylation quantitative mixtures of the linear product **219** and the branced isomer **220** were observed, with uniform product distributions for all complexes. Quantitative yields were obtained with the complexes featuring propylene linkers between the NHC and thioether moieties, and somewhat lower yields for the ethylene-tethered congeners. The main factor contribution to high yields in this reaction seems to be the solubility in the very unpolar reaction medium, and the use of more lipophilic side chains leads to higher yields.

Given the excellent catalytic activities of these complexes, the synthesis of more lipophilic analogues of complexes **214**-**216** and a systematic exploration of the substrate scope of this reaction are potential areas for further research. An additional possibility is the introduction of

less lightly bound coligands, which holds the potential of further enhancing the catalytic activities of these complexes.

The corresponding mono-NHC complexes of palladium(II) **221**-**226** showed higher molecular dynamic due to the weaker Pd-S bond. At ambient temperature, the methylene and methine resonances of the thioether side chain in these complexes could not be observed due to a coalescence temperature of the interconversions close to 298 K. For complex **221**, variable-temperature measurements up to 368 K in DMSO-d_6 allowed to observe these groups, but for the other complexes, decomposition occurred before the coalescence temperature was reached. For the complexes **221**-**223** featuring ethylene tethers in the ligand the addition of pyridine to the NMR sample suppressed the coordination and decoordination processes of the thioether moiety by blocking the coordination site, and clear NMR spectra were obtained. This strategy was unsuccessful for the remaining three complexes. The lability of the thioether moiety allowed to introduce an additional $^{i}Pr_2$-bimy ligand, giving rise to the hetero-bis(NHC) complexes **227**-**232**, which could be fully characterized, including most of their molecular structures. For complexes **222** and **223**, instead of the expected κ^2-*C*,*S* chelating coordination mode of the ligand, dimeric species with the NHC and the thioether moieties bound to different metal centers. Similar species had been proposed previously, but no evidence for their existence had been provided before.

Complexes **221**-**232** were tested as precatalysts for the direct arylation of phenylacetylene under the same conditions as the indy-5 and indy-6 complexes. Reactions run in the absence of triflic acid produced the desired imine, albeit yields were generally low. With the additive, higher yields were observed for the mono-NHC complexes than for the hetero-bis(NHC) complexes, and the six-membered metallacycles in **221**-**223** performed better than the seven-membered metallacycles **224**-**226**, although the best-performing complex **221** fell short of the yields obtained with indy complex **139**. The complexes **221**-**232** were also tested in the direct arylation of 1-methylpyrrole, under identical conditions as **156**-**161**. In this reaction, the hetero-bis(NHC) complexes performed slightly better than their mono-NHC congeners, and bulky wingtip substituents favored the reaction. However, no discernible influence of the linker lengths in the thioether side chain was observed. When compared to the indy complexes, the benzimidazolin-2-ylidene complexes gave lower yields.

The homo-bis(NHC) complexes of nickel(II) **233**, **234**, **236** and **237** were isolated as inseparable mixtures of *trans-syn* and *trans-anti* rotamers, and this isomerism was studied by means of NMR

spectroscopy and DFT calculations. The energy difference between the rotamers of a simplified model was calculated as 1.85 kJ/mol, which corresponds well to the 3:2 ratio observed for the *trans-anti* and *trans-syn* rotamers of complex **233**. The complexes, which were uncommonly soluble in organic solvents due to the long, lipophilic side chains, were used as precatalysts for the Suzuki-Miyaura coupling of aryl bromides and aryl chlorides. In the presence of triphenylphosphine, complex **233** was found to be an active catalyst, and it was possible to lower reaction temperatures and base loading with activated substrates without compromising the yields. All complexes were able to cross-couple unactivated substrates, albeit yields were low. With the best-performing complex **233**, the substrate scope was explored. Activated aryl bromides and aryl chlorides were cross-coupled in good yields, although nitro groups were not tolerated. Less activated substrates and heteroaryl bromides were challenging substrates, or didn't undergo the reaction at all. Future work in this field should aim to include harder donor sites in the side chain, which are more suited to the hard nickel(II) center, or a phosphine functionality, which has been used to great success in related systems. The preparation of mono-NHC complexes with thioether-functionalized NHCs is also of interest.

The last section of chapter 5 deals with the pincer-pseudopincer isomerism observed in palladium(II) complexes of thioether-tethered bis(NHC) ligands. These can either bind as a κ_3-*C,S,C* ligand and form cationic pincer complexes, or as κ^2-*C,C* ligands forming neutral pseudopincers. It has been demonstrated that the preference for one or the other is linked to the ligand donor strength of the carbene moieties. More electron-rich NHCs stabilize the cationic pincer form, while less electron-rich NHCs lead to a preference for the neutral pseudopincers. These results might be useful in fine-tuning pincer ligands with hemilabile coordination sites for catalytic applications.

7. Experimental Section

General Considerations

Unless otherwise noted all operations were performed without taking precautions to exclude air and moisture. All solvents and chemicals were used as received without any further treatment if not indicated otherwise. Anhydrous solvents were prepared by drying over sodium and benzophenone (tetrahydrofurane, benzene) or calcium hydride (dichloromethane, acetonitrile), and distilled under nitrogen prior to use. ^{1}H, ^{13}C, ^{19}F and ^{31}P NMR spectra were recorded on a Bruker ACF 300 or a Bruker AMX 500 spectrometer. NMR Chemical shifts (δ) were referenced internally to the residual solvent signals relative to tetramethylsilane (^{1}H and ^{13}C), or externally to CF_3CO_2H (^{19}F) and 85% H_3PO_4 (^{31}P). ESI mass spectra were recorded using a Finnigan LCQ spectrometer. GC-MS were obtained using an Agilent 7890A Gas Chromatograph together with an Agilent 5975 mass spectrometer (EI). X-ray diffraction analyses were performed by the staff at the X-ray diffraction laboratory, Department of Chemistry, National University of Singapore, using a Bruker D8 VENTURE or a Bruker SMART APEX Single Crystal X-ray Diffractometer. Elemental analyses were done using an Elementar Vario Micro Cube by the staff at the elemental analyses laboratory, Department of Chemistry, National University of Singapore.

The dimer $[PdBr_2(^{i}Pr_2\text{-bimy})]_2$,[29] 1,3-dibenzhydrylbenzimidazolium bromide,[124] IPr·HBr,[27] IPr·HCl,[27] IMes·HBr,[27] SIPr·HBr,[28] SIMes·HBr,[28] *trans*-$[PdCl_2(IPr)(pyridine)]$,[74a] $[NiBr_2(PPh_3)_2]$, [211] 1-benzylbenzimidazole,[124] 1-isobutylbenzimidazole,[173] 1-benzhydryl-benzimidazole,[124] benzimidazolium salt **199**,[55f] and benzimidazolium salt **202**[155] were prepared according to reported procedures.

5-ethoxy-3-methyl-1-phenyl-1*H*-pyrazole (60).

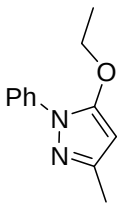

Ethyl acetoacetate (1.00 g, 7.69 mmol, 1.00 equiv.) and phenylhydrazine-hydrochloride (1.17 g, 8.07 mmol, 1.05 equiv.) were dissolved in absolute ethanol (45 mL). The resulting mixture was heated to reflux for 11 h. After that time, it was allowed to cool to ambient temperature, and the solvent was evaporated *in vacuo*. The residue was suspended in dichloromethane (60 mL) and the solution was washed with sodium bicarbonate solution (1 M, 4 × 50 mL). The organic phase was dried over sodium sulfate, filtered, and the solvent was removed *in vacuo*. Upon addition of hexane/ethyl acetate 3:1, an off-white

precipitate formed. The solution was filtered again, concentrated *in vacuo*, and the oily residue was purified by column chromatography (silica gel, hexane/ethyl acetate 3:1). The product was isolated as an orange liquid (210 mg, 1.04 mmol, 13%). **^{1}H-NMR** (300 MHz, $CDCl_3$): δ 7.70 (dd, J = 1 Hz, 9 Hz, 2 H, Ar-H), 7.43 (t, J = 8 Hz, 2 H, Ar-H), 7.29 (d, J = 8 Hz, 1 H, Ar-H), 5.56 (s, 1 H, CH), 4.19 (q, $^3J_{H\text{-}H}$ = 7 Hz, 2 H, OCH_2), 2.37 (s, 3 H, CH_3), 1.45 (t, ^3J = 7 Hz, 3 H, CH_2CH_3),. The analytical data was in accordance with reported values.[108]

5-aminophenyl-3-methyl-1-phenyl-1*H*-pyrazole (63).

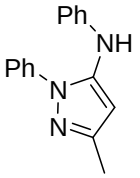

Pyrazolone **61** (600 mg, 3.44 mmol, 1.00 equiv), phosphorous pentoxide (293 mg, 2.06 mmol, 0.60 eq) and anilinium chloride (535 mg, 4.13 mmol, 1.10 equiv.) were thoroughly mixed and heated to 210°C for 30 min by microwave irradiation in a pressure tube. The black solid formed during the reaction was dissolved in water and ethanol (1:1, 10 mL). The aqueous phase was extracted with ethyl acetate (2 × 50 mL), the combined organic layers were dried over sodium sulfate, filtered and the solvent was evaporated *in vacuo*. Recrystallization of the residue from hexane/ethyl acetate yielded the product as a dark orange solid (522 mg, 2.09 mmol, 61%). ^{1}H-NMR (300 MHz, $CDCl_3$): δ 7.58–7.53 (m, 2 H, Ar-H), 7.59–7. 44 (m, 2 H, Ar-H), 7.39–7. 27 (m, 4 H, Ar-H), 7.00–6.59 (m, 2 H, Ar-H), 6.01 (s, 1 H, CH), 5.64 (br, 1 H, NH), 2.36 (s, 3 H, CH_3). The analytical data was in accordance with reported values.[212]

5-methoxy-3-methyl-1-phenyl-1*H*-pyrazole (64).

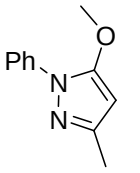

Pyrazolone **61** (400 mg, 2.30 mmol, 1.00 equiv.), methanol (91.8 mg), 2.87 mmol, 0.12 mL, 1.25 eq) and triphenylphosphine (902 mg, 3.44 mmol, 1.50 equiv.) were dissolved in anhydrous toluene under inert atmosphere. Diethyl azodicarboxylate (599 mg, 3.44 mmol, 0.54 mL, 1.50 equiv.) was added, and the mixture was stirred at ambient temperature for 20 h. After this time, methanol (1 mL) was added, and after 1 min, the solution was poured into water (20 mL). The aqueous phase was extracted with dichloromethane (2 × 20 mL). The combined organic layers were washed with sodium hydroxide solution (2 M, 20 mL) and water (2 × 20 mL), dried over sodium sulfate, filtered, and the solvent was removed *in vacuo*. The residue was purified by column chromatrography (silica gel, ethyl acetate/hexane 1:3). The product was obtained as pale yellow liquid (202 mg, 1.07 mmol, 47%) ^{1}H-NMR (300

MHz, $CDCl_3$): δ 7.71–7.63 (m, 2 H, Ar-H), 7.44–7.35 (m, 2 H, Ar-H), 7.27–7.18 (m, 1 H, Ar-H), 5.50 (s, 1 H, CH), 3.89 (s, 3 H, OCH_3), 2.28 (s, 3 H, CH_3). The analytical data was in accordance with reported values.[108]

1,3,5-Triphenyl-1*H*-pyrazole (68).

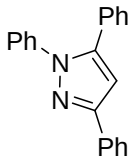

Dibenzoylmethane (12.0 g, 53.5 mmol, 1.00 equiv.) and phenylhydrazine-hydrochloride (8.50 g, 58.8 mmol, 1.10 equiv.) were dissolved in 2-propanol (120 mL). The resulting mixture was heated to reflux for 14 h. After that time, it was allowed to cool to ambient temperature, and the solvent was evaporated *in vacuo*. The residue was suspended in dichloromethane (100 mL) and the solution was washed with sodium bicarbonate solution (1 M, 250 mL). The organic phase was dried over sodium sulfate, filtered, and the solvent was removed *in vacuo*. The residue was purified by recrystallization from methanol. The product was isolated as pale yellow solid (13.2 g, 44.5 mmol, 83%). ^{1}H NMR (300 MHz, $CDCl_3$): δ 8.00–7.94 (m, 2 H, Ar-H), 7.28–7.49 (m, 13 H, Ar-H), 6.85 (s, 1 H, CH). The analytical data was in accordance with reported values.[213]

3,5-Dimethyl-1-phenyl-1*H*-pyrazole (69).

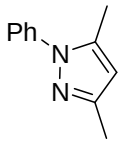

Pyrazole **69** was prepared from acetylacetonate (5.00 g, 50.0 mmol, 1.00 equiv.) and phenylhydrazine-hydrochloride (7.59 g, 52.5 mmol, 1.05 equiv.) in absolute ethanol (300 mL) in analogy to **68**. The product was purified by Kugelrohr distillation (p = 1 mbar, T = 120 °C), and isolated as pale yellow liquid (7.54 g, 43.8 mmol, 88% yield). ^{1}H NMR (300 MHz, $CDCl_3$): δ 7.45–7. 38 (m, 4 H, Ar-H), 7.36–7.28 (m, 1 H, Ar-H), 5.98 (s, 1 H, CH), 2.29 (s, 3 H, CH_3), 2.28 (s, 3 H, CH_3). The analytical data was in accordance with reported values.[110]

3,5-Diisopropyl-1-phenyl-1*H*-pyrazole (70).

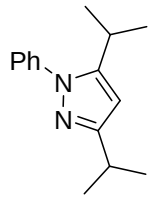

Pyrazole **70** was prepared from **67** (970 mg, 6.21 mmol, 1.00 equiv.) and phenylhydrazine-hydrochloride (988 mg, 6.83 mmol, 1.10 equiv.) in 2-propanol (14 mL) in analogy to **68**. The product was isolated as an orange liquid (1.32 g, 5.78 mmol, 93%). ^{1}H NMR (300 MHz, $CDCl_3$): δ 7.49–7. 32 (m, 5 H, Ar-H), 6.04 (s, 1 H, CH), 3.00 (sept, $^3J_{H\text{-}H}$ = 7 Hz, 1 H, CH), 3.00 (sept, $^3J_{H\text{-}H}$ = 7 Hz, 1 H, CH), 1.30 (d, $^3J_{H\text{-}H}$

= 7 Hz, 3 H, CH_3), 1.17 (d, $^3J_{H\text{-}H}$ = 7 Hz, 3 H, CH_3). The analytical data was in accordance with the reported values.[42d]

4-Chloro-1,3,5-triphenyl-1*H*-pyrazole (71).

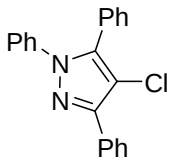

Pyrazole (**68**) (500 mg, 1.68 mmol, 1.00 equiv.) and N-chlorosuccinimide (561 mg, 4.20 mmol, 2.50 equiv) were dissolved in ethyl acetate (8 mL). The solution was sonicated at ambient temperature for 4 h. The reaction mixture was washed with saturated sodium thiosulfate (2 × 20 mL) and water (20 mL), dried over sodium sulfate, and filtered. The solvent was removed *in vacuo*. The product was obtained as an orange solid (556 mg, 1.68 mmol, > 99%). ^{1}H NMR (300 MHz, $CDCl_3$): δ 8.07–8.00 (m, 2 H, Ar-H), 7.52–7.27 (m, 13 H, Ar-H). $^{13}C\{^1H\}$ NMR (75 MHz, $CDCl_3$): δ 148.8 (C=N), 141.0 (C-N), 140.5, 132.3, 130.7, 129.6, 129.6, 129.2, 129.2, 129.1, 129.1, 129.0, 128.4, 128.3 (Ar-C), 125.5 (C-Cl, Ar-C). Anal. Calcd. for $C_{21}H_{15}BrN_2 \cdot HCl$: C, 68.68; H, 4.39; N, 7.63. Found: C, 68.66; H, 3.93; N 7.68. MS (ESI) *m/z* 331 $[M + H]^+$.

4-Bromo-1,3,5-triphenyl-1*H*-pyrazole (72).

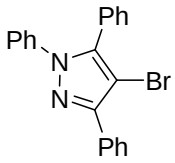

Bromopyrazole **72** was prepared in analogy to **71** from **68** (500 mg, 1.68 mmol, 1.00 equiv) and N-bromosuccinimide (1.03 g, 5.80 mmol, 2.00 equiv) in ethyl acetate (13 mL). The product was obtained as a pale yellow oil (630 mg, 1.68 mmol, >99%). ^{1}H NMR (300 MHz, $CDCl_3$): δ δ 8.05–7.97 (m, 2 H, Ar-H), 7.53–7.27 (m, 13 H, Ar-H). The analytical data was in accordance with reported values.[214]

4-Iodo-1,3,5-triphenyl-1*H*-pyrazole (73).

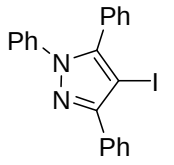

Iodopyrazole **73** was prepared in analogy to **71** from **68** (2.58 g, 8.71 mmol, 1.00 equiv.) and N-iodosuccinimide (2.94 g, 13.1 mmol, 1.50 equiv.) in ethyl acetate (20 mL). The product was obtained as an off-white solid (3.37 g, 7.98 mmol, 92%). ^{1}H NMR (300 MHz, $CDCl_3$): δ 8.02–7.92 (m, 2 H, Ar-H), 7.52–7.27 (m, 13 H, Ar-H). The analytical data was in accordance with reported values.[215]

4-Bromo-3,5-dimethyl-1-phenyl-1*H*-pyrazole (75).

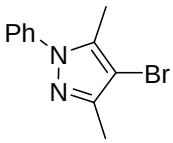

Bromopyrazole **75** was prepared in analogy to **71** from **69** (500 mg, 2.90 mmol, 1.00 equiv) and N-bromosuccinimide (1.03 g, 5.80 mmol, 2.00 equiv) in ethyl acetate (13 mL). The product was obtained as a pale yellow oil (700 mg, 2.79 mmol, 96%). ^{1}H NMR (300 MHz, $CDCl_3$): δ 7.50–7.33 (m, 5 H, Ar-H), 2.30 (s, 3 H, CH_3), 2.30 (s, 3 H, CH_3). The analytical data was in accordance with reported values.[112]

4-Iodo-3,5-dimethyl-1-phenyl-1*H*-pyrazole (76).

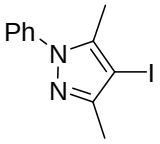

Iodopyrazole **76** was prepared in analogy to **71** from **69** (1.50 g, 8.71 mmol, 1.00 equiv) and N-iodosuccinimide (2.94 g, 13.1 mmol, 1.50 equiv) in ethyl acetate (20 mL). The product was obtained as a light brown oil (2.46 g, 8.25 mmol, 95% yield). ^{1}H NMR (300 MHz, $CDCl_3$): δ 7.33 – 7.50 (m, 5 H, Ar-H), 2.33 (s, 3 H, CH_3), 2.30 (s, 3 H, CH_3). The analytical data was in accordance with the reported values.[112]

4-Bromo-2-Methyl-1,3,5-triphenyl-1*H*-pyrazolium tetrafluoroborate (79).

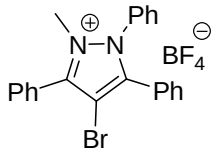

Salt **41** was prepared following the general procedure using bromopyrazole **72** (555 mg, 1.55 mmol). The product was obtained as a white solid (521 mg, 1.09 mmol, 70% yield). ^{1}H NMR (300 MHz, $CDCl_3$): δ 7.87–7. 74 (m, 4 H, Ar-H), 7.59–7.40 (m, 8 H, Ar-H), 7.39–7.34 (m, 1 H, Ar-H), 7.31–7.24 (m, 2 H, Ar-H), 3.73 (s, 3 H, CH_3).

4-Iodo-2-Methyl-1,3,5-triphenyl-1*H*-pyrazolium tetrafluoroborate (80).

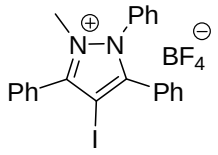

Salt **39** was prepared following the general procedure using iodopyrazole **73** (641 mg, 1.52 mmol). The product was obtaines as a white solid (530 mg, 1.01 mmol, 67% yield). ^{1}H NMR (300 MHz, $CDCl_3$): δ 7.92 – 7.98 (m, 1 H, Ar-.H), 7.74 – 7.79 (m, 1 H, Ar-H), 7.68 – 7.73 (m, 1 H, Ar-H), 7.54 – 7.60 (m, 2 H, Ar-H), 7.45 – 7.52 (m, 3 H, Ar-H), 7.39 – 7.45 (m, 3 H, Ar-H), 7.29 – 7.37 (m, 4 H, Ar-H), 3.74 (s, 3 H, CH_3).

***trans*-Dibromido-(5-aminophenyl-3-methyl-1-phenyl-1*H*-pyrazole)(1,3-diisopropyl-benzimidazolin-2-ylidene)palladium(II) (81).**

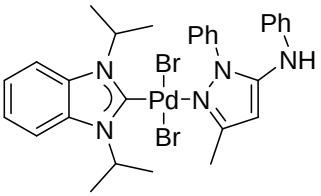

Complex **81** was prepared following the general procedure using 5-aminophenylpyrazole **63** (25 mg, 0.10 mmol, 2.0 equiv). A yellow solid was obtained (75 mg, 0.10 mmol, >99%). ^{1}H NMR (300 MHz, $CDCl_3$): δ 7.93–7.88 (m, 2 H, Ar-H), 7.69–7.60 (m, 3 H, Ar-H), 7.52–7.47 (m, 1 H, Ar-H), 7.46–7.41 (m, 1 H, Ar-H), 7.29–7.20 (m, 2 H, Ar-H), 7.15–7.10 (m, 2 H, Ar-H), 7.00–6.94 (m, 3 H, Ar-H), 6.26 (sept, $^{3}J_{H-H}$ = 7 Hz, 1 H, NCH), 6.00 (s, 1 H, CH), 5.55 (s_{br}, 1 H, NH), 5.32 (sept, $^{3}J_{H-H}$ = 7 Hz, 1 H, NCH), 2.75 (s, 3 H, CH_3), 1.78 (d, $^{3}J_{H-H}$ = 7 Hz, 6 H, CH_3), 1.44 (d, $^{3}J_{H-H}$ = 7 Hz, 6 H, CH_3). $^{13}C\{^{1}H\}$ NMR (75 MHz, $CDCl_3$): δ 162.8 ($C_{carbene}$), 151.0 (C=N), 145.2 (C-N), 141.8, 137.1, 134.1, 133.9, 130.7, 130.1, 130.0, 129.9, 122.7, 122.6, 117.9, 113.0, 113.0 (Ar-C), 94.5 (CH), 54.9 (NCH), 54.4 (NCH), 21.4 (CH_3), 20.8 (CH_3), 15.9 (CH_3). Anal. Calcd. for $C_{29}H_{33}Br_2N_5Pd$: C, 48.52; H, 4.63; N, 9.76. Found: C, 48.15; H, 3.93; N, 9.40. MS (ESI) *m*/*z* 636 $[M - Br]^+$.

***trans*-Dibromido(5-methoxy-3-methyl-1-phenyl-1*H*-pyrazole)(1,3-diisopropylbenzimidazolin-2-ylidene)palladium(II) (82).**

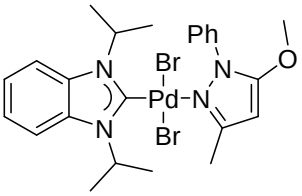

Complex **82** was prepared following the general procedure using 5-methoxypyrazole **64** (19 mg, 0.10 mmol, 2.0 equiv.). A yellow solid was obtained (66 mg, 0.10 mmol, >99%). ^{1}H NMR (300 MHz, $CDCl_3$): δ 7.93–7.87 (m, 2 H, Ar-H), 7.66–7.59 (m, 2 H, Ar-H), 7.59–7.53 (m, 1 H, Ar-H), 7.53–7.48 (m, 1 H, Ar-H), 7.47–7.42 (m, 1 H, Ar-H), 7.16–7.11 (m, 2 H, Ar-H), 6.26 (sept, $^{3}J_{H-H}$ = 7 Hz, 1 H, NCH), 5.60 (s, 1 H, CH), 5.43 (sept, $^{3}J_{H-H}$ = 7 Hz, 1 H, C*H*$(CH_3)_2$), 3.84 (s, 3 H, OCH_3), 2.76 (s, 3 H, CH_3), 1.77 (d, $^{3}J_{H-H}$ = 7 Hz, 6 H, CH_3), 1.45 (d, $^{3}J_{H-H}$ = 7 Hz, 6 H, CH_3). $^{13}C\{^{1}H\}$ NMR (75 MHz, $CDCl_3$): δ 162.3 ($C_{carbene}$), 157.5 (C=N), 151.0 (C-N), 137.2, 134.1, 133.9, 129.7, 129.4, 129.2, 122.6, 113.0, 113.0 (Ar-C), 87.8 (CH), 59.4 (OCH_3), 54.9 (NCH), 54.4 (NCH), 21.4 (CH_3), 20.8 (CH_3), 16.3 (CH_3). Anal. Calcd for $C_{24}H_{30}Br_2N_4OPd$: C, 43.89; H, 4.60; N, 8.53. Found: C, 43.61; H, 4.15; N, 8.85. MS (ESI) *m*/*z* 577 $[M - Br]^+$.

***trans*-Dibromido(1,3,5-triphenyl-1*H*-pyrazole)(1,3-diisopropylbenzimidazolin-2-ylidene)palladium(II) (83).**

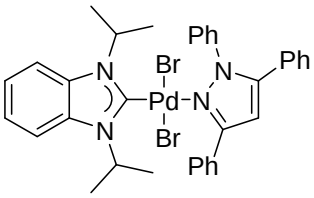

Complex **83** was prepared following the general procedure using 1,3,5-triphenyl-1*H*-pyrazole (**68**) (30 mg, 0.10 mmol, 2.0 equiv.). A pale yellow solid was obtained (73 mg, 0.10 mmol 95% yield). ^{1}H NMR (300 MHz, $CDCl_3$): δ 8.48–8.41 (m, 2 H, Ar-H), 7.94–7.86 (m, 2 H, Ar-H), 7.63–7.56 (m, 5 H, Ar-H), 7.47–7.36 (m, 2 H, Ar-H), 7.31–7.22 (m, 6 H, Ar-H), 7.14–7.07 (m, 2 H, Ar-H), 6.76 (s, 1 H, CH), 5.93 (sept, $^{3}J_{H\text{-}H}$ = 7 Hz, 1 H, NCH), 5.07 (sept, $^{3}J_{H\text{-}H}$ = 7 Hz, 1 H, NCH), 1.55 (d, $^{3}J_{H\text{-}H}$ = 7 Hz, 6 H, CH_3), 1.41 (d, $^{3}J_{H\text{-}H}$ = 7 Hz, 6 H, CH_3). ^{13}C{^{1}H} NMR (75 MHz, $CDCl_3$): δ 161.6 ($C_{carbene}$), 154.9 (C=N), 147.9 (C-N), 139.4, 134.0, 133.9, 133.2, 131.6, 130.4, 129.9, 129.6, 129.5, 129.4, 129.3, 129.3, 129.1, 128.8, 122.6, 122.5, 113.0, 113.0 (Ar-C), 107.8 (CH), 54.7 (NCH), 54.3 (NCH), 20.9 (CH_3), 20.9 (CH_3). Anal. Calcd. for $C_{34}H_{34}Br_2N_4Pd$: C, 53.39; H, 4.48; N, 7.32. Found: C, 53.15; H, 4.27; N, 7.31.

***trans*-Dibromido(3,5-dimethyl-1-phenyl-1*H*-pyrazole)(1,3-diisopropylbenzimidazolin-2-ylidene)palladium(II) (84).**

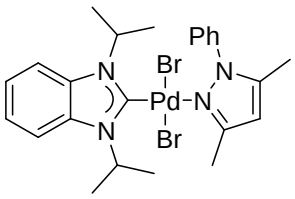

Complex **84** was prepared following the general procedure using 3,5-dimethylpyrazole **69** (17 mg, 0.10 mmol, 2.0 equiv). A pale yellow solid was obtained (56 mg, 0.09 mmol, 87%). ^{1}H NMR (300 MHz, $CDCl_3$): δ 7.83–7.73 (m, 2 H, Ar-H), 7.71–7.56 (m, 3 H, Ar-H), 7.55–7.39 (m, 2 H, Ar-H), 7.18–7.08 (m, 2 H, Ar-H), 6.25 (sept, $^{3}J_{H\text{-}H}$ = 7.Hz, 1 H, NCH), 6.08 (s, 1 H, CH), 5.27 (sept, $^{3}J_{H\text{-}H}$ = 7 Hz, 1 H, NCH), 2.75 (s, 3 H, CH_3), 2.15 (s, 3 H, CH_3), 1.77 (d, $^{3}J_{H\text{-}H}$ = 7 Hz, 6 H, CH_3), 1.43 (d, $^{3}J_{H\text{-}H}$ = 7 Hz, 6 H, CH_3). ^{13}C{^{1}H} NMR (75 MHz, $CDCl_3$): δ 163.0 ($C_{carbene}$), 150.1 (C=N), 143.3 (C-N), 138.8, 134.0, 133.9, 130.6, 129.7, 129.4, 122.6, 113.1, 113.0 (Ar-C), 108.0 (CH), 54.9 (NCH), 54.4 (NCH), 21.4 (CH_3), 20.8 (CH_3), 15.3 (CH_3), 12.7 (CH_3). Anal. Calcd. for $C_{24}H_{30}Br_2N_4Pd$: C, 44.99; H, 4.72; N, 8.74. Found: C, 44.77; H, 4.58; N, 8.21. MS (ESI) *m*/*z* 560 $[M - Br]^+$, 663 $[M + Na]^+$.

***trans*-Dibromido(3,5-diisopropyl-1-phenyl-1*H*-pyrazole)(1,3-diisopropylbenzimidazolin-2-ylidene)palladium(II) (85).**

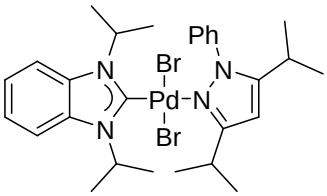

Complex **85** was prepared following the general procedure using 3,5-diisopropylpyrazole **70** (23 mg, 0.10 mmol, 2.0 equiv.). A yellow solid was obtained (70 mg, 0.10 mmol, >99%). ^{1}H NMR (300 MHz, $CDCl_3$): δ 7.83–7.75 (m, 2 H, Ar-H), 7.68–7.59 (m, 3 H, Ar-H), 7.53–7.46 (m, 1 H, Ar-H), 7.45–7.39 (m, 1 H, Ar-H), 7.16–7.08 (m, 2 H, Ar-H), 6.29 (sept, $^{3}J_{H-H}$ = 7 Hz, 1 H, NCH), 6.09 (s, 1 H, CH), 5.10 (sept, $^{3}J_{H-H}$ = 7 Hz, 1 H, NCH), 3.98 (sept, $^{3}J_{H-H}$ = 7 Hz, 1 H, CH), 2.77 (sept, $^{3}J_{H-H}$ = 7 Hz, 6 H, CH), 1.76 (d, $^{3}J_{H-H}$ = 7 Hz, 6 H, CH_3), 1.54 (d, $^{3}J_{H-H}$ = 7 Hz, 6 H, CH_3), 1.42 (d, $^{3}J_{H-H}$ = 7 Hz, 6 H, CH_3), 1.12 (d, $^{3}J_{H-H}$ = 7 Hz, 6 H, CH_3). $^{13}C\{^{1}H\}$ NMR (75 MHz, $CDCl_3$): δ 163.1 ($C_{carbene}$), 160.3 (C=N), 154.1 (C-N), 139.0, 134.0, 133.9, 131.4, 129.8, 129.3, 122.6, 122.5, 113.0, 113.0 (Ar-C), 100.5 (CH), 54.9 (NCH), 54.3 (NCH), 29.1 (CH), 26.4 (CH), 23.4 (CH_3), 23.1 (CH_3), 21.3 (CH_3), 20.9 (CH_3). Anal. Calcd. for $C_{28}H_{39}Br_2N_4Pd$: C, 48.26; H, 5.50; N, 8.04. Found: C, 48.48; H, 4.99; N 8.06.

***trans*-Dibromido(4-chloro-1,3,5-triphenyl-1*H*-pyrazole)(1,3-diisopropylbenzimidazolin-2-ylidene)palladium(II) (86).**

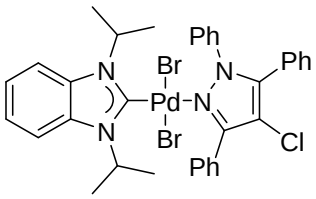

Complex **86** was prepared following the general procedure using pyrazole **71** (33 mg, 0.10 mmol, 2.0 equiv). An orange solid was obtained (80 mg 0.10 mmol, >99%). ^{1}H NMR (300 MHz, $CDCl_3$): δ 8.35–8.26 (m, 2 H, Ar-H), 7.89–7.82 (m, 2 H, Ar-H), 7.70–7.53 (m, 6 H, Ar-H), 7.45–7.31 (m, 7 H, Ar-H), 7.14–7.06 (m, 2 H, Ar-H), 5.67 (sept, $^{3}J_{H-H}$ = 7 Hz, 1 H, NCH), 5.11 (sept, $^{3}J_{H-H}$ = 7 Hz, 1 H, NCH), 1.50 (d, $^{3}J_{H-H}$ = 7 Hz, 6 H, CH_3), 1.41 (d, $^{3}J_{H-H}$ = 7 Hz, 6 H, CH_3). $^{13}C\{^{1}H\}$ NMR (75 MHz, $CDCl_3$): δ 160.8 ($C_{carbene}$), 151.5 (C=N), 144.0 (C-N), 139.1, 133.9, 133.8, 131.7, 131.3, 130.7, 130.5, 130.1, 130.1, 129.8, 129.4, 129.1, 128.7, 127.4, 122.6, 122.6, 113.0, 113.0 (Ar-C), 110.6 (C-Cl), 54.6 (NCH), 54.4 (NCH), 20.8 (CH_3), 20.8 (CH_3). Anal. Calcd. for $C_{34}H_{33}Br_2ClN_4Pd$: C, 51.09; H, 4.16; N, 7.01. Found: C, 51.29; H, 4.45; N, 7.09.

***trans*-Dibromido(4-bromo-1,3,5-triphenyl-1*H*-pyrazole)(1,3-diisopropylbenzimidazolin-2-ylidene)palladium(II) (87).**

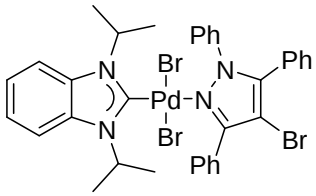

Complex **87** was prepared following the general procedure using pyrazole **72** (38 mg, 0.10 mmol, 2.0 equiv.). An orange solid was obtained (84 mg, 0.10 mmol, >99%). ^{1}H NMR (300 MHz, $CDCl_3$): δ 8.30–8.20 (m, 2 H, Ar-H), 7.88–7.81 (m, 2 H, Ar-H), 7.68–7.52 (m, 6 H, Ar-H), 7.44–7.32 (m, 7 H, Ar-H), 7.15–7.05 (m, 2 H, Ar-H), 5.61 (sept, $^{3}J_{H\text{-}H}$ = 7 Hz, 1 H, NCH), 5.10 (sept, $^{3}J_{H\text{-}H}$ = 7 Hz, 1 H, NCH), 1.48 (d, $^{3}J_{H\text{-}H}$ = 7 Hz, 6 H, CH_3), 1.40 (d, $^{3}J_{H\text{-}H}$ = 7 Hz, 6 H, CH_3). $^{13}C\{^{1}H\}$ NMR (75 MHz, $CDCl_3$): δ 160.8 ($C_{carbene}$), 152.9 (C=N), 145.7 (C-N), 139.1, 133.9, 133.8, 131.9, 131.4, 131.2, 130.7, 130.3, 130.1, 129.7, 129.3, 129.0, 128.6, 128.0, 122.6, 122.6, 113.0, 113.0 (Ar-C), 96.8 (C-Br), 54.6 (NCH), 54.4 (NCH), 20.8 (CH_3), 20.8 (CH_3). Anal. Calcd. for $C_{34}H_{33}Br_3N_4Pd$: C, 48.40; H, 3.94; N, 6.64. Found: C, 48.74; H, 4.16; N, 7.32.

***trans*-Dibromido(4-iodo-1,3,5-triphenyl-1*H*-pyrazole)(1,3-diisopropylbenzimidazolin-2-ylidene)palladium(II) (88).**

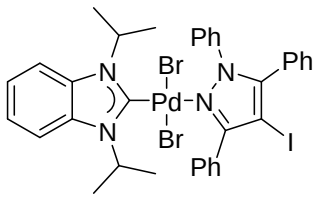

Complex **88** was prepared following the general procedure pyrazole **73** (42 mg, 0.10 mmol, 2.0 equiv.). An off-white solid was obtained (87 mg, 0.10 mmol, 98%). ^{1}H NMR (300 MHz, $CDCl_3$): δ 8.23–8. 15 (m, 2 H, Ar-H), 7.86–7.84 (m, 2 H, Ar-H), 7.69–7.49 (m, 6 H, Ar-H), 7.45–7.31 (m, 7 H, Ar-H), 7.13–7.06 (m, 2 H, Ar-H), 5.55 (sept, $^{3}J_{H\text{-}H}$ = 7 Hz, 1 H, NCH), 5.11 (sept, $^{3}J_{H\text{-}H}$ = 7 Hz, 1 H, NCH), 1.47 (d, $^{3}J_{H\text{-}H}$ = 7 Hz, 6 H, CH_3), 1.40 (d, $^{3}J_{H\text{-}H}$ = 7 Hz, 6 H, CH_3). $^{13}C\{^{1}H\}$ NMR (75 MHz, $CDCl_3$): δ 160.9 ($C_{carbene}$), 156.0 (C=N), 149.0 (C-N), 139.2, 133.9, 133.8, 132.6, 132.2, 131.1, 130.9, 130.1, 130.0, 129.7, 129.3, 129.0, 128.6, 122.6, 122.6, 113.0, 113.0 (Ar-C), 65.8 (C-I), 54.6 (NCH), 54.4 (NCH), 20.8 (CH_3), 20.8 (CH_3). Anal. Calcd. for $C_{34}H_{33}Br_2IN_4Pd$: C, 45.84; H, 3.73; N, 6.29. Found: C, 45.93; H, 3.49; N, 6.57.

***trans*-Dibromido(4-bromo-3,5-dimethyl-1-phenyl-1*H*-pyrazole)(1,3-diisopropylbenzimidazolin-2-ylidene)palladium(II) (89).**

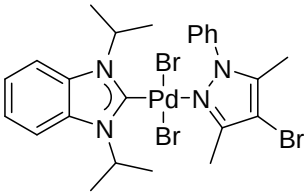

Complex **89** was prepared following the general procedure using pyrazole **75** (25 mg, 0.10 mmol, 2.0 equiv.). A pale yellow solid was obtained (70 mg , mmol, 97%). ^{1}H NMR (300 MHz, $CDCl_3$): δ 7.82–7.61 (m, 5 H, Ar-H), 7.54–7.39 (m, 2 H, Ar-H), 7.18–7.08 (m, 2 H, Ar-H), 6.22 (sept, $^{3}J_{H\text{-}H}$ = 7 Hz, 1 H, NCH), 5.22 (sept, $^{3}J_{H\text{-}H}$ = 7 Hz, 1 H, NCH), 2.76 (s, 3 H, CH_3), 2.17 (s, 3 H, CH_3), 1.77 (d, $^{3}J_{H\text{-}H}$ = 7 Hz, 6 H, CH_3), 1.42 (d, $^{3}J_{H\text{-}H}$ = 7 Hz, 6 H, CH_3). $^{13}C\{^{1}H\}$ NMR (75 MHz, $CDCl_3$): δ 161.8 ($C_{carbene}$), 148.9 (C=N), 142.0 (C-N), 138.7, 134.0, 133.9, 130.5, 130.2, 129.6, 122.7, 113.1, 113.0 (Ar-C), 97.2 (C-Br), 55.1 (NCH), 54.4 (NCH), 21.3 (CH_3), 20.8 (CH_3), 14.3 (CH_3), 12.1 (CH_3). Anal. Calcd. for $C_{24}H_{29}Br_3N_4Pd\cdot CHCl_3$: C, 35.79; H, 3.60; N, 6.68. Found: C, 36.05; H, 3.18; N, 6.68. MS (ESI) *m*/*z* 637 $[M - Br]^+$.

***trans*-Dibromido(4-iodo-3,5-dimethyl-1-phenyl-1*H*-pyrazole)(1,3-diisopropylbenzimidazolin-2-ylidene)palladium(II) (90).**

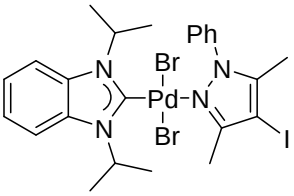

Complex **90** was prepared following the general procedure using pyrazole **76** (30 mg, 0.10 mmol, 2.0 equiv.). A pale yellow solid was obtained (79 mg, 0.10 mmol, >99%). ^{1}H NMR (300 MHz, $CDCl_3$): δ 7.81–7.75 (m, 2 H, Ar-H), 7.71–7.62 (m, 3 H, Ar-H), 7.53–7.48 (m, 1 H, Ar-H), 7.46–7.41 (m, 1 H, Ar-H), 7.17–7.11 (m, 2 H, Ar-H), 6.22 (sept, $^{3}J_{H\text{-}H}$ = 7 Hz, 1 H, NCH), 5.21 (sept, $^{3}J_{H\text{-}H}$ = 7 Hz, 1 H, NCH), 2.78 (s, 3 H, CH_3), 2.20 (s, 3 H, CH_3), 1.77 (d, $^{3}J_{H\text{-}H}$ = 7 Hz, 6 H, CH_3), 1.43 (d, $^{3}J_{H\text{-}H}$ = 7 Hz, 6 H, CH_3). $^{13}C\{^{1}H\}$ NMR (75 MHz, $CDCl_3$): δ 161.8 ($C_{carbene}$), 152.0 (C=N), 145.4 (C-N), 139.0, 134.1, 133.9, 130.6, 130.2, 129.6, 122.7, 113.2, 113.0 (Ar-C), 65.9 (C-I), 55.1 (NCH), 54.5 (NCH), 21.4 (CH_3), 20.9 (CH_3), 16.2 (CH_3), 14.0 (CH_3). Anal. Calcd. for $C_{24}H_{29}Br_2IN_4Pd\cdot CH_2Cl_2$: C, 35.26; H, 3.67; N, 6.58. Found: C, 34.81; H, 3.19; N, 6.65. MS (ESI) *m*/*z* 685 $[M - Br]^+$.

2-Ethyl-3,5-dimethyl-1-phenyl-1*H*-pyrazolium bromide (91).

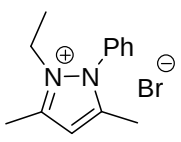

Salt **91** was prepared following the general procedure using 3,5-dimethylpyrazole **69** (258 mg, 1.50 mmol). An off-white solid was obtained (47 mg, mixture of starting material and product, 7% yield as determined by

NMR). ^{1}H NMR (300 MHz, $CDCl_3$): δ 7.78–7.63 (m, 5 H, Ar-H), 6.59 (s, 1 H, CH), 4.34 (q, $^{3}J_{H-H}$ = 7 Hz, 2 H, NCH_2), 2.67 (s, 3 H, CH_3), 2.23 (s, 3 H, CH_3), 1.19 (t, $^{3}J_{H-H}$ = 7 Hz, 3 H, CH_3).

2-Ethyl-3,5-diisopropyl-1-phenyl-1*H*-pyrazolium bromide (92).

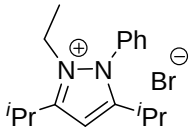

Salt **92** was prepared following the general procedure using 3,5-diisopropylpyrazole **70** (342 mg, 1.50 mmol). Trace amounts of a brown solid were obtained. ^{1}H NMR (300 MHz, $CDCl_3$): δ 7.83–7.77 (m, 2 H, Ar-H), 7.75–7.68 (m, 3 H, Ar-H), 6.46 (s, 1 H, CH), 4.43 (q, J = 7 Hz, 2 H, NCH_2), 3.35 (sept, $^{3}J_{H-H}$ = 7 Hz, 1 H, CH), 2.66 (sept, $^{3}J_{H-H}$ = 7 Hz, 1 H, CH), 1.44 (d, $^{3}J_{H-H}$ = 7 Hz, 6 H, CH_3), 1.22 (d, $^{3}J_{H-H}$ = 7 Hz, 6 H, CH_3), 1.20 (t, J = 7 Hz, 3 H, CH_3).

5-Aminophenyl-2-ethyl-3-methyl-1-phenyl-1*H*-pyrazolium iodide (93).

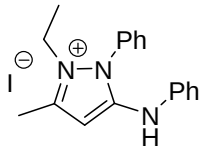

Salt **93** was prepared following the general procedure using amine-functionalized pyrazole **63** (150 mg, 0.60 mmol). A light brown solid was obtainted (142 mg, 0.35 mmol, 58%). ^{1}H NMR (300 MHz, $CDCl_3$): δ 7.85–7.78 (m, 2 H, Ar-H), 7.73–7.69 (m, 2 H, Ar-H), 7.62–7.58 (m, 1 H, Ar-H), 7.38–7.28 (m, 4 H, Ar-H), 7.19–7.11 (m, 1 H, Ar-H), 6.09 (s, 1 H, CH), 4.04 (q, $^{3}J_{H-H}$ = 7 Hz, 2 H, NCH_2), 2.52 (s, 3 H, CH_3), 1.20 (t, $^{3}J_{H-H}$ = 7 Hz, 3 H, CH_3).

2-Ethyl-3,5-dimethyl-1-phenyl-1*H*-pyrazolium iodide (94).

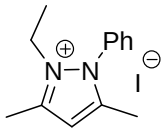

Salt **94** was prepared following the general procedure using 3,5-dimethylpyrazole **69** (258 mg, 1.50 mmol). A light grey solid was obtainted (488 mg, 1.49 mmol, 99%). ^{1}H NMR (300 MHz, $CDCl_3$): δ 7.83–7.77 (m, 2 H, Ar-H), 7.74–7.68 (m, 3 H, Ar-H), 6.57 (s, 1 H, CH), 4.32 (q, $^{3}J_{H-H}$ = 7 Hz, 2 H, NCH_2), 2.68 (s, 3 H, CH_3), 2.24 (s, 3 H, CH_3), 1.22 (t, $^{3}J_{H-H}$ = 7 Hz, 3 H, CH_3).

2-Ethyl-3,5-diisopropyl-1-phenyl-1*H*-pyrazolium iodide (95).

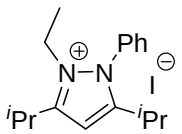

Salt **95** was prepared following the general procedure using 3,5-diisopropylpyrazole **70** (342 mg, 1.50 mmol). A light brown solid was obtained (433 mg, 1.13 mmol, 75%). ^{1}H NMR (300 MHz, $CDCl_3$): δ 7.91–7.84 (m, 2 H, Ar-H), 7.76–7.66 (m, 3 H, Ar-H), 6.46 (s, 1 H, CH), 4.39 (q, J = 7 Hz, 2 H, NCH_2), 3.31 (sept,

$^3J_{H-H}$ = 7 Hz, 1 H, CH), 2.67 (sept, $^3J_{H-H}$ = 7 Hz, 1 H, CH), 1.48 (d, $^3J_{H-H}$ = 7 Hz, 6 H, CH_3), 1.24 (d, *J* = 7 Hz, 6 H, CH_3), 1.22 (t, $^3J_{H-H}$ = 7 Hz, 3 H, CH_3).

4-Bromo-2-ethyl-3,5-dimethyl-1-phenyl-1*H*-pyrazolium iodide (96).

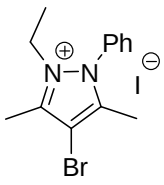

Salt **96** was prepared following the general procedure using pyrazole **89** (126 mg, 0.50 mmol). A light brown solid was obtainted (60 mg, mixture of starting material and product, 24% yield as determined by NMR). ^{1}H NMR (300 MHz, $CDCl_3$): δ 7.82 – 7.89 (m, 2 H, Ar-H), 7.67 – 7.77 (m, 3 H, Ar-H), 4.45 (q, $^3J_{H-H}$ = 7.3 Hz, 2 H, CH_2CH_3), 2.76 (s, 3 H, CH_3), 2.70 (s, 3 H, CH_3), 1.24 (t, $^3J_{H-H}$ = 7.3 Hz, 3 H, CH_2CH_3).

2,3-Dimethyl-5-methoxy-1-phenyl-1*H*-pyrazolium tetrafluoroborate (97).

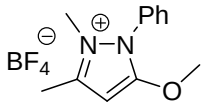

Salt **97** was prepared following the general procedure using methoxy-functionalized pyrazole **64** (49 mg, 0.26 mmol). A white solid was obtained (47 mg, 0.16 mmol, 62%). ^{1}H NMR (300 MHz, $CDCl_3$): *δ* 7.55–7.36 (m, 5 H, Ar-H), 6.10 (s, 1 H, CH), 3.91 (s, 3 H, OCH_3), 3.47 (s, 3 H, NCH_3), 2.41 (s, 3 H, CH_3).

2-Methyl-1,3,5-triphenyl-1*H*-pyrazolium tetrafluoroborate (98).

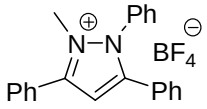

Salt **98** was prepared following the general procedure using 1,3,5-triphenyl-1*H*-pyrazole (**68**) (296 mg, 1.00 mmol). An off-white solid was obtained (221 mg 0.55 mmol, 55%). ^{1}H NMR (300 MHz, $CDCl_3$): *δ* =7.80–7. 31 (m, 15 H, Ar-H) 6.89 (s, 1 H, CH), 3.81 (s, 3 H, NCH_3).

2,3,5-Trimethyl-1-phenyl-1*H*-pyrazolium tetrafluoroborate (99).

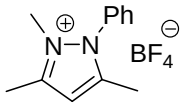

Salt **99** was prepared following the general procedure using 3,5-dimethylpyrazole **69** (172 mg, 1.50 mmol). A white solid was obtained (210 mg, 0.77 mmol, 77%). ^{1}H NMR (300 MHz, $CDCl_3$): *δ* 7.74–7.46 (m, 5 H, Ar-H), 6.48 (s, 1 H, CH), 3.65 (s, 3 H, NCH_3), 2.53 (s, 3 H, CH_3), 2.20 (s, 3 H, CH_3).

3,5-Diisopropyl-2-methyl-1-phenyl-1*H*-pyrazolium tetrafluoroborate (100).

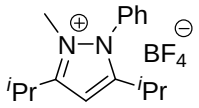

Salt **100** was prepared following the general procedure using 3,5-diisopropylpyrazole **70** (228 mg, 1.00 mmol). A brown solid was obtained (234 mg, 0.74 mmol, 74%). ^{1}H NMR (300 MHz, $CDCl_3$): δ 7.73–7.57 (m, 5 H, Ar-H), 6.41 (s, 1 H, CH), 3.65 (s, 3 H, NCH_3), 3.20 (sept, $^{3}J_{H\text{-}H}$ = 7 Hz, 1 H, CH), 2.68 (sept, J = 7 Hz, 1 H, CH), 1.39 (d, $^{3}J_{H\text{-}H}$ = 7 Hz, 6 H, CH_3), 1.21 (d, J = 7 Hz, 6 H, CH_3).

4-Chloro-2-methyl-1,3,5-triphenyl-1*H*-pyrazolium tetrafluoroborate (101).

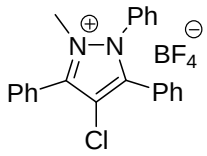

Salt **101** was prepared following the general procedure using pyrazole **71** (165 mg, 0.50 mmol). A white solid was obtained (79 mg, 0.18 mmol, 37%). ^{1}H NMR (300 MHz, $CDCl_3$): δ 7.84–7.70 (m, 4 H, Ar-H), 7.61–7.27 (m, 11 H, Ar-H), 3.73 (s, 3 H, NCH_3).

4-Bromo-2-Methyl-1,3,5-triphenyl-1*H*-pyrazolium tetrafluoroborate (102).

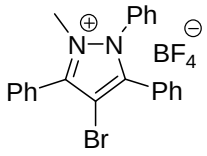

Salt **102** was prepared following the general procedure using pyrazole **72** (555 mg, 1.55 mmol). A white solid was obtained (521 mg, 1.09 mmol, 70%). ^{1}H NMR (300 MHz, $CDCl_3$): δ 7.84–7.74 (m, 4 H, Ar-H), 7.59–7.40 (m, 8 H, Ar-H), 7.39–7.34 (m, 1 H, Ar-H), 7.31–7.24 (m, 2 H, Ar-H), 3.73 (s, 3 H, NCH_3).

4-Iodo-2-Methyl-1,3,5-triphenyl-1*H*-pyrazolium tetrafluoroborate (103).

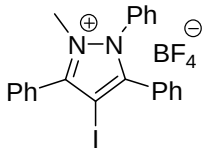

Salt **103** was prepared following the general procedure using pyrazole **73** (641 mg, 1.52 mmol). A white solid was obtained (530 mg , 1.01 mmol, 67%). ^{1}H NMR (300 MHz, $CDCl_3$): δ 7.98–7.92 (m, 1 H, Ar-H), 7.79–7.74 (m, 1 H, Ar-H), 7.73–7.68 (m, 1 H, Ar-H), 7.60–7.54 (m, 2 H, Ar-H), 7.52–7.45 (m, 3 H, Ar-H), 7.45–7.39 (m, 3 H, Ar-H), 7.37–7.29 (m, 4 H, Ar-H), 3.74 (s, 3 H, NCH_3).

5-Chloro-3-methyl-1-phenyl-1*H*-pyrazole (104).

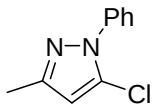

Pyrazolone **61** (5.00 g, 28.7 mmol, 1.00 equiv.) and phosphorous trichloride (5.91 g, 43.1 mmol, 1.50 equiv.) were thoroughly mixed and heated to 160 °C under microwave irradiation for 2 h. After cooling to ambient temperature, ice water (30 mL) was added slowly. The aqueous phase was extracted with diethyl ether

(2 × 45 mL). The combined organic layers were successively washed with aqueous sodium hydroxide solution (2 N, 2 × 40 mL) and water (40 mL), dried over sodium sulfate, filtered, and the solvent was removed *in vacuo*. The product was obtained as a colourless liquid (4.49 g, 23.3 mmol, 81%). ^{1}H NMR (300 MHz, $CDCl_3$): δ 7.57–7.51 (m, 2 H, Ar-H), 7.50–7.43 (m, 2 H, Ar-H), 7.41–7.35 (m, 1 H, Ar-H), 6.19 (s, 1 H, CH), 2.32 (s, 3 H, CH_3). The analytical data was in accordance with reported values.[216]

3-Methyl-1-phenyl-1*H*-pyrazol-5-yl-trifluoromethanesulfonate (105).

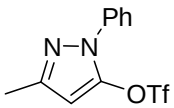

Pyrazolone **61** (600 mg, 3.44 mmol, 1.00 equiv.) was dissolved in anhydrous dichloromethane (40 mL). N-Phenylbis-(trifluoromethanesulfoneimide) (1.47 g, 4.13 mmol, 1.20 equiv.) and triethylamine (1.04 g, 1.40 mL, 10.3 mmol, 3.00 equiv.) were added and the mixture was heated to reflux for 3 h. After cooling to ambient temperature, it was diluted with dichloromethane (20 mL), washed with water (60 mL), dried over sodium sulfate, filtered and concentrated *in vacuo*. The residue was purified by column chromatography (silica gel, ethyl acetate/hexane 1:3) to give the product as a pale yellow liquid (1.04 g, 3.40 mmol, 99%). ^{1}H NMR (300 MHz, $CDCl_3$): δ 7.54–7.33 (m, 5 H, Ar-H), 6.14 (s, 1 H, CH), 2.34 (s, 3 H, CH_3). The analytical data was in accordance with reported values.[122]

5-Chloro-2,3-dimethyl-1-phenyl-pyrazolium tetrafluoroborate (107).

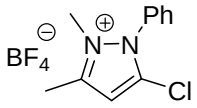

Pyrazole **104** (384 mg, 2.00 mmol, 1.00 equiv.) was dissolved in anhydrous dichloromethane (6 mL). Trimethyloxonium tetrafluoroborate (473 mg, 3.20 mmol, 1.6 equiv.) was added, and the mixture was heated to reflux for 20 h under a dry nitrogen atmosphere. After cooling to ambient temperature, the solvent was removed *in vacuo*. The residue was washed with diethyl ether (3 mL) and dried *in vacuo*. The product was obtained as a white solid (350 mg, 1.19 mmol, 60%). ^{1}H NMR (300 MHz, DMSO-d_6): δ 7.87–7.72 (m, 5 H, Ar-H), 7.29 (s, 1 H, CH), 3.68 (s, 3 H, NCH_3), 2.58 (s, 3 H, CH_3). ^{13}C{^{1}H} NMR (75 MHz, DMSO-d_6): δ 149.0 (C=N), 135.5 (Cl-C-N), 133.0, 130.6, 130.2, 129.1 (Ar-C), 107.8 (CH), 35.5 (NCH_3), 11.9 (CH_3). ^{19}F NMR (170 MHz, DMSO-d_6): δ -77.23, -77.18 (BF_4). Anal. Calcd. for $C_{11}H_{12}BClF_4N_2$: C, 44.86; H, 4.11; N, 9.51. Found: C, 44.57; H, 4.13; N, 9.52. MS (ESI) *m*/*z* 207 $[M - BF_4]^+$.

5-Trifluoromethanesulfonyl-2,3-dimethyl-1-phenyl-pyrazolium tetrafluoroborate (108).

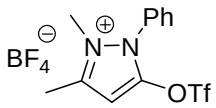

Pyrazole **105** (3.34 g, 10.9 mmol, 1.00 equiv.) was dissolved in anhydrous dichloromethane (50 mL). Trimethyloxonium tetrafluoroborate (1.94 g, 13.1 mmol, 1.20 equiv.) was added, and the mixture was heated to reflux for 10 h under dry nitrogen atmosphere. After cooling to ambient temperature, the solvent was removed *in vacuo*. The residue was dissolved in THF and precipitated by addition of diethyl ether, collected by filtration, and dried *in vacuo*. The product was obtained as an off-white solid (3.36 g, 8.23 mmol, 76%). ^{1}H NMR (300 MHz, $CDCl_3$): δ 7.82–7.62 (m, 5 H, Ar-H), 6.67 (s, 1 H, CH), 3.77 (s, 3 H, NCH_3), 2.67 (s, 3 H, CH_3). $^{13}C\{^{1}H\}$ NMR (75 MHz, $CDCl_3$): δ 151.6 (C=N), 145.4 (O-C-N), 134.2, 131.5, 129.8, 128.8 (Ar-C), 98.9 (CH), 35.7 (NCH_3), 13.4 (CH_3); CF_3 not observed. ^{19}F NMR (170 MHz, $CDCl_3$): δ -77.83, -77.78 (BF_4), -4.38 (OTf). Anal. Calcd. for $C_{12}H_{12}BF_7N_2O_3S$: C, 35.32; H, 2.96; N, 6.86. Found: C, 35.09; H, 2.61; N, 6.78. MS (ESI) *m*/*z* 321 $[M - BF_4]^+$.

2,3-Dimethyl-1-phenyl-1*H*-pyrazolium tetrafluoroborate (109).

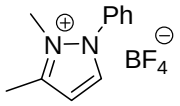

Pyrazole **106** (1.00 g, 6.32 mmol, 1.00 equiv.) was dissolved in anhydrous dichloromethane (15 mL). Trimethyloxonium tetrafluoroborate (1.12 g, 7.59 mmol, 1.20 equiv.) was added, and the mixture was heated to reflux for 15 h under a dry nitrogen atmosphere. After cooling to ambient temperature, the solvent was removed *in vacuo* and the residue was washed with diethyl ether (5 mL). The product was obtained as a white solid (1.64 g, 6.31 mmol, >99%). ^{1}H NMR (300 MHz, $CDCl_3$): δ 7.91 (d, $^{3}J_{H\text{-}H}$ = 3 Hz, 1 H, 5-H), 7.71–7.51 (m, 5 H, Ar-H), 6.69 (d, $^{3}J_{H\text{-}H}$ = 3 Hz, 1 H, 4-H), 3.75 (s, 3 H, NCH_3), 2.56 (s, 3 H, CH_3). $^{13}C\{^{1}H\}$ NMR (75 MHz, $CDCl_3$): δ 149.9 (C-3), 137.2 (C-5), 133.3, 133.2, 131.2, 128.5 (Ar-C), 109.4 (C-4), 35.2 (NCH_3), 13.0 (CH_3). ^{19}F NMR (170 MHz, $CDCl_3$): δ -76.92, -76.87 (BF_4). Anal. Calcd. for $C_{11}H_{13}BF_4N_2$: C, 50.81; H, 5.04; N, 10.77. Found: C, 50.43; H, 4.76; N, 10.62. MS (ESI) *m*/*z* = 173 $[M - BF_4]^+$.

***trans*-Chlorido(2,3-dimethyl-1-phenyl-pyrazolin-5-ylidene)bis(triphenylphosphine)-palladium(II) tetrafluoroborate/triflate (112).**

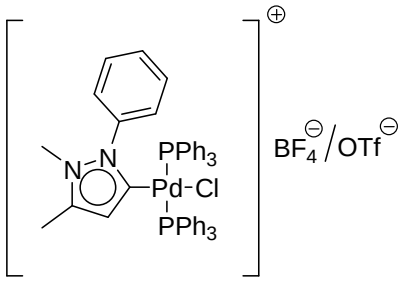

Tetrakis(triphenylphosphine)palladium (1.16 g, 1.00 mmol, 1.00 equiv.) was dissolved in anhydrous dichloromethane (15 mL), and pyrazolium salt **108** (429 mg, 1.05 mmol, 1.05 equiv) and TBACl (292 mg, 1.05 mmol, 1.05 equiv) were added. The mixture was heated to reflux for 10 h under a dry nitrogen atmosphere. After cooling to ambient temperature, the solvent was evaporated *in vacuo*. The residue was washed with diethyl ether/THF mixture (1:1, 5 mL), and dried *in vacuo*. After recrystallization from $CHCl_3$/hexane, the product was obtained as a pale yellow solid (477 mg, 0.515 mmol, 52%). ^{1}H NMR (300 MHz, $CDCl_3$): δ 7.80–7.29 (m, 35 H, Ar-H), 6.63 (s, 1 H, CH), 3.35 (s, 3 H, NCH_3), 2.05 (s, 3 H, CH_3). $^{13}C\{^1H\}$ NMR (75 MHz, $CDCl_3$): δ 165.6 ($C_{carbene}$), 148.7 (C=N), 136.3 (Ar-C), 135.0 (t, $J_{C\text{-}P}$ = 6 Hz, Ar-C), 132.1, 131.3, 130.4, 130.0, 129.7 (Ar-C), 129.3 (t, $J_{C\text{-}P}$ = 5 Hz, Ar-C), 127.3 (CH), 36.2 (NCH_3), 12.7 (CH_3). ^{19}F NMR (170 MHz, $CDCl_3$): δ -77.06, -77.00 (BF_4), -2.22 (OTf). ^{31}P NMR (158 MHz, $CDCl_3$): δ 22.9. Anal. Calcd. for ($C_{47}H_{42}ClN_2P_2Pd(BF_4)_{2/3}OTf_{1/3}$): C, 60.08; H, 4.47; N, 2.96. Found: C, 59.50; H, 4.83; N, 3.73. MS (ESI) *m*/*z* 837 $[M - BF_4]^+$.

(3-Methyl-1-phenyl-1*H*-pyrazol-5-yl)triphenylphosphonium tetrafluoroborate (114).

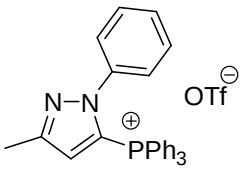

Pyrazole **105** (37 mg, 0.12 mmol, 1.20 equiv.) and $[Pd(PPh_3)_4]$ (116 mg, 0.10 mmol, 1.00 equiv.) were dissolved in anhydrous toluene (2 mL) and heated to 75° C for 20 h. After the mixture had cooled to ambient temperature, the solution was filtered over a short plug of Celite. It was diluted with dichloromethane (5 mL), extracted with water (10 mL), dried over sodium sulfate, and filtered. The solvent was almost completely removed under reduced pressure, and pentane (10 mL) was added. A white precipitate was isolated (31 mg, 0.05 mmol, 54%). ^{1}H NMR (300 MHz, $CDCl_3$): δ 7.94–7.80 (m, 3 H, Ar-H), 7.80–7.54 (m, 13 H, Ar-H), 7.15–7.03 (m, 2 H, Ar-H), 6.97–6.88 (m, 2 H, Ar-H), 6.83–6.75 (m, 1 H, CH), 2.48 (s, 3 H, CH_3). ^{19}F NMR (170 MHz, $CDCl_3$): δ -2.10 (OTf). ^{31}P NMR (158 MHz, $CDCl_3$): δ 9.88. MS (ESI) *m*/*z* 419 $[M - OTf]^+$.

***trans*-Dibromido(2,3-dimethyl-1-phenyl-1*H*-pyrazolin-5-ylidene)(1,3-diisopropyl-benzimidazolin-2-ylidene)palladium(II) (116)**.

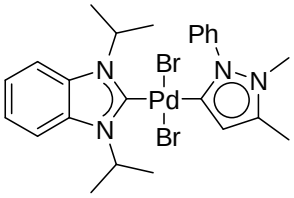

Pyrazolium salt **109** (52 mg, 0.20 mmol, 1.00 equiv.), tetrabutylammonium bromide (64 mg, 0.20 mmol, 1.00 equiv.) and silver(I) oxide (23 mg, 0.10 mmol, 0.50 equiv.) were dissolved in dichloromethane (25 mL) and stirred shielded from light for 15 h at ambient temperature. $[PdBr_2(^iPr_2\text{-bimy})]_2$ (94 mg, 0.10 mmol, 0.50 equiv.) was added, and the solution was stirred at ambient temperature for another 2 h shielded from light. The resulting suspension was filtered over a short plug of Celite and concentrated *in vacuo*. The solid residue was washed with diethyl ether (5 mL), and dried *in vacuo*. The product was obtained as a yellow solid (103 mg, 0.160 mmol, 80%). ^{1}H NMR (300 MHz, $CDCl_3$): δ 7.90–7.80 (m, 2 H, Ar-H), 7.68–7.60 (m, 3 H, Ar-H), 7.50–7.40 (m, 2 H, Ar-H), 7.14–7.06 (m, 2 H, Ar-H), 6.51 (s, 1 H, 4-H), 5.72 (sept, $^3J_{H\text{-}H}$ = 7 Hz, 2 H, NCH), 3.49 (s, 3 H, NCH_3), 2.31 (s, 3 H, CH_3), 1.57 (d, $^3J_{H\text{-}H}$ = 7 Hz, 12 H, CH_3). $^{13}C\{^1H\}$ NMR (75 MHz, $CDCl_3$): δ 182.8 ($C_{carbene}$, bimy), 175.4 ($C_{carbene}$, pyry), 144.0 (C=N), 138.6, 134.2, 131.0, 130.5, 129.8, 122.1, 116.1, 113.0 (Ar-C), 53.9 (NCH), 34.1 (NCH_3), 21.6 (CH_3), 12.7 (CH_3). Anal. Calcd. for $C_{24}H_{30}Br_2N_4Pd$: C, 44.99; H, 4.72; N, 8.74. Found: C, 44.96; H, 4.73; N, 8.84. MS (ESI) *m*/*z* 559 $[M - Br]^+$.

***trans*-Dibromido(acetonitrile)(2,3-dimethyl-1-phenyl-pyrazolin-5-ylidene)palladium(II) (117).**

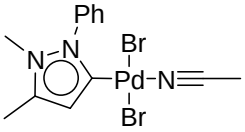

Pyrazolium salt **109** (650 mg, 2.50 mmol, 1.00 equiv.), silver(I) oxide (290 mg, 1.25 mmol, 0.50 equiv.) and tetrabutylammonium bromide (806 mg, 2.50 mmol, 1.00 equiv.) were suspended in dichloromethane (60 mL) and stirred at ambient temperature for 15 h shielded from light. Palladium(II) bromide (660 mg, 2.50 mmol, 1.00 equiv.) was dissolved in acetonitrile (60 mL) and heated to 50 °C for 20 min. The resulting $[PdBr_2(acetonitrile)_2]$ solution was slowly added to the reaction mixture. After stirring for an additional 2 h, the mixture was filtered over a short plug of Celite, and the solvent was concentrated to 10 mL. The precipitate was collected and dried under reduced pressure. The product was obtained as a yellow solid (937 mg, 1.95 mmol, 78%). ^{1}H NMR (300 MHz, $CDCl_3$): δ 7.72–7.78 (m, 5 H, Ar-H), 6.40 (s, 1 H, CH), 3.43 (s, 3 H, NCH_3), 2.29 (s, 3 H, CH_3), 2.01 (s, 3 H, CH_3). $^{13}C\{^1H\}$ NMR (75 MHz, $CDCl_3$/CD_3CN): δ 150.0

($C_{carbene}$), 144.5 (C=N), 137.0, 131.1, 130.0, 129.9, 129.8 (Ar-C), 115.9 (CN), 34.3 (NCH_3), 12.3 (CH_3), 2.1 (CH_3). Anal. Calcd. for $C_{13}H_{15}Br_2N_3Pd$: C, 32.56; H, 3.15; N, 8.76. Found: C, 32.98; H, 3.32; N, 8.45. MS (ESI) *m*/*z* 397 $[M - Br]^+$.

***trans*-Dibromido(2,3-dimethyl-1-phenyl-pyrazolin-5-ylidene)(pyridine)palladium(II) (118).**

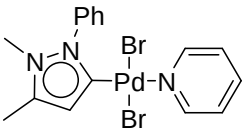

Pyridine (8.0 µL, 0.10 mmol, 1.00 equiv.) and complex **117** (50 mg, 0.10 mmol, 1.00 equiv) were dissolved in dichloromethane (5 mL). The solution was stirred for 30 min at ambient temperature. Then, the solvent was evaporated *in vacuo*. The product was obtained as a yellow solid (52 mg, 0.10 mmol, >99%). ^{1}H NMR (300 MHz, $CDCl_3$): δ 8.80–8.75 (m, 2 H, Ar-H), 7.84–7.77 (m, 2 H, Ar-H), 7.65–7.57 (m, 4 H, Ar-H), 7.22–7.14 (m, 2 H, Ar-H), 6.50 (s, 1 H, CH), 3.48 (s, 3 H, NCH_3), 2.31 (s, 3 H, CH_3). $^{13}C\{^1H\}$ NMR (75 MHz, $CDCl_3$): δ 154.1 ($C_{carbene}$), 153.0 (Ar-C), 144.4 (C=N), 137.9, 137.7, 131.3, 130.4, 130.1, 124.8 (Ar-C), 116.9 (CH), 34.5 (NCH_3), 12.9 (CH_3). Anal. Calcd. for $C_{16}H_{17}Br_2N_3Pd \cdot CH_2Cl_2$: C, 33.89; H, 3.18; N, 6.97. Found: C, 33.94; H, 3.16; N, 6.94. MS (ESI) *m*/*z* 436 $[M - Br]^+$.

***cis*-Dibromido(2,3-dimethyl-1-phenyl-pyrazolin-5-ylidene)(triphenylphosphine)-palladium(II) (119).**

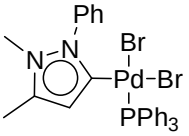

Triphenylphosphine (26 mg, 0.10 mmol, 1.00 equiv.) and complex **117** (50 mg, 0.10 mmol, 1.00 equiv.) were dissolved in dichloromethane (5 mL). The solution was stirred for 30 min at ambient temperature. Then, the solvent was evaporated *in vacuo*. The residue was washed with diethyl ether (5 mL) and dried. The product was obtained as a yellow solid (71 mg, 0.10 mmol, >99%). ^{1}H NMR (300 MHz, CD_2Cl_2): δ 7.77–7.41 (m, 8 H, Ar-H), 7.35–7.24 (m, 12 H, Ar-H), 6.39 (s, 1 H, CH), 3.31 (s, 3 H, NCH_3), 2.27 (s, 3 H, CH_3). $^{13}C\{^1H\}$ NMR (75 MHz, CD_2Cl_2): δ 166.5 ($C_{carbene}$), 145.0 (C=N), 136.0 (Ar-C), 135.6 (d, $J_{C\text{-}P}$ = 11 Hz, Ar-H), 131.4, 130.7 (Ar-C), 130.5 (d, $J_{C\text{-}P}$ = 3 Hz, Ar-H), 130.3, 129.7 (Ar-C), 127.7 (d, $J_{C\text{-}P}$ = 11 Hz, Ar-C), 115.8 (CH), 34.4 (NCH_3), 11.9 (CH_3). ^{31}P NMR (158 MHz, $CDCl_3$): δ 27.3. Anal. Calcd. for $C_{29}H_{27}Br_2N_2Pd$: C, 49.71; H, 3.88; N, 4.00. Found: C, 50.01; H, 3.64; N, 4.06. MS (ESI) *m*/*z* 619 $[M - Br]^+$.

***trans*-Dibromido(2,3-dimethyl-1-phenyl-1*H*-pyrazolin-5-ylidene)(1,3-dibenzhydryl-benzimidazolin-2-ylidene)palladium(II) (120).**

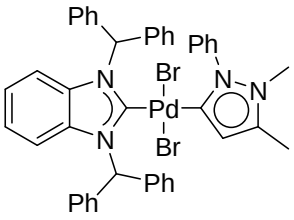

1,3-Dibenzhydrylbenzimidazolium bromide (106 mg, 0.20 mmol, 1.00 equiv.) and silver(I) oxide (23 mg, 0.10 mmol, 0.50 equiv.) were dissolved in dichloromethane (10 mL) and stirred shielded from light for 15 h at ambient temperature. Complex **117** (96 mg, 0.20 mmol, 1.00 equiv.) was added, and the solution was stirred at ambient temperature for another 1 h shielded from light. The resulting suspension was filtered over a short plug of Celite and concentrated *in vacuo*. The solid residue was washed with diethyl ether (5 mL), and dried *in vacuo*. The product was obtained as a yellow solid (179 mg, 0.20 mmol, >99%). ^{1}H NMR (300 MHz, $CDCl_3$): δ 8.46–8.36 (m, 2 H, CH), 7.84–7.78 (m, 2 H, Ar-H), 7.49–7.17 (m, 23 H, Ar-H), 6.83 (s, 4 H, Ar-H), 6.53, (s, 1 H, CH), 3.39 (s, 3 H, NCH_3), 2.28 (s, 3 H, CH_3). ^{13}C{1H} NMR (75 MHz, $CDCl_3$): δ 189.7 ($C_{carbene}$, bimy), 174.3 ($C_{carbene}$, pyry), 144.0 (C=N), 138.5, 138.4, 134.9, 130.6, 130.3, 130.0, 129.8, 128.8, 128.2, 122.4 (Ar-C), 116.2 (CH), 114.3 (Ar-C), 68.1 (CH), 34.1 (NCH_3), 12.2 (CH_3). Anal. Calcd. for $C_{44}H_{38}Br_2N_4Pd$: C, 59.44; H, 4.31; N, 6.30. Found: C, 60.28; H, 4.98; N, 6.01. MS (ESI) *m*/*z* 809 $[M - Br]^+$.

***trans*-Dibromido(IPr)(1-phenyl-2,3-dimethylpyrazolin-5-ylidene)palladium(II) (121).**

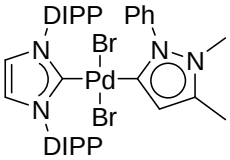

IPr·HBr (70 mg, 0.15 mmol, 1.00 equiv) and potassium *tert*-butoxide (17 mg, 0.15 mmol, 1.00 equiv) were dissolved in anhydrous THF (15 mL) and stirred for 30 min at ambient temperature under dry nitrogen atmosphere. Then complex **117** (72 mg, 0.15 mmol, 1.00 equiv.) was added, and stirring was continued for another 2 h. The solvent was removed *in vacuo*, and the solid residue was taken up in dichloromethane (20 mL) and filtered over a short plug of Celite. The solvent was removed *in vacuo*. The product was obtained as a yellow solid (124 mg, 0.15 mmol, >99%). ^{1}H NMR (300 MHz, $CDCl_3$): δ 7.50–7.42 (m, 2 H, Ar-H), 7.39–7.22 (m, 7 H, Ar-H), 7.18–7.10 (m, 2 H, Ar-H), 6.94 (s, 2 H, HC=CH), 6.06 (s, 1 H, CH), 3.25 (s, 3 H, NCH_3), 3.14 (sept, $^{3}J_{H\text{-}H}$ = 7 Hz, 4 H, CH), 2.12 (s, 3 H, CH_3), 1.39–1.24 (m, 12 H, CH_3), 1.01 (d, $^{3}J_{H\text{-}H}$ = 7 Hz, 12 H, CH_3). ^{13}C{^{1}H} NMR (75 MHz, $CDCl_3$): δ 179.4 ($C_{carbene}$, IPr), 173.2 ($C_{carbene}$, pyry), 147.3 (Ar-C), 143.8 (C=N), 137.8, 136.8, 130.0, 129.6, 129.4, 129.2 (Ar-C), 124.7 (C-sp^2), 124.3 (Ar-C), 116.1 (CH), 34.1 (NCH_3), 29.2 (CH), 26.9 (CH_3), 24.0 (CH_3), 12.6 (CH_3). Anal. Calcd.

for $C_{38}H_{48}Br_2N_4Pd \cdot CH_2Cl_2$: C, 51.36; H, 5.53; N, 6.14. Found: C, 51.90; H, 5.82; N, 5.92. MS (ESI) *m*/*z* 747 $[M - Br]^+$.

***trans*-Dibromido(SIPr)(1-phenyl-2,3-dimethylpyrazolin-5-ylidene)palladium(II) (122).**

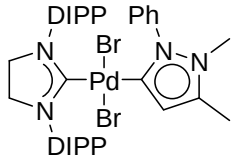

SIPr·HBr (71 mg, 0.15 mmol, 1.00 equiv.) and potassium *tert*-butoxide (26 mg, 0.23 mmol, 1.50 equiv.) were dissolved in anhydrous THF (15 mL) and stirred for 30 min at ambient temperature under dry nitrogen atmosphere. Then complex **117** (72 mg, 0.15 mmol, 1.00 equiv.) was added, and stirring was continued for another 2 h. The solvent was removed *in vacuo*, and the solid residue was taken up in dichloromethane (20 mL) and filtered over a short plug of Celite. The solvent was removed *in vacuo*. The product was obtained as a dark yellow solid (107 mg, 0.13 mmol, 86%). ^{1}H NMR (300 MHz, $CDCl_3$): δ 7.42–7.28 (m, 5 H, Ar-H), 7.25–7.17 (m, 4 H, Ar-H), 7.11–7.03 (m, 2 H, Ar-H), 6.03 (s, 1 H, CH), 3.87 (s, 4 H, CH_2), 3.55 (sept, $^3J_{H\text{-}H}$ = 7 Hz, 4 H, CH), 3.23 (s, 3 H, NCH_3), 2.10 (s, 3 H, CH_3), 1.51–1.22 (m, 12 H, CH_3), 1.16 (d, $^3J_{H\text{-}H}$ = 7 Hz, 12 H, CH_3). ^{13}C{1H} NMR (75 MHz, $CDCl_3$): δ 207.6 ($C_{carbene}$, SIPr), 173.4 ($C_{carbene}$, pyry), 148.3 (Ar-C), 143.7 (C=N), 137.7, 137.2, 129.7, 129.4, 129.2, 129.1, 124.8 (Ar-C), 116.1 (CH), 54.4 (CH_2), 34.1 (NCH_3), 29.1 (CH), 27.4 (CH_3), 25.0 (CH_3), 12.6 (CH_3). Anal. Calcd. for $C_{38}H_{50}Br_2N_4Pd \cdot CH_2Cl_2$: C, 51.25; H, 5.73; N, 6.13. Found: C, 50.62; H, 5.82; N, 6.41. MS (ESI) *m*/*z* 749 $[M - Br]^+$.

***trans*-Dibromido(IMes)(1-phenyl-2,3-dimethylpyrazolin-5-ylidene)palladium(II) (123).**

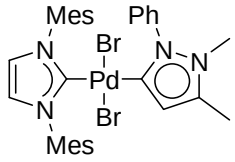

IMes·HBr (58 mg, 0.15 mmol, 1.00 equiv.) and potassium *tert*-butoxide (17 mg, 0.15 mmol, 1.00 equiv.) were dissolved in anhydrous THF (15 mL) and stirred for 30 min at ambient temperature under dry nitrogen atmosphere. Then complex **117** (72 mg, 0.15 mmol, 1.00 equiv.) was added, and stirring was continued for another 2 h. The solvent was removed *in vacuo*, and the solid residue was taken up in dichloromethane (20 mL) and filtered over a short plug of Celite. The solvent was removed *in vacuo*. The product was obtained as a yellow solid (107 mg, 0.14 mmol, 96%). ^{1}H NMR (300 MHz, $CDCl_3$): δ 7.51–7.38 (m, 3 H, Ar-H), 7.35–7.27 (m, 2 H, Ar-H), 6.97–6.88 (m, 4 H, Ar-H), 6.83 (s, 2 H, HC=CH), 6.08 (s, 1 H, CH), 3.27 (s, 3 H, NCH_3), 2.40 (s, 6 H, CH_3), 2.23 (s_{br}, 12 H, CH_3), 2.14 (s, 3 H, CH_3). ^{13}C{1H} NMR (75 MHz, $CDCl_3$): δ 176.6

($C_{carbene}$, IMes), 172.6 ($C_{carbene}$, pyry), 143.5 (C=N), 137.9, 136.7, 129.7, 129.6, 129.6, 129.3 (Ar-C), 123.5 (C(sp^2)), 123.4 (Ar-C), 115.6 (CH), 34.0 (NCH_3), 21.9 (CH_3), 20.3 (CH_3), 12.6 (CH_3). Anal. Calcd. for $C_{32}H_{36}Br_2N_4Pd$: C, 51.74; H, 4.88; N, 7.54. Found: C, 51.62; H, 5.09; N, 7.24. MS (ESI) *m*/*z* 663 $[M - Br]^+$.

cis-Dibromido-bis(2,3-dimethyl-1-phenyl-1*H*-pyrazolin-5-ylidene)palladium(II) (124).

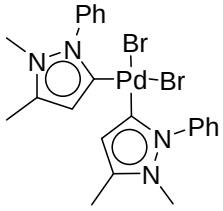

Pyrazolium salt **109** (52 mg, 0.20 mmol, 1.00 equiv.), silver(I) oxide (23 mg, 0.10 mmol, 0.50 equiv.) and tetrabutylammonium bromide (64 mg, 0.10 mmol, 1.00 equiv.) were suspended in dichloromethane (10 mL) and stirred at ambient temperature for 15 h shielded from light. Complex **117** (96 mg, 0.20 mmol, 1.00 equiv.) was added and stirring was continued for 2 h. Then, the solution was filtered over a short plug of Celite and concentrated *in vacuo*. The residue was washed with a mixture of diethyl ether and dichloromethane (3:1, 5 mL). The product was obtained as a yellow solid (113 mg, 0.19 mmol, 93%). ^{1}H NMR (300 MHz, CD_2Cl_2): δ 7.58–7.52 (m, 6 H, Ar-H), 7.50–7.44 (m, 4 H, Ar-H), 6.29 (s, 2 H, CH), 3.39 (s, 6 H, NCH_3), 2.30 (s, 6 H, CH_3). ^{13}C{1H} NMR (75 MHz, DMSO-d_6): δ 181.8 ($C_{carbene}$), 136.7 (C=N), 130.2, 129.3, 128.9, 128.3 (Ar-C), 79.2 (CH), 34.5 (NCH_3), 11.4 (CH_3). Anal. Calcd. for $C_{22}H_{24}Br_2N_4Pd \cdot CH_2Cl_2$: C, 39.71; H, 3.77; N, 8.05. Found: C, 41.20; H, 4.37; N, 7.68. MS (ESI) *m*/*z* 531 $[M - Br]^+$.

2,3-dihydro-1*H*-pyrazolo[1,2-*a*]indazolium bromide (131).

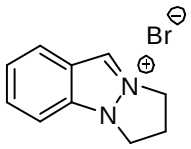

Sodium hydroxide (1.20 g, 30.0 mmol, 1.50 equiv.) was added to a solution of indazole (2.36 g, 20.0 mmol, 1.00 equiv.) in acetonitrile (250 mL). After stirring for 30 min at ambient temperature, 1,3-dibromopropane (2.84 mL, 28.0 mmol, 1.40 equiv.) was added. The reaction mixture was stirred at ambient temperature for 6 h, and then the temperature was increased to 90 °C for 15 h. The mixture was allowed to cool to ambient temperature, and the solvent was distilled under reduced pressure. The residue was taken up in dichloromethane (150 mL), and the resulting suspension was filtered. The solvent was removed in vacuo to yield an off-white solid (4.18 g, 17.5 mmol, 88%). ^{1}H NMR (300 MHz, $CDCl_3$): δ 9.55 (s, 1 H, NCH), 7.96 (d, $^3J_{H-H}$ = 9 Hz, 1 H, Ar-H), 7.78–7.71 (m, 1 H, Ar-H), 7.69–7.62 (m, 1 H, Ar-H), 7.47–7.38 (m, 1 H, Ar-H), 5.27 (t, $^3J_{H-H}$ = 8 Hz, 2 H, NCH_2), 4.84 (t, $^3J_{H-H}$ = 7 Hz,

2 H, NCH_2), 3.22 (quint, 3JH-H = 8 Hz, 2 H, CH_2). $^{13}C\{^1H\}$ NMR (75 MHz, $CDCl_3$): δ 136.4 (Ar-C), 133.5 (NCH), 128.5, 125.8, 125.0, 124.2, 111.6 (Ar-C), 51.1 (NCH_2), 47.7 (NCH_2), 28.3 (CH_2). Because of the hygroscopic nature of **131**, an elemental analysis could not be obtained. ESI (MS) m/z 159 $[M - Br]^+$.

di-μ-Bromido-bis(indy-5)dibromidodipalladium(II) (133).

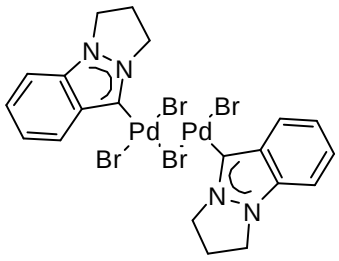

Indazolium salt **131** (475 mg, 2.00 mmol, 1.10 equiv.), palladium(II) acetate (405 mg, 1.80 mmol, 1.00 equiv.) and sodium bromide (740 mg, 7.20 mmol, 4.00 equiv.) were dissolved in DMSO (30 mL) and the mixture was heated to 70 °C for 24 h. Then the solvent was distilled off under reduced pressure. The residue was taken up in dichloromethane (100 mL) and the resulting suspension was extracted with water (3 × 50 mL), dried over Na_2SO_4, filtered and concentrated in vacuo. The solid residue was washed with diethyl ether (100 mL) and dried in vacuo. The product was obtained as an orange solid (764 mg, 0.90 mmol, >99%). ^1H NMR (500 MHz, CD_3CN): δ 8.17 (d, $^3J_{H-H}$ = 8 Hz, 2 H, Ar-H), 7.67–7.63 (m, 2 H, Ar-H), 7.43 (d, $^3J_{H-H}$ = 9 Hz, 2 H, Ar-H), 7.30 (t, $^3J_{H-H}$ = 8 Hz, 2 H, Ar-H), 4.77 (t, $^3J_{H-H}$ = 7 Hz, 4 H, NCH_2), 4.45 (t, $^3J_{H-H}$ = 7 Hz, 4 H, NCH_2), 2.96 (quint, $^3J_{H-H}$ = 7 Hz, 4 H, CH_2). $^{13}C\{^1H\}$ NMR (75 MHz, CD_3CN): δ 141.0 ($C_{Carbene}$), 136.3, 133.8, 131.8, 128.6, 122.4, 110.6 (Ar-C), 50.2 (NCH_2), 46.2 (NCH_2), 27.6 (CH_2). Anal. Calcd. for $C_{20}H_{20}N_4Br_4Pd_2$: C, 28.30; H, 2.37; N, 6.60. Found: C, 28.02; H, 2.22; N, 6.82. ESI (MS) m/z 427 $[0.5\ M + H]^+$, 812 $[M - Br + CH3CN]^+$.

***trans*-Dibromido(indy-5)(pyridine)palladium(II) (135).**

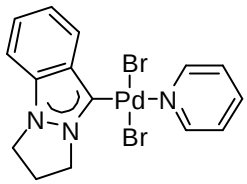

Pyridine (0.25 mL) was added to dimer **133** (100 mg, 0.12 mmol) in dichloromethane (25 mL) and the resulting solution was stirred at ambient temperature for 1 h. The reaction mixture was filtered and the filtrate was dried in *vacuo*. The solid residue was washed repeatedly with diethyl ether (2 × 10 mL) and dried *in vacuo* to afford a pale yellow solid (115 mg, 0.23 mmol, 95%). ^1H NMR (300 MHz, $CDCl_3$): δ 9.15–9.05 (m, 2 H, Ar-H), 8.44 (d, 1 H, $^3J_{H-H}$ = 8 Hz, Ar-H), 7.79–7.18 (m, 1 H, Ar-H), 7.60–7.53 (m, 1 H, Ar-H), 7.40–7.28 (m, 3 H, Ar-H), 7.24–7.18 (m, 1 H, Ar-H) 4.95 (t, 2 H, $^3J_{H-H}$ = 8 Hz, NCH_2), 4.36 (t, 2 H, $^3J_{H-H}$ = 7 Hz, NCH_2), 3.00 (quin, $^3J_{H-H}$ =

7 Hz, 2 H, CH_2). $^{13}C\{^1H\}$ NMR (75 MHz, $CDCl_3$): δ 153.3 (Ar-C), 145.7 ($C_{carbene}$), 138.4, 136.4, 135.0, 132.0, 130.0, 125.1, 122.8, 109.5 (Ar-C), 49.6 (NCH_2), 45.6 (NCH_2), 27.7 (CH_2). Anal. Calcd. for $C_{15}H_{15}Br_2N_3Pd$: C, 35.78; H, 3.00; N, 8.35. Found: C, 35.50; H, 3.06; N, 7.99. ESI (MS) *m/z* 456 $[M - Br + MeOH]^+$, 503 $[M - Br + py]^+$.

cis-Dibromido(indy-5)(triphenylphosphine)palladium(II) (136).

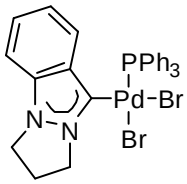

Triphenylphosphine (37 mg, 0.14 mmol, 1.00 equiv.) was added to **133** (60 mg, 0.07 mmol, 0.50 equiv.) in dichloromethane (15 mL) and the reaction mixture was stirred at ambient temperature for 2 h. The resulting suspension was filtered and the filtrate was dried under reduced pressure. The solid residue was washed with hexane (10 mL) and diethyl ether (10 mL) and dried *in vacuo* to give a pale yellow solid (92 mg, 0.13 mmol, 96%). ^1H and $^{13}C\{^1H\}$ NMR spectra could not be measured due to poor solubility. Anal. Calcd. for $C_{28}H_{25}Br_2N_2PPd$: C, 48.97; H, 3.67; N, 4.08. Found: C, 48.62; H, 3.99; N, 4.00. ESI (MS) *m/z* 607 $[M – Br]^+$.

cis-Ditrifluoroacetato(indy-5)(triphenylphosphine)palladium(II) (137).

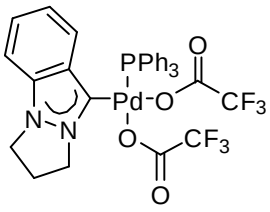

Complex **136** (44 mg, 0.06 mmol, 1.00 equiv.) and silver(I) trifluoroacetate (31 mg, 0.14 mmol, 2.30 equiv.) were suspended in acetonitrile (15 mL) and stirred at ambient temperature for 15 h shielded from light. The resulting suspension was filtered, and the filtrate was concentrated under reduced pressure. The yellow residue was redissolved in dichloromethane (5 mL), and the crude product was precipitated out by addition of diethyl ether (20 mL). The solid was isolated, washed with diethyl ether (3 × 20 mL) and dried *in vacuo* to afford a pale yellow solid (36 mg, 0.05 mmol, 80%). ^1H NMR (300 MHz, CD_2Cl_2): δ 8.12 (d, 1 H, Ar-H), 7.60–7.41 (m, 10 H, Ar-H), 7.39–7.28 (m, 6 H, Ar-H), 7.24–7.13 (m, 2 H, Ar-H), 5.17–5.04 (m, 1 H, NCH_2), 4.26–4.09 (m, 1 H, NCH_2), 3.99–3.84 (m, 1 H, NCH_2), 3.75–3.58 (m, 1 H, NCH_2), 2.85–2.67 (m, 1 H, CH_2), 2.38–2.19 (m, 1 H, CH_2). $^{13}C\{^1H\}$ NMR (75 MHz, CD_2Cl_2): δ 149.2 (d, $^2J_{P\text{-}C}$ = 10 Hz, $C_{carbene}$), 135.9 (Ar-C), 134.3 (d, $^2J_{P\text{-}C}$ = 11 Hz, Ar-C), 132.7 (d, $^1J_{P\text{-}C}$ = 2 Hz, Ar-C), 132.1 (Ar-C), 132.0 (d, $^4J_{C\text{-}P}$ = 3 Hz, Ar-C), 128.9 (d, $^3J_{P\text{-}C}$ = 12 Hz, Ar-C), 128.2, 127.4, 127.1, 123.0, 109.5 (Ar-C), 48.9 (NCH_2), 45.5 (NCH_2), 27.0 (CH_2), trifluoroacetate not observed. $^{19}F\{^1H\}$ NMR (282 MHz, CD_2Cl_2): δ 1.3 (CF_3), 0.5 (CF_3). $^{31}P\{^1H\}$

NMR (122 MHz, CD_2Cl_2): δ 27.9 (PPh_3). Anal. Calcd. for $C_{32}H_{25}F_6N_2O_4PPd \cdot 1/3CH_2Cl_2$: C, 49.71; H, 3.31; N, 3.59. Found: C, 49.79; H, 3.50; N, 3.36. ESI (MS) *m/z* 639 $[M - O_2CCF_3]^+$.

***trans*-Bromido(indy-5)bis(triphenylphosphine)palladium(II) tetrafluoroborate (138).**

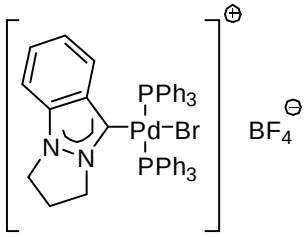

Triphenylphosphine (139 mg, 0.53 mmol, 2.20 equiv.) and sodium tetrafluoroborate (29 mg, 0.26 mmol, 1.10 equiv.) were added to **133** (100 mg, 0.12 mmol, 0.50 equiv.) in dichloromethane (25 mL). The reaction mixture was stirred at ambient temperature for 15 h. The resulting suspension was filtered over a short plug of Celite, and the filtrate was dried under reduced pressure. The solid residue was washed with hexane (2 × 10 mL) and dried *in vacuo* to afford a pale yellow solid (168 mg, 0.17 mmol, 70%). ^{1}H NMR (500 MHz, CD_3CN): δ 7.74 (d, $J_{H\text{-}H}$ = 8 Hz, 1 H, Ar-H), 7.56–7.50 (m, 12 H, Ar-H), 7.49–7.44 (m, 7 H, Ar-H), 7.38–7.32 (m, 12 H, Ar-H), 7.10–7.02 (m, 2 H, Ar-H), 3.80–3.72 (m, 4 H, NCH_2), 2.29 (quint, $^3J_{H\text{-}H}$ = 7 Hz, 2 H, CH_2). ^{13}C{^{1}H} NMR (125 MHz, CD_3CN): δ 156.4 (d, $^2J_{P\text{-}C}$ = 10 Hz, $C_{carbene}$), 136.6 (Ar-C), 135.2 (t, $J_{C\text{-}P}$ = 6 Hz, Ar-C), 132.8, 132.7, 132.4 (Ar-C), 130.4 (t, $J_{C\text{-}P}$ = 25 Hz, Ar-C), 129.6 (t, $J_{C\text{-}P}$ = 5 Hz, Ar-C), 126.2, 123.6, 111.1 (Ar-C), 49.2 (NCH_2), 46.2 (NCH_2), 27.0 (CH_2). ^{19}F{^{1}H} NMR (282 MHz, CD_3CN): δ -75.5 (BF_4), -75.6 (BF_4). ^{31}P{^{1}H} NMR (202 MHz, CD_3CN): δ 23.2 (PPh_3). Anal. Calcd. for $C_{46}H_{40}BBrF_4N_2P_2Pd \cdot 0.5CH_2Cl_2$: C, 55.94; H, 4.14; N, 2.81. Found: C, 56.10; H, 4.54; N, 3.14. ESI (MS) *m/z* 869 $[M - BF_4]^+$.

***cis*-Bromido(indy-5)(dppe)palladium(II) tetrafluoroborate (139).**

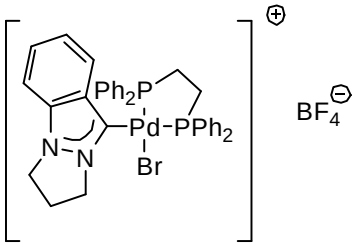

1,2-Bis(diphenylphosphino)ethane (104 mg, 0.26 mmol, 1.1 equiv.) and sodium tetrafluoroborate (29 mg, 0.26 mmol, 1.10 equiv) were added to **133** (100 mg, 0.12 mmol, 0.50 equiv.) in dichloromethane (25 mL). The reaction mixture was stirred at ambient temperature for 15 h. The resulting suspension was filtered over a short plug of Celite, and the filtrate was dried under reduced pressure. The solid residue was washed with hexane (2 × 10 mL) and dried *in vacuo* to afford a yellow solid (199 mg, 0.24 mmol, >99%). ^{1}H NMR (500 MHz, CD_3CN): δ 8.02–7.89 (m, 4 H, Ar-H), 7.81 (d, $J_{H\text{-}H}$ = 8 Hz, 1 H, Ar-H), 7.74–7.45 (m, 11 H, Ar-H), 7.43–7.33 (m, 5 H, Ar-H), 7.15 (dd, $J_{H\text{-}H}$ = 8 H, $J_{H\text{-}H}$ = 12 Hz, 2 H, Ar-H), 7.08 (t, $J_{H\text{-}H}$ = 1 H, 8 Hz, Ar-H), 4.43–4.35 (m, 1 H, NCH_2), .4.31–4.25 (m, 1 H,

NCH_2), 4.21–4.14 (m, 1 H, NCH_2), 3.58–3.50 (m, 1 H, NCH_2), 2.84–2.67 (m, 4 H, CH_2), 2.43–2.26 (m, 2 H, CH_2). $^{13}C\{^1H\}$ NMR (125 MHz, CD_3CN): δ 163.5 (d, $^2J_{C\text{-}P}$ = 145 Hz, $C_{carbene}$), 136.9 (d, $J_{C\text{-}P}$ = 4 Hz, Ar-C), 135.0 (d, $J_{C\text{-}P}$ = 11 Hz, Ar-C), 134.9 (d, $J_{C\text{-}P}$ = 12 Hz, Ar-C), 134.6 (d, $J_{C\text{-}P}$ = 11 Hz, Ar-C), 133.8 (d, $J_{C\text{-}P}$ = 3 Hz, Ar-C), 133.4 (d, $J_{C\text{-}P}$ = 3 Hz, Ar-C), 133.0 (d, $J_{C\text{-}P}$ = 11 Hz, Ar-C), 132.1 (Ar-C), 130.4, 130.4 (d, $J_{C\text{-}P}$ = 3 Hz, Ar-C), 130.3 (d, $J_{C\text{-}P}$ = 4 Hz, Ar-C), 130.2 (Ar-C), 130.2 (d, $J_{C\text{-}P}$ = 3 Hz, Ar-C), 130.1, 129.7, 129.6, 129.1, 129.0, 128.5, 127.8, 122.9, 111.0 (Ar-C), 49.6 (NCH_2), 46.0 (NCH_2), 29.9 (dd, $^2J_{C\text{-}P}$ = 17 Hz, $^1J_{C\text{-}P}$ = 34 Hz, PCH_2), 27.6 (CH_2), 25.3 (dd, $^2J_{C\text{-}P}$ = 12 Hz, $^1J_{C\text{-}P}$ = 31 Hz, PCH_2). $^{19}F\{^1H\}$ NMR (282 MHz, CD_3CN): δ –75.5 (BF_4), –75.5 (BF_4). $^{31}P\{^1H\}$ NMR (202 MHz, CD_3CN): δ 61.1 (d, $^2J_{P\text{-}P}$ = 15 Hz), 50.7 (d, $^2J_{P\text{-}P}$ = 15 Hz). Anal. Calcd. for $C_{36}H_{34}BBrF_4N_2P_2Pd$: C, 52.11; H, 4.13; N, 3.38. Found: C, 52.05; H, 4.13; N, 3.00. ESI (MS) *m/z* 743 $[M - BF_4]^+$.

***cis*-Bromido(indy-5)(dppp)palladium(II) tetrafluoroborate (140).**

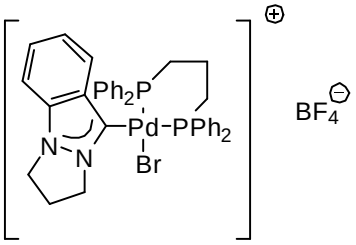

1,3-Bis(diphenylphosphino)propane (107 mg, 0.26 mmol, 1.10 equiv.) and sodium tetrafluoroborate (29 mg, 0.26 mmol, 1.10 equiv.) were added to **133** (100 mg, 0.12 mmol, 0.50 equiv) in dichloromethane (25 mL). The reaction mixture was stirred at ambient temperature for 15 h. The resulting suspension was filtered over a short plug of Celite, and the filtrate was dried under reduced pressure. The solid residue was washed with hexane (2 × 20 mL) and dried *in vacuo* to afford a pale orange solid (145 mg, 0.17 mmol, 72%). ^1H NMR (500 MHz, CD_3CN): δ 7.98–7.92 (m, 2 H, Ar-H), 7.88 (d, $^3J_{H\text{-}H}$ = 9 Hz, 1 H, Ar-H), 7.75–7.69 (m, 2 H, Ar-H), 7.66–7.56 (m, 3 H, Ar-H), 7.55–7.45 (m, 6 H, Ar-H), 7.39–7.34 (m, 1 H, Ar-H), 7.32–7.27 (m, 1 H, Ar-H), 7.24 (d, $^3J_{H\text{-}H}$ = 9 Hz, 1 H, Ar-H), 7.16–7.03 (m, 7 H, Ar-H), 4.48–4.41 (m, 1 H, NCH_2), 4.24–4.18 (m, 1 H, NCH_2), 4.06–4.00 (m, 1 H, NCH_2), 3.99–3.93 (m, 1 H, NCH_2), 2.95–2.87 (m, 1 H, CH_2), 2.81–2.60 (m, 4 H, CH_2), 2.54–2.44 (m, 2 H, CH_2), 1.79–1.67 (m, 1 H, CH_2). $^{13}C\{^1H\}$ NMR (125 MHz, CD_3CN): δ 161.8 (dd, $^2J_{C\text{-}P}$ = 4 Hz, $^2J_{C\text{-}P}$ = 148 Hz, $C_{carbene}$), 136.7 (d, $J_{C\text{-}P}$ = 4 Hz, Ar-C), 134.7 (d, $J_{C\text{-}P}$ = 10 Hz, Ar-C), 134.6 (d, $J_{C\text{-}P}$ = 12 Hz, Ar-C), 134.3 (d, $J_{C\text{-}P}$ = 11 Hz, Ar-C), 132.9 (d, $J_{C\text{-}P}$ = 3 Hz, Ar-C), 132.8 (d, $J_{C\text{-}P}$ = 10 Hz, Ar-C), 132.4 (d, $J_{C\text{-}P}$ = 2 Hz, Ar-C), 132.3 (d, $J_{C\text{-}P}$ = 3 Hz, Ar-C), 132.2, 132.1 (Ar-C), 131.9 (d, $J_{C\text{-}P}$ = 2 Hz, Ar-C), 131.8, 131.5, 131.1, 130.3, 130.1, 130.0, 129.9 129.7, 129.7 (Ar-C), 129.6 (d, $J_{C\text{-}P}$ = 1 Hz, Ar-C), 129.5 (d, $J_{C\text{-}P}$ = 3 Hz, Ar-C), 129.4, 127.7, 122.8, 110.7 (Ar-C), 49.6

(NCH_2), 45.9 (NCH_2), 27.5 (CH_2), 25.8 (dd, $^3J_{C\text{-}P}$ = 7 Hz, $^1J_{C\text{-}P}$ = 30 Hz, PCH_2), 24.9 (dd, $^3J_{C\text{-}P}$ = 7 Hz, $^1J_{C\text{-}P}$ = 28 Hz, PCH_2), 19.2 (CH_2). $^{19}F\{^1H\}$ NMR (282 MHz, CD_3CN): δ -75.5 (BF_4), -75.5 (BF_4). $^{31}P\{^1H\}$ NMR (202 MHz, CD_3CN): δ 13.3 (d, $^2J_{P\text{-}P}$ = 42 Hz), -4.0 (d, $^2J_{P\text{-}P}$ = 42 Hz). Anal. Calcd. for $C_{37}H_{36}BBrF_4N_2P_2Pd$: C, 52.67; H, 4.30; N, 3.32. Found: C, 52.58; H, 4.31; N, 3.00. ESI (MS) *m/z* 757 $[M - BF_4]^+$.

1-Phenylpyrrolidine (166).

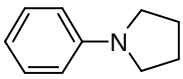

Complex *trans*-[$PdCl_2$(IPr)(pyridine)] (59 mg, 0.08 mmol, 4 mol%) was dissolved in anhydrous THF (5 mL) under an atmosphere of dry nitrogen. Chlorobenzene (203 µL, 2.00 mmol, 1.00 equiv.), potassium tert-butoxide (337 mg, 3.00 mol, 1.50 equiv.), and pyrrolidine (246 µL, 3.00 mmol, 1.50 equiv.) were added, and the mixture was heated to 50 °C for 2 h. Then the solution was diluted with diethyl ether (10 mL), filtered over a short plug of Celite, and concentrated under reduced pressure. The residue was purified by column chromatography (silica, pentane + 10 % diethyl ether). A colorless liquid was obtained (210 mg, 1.43 mmol, 71%). ^1H NMR (300 MHz, $CDCl_3$): δ 7.37–7.27 (m, 2 H, Ar-H), 6.80–6.70 (m, 1 H, Ar-H), 6.69–6.61 (m, 2 H, Ar-H), 3.43–3.28 (m, 4 H, NCH_2), 2.15–2.00 (m, 4 H, CH_2). The analytical data was in accordance with reported values.[162h]

2-Phenylindazole (179).

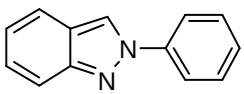

Copper(I) iodide (29 mg, 0.15 mmol, 0.10 equiv.), 2-bromobenzaldehyde (175 µL, 1.50 mmol, 1.00 equiv.), sodium azide (195 mg, 3.00 mmol, 2.00 equiv.), tetramethylethylenediamine (22 µL, 0.15 mmol, 0.10 equiv.), and aniline (164 µL, 1.80 mmol, 1.20 equiv.) were dissolved in DMSO (5 mL) and heated to 120 °C for 16 h under an atmosphere of dry nitrogen. After this time, the reaction mixture was allowed to cool to ambient temperature, and poured into a mixture of ethyl acetate and hexane (160 mL, 2:1). The resulting solution was washed with water (3 × 40 mL). The organic layer was dried over sodium sulfate, filtered and concentrated under reduced pressure. The residue was purified by column chromatography (silica, hexane/ethyl acetate 10:1). A slowly solidifying orange oil was obtained (185 mg, 0.95 mmol, 64%). ^1H NMR (300 MHz, $CDCl_3$): δ 8.46 (s, 1 H, Ar-H), 7.96 (d, $J_{H\text{-}H}$ = 8 Hz, 2 H, Ar-H), 7.85 (d, $J_{H\text{-}H}$ = 8 Hz, 1 H, Ar-H), 7.76 (d, $J_{H\text{-}H}$ = 8 Hz, 1 H, Ar-H), 7.58 (t, $J_{H\text{-}H}$

= 8 Hz, 2 H, Ar-H), 7.45 (t, J_{H-H} = 7 Hz, 1 H, Ar-H), 7.41–7.34 (m, 1 H, Ar-H), 7.20–7.13 (m, 1 H, Ar-H). The analytical data was in accordance with reported values.[166]

2-(2-Pyridyl)indazole (181).

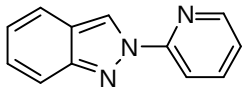

Copper(I) iodide (29 mg, 0.15 mmol, 0.10 equiv.), 2-bromobenzaldehyde (175 µL, 1.50 mmol, 1.00 equiv.), sodium azide (195 mg, 3.00 mmol, 2.00 equiv.), tetramethylethylenediamine (22 µL, 0.15 mmol, 0.10 equiv.), and 2-aminopyridine (169 mg, 1.80 mmol, 1.20 equiv.) were dissolved in DMSO (5 mL) and heated to 120 °C for 16 h under an atmosphere of dry nitrogen. After this time, the reaction mixture was allowed to cool to ambient temperature, and poured into a mixture of ethyl acetate and hexane (100 mL, 1:1). The resulting solution was washed with water (3 × 40 mL). The organic layer was dried over sodium sulfate, filtered and concentrated under reduced pressure. The residue was purified by column chromatography (silica, hexane + 5% ethyl acetate). A yellow solid was obtained (54 mg, 0.28 mmol, 64%). ^{1}H NMR (300 MHz, $CDCl_3$): δ 9.16 (s, 1 H, Ar-H), 8.54 (s, br, 1 H, Ar-H), 8.35 (d, J_{H-H} = 8 Hz, 1 H, Ar-H), 7.97–7.87 (m, 1 H, Ar-H), 7.85–7.73 (m, 2 H, Ar-H), 7.41–7.28 (m, 2 H, Ar-H), 7.20–7.10 (m, 1 H, Ar-H). The analytical data was in accordance with reported values.[166]

2-(1-Adamantyl)indazole (182).

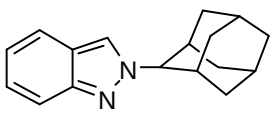

Copper(I) iodide (29 mg, 0.15 mmol, 0.10 equiv.), 2-bromobenzaldehyde (175 µL, 1.50 mmol, 1.00 equiv.), sodium azide (195 mg, 3.00 mmol, 2.00 equiv.), tetramethylethylenediamine (22 µL, 0.15 mmol, 0.10 equiv.), and 1-adamantylamine (272 mg, 1.80 mmol, 1.20 equiv.) were dissolved in DMSO (5 mL) and heated to 120 °C for 16 h under an atmosphere of dry nitrogen. After this time, the reaction mixture was allowed to cool to ambient temperature, and poured into a mixture of hexane and ethyl acetate (100 mL, 2:1). The resulting solution was washed with water (3 × 40 mL). The organic layer was dried over sodium sulfate, filtered and concentrated under reduced pressure. The residue was purified by column chromatography (silica, hexane → hexane + 5% ethyl acetate). An off-white solid was obtained (151 mg, 0.60 mmol, 40%). ^{1}H NMR (300 MHz, $CDCl_3$): δ 8.06 (s, 1 H, Ar-H), 7.77 (d, J_{H-H} = 9 Hz, 1 H, Ar-H), 7.65 (d, J_{H-H} = 8 Hz, 1 H, Ar-H),

7.33–7.26 (m, 1 H, Ar-H), 7.11–7.03 (m, 1 H, Ar-H), 2.38–2.23 (m, 9 H, adamantyl), 1.84–1.79 (m, 1 H, adamantyl). The analytical data was in accordance with reported values.[166]

1-Methyl-2-cyclohexylindazolium triflate (187).

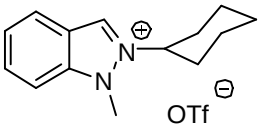

Copper(I) iodide (191 mg, 1.00 mmol, 0.10 equiv.), 2-bromobenzaldehyde (1.16 mL, 10.0 mmol, 1.00 equiv.), sodium azide (1.30 g, 20.0 mmol, 2.00 equiv.), tetramethylethylenediamine (149 µL, 1.00 mmol, 0.10 equiv.) and cyclohexylamine (1.38 mL, 12.0 mmol, 1.20 equiv) were dissolved in DMSO (40 mL) and heated to 120 °C for 6 h. After this time, the solvent was distilled off and the residue was taken up in ethyl acetate (100 mL). The resulting suspension was filtered and concentrated under reduced pressure. The residue was passed over a column of silica gel using hexane + 5% ethyl acetate as eluent. After evaporation of the solvent, 800 mg of an oily residue were obtained, which was taken up anhydrous dichloromethane (40 mL). Methyl triflate (873 µL, 7.98 mmol, 2.00 equiv with respect to the intermediate) was added and the mixture was heated to 40 °C for 24 h under an atmosphere of dry nitrogen. Then the solvent was evaporated and the residue was washed with diethyl ether (2 × 25 mL). The product was obtained as a pale orange solid solid (1.18 g, 3.24 mmol, 32%). ^{1}H NMR (300 MHz, $CDCl_3$): δ 9.02 (s, 1 H, NCH), 7.99 (d, $^{3}J_{H\text{-}H}$ = 8 Hz, 1 H, Ar-H), 7.74 (t, $^{3}J_{H\text{-}H}$ = 7 Hz, 1 H, Ar-H), 7.63 (d, $^{3}J_{H\text{-}H}$ = 9 Hz, 1 H, Ar-H), 7.38 (d, $^{3}J_{H\text{-}H}$ = 8 Hz, 1 H, Ar-H), 4.93–4.74 (m, 1 H, NCH), 4.31 (s, 3 H, NCH_3), 2.36–2.21 (m, 2 H, CH_2), 1.98–1.71 (m, 5 H, CH_2), 1.70–1.52 (m, 2 H, CH_2), 1.39–1.22 (m, 1 H, CH_2). ^{13}C{^{1}H} NMR (75 MHz, $CDCl_3$): δ 141.4 (NCH), 134.4, 130.9, 126.1, 124.1, 120.4, 111.1 (Ar-C), 61.9 (NCH), 34.5 (NCH_3), 33.8 (CH_2), 25.6 (CH_2), 25.2 (CH_2). ^{19}F{^{1}H} NMR (282 MHz, $CDCl_3$): δ -2.42. Anal. Calcd. for $C_{15}H_{19}F_3N_2O_3S$: C, 49.44; H, 5.26; N, 7.69. Found: C, 49.24; H, 4.91; N, 7.41. ESI (MS) *m/z* 215 $[M - Br]^+$.

***trans*-Dibromido(1,3-diisopropylbenzimidazolin-2-ylidene)(indy-Cy)palladium(II) (188).**

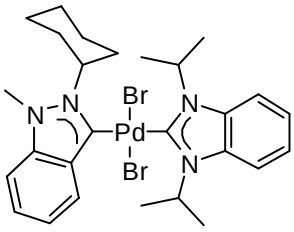

Indazolium salt **187** (182 mg, 0.50 mmol, 1.00 equiv.), silver(I) oxide (58 mg, 0.25 mmol, 0.50 equiv.) and tetrabutylammonium bromide (161 mg, 0.50 mmol, 1.00 equiv.) were stirred in dichloromethane (30 mL) for 15 h at ambient temperature shielded from light. $[PdBr_2(^{i}Pr_2\text{-bimy})]_2$ (234 mg, 0.25 mmol, 0.50 equiv.) was added and

stirring was continued for 1 h. Then the resulting suspension was filtered over a short plug of Celite and the solvent was removed under reduced pressure. The residue was washed with methanol (10 mL) and diethyl ether (3 × 15 mL), and dried *in vacuo*. The product was obtained as a yellow solid (265 mg, 0.39 mmol, 78%). ^{1}H NMR (300 MHz, $CDCl_3$): δ 8.55 (d, $^{3}J_{H\text{-}H}$ = 8 Hz, 1 H, Ar-H), 7.63–7.52 (m, 3 H, Ar-H), 7.34–7.28 (m, 1 H, Ar-H), 7.23–7:15 (m, 3 H, Ar-H), 6.47 (sept, $^{3}J_{H\text{-}H}$ = 7 Hz, 2 H, NCH_2), 5.32–5.27 (m, 1 H, NCH), 3.90 (s, 3 H, NCH_3), 3.04–2.87 (m, 2 H, CH_2), 2.53–2.42 (m, 2 H, CH_2), 2.17–2.06 (m, 2 H, CH_2), 1.92 (d, $^{3}J_{H\text{-}H}$ = 7 Hz, 6 H, CH_3), 1.85 (d, $^{3}J_{H\text{-}H}$ = 7 Hz, 6 H, CH_3), 1.67–1.43 (m, 1 H, CH_2). $^{13}C\{^{1}H\}$ NMR (75 MHz, $CDCl_3$): δ 181.6 ($C_{carbene}$, bimy), 177.8 ($C_{carbene}$, indy) 141.9, 134.5, 134.1, 132.0, 131.2, 130.5, 122.7, 122.5, 113.3, 113.1, 109.3 (Ar-C), 64.6 (NCH), 54.5 (NCH), 54.5 (NCH), 35.4 (NCH_3), 34.1 (CH_2), 30.3 (CH_2), 27.1 (CH_2), 26.1 (CH_2), 22.0 (CH_3), 21.6 (CH_3). Anal. Calcd. for $C_{27}H_{36}Br_2N_4Pd$: C, 47.49; H, 5.31; N, 8.21. Found: C, 47.43; H, 5.44; N, 7.76. ESI (MS) *m/z* 603 $[M - Br]^{+}$.

di-μ-Bromido-bis(indy-Cy)dibromidodipalladium(II) (189).

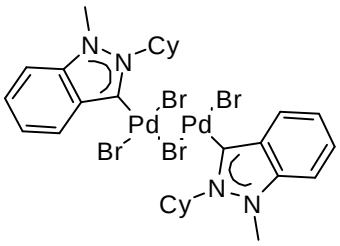

Indazolium salt **187** (182 mg, 0.50 mmol, 1.00 equiv.), silver(I) oxide (58 mg, 0.25 mmol, 0.50 equiv.) and tetrabutylammonium bromide (161 mg, 0.50 mmol, 1.00 equiv.) were stirred in dichloromethane (30 mL) for 15 h at ambient temperature shielded from light. Then the solution was filtered over a short pad of Celite. A solution of [$PdBr_2$(acetonitrile)$_2$] was prepared by dissolving palladium(II) bromide (133 mg, 0.50 mmol, 1.00 equiv.) in acetonitrile (10 mL). Both solutions were combined and stirred for 1 h at ambient temperature. Then the mixture was filtered over a short pad of Celite, concentrated under reduced pressure, and the residue was washed with methanol (15 mL) and diethyl ether (2 × 20 mL). A yellow solid was obtained (170 mg, 0.18 mmol, 71%). ^{1}H NMR (500 MHz, DMSO-d_6): δ 8.30–8.17 (m, 2 H, Ar-H), 7.78–7.60 (m, 4 H, Ar-H), 7.39–7.29 (m, 2 H, Ar-H), 5.29–5.11 (m, 2 H, NCH), 4.14 (s. 6 H, NCH_3), 2.98–2.74 (m, 2 H, CH_2), 2.31–2.14 (m, 4 H, CH_2), 2.14–1.86 (m, 4 H, CH_2), 1.85–1.72 (m, 2 H, CH_2), 1.71–1.48 (m, 4 H, CH_2), 1.44–1.25 (m, 2 H, CH_2), two CH_2 protons not observed due to overlap with the water signal. $^{13}C\{^{1}H\}$ NMR (125 MHz, DMSO-d_6): δ 157.0 ($C_{carbene}$), 149.7, 140.3, 132.1, 128.9, 122.5, 110.6 (Ar-C), 63.0 (NCH), 35.3 (NCH_3), 32.9 (CH_2), 26.0 (CH_2), 25.3 (CH_2). Anal. Calcd. for $C_{28}H_{36}Br_4N_4Pd_2$: C, 34.99; H,

3.78; N, 5.83. Found: C, 34.45; H, 3.89; N, 5.55. ESI (MS) *m/z* 479 [½ M-Br+DMSO]$^+$, 557 [½ M - Br + 2 DMSO]$^+$.

1-Isobutyl-3-(2-bromoethyl)-benzimidazolium bromide (200).

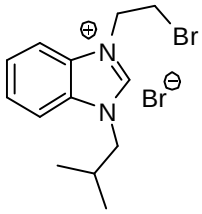

1-Isobutylbenzimidazole **(197)** (8.00 g, 46.0 mmol) was dissolved in 1,2-dibromoethane (50 mL) and heated to 85 °C for 15 h. Then the volatiles were distilled off under reduced pressure, and the solid residue was extracted with dichloromethane (150 mL). The resulting suspension was filtered, and the solvent of the filtrate was evaporated. The residue was washed with acetone (50 mL). An off-white solid was obtained (8.52 g, 23.5 mmol, 51%). ^{1}H NMR (300 MHz, $CDCl_3$): δ 11.14 (s, 1 H, NCHN), 8.00–7.91 (m, 1 H, Ar-H), 7.76–7.60 (m 3 H, Ar-H), 5.25 (t, $^3J_{H\text{-}H}$ = 6 Hz, 2 H, NCH_2), 4.41 (d, $^3J_{H\text{-}H}$ = 7 Hz, 2 H, NCH_2), 4.07 (t, $^3J_{H\text{-}H}$ = 6 Hz, 2 H, CH_2Br), 2.41 (sept, $^3J_{H\text{-}H}$ = 7 Hz, 1 H, CH), 1.03 (d, $^3J_{H\text{-}H}$ = 7 Hz, 6 H, CH_3). $^{13}C\{^1H\}$ NMR (75 MHz, $CDCl_3$): δ 143.8 (NCHN), 132.0, 131.9, 128.1, 128.0, 114.3, 113.8 (Ar-C), 55.2 (NCH_2), 49.4 (NCH_2), 30.9 (CH), 29.5 (CH_2Br), 20.5 (CH_3). Anal. Calcd. for $C_{13}H_{18}Br_2N_2 \cdot H_2O$: C, 41.08; H, 5.30; N, 7.37. Found: C, 40.77; H, 4.98; N, 7.66. MS (ESI) *m/z* 281 [M - Br]$^+$.

1-Benzhydryl-3-(2-bromoethyl)-benzimidazolium bromide (201).

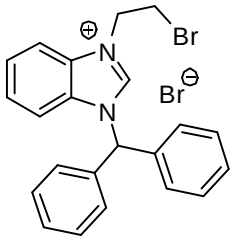

Benzimidazolium salt **201** was prepared in analogy to salt **200** from 1-benzhydrylbenzimidazole (**198)** (1.80 g, 6.34 mmol) and 1,2-dibromoethane (10 mL). A white solid was obtained (1.09 g, 2.31 mmol, 37%). ^{1}H NMR (300 MHz, $CDCl_3$): δ 10.21 (s, 1 H, NCHN), 7.96 (d, $^3J_{H\text{-}H}$ = 8 Hz, 2 H, Ar-H), 7.62 (t, $^3J_{H\text{-}H}$ = 8 Hz, 1 H, Ar-H), 7.49–7.33 (m, 12 H, Ar-H), 7.21 (s, 1 H, $NCHPh_2$), 5.28 (t, $^3J_{H\text{-}H}$ = 5 Hz, 2 H, NCH_2), 4.00 (t, $^3J_{H\text{-}H}$ = 5 Hz, 2 H, CH_2Br). $^{13}C\{^1H\}$ NMR (75 MHz, DMSO-d_6): δ 143.7 (NCHN), 136.2, 132.0, 131.1, 129.5, 129.5, 128.8, 127.3, 114.0 (Ar-C), 65.3 ($NCHPh_2$), 48.6 (NCH_2), 31.4 (CH_2Br). Anal. Calcd. for $C_{22}H_{20}Br_2N_2$: C, 55.96; H, 4.27; N, 5.93. Found: C, 56.03; H, 4.36; N, 5.73. MS (ESI) *m/z* 391 [M - Br]$^+$.

1-Isobutyl-3-(3-bromopropyl)-benzimidazolium bromide (203).

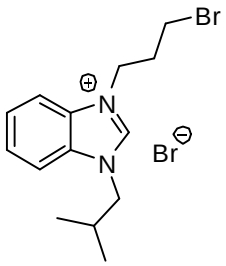

1-Isobutylbenzimidazole **(197)** (8.00 g, 46.0 mmol) was dissolved in 1,3-dibromopropane (50 mL) and heated to 85 °C for 15 h. Then the volatiles were distilled off under reduced pressure, and the solid residue was extracted with dichloromethane (150 mL). The resulting suspension was filtered, and the solvent of the filtrate was evaporated. The residue was washed with acetone (50 mL) to yield a white solid (8.57 g, 22.8 mmol, 50%). ^{1}H NMR (300 MHz, $CDCl_3$): δ 11.25 (s, 1 H, NCHN), 7.88–7.83 (m, 1 H, Ar-H), 7.74–7.63 (m 3 H, Ar-H), 4.90 (t, $^{3}J_{H\text{-}H}$ = 7 Hz, 2 H, NCH_2), 4.41 (d, $^{3}J_{H\text{-}H}$ = 7 Hz, 2 H, NCH_2), 3.56 (t, $^{3}J_{H\text{-}H}$ = 6 Hz, 2 H, CH_2Br), 2.71 (tt, $^{3}J_{H\text{-}H}$ = 6 Hz, $^{3}J_{H\text{-}H}$ = 7 Hz, 2 H, CH_2), 2.41 (sept, $^{3}J_{H\text{-}H}$ = 7 Hz, 1 H, CH), 1.01 (d, $^{3}J_{H\text{-}H}$ = 7 Hz, 6 H, CH_3). $^{13}C\{^{1}H\}$ NMR (75 MHz, $CDCl_3$): δ 143.7 (NCHN), 132.1, 132.0, 128.0, 127.9, 113.9, 113.8 (Ar-C), 55.2 (NCH_2), 46.5 (NCH_2), 32.8 (CH_2), 30.4 (CH_2), 29.6 (CH_2Br), 20.6 (CH_3). Anal. Calcd. for $C_{14}H_{20}Br_2N_2 \cdot CH_2Cl_2$: C, 43.07; H, 5.20; N, 7.05. Found: C, 42.76; H, 5.15; N, 7.45. MS (ESI) *m*/*z* 295 $[M - Br]^+$.

1-Benzhydryl-3-(3-bromopropyl)-benzimidazolium bromide (204).

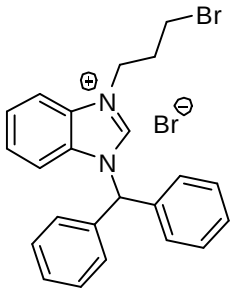

Benzimidazolium salt **204** was prepared in analogy to salt **203** from 1-benzhydrylbenzimidazole (**198)** (1.80 g, 6.34 mmol) and 1,3-dibromopropane (10 mL). A white solid was obtained (1.74 g, 3.58 mmol, 57%). ^{1}H NMR (300 MHz, $CDCl_3$): δ 10.82 (s, 1 H, NCHN), 7.86 (d, $^{3}J_{H\text{-}H}$ = 8 Hz, 1 H, Ar-H), 7.68–7.59 (m, 1 H, Ar-H), 7.51–7.27 (m, 12 H, Ar-H) 7.30 (s, 1 H, $NCHPh_2$), 4.95 (t, $^{3}J_{H\text{-}H}$ = 7 Hz, 2 H, NCH_2), 3.58 (t, $^{3}J_{H\text{-}H}$ = 6 Hz, 2 H, CH_2Br), 2.77–2.65 (m, 2 H, CH_2). $^{13}C\{^{1}H\}$ NMR (75 MHz, $CDCl_3$): δ 143.6 (NCHN), 135.9, 135.7, 132.6, 130.2, 130.1, 129.1, 128.1, 127.9, 115.7, 114.0 (Ar-C), 67.6 ($NCHPh_2$), 47.0 (NCH_2), 32.6 (CH_2Br), 30.5 (CH_2). Anal. Calcd. for $C_{23}H_{22}Br_2N_2$: C, 56.81; H, 4.56; N, 5.76. Found: C, 56.44; H, 4.33; N, 5.58. MS (ESI) *m*/*z* 405 $[M - Br]^+$.

1-Benzyl-3-(2-(isopropylthio)ethyl)-benzimidazolium bromide (205).

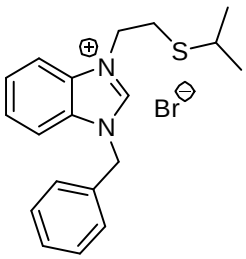

2-Mercaptopropane (351 µL, 3.78 mmol, 1.50 equiv.) was dissolved in degassed acetonitrile (30 mL). Sodium hydroxide (151 mg, 3.78 mmol, 1.50 equiv.) in water (1 mL) was added, and the resulting mixture was stirred for 30 min at ambient temperature. Then, salt **199** (1.00 g, 2.52 mmol, 1.00 equiv.) was added, and stirring was continued for 15 h at ambient temperature. After this time, the volatiles were removed under reduced pressure. The solid residue was suspended in dichloromethane (10 mL) and filtered. The solvent was removed under reduced pressure, and the residue washed with diethyl ether (5 mL). A white solid was obtained (978 mg, 2.50 mmol, 99%). ^{1}H NMR (300 MHz, $CDCl_3$): δ 11.60 (s, 1 H, NCHN), 7.69–7.74 (m, 1 H, Ar-H), 7.46–7.65 (m, 6 H, Ar-H), 7.36–7.40 (m, 2 H, Ar-H), 5.84 (s, 2 H, NCH_2Ph), 4.87 (t, $^{3}J_{H-H}$ = 7 Hz, 2 H, NCH_2), 3.19 (t, $^{3}J_{H-H}$ = 7 Hz, 2 H, SCH_2), 3.17 (sept, $^{3}J_{H-H}$ = 7 Hz, 1 H, SCH), 1.26 (d, $^{3}J_{H-H}$ = 7 Hz, 6 H, CH_3). $^{13}C\{^{1}H\}$ NMR (75 MHz, $CDCl_3$): δ 144.0 (NCHN), 133.3, 132.1, 131.7, 130.0, 129.9, 128.9, 127.8, 114.4, 113.8 (Ar-C), 52.1 (NCH_2Ph), 47.8 (NCH_2), 35.9 (SCH), 30.5 (SCH_2), 24.0 (CH_3). Anal. Calcd. for $C_{19}H_{23}BrN_2S \cdot H_2O$: C, 55.74; H, 6.16; N, 6.84. Found: C, 56.11; H, 5.80; N, 6.88. MS (ESI) *m*/*z* 311 $[M - Br]^+$.

1-Isobutyl-3-(2-(isopropylthio)ethyl)-benzimidazolium bromide (206).

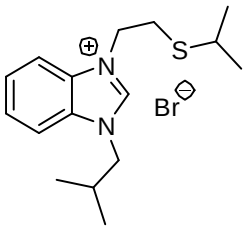

Salt **206** was prepared in analogy to salt **205** from 2-mercaptopropane (628 µL, 6.80 mmol, 1.51 equiv.), sodium hydroxide (272 mg, 6.80 mmol, 1.51 equiv.) and salt **200** (1.63 g, 4.50 mmol, 1.00 equiv.). A white solid was obtained (1.26 g, 3.53 mmol, 78%). ^{1}H NMR (300 MHz, $CDCl_3$): δ 11.33 (s, 1 H, NCHN), 7.79–7.59 (m, 4 H, Ar-H), 4.91 (t, $^{3}J_{H-H}$ = 7 Hz, 2 H, NCH_2), 4.40 (d, $^{3}J_{H-H}$ = 7 Hz, 2 H, NCH_2), 3.19 (sept, $^{3}J_{H-H}$ = 7 Hz, 1 H, SCH), 3.17 (t, $^{3}J_{H-H}$ = 7 Hz, 2 H, SCH_2), 2.41 (m, 1 H, CH), 1.24 (d, $^{3}J_{H-H}$ = 7 Hz, 6 H, CH_3), 1.05 (d, $^{3}J_{H-H}$ = 7 Hz, 6 H, CH_3). $^{13}C\{^{1}H\}$ NMR (75 MHz, $CDCl_3$): δ 144.3 (NCHN), 132.1, 131.9, 127.8, 113.8 (Ar-C), 55.1 (NCH_2), 47.6 (NCH_2), 35.7 (SCH), 30.6 (CH), 29.6 (SCH_2), 24.0 (CH_3), 20.5 (CH_3). Anal. Calcd. for $C_{16}H_{25}BrN_2S \cdot 1/5CH_2Cl_2$: C, 51.98; H, 6.84; N, 7.48. Found: C, 52.37; H, 6.68; N, 7.67. MS (ESI) *m*/*z* 277 $[M - Br]^+$.

1-Benzhydryl-3-(2-(isopropylthio)ethyl)-benzimidazolium bromide (207).

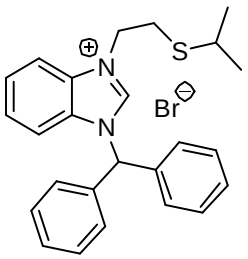

Salt **207** was prepared in analogy to salt **205** from 2-mercaptopropane (903 µL, 9.78 mmol, 1.50 equiv.), sodium hydroxide (391 mg, 9.78 mmol, 1.50 equiv.) and salt **201** (3.08 g, 6.52 mmol, 1.00 equiv.). A white solid was obtained (2.03 g, 4.34 mmol, 67%). ^{1}H NMR (300 MHz, $CDCl_3$): δ 10.42 (s, 1 H, NCHN), 7.80 (d, $^{3}J_{H\text{-}H}$ = 9 Hz, 1 H, Ar-H), 7.58 (dt, $^{4}J_{H\text{-}H}$ = 1 Hz, $^{3}J_{H\text{-}H}$ = 8 Hz, 1 H, Ar-H), 7.50–7.35 (m, 12 H, Ar-H), 7.27 (s, 1 H, $NCHPh_2$), 4.99 (t, $^{3}J_{H\text{-}H}$ = 6 Hz, 2 H, NCH_2), 3.10 (t, $^{3}J_{H\text{-}H}$ = 6 Hz, 2 H, SCH_2), 3.09 (sept, $^{3}J_{H\text{-}H}$ = 7 Hz, 1 H, SCH), 1.16 (d, $^{3}J_{H\text{-}H}$ = 7 Hz, 6 H, CH_3). $^{13}C\{^{1}H\}$ NMR (75 MHz, $CDCl_3$): δ 144.0 (NCHN), 135.7, 132.5, 131.7, 130.3, 129.2, 127.9, 127.7, 115.4, 114.0 (Ar-C), 67.4 ($NCHPh_2$), 47.9 (NCH_2), 35.6 (SCH), 30.5 (SCH_2), 24.0 (CH_3). Anal. Calcd. for $C_{25}H_{27}BrN_2S$: C, 64.23; H, 5.82; N, 5.99. Found: C, 64.25; H, 5.58; N, 5.90. MS (ESI) *m*/*z* 387 $[M - Br]^+$.

1-Benzyl-3-(3-(isopropylthio)propyl)-benzimidazolium bromide (208).

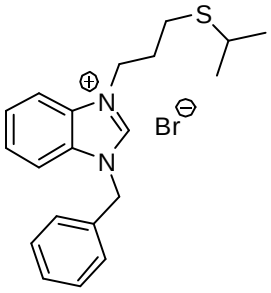

Salt **208** was prepared in analogy to salt **205** from 2-mercaptopropane (3.05 mL, 33.0 mmol, 1.50 equiv.), sodium hydroxide (1.32 g, 33.0 mmol, 1.50 equiv.) and salt **202** (9.02 g, 22.0 mmol, 1.00 equiv.). An off-white solid was obtained (5.24 g, 12.9 mmol, 58%). ^{1}H NMR (300 MHz, $CDCl_3$): δ 11.70 (s, 1 H, NCHN), 7.81–7.75 (m, 1 H, Ar-H), 7.63–7.47 (m, 5 H, Ar-H), 7.39–7.30 (m, 3 H, Ar-H), 5.87 (s, 2 H, NCH_2Ph), 4.77 (t, $^{3}J_{H\text{-}H}$ = 8 Hz, 2 H, NCH_2), 2.90 (sept, $^{3}J_{H\text{-}H}$ = 7 Hz, 1 H, SCH), 2.67 (t, $^{3}J_{H\text{-}H}$ = 7 Hz, 2 H, SCH_2), 2.40 (tt, $^{3}J_{H\text{-}H}$ = 7 Hz, $^{3}J_{H\text{-}H}$ = 8 Hz, 2 H, CH_2), 1.21 (d, $^{3}J_{H\text{-}H}$ = 7 Hz, 6 H, CH_3). $^{13}C\{^{1}H\}$ NMR (75 MHz, $CDCl_3$): δ 143.9 (NCHN), 133.3, 132.3, 131.8, 130.0, 129.9, 129.1, 127.9, 127.8, 114.4, 113.8 (Ar-C), 52.1 (NCH_2Ph), 46.9 (NCH_2), 36.0 (SCH), 29.8 (SCH_2), 27.9 (CH_2), 24.0 (CH_3). Anal. Calcd. for $C_{20}H_{25}BrN_2S \cdot 1/4CH_2Cl_2$: C, 57.01; H, 6.02; N, 6.57. Found: C, 57.03; H, 5.95; N, 6.82. MS (ESI) *m*/*z* 325 $[M - Br]^+$.

1-Isobutyl-3-(3-(isopropylthio)propyl)-benzimidazolium bromide (209).

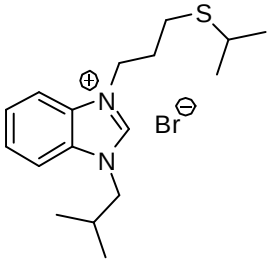

Salt **209** was prepared in analogy to salt **205** from 2-mercaptopropane (849 µL, 9.20 mmol, 1.50 equiv.), sodium hydroxide (369 mg, 9.20 mmol, 1.50 equiv.) and salt **203** (2.31 g, 6.10 mmol, 1.00 equiv.). A brown oil was obtained (1.76 g, 4.74 mmol, 78%). ^{1}H NMR (300 MHz, $CDCl_3$): δ 11.49 (s, 1 H, NCHN), 7.84–7.78 (m, 1 H, Ar-H), 7.72–7.60 (m, 3 H, Ar-H), 4.80 (t, $^{3}J_{H\text{-}H}$ = 7 Hz, 2 H, NCH_2), 4.41 (d, $^{3}J_{H\text{-}H}$ = 8 Hz, 2 H, NCH_2), 2.89 (sept, $^{3}J_{H\text{-}H}$ = 7 Hz, 1 H, SCH), 2.66 (t, $^{3}J_{H\text{-}H}$ = 7 Hz, 2 H, SCH_2), 2.43–2.30 (m, 3 H, CH, CH_2), 1.21 (d, $^{3}J_{H\text{-}H}$ = 7 Hz, 6 H, CH_3), 1.02 (d, $^{3}J_{H\text{-}H}$ = 7 Hz, 6 H, CH_3). $^{13}C\{^{1}H\}$ NMR (75 MHz, $CDCl_3$): δ 143.9 (NCHN), 132.1, 132.0, 127.8, 113.8 (Ar-C), 55.0 (NCH_2), 46.8 (NCH_2), 36.0 (SCH); 29.9 (CH), 29.6 (SCH_2), 27.8 (CH_2), 24.0 (CH_3), 20.5 (CH_3). No correct elemental analysis could be obtained for this compound despite several attempts. MS (ESI) *m*/*z* 291 $[M - Br]^{+}$.

1-Benzhydryl-3-(3-(isopropylthio)propyl)-benzimidazolium bromide (210).

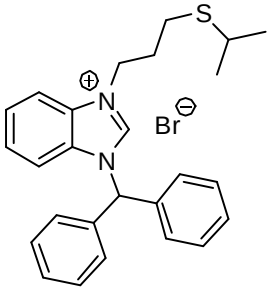

Salt **210** was prepared in analogy to salt **205** from 2-mercaptopropane (1.48 mL, 16.1 mmol, 1.50 equiv.), sodium hydroxide (644 mg, 16.1 mmol, 1.50 equiv.) and salt **204** (5.21 g, 10.7 mmol, 1.00 equiv.). A white solid was obtained (3.09 g, 6.42 mmol, 60%). ^{1}H NMR (300 MHz, $CDCl_3$): δ 10.88 (s, 1 H, NCHN), 7.82 (d, $^{3}J_{H\text{-}H}$ = 8 Hz, 1 H, Ar-H), 7.58 (dt, $^{4}J_{H\text{-}H}$ = 1 Hz, $^{3}J_{H\text{-}H}$ = 7 Hz, 1 H, Ar-H), 7.47–7.33 (m, 12 H, Ar-H), 7.29 (s, 1 H, $NCHPh_2$), 4.87 (t, $^{3}J_{H\text{-}H}$ = 7 Hz, 2 H, NCH_2), 2.85 (sept, $^{3}J_{H\text{-}H}$ = 7 Hz, 1 H, SCH), 2.65 (t, $^{3}J_{H\text{-}H}$ = 7 Hz, 2 H, SCH_2), 2.34 (quint, $^{3}J_{H\text{-}H}$ = 7 Hz, 2 H, CH_2), 1.18 (d, $^{3}J_{H\text{-}H}$ = 7 Hz, 6 H, CH_3). $^{13}C\{^{1}H\}$ NMR (75 MHz, $CDCl_3$): δ 143.8 (NCHN), 135.8, 132.6, 131.7, 130.1, 129.2, 127.8, 127.7, 115.7, 114.0 (Ar-C), 67.4 ($NCHPh_2$), 47.3 (NCH_2), 36.0 (SCH), 29.6 (SCH_2), 27.9 (CH_2), 24.0 (CH_3). Anal. Calcd. for $C_{26}H_{29}BrN_2S$: C, 64.86; H, 6.07; N, 5.84. Found: C, 64.80; H, 5.73; N, 5.88. MS (ESI) *m*/*z* 401 $[M - Br]^{+}$.

***cis*-Dibromido(1-benzyl-3-(2-(isopropylthio)ethyl)-benzimidazolin-2-ylidene-κ^2-CS)-platinum(II) (211).**

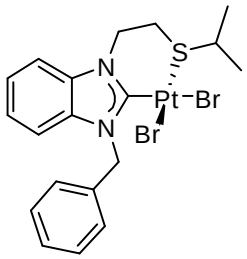

Benzimidazolium salt **205** (117 mg, 0.30 mmol, 1.00 equiv.) and silver(I) oxide (35 mg, 0.15 mmol, 0.50 equiv.) were suspended in dichloromethane (15 mL) and stirred at ambient temperature for 15 h shielded from light. Platinum(II) bromide (106 mg, 0.30 mmol, 1.00 equiv.) was dissolved in DMSO (5 mL) by stirring for 10 min at 80 °C. After the [$PtBr_2(dmso)_2$] solution had cooled to ambient temperature, the silver complex solution was added by filtration over a short plug of Celite, and the resulting mixture was stirred for 1 h at ambient temperature. Then the solution was filtered over Celite. The solution was extracted with water (2 × 50 mL), dried over sodium sulfate, filtered, and the solvent was removed under reduced pressure. The residue was washed with small quantities of dichloromethane. The product was obtained as an off-white solid (176 mg, 0.26 mmol, 88%). ^{1}H NMR (300 MHz, DMSO-d_6): δ 7.93 (d, $^3J_{H\text{-}H}$ = 8 Hz, 1 H, Ar-H), 7.61 (d, $^3J_{H\text{-}H}$ = 8 Hz, 1 H, Ar-H), 7.49–7.23 (m, 9 H, Ar-H, NCH_2Ph), 6.45 (d, $^2J_{H\text{-}H}$ = 16 Hz, 1 H, NCH_2), 5.82 (d, $^2J_{H\text{-}H}$ = 16 Hz, 1 H, NCH_2), 5.04 (d, $^2J_{H\text{-}H}$ = 15 Hz, 1 H, SCH_2), 4.35 (t, $^2J_{H\text{-}H}$ = 13 Hz, 1 H, SCH_2), 2.69–2.52 (m, 1 H, SCH), 1.04 (d, $^3J_{H\text{-}H}$ = 6 Hz, 3 H, CH_3), 0.87 (d, $^3J_{H\text{-}H}$ = 6 Hz, 3 H, CH_3). ^{13}C{^{1}H} NMR (75 MHz, DMSO-d_6): δ 152.3 ($C_{carbene}$), 136.1, 133.8, 132.7, 128.6, 127.8, 127.4, 124.1, 123.9, 112.0, 111.7 (Ar-C), 50.4 (NCH_2Ph), 45.9 (NCH_2), 45.0 (SCH), 30.1 (SCH_2), 22.3 (CH_3), 21.1 (CH_3). Anal. Calcd. for $C_{19}H_{22}Br_2N_2PtS\cdot 1.5CH_2Cl_2$: C, 31.06; H, 3.18; N, 3.53. Found: C, 31.43; H, 3.53; N, 3.71. MS (ESI) *m*/*z* 585 [M - Br]$^+$.

***cis*-Dibromido(1-isobutyl-3-(2-(isopropylthio)ethyl)-benzimidazolin-2-ylidene-κ^2-CS)-platinum(II) (212).**

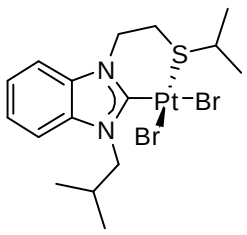

Complex **212** was prepared in analogy to complex **211** from benzimidazolium salt **206** (107 mg, 0.30 mmol, 1.00 equiv.), silver(I) oxide (35 mg, 0.15 mmol, 0.50 equiv.) and platinum(II) bromide (106 mg, 0.30 mmol, 1.00 equiv.). The product was obtained as an off-white solid (102 mg, 0.16 mmol, 54%). ^{1}H NMR (300 MHz, DMSO-d_6): δ 7.96–7.77 (m, 2 H, Ar-H), 7.46–7.30 (m, 2 H, Ar-H), 5.19 (dd, $^3J_{H\text{-}H}$ = 7 Hz, $^2J_{H\text{-}H}$ = 14 Hz, 1 H, NCH_2), 5.01 (d, $^2J_{H\text{-}H}$ = 15 Hz, 1 H, NCH_2), 4.45–4.24 (m, 1 H, NCH_2), 4.09 (dd, $^3J_{H\text{-}H}$ = 9, $^4J_{H\text{-}H}$ = 13 Hz,

1 H, NCH_2), 2.83–2.60 (m, 2 H, SCH_2), 1.33 (d, $^3J_{H-H}$ = 7 Hz, 3 H, CH_3), 1.31–1.23 (m, 1 H, CH), 1.18 (d, $^3J_{H-H}$ = 6 Hz, 3 H, CH_3), 1.00 (d, $^3J_{H-H}$ = 6 Hz, 3 H, CH_3), 0.83 (d, $^3J_{H-H}$ = 6 Hz, 3 H, CH_3), SCH not observed due to overlap with solvent peak. $^{13}C\{^1H\}$ NMR (75 MHz, DMSO-d_6): δ 150.6 ($C_{carbene}$), 134.4, 132.4, 123.8, 123.7, 111.9, 111.5 (Ar-C), 53.8 (NCH_2), 45.7 (NCH_2), 45.2 (SCH), 30.4 (SCH_2), 28.7 (CH), 22.8, 21.3, 19.8, 19.6 (CH_3). Anal. Calcd. for $C_{16}H_{24}Br_2N_2PtS$: C, 30.44; H, 3.83; N, 4.44. Found: C, 30.31; H, 3.83; N, 4.49. MS (ESI) *m*/*z* 550 $[M - Br]^+$.

cis-Dibromido(1-benzhydryl-3-(2-(isopropylthio)ethyl)-benzimidazolin-2-ylidene-κ^2-CS)-platinum(II) (213).

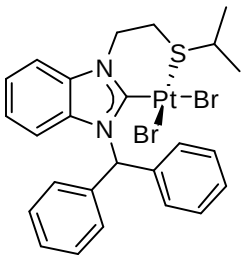

Benzimidazolium salt **207** (468 mg, 1.00 mmol, 1.00 equiv.) and silver(I) oxide (116 mg, 0.50 mmol, 0.50 equiv.) were suspended in dichloromethane (50 mL) and stirred at ambient temperature for 15 h shielded from light. Platinum(II) bromide (355 mg, 1.00 mmol, 1.00 equiv.) was dissolved in DMSO (5 mL) by stirring for 10 min at 80 °C. After the $[PtBr_2(dmso)_2]$ solution had cooled to ambient temperature, the silver complex solution was added by filtration, and the resulting mixture was stirred for 1 h at ambient temperature. Then the solution was filtered and the solvent was removed under reduced pressure. The residue was washed with methanol (40 mL) and diethyl ether (40 mL). The product was obtained as an off-white solid (529 mg, 0.71 mmol, 71%). ^1H NMR (300 MHz, DMSO-d_6): δ 8.60 (s, 1 H, Ar-H), 7.94 (d, $^3J_{H-H}$ = 8 Hz, 1 H, Ar-H), 7.48–7.33 (m, 7 H, Ar-H), 7.31–7.21 (m, 4 H, Ar-H, $NCHPh_2$), 7.17–7.06 (m, 1 H, Ar-H), 6.53 (d, $^3J_{H-H}$ = 8 Hz, 1 H, Ar-H), 5.07 (t, $^2J_{H-H}$ = 15 Hz, 1 H, NCH_2), 4.45 (t, $^2J_{H-H}$ = 13 Hz, 1 H, NCH_2), 2.63–2.52 (m, 1 H, SCH_2), 2.13–1.96 (m, 1 H, SCH), 1.32–1.22 (m, 1 H, SCH_2), 0.89 (d, $^3J_{H-H}$ = 6 Hz, 3 H, CH_3), 0.48 (d, $^3J_{H-H}$ = 7 Hz, 3 H, CH_3). $^{13}C\{^1H\}$ NMR (75 MHz, DMSO-d_6): δ 154.3 ($C_{carbene}$), 137.8, 133.3, 133.2, 129.1, 128.6, 128.4, 127.6, 123.8, 123.7, 113.6, 112.2 (Ar-C), 65.6 ($NCHPh_2$), 46.3 (NCH_2), 45.5 (SCH), 30.4 (SCH_2), 21.9 (CH_3), 20.9 (CH_3). Anal. Calcd. for $C_{25}H_{26}Br_2N_2PtS$: C, 40.50; H, 3.53; N, 3.78. Found: C, 40.62; H, 3.53; N, 3.78. MS (ESI) *m*/*z* 661 $[M - Br]^+$.

***cis*-Dibromido(1-benzyl-3-(3-(isopropylthio)propyl)-benzimidazolin-2-ylidene-κ^2-CS)-platinum(II) (214).**

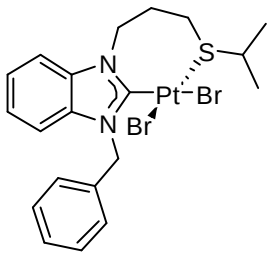

Complex **214** was prepared in analogy to complex **211** from benzimidazolium salt **208** (122 mg, 0.30 mmol, 1.00 equiv.), silver(I) oxide (35 mg, 0.15 mmol, 0.50 equiv.) and platinum(II) bromide (106 mg, 0.30 mmol, 1.00 equiv.). The product was obtained as an off-white solid (205 mg, 0.30 mmol >99%). ^{1}H NMR (300 MHz, DMSO-d_6) (two overlapping sets of signals, ratio ~1:1): δ 7.78 (d, $^3J_{H\text{-}H}$ = 8.0 Hz, 1 H, Ar-H), 7.56–7.13 (m, 10 H, Ar-H, NCH_2Ph), 6.20–6.06 (m, 1 H, NCH_2), 6.06–5.91 (m, 1 H, NCH_2), 5.42–5.22 (m, 1 H, SCH_2), 4.89–4.70 (m, 1 H, SCH_2), 2.86–2.63 (m, 0.5 H, SCH), 2.46–2.16 (m, 2 H, CH_2), 1.95–1.78 (m, 0.5 H, SCH), 1.28–0.99 (m, 6 H, CH_3). ^{13}C{^{1}H} NMR (75 MHz, DMSO-d_6) (two signal sets observed): δ 156.0 ($C_{carbene}$), 135.6, 135.5, 134.1, 133.3, 133.2, 132.6, 128.7, 128.6, 127.9, 127.7, 127.4, 127.0, 124.0, 124.0, 112.4, 112.0, 111.8, 111.3 (Ar-C), 51.2, 51.1 (NCH_2Ph), 46.8, 42.8 (NCH_2), 42.6, 33.8 (SCH), 29.1, 28.5 (SCH_2), 26.7, 24.3 (CH_2), 23.3, 23.2 (CH_3), 21.7, 20.9 (CH_3). Anal. Calcd. for $C_{20}H_{24}Br_2N_2PtS$: C, 35.36; H, 3.56; N, 4.12. Found: C, 35.73; H, 3.72; N, 4.16. MS (ESI) *m*/*z* 599 [M - Br]$^+$.

***cis*-Dibromido(1-isobutyl-3-(3-(isopropylthio)propyl)-benzimidazolin-2-ylidene-κ^2-CS)-platinum(II) (215).**

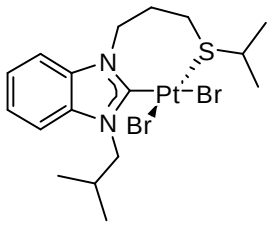

Complex **215** was prepared in analogy to complex **213** from benzimidazolium salt **209** (371 mg, 1.00 mmol, 1.00 equiv.), silver(I) oxide (116 mg, 0.50 mmol, 0.50 equiv.) and platinum(II) bromide (355 mg, 1.00 mmol, 1.00 equiv.). The product was obtained as an off-white solid (283 mg, 0.44 mmol, 44%). ^{1}H NMR (300 MHz, DMSO-d_6): δ 7.94–7.70 (m, 2 H, Ar-H), 7.55–7.25 (m, 2 H, Ar-H), 5.39–5.12 (m, 1 H, NCH_2), 5.00–4.60 (m, 2 H, NCH_2), 4.55–4.04 (m, 1 H, NCH_2), 2.98–2.58 (m, 2 H, SCH_2), 2.48–1.60 (m, 4 H, SCH, CH, CH_2), 1.47–1.13 (m, 6 H, CH_3), 1.06–0.82 (m, 6 H, CH_3). ^{13}C{^{1}H} NMR (75 MHz, DMSO-d_6): δ 154.9 ($C_{carbene}$), 134.0, 132.8, 123.9, 112.1, 111.0 (Ar-C), 54.9 (NCH_2), 46.7 (NCH_2), 33.8 (SCH), 28.6 (SCH_2), 28.4 (CH), 26.7 (CH_2), 23.3 (CH_3), 23.2 (CH_3), 19.9 (CH_3), 19.8 (CH_3). Anal. Calcd. for $C_{17}H_{26}Br_2N_2PtS$: C, 31.64; H, 4.06; N, 4.34. Found: C, 31.44; H, 3.90; N, 4.27. MS (ESI) *m*/*z* 1210 [2 M - Br]$^+$.

cis-Dibromido(1-benzhydryl-3-(3-(isopropylthio)propyl)-benzimidazolin-2-ylidene-κ^2-CS)-platinum(II) (216).

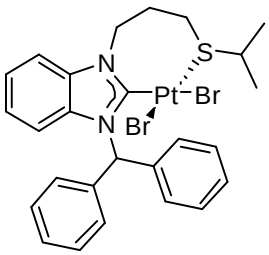

Complex **216** was prepared in analogy to complex **213** from benzimidazolium salt **210** (482 mg, 1.00 mmol, 1.00 equiv.), silver(I) oxide (116 mg, 0.50 mmol, 0.50 equiv.) and platinum(II) bromide (355 mg, 1.00 mmol, 1.00 equiv.). The product was obtained as an off-white solid (405 mg, 0.54 mmol, 54%). ^{1}H NMR (300 MHz, DMSO-d_6) (two signal sets observed, ratio 1:0.6): δ (major) 8.35 (s, 1 H, Ar-H), 7.92–7.85 (m, 1 H, Ar-H), 7.47–7.33 (m, 7 H, Ar-H), 7.31–7.21 (m, 4 H, Ar-H, NC*H*Ph$_2$), 7.10 (t, $^3J_{H-H}$ = 8 Hz, 1 H, Ar-H), 6.48 (d, $^3J_{H-H}$ = 8 Hz, 1 H, Ar-H), 5.55–5.38 (m, 1 H, NCH$_2$), 4.86 (dd, $^3J_{H-H}$ = 8 Hz, $^4J_{H-H}$ = 15 Hz, 1 H, NCH$_2$), 3.31–2.59 (m, 2 H, SCH$_2$/SCH/CH$_2$), 2.45–2.10 (m, 2 H, SCH$_2$/SCH/CH$_2$), 1.53–1.31 (m, 1 H, SCH$_2$/SCH/CH$_2$), 1.00 (d, $^3J_{H-H}$ = 7 Hz, 3 H, CH$_3$), 0.59 ($^3J_{H-H}$ = 6 Hz, 3 H, CH$_3$); (minor) 8.42 (s, 1 H, Ar-H), 7.92–7.85 (m, 1 H, Ar-H), 7.47–7.33 (m, 7 H, Ar-H), 7.31–7.21 (m, 4 H, Ar-H, NC*H*Ph$_2$), 7.10 (t, $^3J_{H-H}$ = 8 Hz, 1 H, Ar-H), 6.57 (d, J_{H-H} = 8 Hz, 1 H, Ar-H), 5.02–4.90 (m, 1 H, NCH$_2$), 4.72–4.55 (m, 1 H, NCH$_2$), 3.31–2.59 (m, 2 H, SCH$_2$/SCH/CH$_2$), 2.45–2.10 (m, 2 H, SCH$_2$/SCH/CH$_2$), 1.53–1.31 (m, 1 H, SCH$_2$/SCH/CH$_2$), 1.23 (d, $^3J_{H-H}$ = 7 Hz, 3 H, CH$_3$), 1.22 (d, $^3J_{H-H}$ = 7 Hz, 3 H, CH$_3$). Due to the low solubility of this compound, no ^{13}C NMR spectrum could be obtained. Anal. Calcd. for $C_{26}H_{28}Br_2N_2PtS$: C, 41.34; H, 3.74; N, 3.71. Found: C, 41.71; H, 3.54; N, 3.74. MS (ESI) *m*/*z* 675 [M - Br]$^+$.

cis-Dibromido(1-benzyl-3-(2-(isopropylthio)ethyl)-benzimidazolin-2-ylidene-κ^2*C*,*S*)-palladium (II) (221).

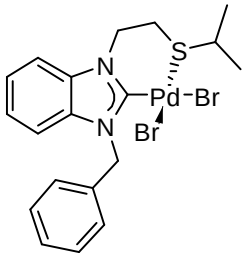

Benzimidazolium salt **205** (117 mg, 0.30 mmol, 1.00 equiv.) and silver(I) oxide (35 mg, 0.15 mmol, 0.50 equiv.) were suspended in dichloromethane (15 mL) and stirred at ambient temperature for 15 h shielded from light. Palladium(II) bromide (80 mg, 0.30 mmol, 1.00 equiv.) was dissolved in acetonitrile (10 mL) by stirring for 30 min at 50 °C. After cooling to ambient temperature, the silver carbene complex solution was added by filtration over a short plug of Celite, and stirring was continued for 1 h at ambient temperature. Then the solution was filtered over Celite and the solvent was removed under reduced pressure. The residue was washed

with diethyl ether (10 mL). The product was obtained as a yellow solid (111 mg, 0.19 mmol, 64%). ^{1}H NMR (300 MHz, DMSO-d_6, 358 K): δ 7.87 (d, $^{3}J_{H\text{-}H}$ = 8 Hz, 1 H, Ar-H), 7.56 (d, $^{3}J_{H\text{-}H}$ = 8 Hz, 1 H, Ar-H), 7.49–7.25 (m, 9 H, Ar-H, NCH_2Ph), 6.19–6.05 (m, 2 H, NCH_2), 4.98–4.72 (m, 2 H, SCH_2), 2.85–2.73 (m, 1 H, SCH), 1.09–1.02 (m, 6 H, CH_3). $^{13}C\{^{1}H\}$ NMR (75 MHz, DMSO-d_6): δ 136.4, 134.4, 133.3, 129.1, 128.4, 127.9, 124.6, 124.4, 112.3 (Ar-C), 51.6 (NCH_2Ph), 47.2 (NCH_2), 44.3 (SCH), 30.8 (SCH_2), 22.6 (CH_3), $C_{carbene}$ not observed. ^{1}H NMR (300 MHz, $CDCl_3$, as pyridine adduct): δ 9.06–8.99 (m, 2 H, Ar-H), 7.81–7.77 (m, 1 H, Ar-H), 7.60–7.52 (m, 2 H, Ar-H), 7.47–7.42 (m, 1 H, Ar-H), 7.38–7.30 (m, 5 H, Ar-H), 7.25–7.21 (m, 1 H, Ar-H), 7.14–7.01 (m, 2 H, Ar-H), 6.16 (s, 2 H, NCH_2Ph), 5.11–5.01 (m, 2 H, NCH_2), 3.47–3.34 (m, 2 H, SCH_2), 3.22 (sept, $^{3}J_{H\text{-}H}$ = 7 Hz, 1 H, CH), 1.41 (d, $^{3}J_{H\text{-}H}$ = 7 Hz, 6 H, CH_3). $^{13}C\{^{1}H\}$ NMR (75 MHz, $CDCl_3$, as pyridine adduct): δ 164.2 ($C_{carbene}$), 153.2, 138.7, 135.4, 135.4, 134.9, 129.5, 128.9, 128.8, 125.3, 123.9, 123.9, 112.3, 110.9 (Ar-C), 54.3 (NCH_2Ph), 49.6 (NCH_2), 36.1 (SCH), 29.6 (SCH_2), 24.5 (CH_3). Anal. Calcd. for $C_{19}H_{22}Br_2N_2PdS$: C, 39.57; H, 3.85; N, 4.86. Found: C, 39.45; H, 3.89; N, 4.85. MS (ESI) *m*/*z* 497 $[M - Br]^+$.

cis-Dibromido(1-isobutyl-3-(2-(isopropylthio)ethyl)-benzimidazolin-2-ylidene-κ^2*C*,*S*)-palladium(II) (222).

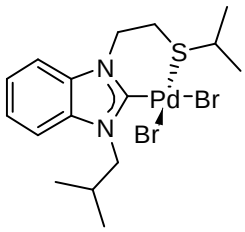

Complex **222** was prepared in analogy to complex **221** from benzimidazolium salt **206** (107 mg, 0.30 mmol, 1.00 equiv.), silver(I) oxide (35 mg, 0.15 mmol, 0.50 equiv.) and palladium(II) bromide (80 mg, 0.30 mmol, 1.00 equiv.). The product was obtained as a yellow solid (139 mg, 0.26 mmol, 85%). ^{1}H NMR (300 MHz, $CDCl_3$, as pyridine adduct): δ 9.08–8.97 (m, 2 H, Ar-H), 7.85–7.74 (m, 1 H, Ar-H), 7.49–7.34 (m, 4 H, Ar-H), 7.33–7.26 (m, 2 H, Ar-H), 5.10–4.97 (m, 2 H, NCH_2), 4.55 (d, $^{3}J_{H\text{-}H}$ = 8 Hz, 2 H, NCH_2), 3.42–3.30 (m, 2 H, SCH_2), 3.26–3.06 (m, 2 H, SCH, CH), 1.39 (d, $^{3}J_{H\text{-}H}$ = 7 Hz, 6 H, CH_3), 1.11 (d, $^{3}J_{H\text{-}H}$ = 7 Hz, 6 H, CH_3). $^{13}C\{^{1}H\}$ NMR (75 MHz, $CDCl_3$, as pyridine adduct): δ 163.3 ($C_{carbene}$), 153.2, 138.7, 136.1, 134.8, 125.3, 123.8, 111.5, 110.9 (Ar-C), 56.7 (NCH_2), 49.7 (NCH_2), 36.1 (SCH), 29.8 (SCH_2), 29.6 (CH), 24.5 (CH_3), 21.5 (CH_3). Anal. Calcd. for $C_{16}H_{24}Br_2N_2PdS$: C, 35.41; H, 4.46; N, 5.16. Found: C, 35.36; H, 4.72; N, 5.08. MS (ESI) *m*/*z* 1005 $[2 M - Br]^+$.

***cis*-Dibromido(1-benzhydryl-3-(2-(isopropylthio)ethyl)-benzimidazolin-2-ylidene-κ^2*C*,*S*)-palladium(II) (223).**

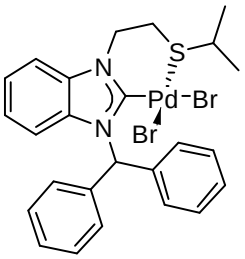

Complex **223** was prepared in analogy to complex **221** from benzimidazolium salt **207** (140 mg, 0.30 mmol, 1.00 equiv.), silver(I) oxide (35 mg, 0.15 mmol, 0.50 equiv.) and palladium(II) bromide (80 mg, 0.30 mmol, 1.00 equiv.). The product was obtained as a yellow solid (197 mg, 0.30 mmol, >99%). ^{1}H NMR (300 MHz, $CDCl_3$, as pyridine adduct): δ 8.98 (d, $J_{H\text{-}H}$ = 5 Hz, 2 H, Ar-H), 8.53 (s, 1 H, Ar-H), 7.74 (t, $J_{H\text{-}H}$ = 8 Hz, 2 H, Ar-H), 7.47–7.39 (m, 4 H, Ar-H), 7.36–7.27 (m, 7 H, Ar-H, $NCHPh_2$), 7.20 (t, $J_{H\text{-}H}$ = 7 Hz, 1 H, Ar-H), 6.96 (t, $J_{H\text{-}H}$ = 8 Hz, 1 H, Ar-H), 6.74 (d, $J_{H\text{-}H}$ = 8 Hz, 1 H, Ar-H), 5.13–5.00 (m, 2 H, NCH_2), 3.47–3.33 (m, 2 H, SCH_2), 3.21 (sept, $^3J_{H\text{-}H}$ = 7 Hz, 1 H, SCH), 1.39 (d, $^3J_{H\text{-}H}$ = 7 Hz, 6 H, CH_3). $^{13}C\{^1H\}$ NMR (75 MHz, $CDCl_3$, as pyridine adduct): δ 165.6 ($C_{carbene}$), 153.1, 138.6, 137.0, 135.5, 129.7, 129.1, 128.8, 125.6, 125.2, 123.6, 123.6, 114.3, 110.9 (Ar-C), 69.0 ($NCHPh_2$), 49.7 (NCH_2), 36.0 (SCH), 29.3 (SCH_2), 24.5 (CH_3). Anal. Calcd. for $C_{25}H_{26}Br_2N_2PdS$: C, 46.00; H, 4.01; N, 4.29. Found: C, 45.89; H, 3.93; N, 4.60. MS (ESI) m/z 572 $[M - Br]^+$.

***cis*-Dibromido(1-benzyl-3-(3-(isopropylthio)propyl)-benzimidazolin-2-ylidene-κ^2*C*,*S*)-palladium(II) (224).**

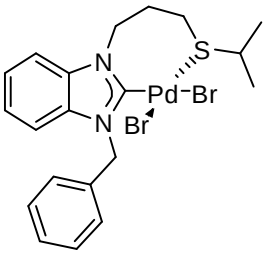

Complex **224** was prepared in analogy to complex **221** from benzimidazolium salt **208** (122 mg, 0.30 mmol, 1.00 equiv.), silver(I) oxide (35 mg, 0.15 mmol, 0.50 equiv.) and palladium(II) bromide (80 mg, 0.30 mmol, 1.00 equiv). The product was obtained as a yellow solid (173 mg, 0.29 mmol, 98%). NMR spectra could not be obtained due to the low solubility of the compound in all common deuterated solvents and the fluxionality of its structure. Anal. Calcd. for $C_{20}H_{24}Br_2N_2PdS$: C, 40.67; H, 4.10; N, 4.74. Found: C, 40.21; H, 4.28; N, 4.57. MS (ESI) *m*/*z* 511 $[M - Br]^+$.

***cis*-Dibromido(1-isobutyl-3-(3-(isopropylthio)propyl)-benzimidazolin-2-ylidene-κ^2*C,S*)-palladium(II) (225).**

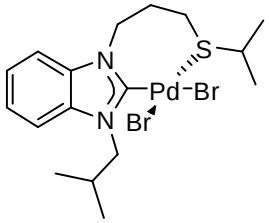

Complex **225** was prepared in analogy to complex **221** from benzimidazolium salt **209** (111 mg, 0.30 mmol, 1.00 equiv.), silver(I) oxide (35 mg, 0.15 mmol, 0.50 equiv.) and palladium(II) bromide (80 mg, 0.30 mmol, 1.00 equiv.). The product was obtained as a yellow solid (167 mg, 0.30 mmol, >99%). NMR spectra could not be obtained due to the low solubility of the compound in all common deuterated solvents and the fluxionality of its structure. Anal. Calcd. for $C_{17}H_{26}Br_2N_2PdS$: C, 36.68; H, 4.71; N, 5.03. Found: C, 36.27; H, 4.55; N, 5.40. MS (ESI) *m*/*z* 1032 [M - Br]+.

***cis*-Dibromido(1-benzhydryl-3-(2-(isopropylthio)propyl)-benzimidazolin-2-ylidene-κ^2*C,S*)-palladium(II) (226).**

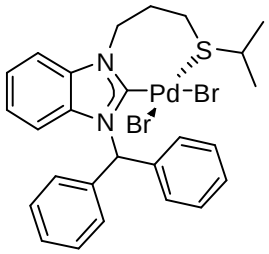

Complex **226** was prepared in analogy to complex **221** from benzimidazolium salt **210** (144 mg, 0.30 mmol, 1.0 equiv.), silver(I) oxide (35 mg, 0.15 mmol, 0.50 equiv.) and palladium(II) bromide (80 mg, 0.30 mmol, 1.00 equiv.). The product was obtained as a yellow solid (200 mg, 0.30 mmol, >99%). NMR spectra could not be obtained due to the low solubility of the compound in all common deuterated solvents and the fluxionality of its structure. Anal. Calcd. for $C_{26}H_{28}Br_2N_2PdS$: C, 46.83; H, 4.23; N, 4.20. Found: C, 46.68; H, 4.30; N, 4.15. MS (ESI) *m*/*z* 585 $[M - Br]^+$.

***trans*-Dibromido(1-benzyl-3-(2-(isopropylthio)ethyl)-benzimidazolin-2-ylidene)(1,3-diisopropyl-benzimidazolin-2-ylidene)-palladium(II) (227).**

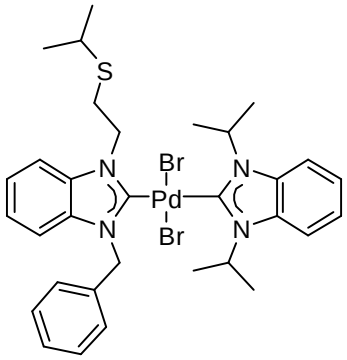

Benzimidazolium salt **205** (391 mg, 1.00 mmol, 1.00 equiv.) and silver(I) oxide (116 mg, 0.50 mmol, 0.50 equiv.) were suspended in dichloromethane (15 mL) and stirred at ambient temperature for 15 h shielded from light. $[PdBr_2(^iPr_2\text{-bimy})]_2$ (**30**) (469 mg, 0.50 mmol, 0.50 equiv.) was suspended in dichloromethane (20 mL), and the filtered silver(I) carbene complex solution was added to this suspension. The resulting mixture was stirred for 1 h at ambient temperature. Then it was filtered and concentrated under reduced pressure. The residue was purified by column chromatography (silica, dichloromethane + 5% EtOH). The product was obtained as a yellow solid (644 mg, 0.83 mmol, 83%). ^{1}H NMR (300 MHz, $CDCl_3$): δ 7.68–7.50 (m, 4 H, Ar-H), 7.47–7.28 (m, 5 H, Ar-H), 7.24–7.13 (m, 4 H, Ar-H), 6.23 (sept, $^3J_{H-H}$ = 7 Hz, 1 H, NCH), 6.12 (s, 2 H, NCH_2Ph), 5.99 (sept, $^3J_{H-H}$ = 7 Hz, 1 H, NCH), 5.13–5.02 (m, 2 H, NCH_2), 3.50–3.38 (m, 2 H, SCH_2), 3.13 (sept, $^3J_{H-H}$ = 7 Hz, 1 H, SCH), 1.86 (d, $^3J_{H-H}$ = 7 Hz, 6 H, CH_3), 1.65 (d, $^3J_{H-H}$ = 7 Hz, 6 H, CH_3) 1.37 (d, $^3J_{H-H}$ = 7 Hz, 6 H, CH_3). $^{13}C\{^1H\}$ NMR (125 MHz, $CDCl_3$): δ 184.5 ($C_{carbene}$), 178.6 ($C_{carbene}$), 136.2, 135.3, 135.2, 134.3, 134.2, 129.5, 128.6, 128.5, 123.8, 123.7, 122.7, 113.4, 113.3, 112.0, 110.9 (Ar-C), 55.4 (NCH), 54.8 (NCH), 54.4 (NCH_2Ph), 49.1 (NCH_2), 36.2 (SCH), 30.5 (SCH_2), 24.4 (CH_3), 21.8 (CH_3) 21.6 (CH_3). Anal. Calcd. for $C_{32}H_{40}Br_2N_4PdS\cdot CH_2Cl_2$: C, 45.88; H, 4.90; N, 6.49. Found: C, 46.30; H, 4.58; N, 6.73. MS (ESI) *m*/*z* 699 $[M - Br]^+$.

***trans*-Dibromido(1-isobutyl-3-(2-(isopropylthio)ethyl)-benzimidazolin-2-ylidene)(1,3-diisopropyl-benzimidazolin-2-ylidene)-palladium(II) (228).**

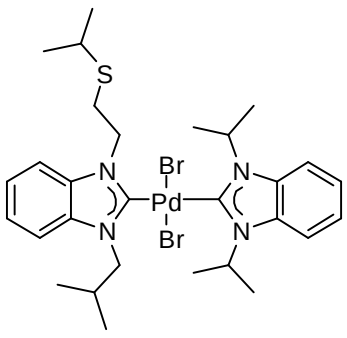

Complex **228** was prepared in analogy to complex **227** from benzimidazolium salt **206** (391 mg, 1.00 mmol, 1.00 equiv.), silver(I) oxide (116 mg, 0.50 mmol, 0.50 equiv.) and $[PdBr_2(^iPr_2\text{-bimy})]_2$ (**30**) (469 mg, 0.50 mmol, 0.50 equiv.). The product was obtained as a yellow solid (635 mg, 0.85 mmol, 85%). ^{1}H NMR (500 MHz, $CDCl_3$): δ 7.62–7.56 (m, 2 H, Ar-H), 7.45–7.39 (m, 2 H, Ar-H), 7.31–7.27 (m, 2 H, Ar-H), 7.23–7.19 (m, 2 H, Ar-H), 6.28

(sept, $^3J_{H\text{-}H}$ = 7 Hz, 1 H, NCH), 6.24 (sept, $^3J_{H\text{-}H}$ = 7 Hz, 1 H, NCH), 5.06–5.01 (m, 2 H, NCH_2), 4.56 (d, $^3J_{H\text{-}H}$ = 8 Hz, 2 H, NCH_2), 3.43–3.38 (m, 2 H, SCH_2), 3.18–3.06 (m, 2 H, SCH, CH), 1.85 (d, $^3J_{H\text{-}H}$ = 7 Hz, 6 H, CH_3), 1.84 (d, $^3J_{H\text{-}H}$ = 7 Hz, 6 H, CH_3), 1.35 (d, $^3J_{H\text{-}H}$ = 7 Hz, 6 H, CH_3), 1.13 (d, $^3J_{H\text{-}H}$ = 7 Hz, 6 H, CH_3). $^{13}C\{^1H\}$ NMR (125 MHz, $CDCl_3$): δ 183.9 ($C_{carbene}$), 179.3 ($C_{carbene}$), 136.1, 134.7, 134.3, 134.2, 123.5, 123.5, 122.7, 113.4, 113.3, 111.5, 110.8 (Ar-C), 56.2 (NCH), 54.9 (NCH), 54.6 (NCH_2), 49.0 (NCH_2), 36.2 (SCH), 30.5 (SCH_2), 30.4 (CH), 24.4 (CH_3), 21.7 (CH_3), 21.8 (CH_3) 21.4 (CH_3). Anal. Calcd. for $C_{29}H_{42}Br_2N_4PdS$: C, 46.76; H, 5.68; N, 7.52. Found: C, 46.83; H, 5.59; N, 7.48. MS (ESI) *m*/*z* 665 $[M - Br]^+$.

***trans*-Dibromido(1-benzhydryl-3-(2-(isopropylthio)ethyl)-benzimidazolin-2-ylidene)(1,3-diisopropyl-benzimidazolin-2-ylidene)-palladium(II) (229).**

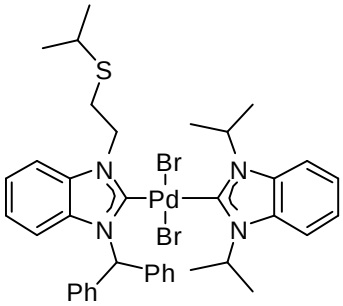

Complex **229** was prepared in analogy to complex **227** from benzimidazolium salt **207** (207 mg, 0.44 mmol, 1.00 equiv.), silver(I) oxide (51 mg, 0.22 mmol, 0.50 equiv.) and $[PdBr_2(^iPr_2\text{-bimy})]_2$ (**30**) (206 mg, 0.22 mmol, 0.50 equiv.). The product was obtained as a yellow solid (229 mg, 0.27 mmol, 61%). ^1H NMR (500 MHz, $CDCl_3$): δ 8.61 (s, 1 H, Ar-H), 7.60–7.57 (m, 1 H, Ar-H), 7.55–7.52 (m, 1 H, Ar-H), 7.44–7.34 (m, 11 H, Ar-H, $NCHPh_2$), 7.22–7.18 (m, 3 H, Ar-H), 6.95 (t, $^3J_{H\text{-}H}$ = 8 Hz, 1 H, Ar-H), 6.67 (d, $^3J_{H\text{-}H}$ = 8 Hz, 1 H, Ar-H), 6.24 (sept, $^3J_{H\text{-}H}$ = 7 Hz, 1 H, NCH), 6.02 (sept, $^3J_{H\text{-}H}$ = 7 Hz, 1 H, NCH), 5.13–5.06 (m, 2 H, NCH_2), 3.52–3.46 (m, 2 H, SCH_2), 3.12 (sept, $^3J_{H\text{-}H}$ = 7 Hz, 1 H, SCH), 1.85 (d, $^3J_{H\text{-}H}$ = 7 Hz, 3 H, CH_3), 1.67 (d, $^3J_{H\text{-}H}$ = 7 Hz, 3 H, CH_3), 1.37 (d, $^3J_{H\text{-}H}$ = 7 Hz, 3 H, CH_3). $^{13}C\{^1H\}$ NMR (125 MHz, $CDCl_3$): δ 186.3 ($C_{carbene}$), 179.2 ($C_{carbene}$), 138.9, 135.6, 134.8, 134.3, 134.2, 129.6, 129.2, 128.7, 123.4, 122.6, 114.3, 113.4, 113.3, 110.9 (Ar-C), 68.3 (NCH_2Ph), 54.8 (NCH), 54.5 (NCH), 49.1 (NCH_2), 36.3 (SCH), 30.4 (SCH_2), 24.4 (CH_3), 21.7 (CH_3), 21.5 (CH_3). Anal. Calcd. for $C_{38}H_{44}Br_2N_4PdS \cdot 0.5CH_2Cl_2$: C, 51.52; H, 5.05; N, 6.24. Found: C, 51.75; H, 5.20; N, 6.35. MS (ESI) *m*/*z* 775 $[M - Br]^+$.

***trans*-Dibromido(1-benzyl-3-(2-(isopropylthio)propyl)-benzimidazolin-2-ylidene)(1,3-diisopropyl-benzimidazolin-2-ylidene)-palladium(II) (230).**

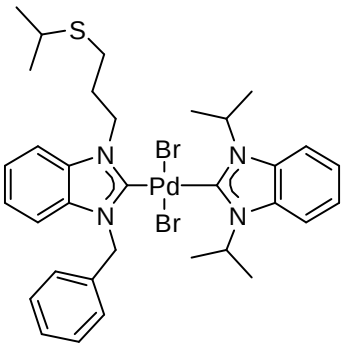

Complex **230** was prepared in analogy to complex **227** from benzimidazolim salt **208** (405 mg, 1.00 mmol, 1.00 equiv.), silver(I) oxide (116 mg, 0.50 mmol, 0.50 equiv.) and $[PdBr_2(^iPr_2\text{-bimy})]_2$ (**30**) (469 mg, 0.50 mmol, 0.50 equiv.). The product was obtained as a yellow solid (485 mg, 0.61 mmol, 61%). ^{1}H NMR (500 MHz, $CDCl_3$): δ 7.73–7.69 (m, 2 H, Ar-H), 7.66–7.63 (m, 1 H, Ar-H), 7.60–7.56 (m, 2 H, Ar-H), 7.47–7.43 (m, 2 H, Ar-H), 7.40–7.36 (m, 1 H, Ar-H),7.34–7.30 (m, 2 H, Ar-H), 7.28–7.26 (m, 1 H, Ar-H), 7.25–7.20 (m, 2 H, Ar-H), 6.29 (sept, $^3J_{H\text{-}H}$ = 7 Hz, 1 H, NCH), 6.22 (s, 2 H, NCH_2Ph), 6.08 (sept, $^3J_{H\text{-}H}$ = 7 Hz, 1 H, NCH), 5.10–5.05 (m, 2 H, NCH_2), 3.07 (sept, $^3J_{H\text{-}H}$ = 7 Hz, 1 H, SCH), 2.87 (t, $^3J_{H\text{-}H}$ = 7 Hz, 2 H, SCH_2), 2.71–2.63 (m, 2 H, CH_2), 1.93 (d, $^3J_{H\text{-}H}$ = 7 Hz, 6 H, CH_3), 1.69 (d, $^3J_{H\text{-}H}$ = 7 Hz, 6 H, CH_3), 1.39 (d, $^3J_{H\text{-}H}$ = 7 Hz, 6 H, CH_3). $^{13}C\{^1H\}$ NMR (125 MHz, $CDCl_3$): δ 184.1 ($C_{carbene}$), 178.8 ($C_{carbene}$), 136.4, 135.5, 135.2, 134.3, 134.2, 129.4, 128.5, 128.4, 123.6, 123.6, 122.7, 113.3, 111.8, 111.1 (Ar-C), 54.5 (NCH), 54.5 (NCH), 53.2 (NCH_2Ph), 48.0 (NCH_2), 36.0 (SCH), 30.5 (SCH_2), 28.9 (CH_2), 24.1 (CH_3), 21.8 (CH_3), 21.5 (CH_3). Anal. Calcd. for $C_{33}H_{42}Br_2N_4PdS$: C, 49.98; H, 5.34; N, 7.07. Found: C, 50.04; H, 5.39; N, 7.07. MS (ESI) *m*/*z* 713 $[M - Br]^+$.

***trans*-Dibromido(1-isobutyl-3-(2-(isopropylthio)propyl)-benzimidazolin-2-ylidene)(1,3-diisopropyl-benzimidazolin-2-ylidene)-palladium(II) (231).**

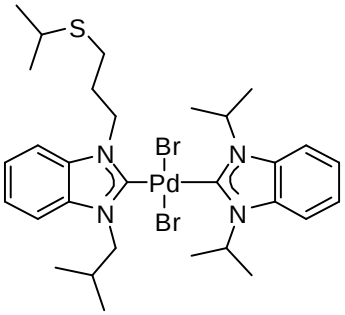

Complex **231** was prepared in analogy to complex **227** from benzimidazolium salt **209** (371 mg, 1.00 mmol, 1.00 equiv.), silver(I) oxide (116 mg, 0.50 mmol, 0.50 equiv.) and $[PdBr_2(^iPr_2\text{-bimy})]_2$ (**30**) (469 mg, 0.50 mmol, 0.50 equiv.). The product was obtained as a yellow solid (541 mg, 0.71 mmol, 71%). ^{1}H NMR (500 MHz, $CDCl_3$): δ 7.63–7.60 (m, 2 H, Ar-H), 7.54–7.51 (m, 1 H, Ar-H), 7.45–7.41 (m, 1 H, Ar-H), 7.31–7.28 (m, 2 H, Ar-H), 7.26–7.23 (m, 2 H, Ar-H), 6.35 (sept, $^3J_{H\text{-}H}$ = 7 Hz, 1 H, NCH), 6.27 (sept, $^3J_{H\text{-}H}$ = 7 Hz, 1 H, NCH), 4.99 (t, $^3J_{H\text{-}H}$ = 7 Hz, 2 H, NCH_2), 4.60 (d, $^3J_{H\text{-}H}$ = 7 Hz, 2 H, NCH_2), 3.16 (sept, $^3J_{H\text{-}H}$ = 7 Hz, 1 H, SCH), 3.01 (sept, $^3J_{H\text{-}H}$ = 7 Hz, 1 H, CH), 2.80 (t, $^3J_{H\text{-}H}$ = 7 Hz, 2 H, SCH_2), 2.62 (quint, $^3J_{H\text{-}H}$ = 7 Hz, 2 H, CH_2), 1.88 (d,

$^{3}J_{H\text{-}H}$ = 7 Hz, 6 H, CH_3), 1.86 (d, $^{3}J_{H\text{-}H}$ = 7 Hz, 6 H, CH_3), 1.34 (d, $^{3}J_{H\text{-}H}$ = 7 Hz, 6 H, CH_3), 1.16 (d, $^{3}J_{H\text{-}H}$ = 7 Hz, 6 H, CH_3). $^{13}C\{^{1}H\}$ NMR (125 MHz, $CDCl_3$): δ 183.5 ($C_{carbene}$), 179.6 ($C_{carbene}$), 136.1, 135.1, 134.3, 134.2, 123.4, 123.4, 122.7, 113.4, 113.3, 111.4, 111.1 (Ar-C), 56.2 (NCH_2), 54.6 (NCH), 48.0 (NCH_2), 36.1 (SCH), 30.5 (SCH_2), 30.5 (CH), 28.9 (CH_2), 24.2 (CH_3), 21.8 (CH_3), 21.6 (CH_3) 21.5 (CH_3). Anal. Calcd. for $C_{30}H_{44}Br_2N_4PdS$: C, 47.47; H, 5.84; N, 7.38. Found: C, 47.97; H, 6.15; N, 7.63. MS (ESI) *m*/*z* 679 $[M - Br]^+$.

***trans*-Dibromido(1-benzhydryl-3-(2-(isopropylthio)propyl)-benzimidazolin-2-ylidene)(1,3-diisopropyl-benzimidazolin-2-ylidene)-palladium(II) (232).**

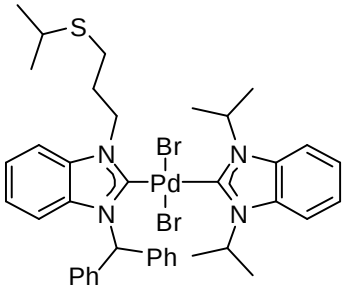

Complex **232** was prepared in analogy to complex **227** from benzimidazolium salt **210** (482 mg, 1.00 mmol, 1.00 equiv.), silver(I) oxide (116 mg, 0.50 mmol, 0.50 equiv.) and $[PdBr_2(^{i}Pr_2\text{-bimy})]_2$ (**30**) (469 mg, 0.50 mmol, 0.50 equiv.). The product was obtained as a yellow solid (649 mg, 0.76 mmol, 76%). ^{1}H NMR (500 MHz, $CDCl_3$): δ 8.66 (s, 1 H, Ar-H), 7.58–7.55 (m, 1 H, Ar-H), 7.54–7.48 (m, 2 H, Ar-H), 7.43–7.33 (m, 10 H, Ar-H, $NCHPh_2$), 7.21–7.16 (m, 3 H, Ar-H), 6.93 (t, $J_{H\text{-}H}$ = 8 Hz, 1 H, Ar-H), 6.66 (d, $J_{H\text{-}H}$ = 8 Hz, 1 H, Ar-H), 6.23 (sept, $^{3}J_{H\text{-}H}$ = 7 Hz, 1 H, NCH), 6.01 (sept, $^{3}J_{H\text{-}H}$ = 7 Hz, 1 H, NCH), 5.04–4.99 (m, 2 H, NCH_2), 3.02 (sept, $^{3}J_{H\text{-}H}$ = 7 Hz, 1 H, SCH), 2.82 (t, $^{3}J_{H\text{-}H}$ = 7 Hz, 2 H, SCH_2), 2.68–2.60 (m, 2 H, CH_2), 1.84 (d, $^{3}J_{H\text{-}H}$ = 7 Hz, 6 H, CH_3), 1.64 (d, $^{3}J_{H\text{-}H}$ = 7 Hz, 6 H, CH_3), 1.33 (d, $^{3}J_{H\text{-}H}$ = 7 Hz, 6 H, CH_3). $^{13}C\{^{1}H\}$ NMR (125 MHz, $CDCl_3$): δ 185.9 ($C_{carbene}$), 179.3 ($C_{carbene}$), 138.9, 135.8, 134.9, 134.2, 134.1, 129.6 129.1, 128.6, 123.3, 122.6, 114.2, 113.3, 113.3, 111.1 (Ar-C), 68.1 ($NCHPh_2$), 54.6 (NCH), 54.5 (NCH), 48.1 (NCH_2), 36.0 (SCH), 30.4 (SCH_2), 28.9 (CH_2), 24.2 (CH_3), 21.8 (CH_3), 21.5 (CH_3). Anal. Calcd. for $C_{39}H_{46}Br_2N_4PdS$: C, 53.90; H, 5.33; N, 6.45. Found: C, 53.64; H, 5.25; N, 6.23. MS (ESI) *m*/*z* 789 $[M - Br]^+$.

***trans*-Dibromido-bis(1-benzyl-3-(2-(isopropylthio)ethyl)-benzimidazolin-2-ylidene)nickel(II) (233).**

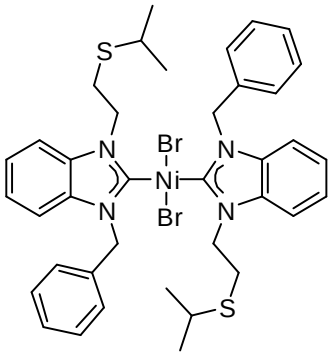

Benzimidazolium salt **205** (783 mg, 2.00 mmol, 2.0 equiv.), nickel(II) acetate (177 mg, 1.00 mmol, 1.0 equiv.) and TBAB (2.00 g) were dried under vaccum at 80 °C for 2 h. Then the temperature was brought slowly to 130 °C and maintained constant for 12 h. After this time the reaction mixture was allowed to cool to ambient temperature. Trituration with water and subsequent filtration gave the product as a red solid (631 mg, 0.75 mmol, 75%, mixture of *trans-syn* and *trans-anti* rotamers). ^{1}H NMR (300 MHz, $CDCl_3$,): δ (*trans-anti*, major rotamer) 7.76–7.53 (m, 3 H, Ar-H), 7.53–7.28 (m, 9 H, Ar-H), 7.22–7.10 (m, 2 H, Ar-H), 7.08–6.87 (m, 4 H, Ar-H), 6.71 (s, 4 H, NCH_2Ph), 5.47–5.35 (m, 4 H, NCH_2), 3.52–3.41 (m, 4 H, SCH_2), 2.90 (sept, $^{3}J_{H\text{-}H}$ = 7 Hz, 2 H, SCH), 1.15 (d, $^{3}J_{H\text{-}H}$ = 7 Hz, 12 H, CH_3). δ (*trans-syn*, minor rotamer) 7.76–7.53 (m, 3 H, Ar-H), 7.53–7.28 (m, 9 H, Ar-H), 7.22–7.10 (m, 2 H, Ar-H), 7.08–6.87 (m, 4 H, Ar-H), 6.46 (s, 4 H, NCH_2Ph), 5.56–5.47 (m, 4 H, NCH_2), 3.73–3.60 (m, 4 H, SCH_2), 3.18 (sept, $^{3}J_{H\text{-}H}$ = 7 Hz, 2 H, SCH), 1.38 (d, $^{3}J_{H\text{-}H}$ = 7 Hz, 12 H, CH_3). $^{13}C\{^{1}H\}$ NMR (75 MHz, $CDCl_3$): δ (*trans-anti*, major rotamer) 185.5 ($C_{carbene}$), 136.1, 135.9, 135.5, 129.5, 128.8, 128.5, 123.2, 112.0, 110.4 (Ar-C), 54.2 (NCH_2Ph), 49.2 (NCH_2), 36.1 (SCH), 30.2 (SCH_2), 24.2 (CH_3). δ (*trans-syn*, minor rotamer) 185.5 ($C_{carbene}$), 136.1, 135.9, 135.2, 129.3, 128.8, 128.5, 123.2, 111.6, 110.7 (Ar-C), 53.5 (NCH_2Ph), 49.4 (NCH_2), 36.3 (SCH), 30.5 (SCH_2), 24.4 (CH_3). Anal. Calcd. for $C_{38}H_{44}Br_2N_4NiS_2$: C, 54.37; H, 5.28; N, 6.67. Found: C, 54.45; H, 4.79; N, 6.59. MS (ESI) *m*/*z* 759 $[M - Br]^+$.

***trans*-Dibromido-bis(1-isobutyl-3-(2-(isopropylthio)ethyl)-benzimidazolin-2-ylidene)nickel(II) (234).**

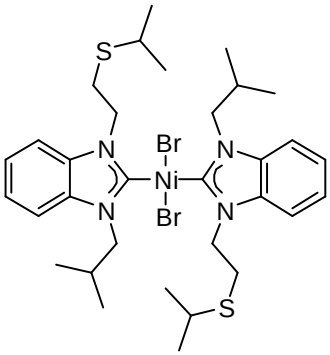

Benzimidazolium salt **206** (357 mg, 1.00 mmol, 2.0 equiv.), nickel(II) acetate (88 mg, 0.50 mmol, 1.0 equiv.) and TBAB (1.00 g) were dried under vaccum at 80 °C for 2 h. Then the temperature was brought slowly to 130 °C and maintained constant for 12 h. After this time the reaction mixture was allowed to cool to ambient temperature. Trituration with water and subsequent filtration gave the product as a red solid (195 mg, 0.25 mmol, 51%, mixture of *trans-syn* and *trans-anti* rotamers). ^{1}H NMR (500 MHz, $CDCl_3$): δ (both rotamers) 7.49–7.30 (m, 4 H, Ar-H), 7.28–7.15 (m, 4 H, Ar-H), 5.71–5.22 (m, 4 H, NCH2), 5.05–4.88 (m, 4 H, NCH_2), 3.71–3.57 (m, 2 H, SCH_2), 3.57–3.45 (m, 2 H, SCH_2), 3.41–3.21 (m, 2 H, SCH), 3.18–3.02 (m, 2 H, CH), 1.33 (d, $^{3}J_{H\text{-}H}$ = 6 Hz, 12 H, CH_3), 1.26 (d, $^{3}J_{H\text{-}H}$ = 6 Hz, 6 H, CH_3), 1.22 (d, $^{3}J_{H\text{-}H}$ = 6 Hz, 6 H, CH_3). $^{13}C\{^{1}H\}$ NMR (125 MHz, $CDCl_3$): δ (both rotamers) 184.5, 184.3 ($C_{carbene}$), 136.5, 136.2, 135.6, 135.2, 122.9, 111.3, 111.2, 110.9, 110.5 (Ar-C), 56.3, 56.3, 49.4, 49.1 (NCH_2), 36.5, 36.3 (SCH), 30.4, 30.1 (SCH_2), 29.9, 29.6 (CH), 24.4, 24.3, 21.8, 21.7 (CH_3). Anal. Calcd. for $C_{32}H_{48}Br_2N_4NiS_2$: C, 49.83; H, 6.27; N, 7.26. Found: C, 49.70; H, 6.23; N, 7.03. MS (ESI) *m*/*z* 691 $[M - Br]^+$.

***trans*-Dibromido-bis(1-benzyl-3-(3-(isopropylthio)propyl)-benzimidazolin-2-ylidene)nickel(II) (236).**

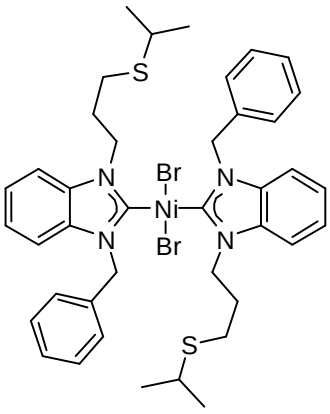

Benzimidazolium salt **208** (405 mg, 1.00 mmol, 2.0 equiv.), nickel(II) acetate (88 mg, 0.50 mmol, 1.0 equiv.) and TBAB (1.00 g) were dried under vaccum at 80 °C for 2 h. Then the temperature was brought slowly to 130 °C and maintained constant for 12 h. After this time the reaction mixture was allowed to cool to ambient temperature. Trituration with water and subsequent filtration gave the product as a red solid (249 mg, 0.29 mmol, 57%, mixture of *trans-syn* and *trans-anti* rotamers). ^{1}H NMR (500 MHz, $CDCl_3$): δ (*trans-anti*, major rotamer) 7.69 (d, $J_{H\text{-}H}$ = 7 Hz, 2 H, Ar-H), 7.48–7.28 (m, 10 H, Ar-H), 7.18–7.12 (m, 2 H, Ar-H), 7.05–6.94 (m, 4 H, Ar-H), 6.69 (s, 4 H, NCH_2Ph), 5.33–5.26 (m, 4 H,

NCH_2), 2.81 (sept, $^3J_{H\text{-}H}$ = 7 Hz, 2 H, SCH), 2.71–2.62 (m, 4 H, SCH_2), 2.59–2.54 (m, 4 H, CH_2), 1.21 (d, $^3J_{H\text{-}H}$ = 7 Hz, 12 H, CH_3). δ (*trans-syn*, minor rotamer) 7.69 (d, $J_{H\text{-}H}$ = 7 Hz, 2 H, Ar-H), 7.48–7.28 (m, 10 H, Ar-H), 7.18–7.12 (m, 2 H, Ar-H), 7.05–6.94 (m, 4 H, Ar-H), 6.46 (s, 4 H, NCH_2Ph), 5.39 (t, $^3J_{H\text{-}H}$ = 7 Hz, 4 H, NCH_2), 3.05 (sept, $^3J_{H\text{-}H}$ = 7 Hz, 2 H, SCH), 2.93–2.83 (m, 8 H, SCH_2, CH_2), 1.35 (d, $^3J_{H\text{-}H}$ = 6.6 Hz, 12 H, CH_3). $^{13}C\{^1H\}$ NMR (125 MHz, $CDCl_3$): δ (*trans-anti*, major rotamer) 185.3 ($C_{carbene}$), 136.3, 136.1, 135.4, 129.6, 128.6, 128.4, 123.1, 123.0, 111.7, 110.5 (Ar-C), 54.0 (NCH_2Ph), 47.9 (NCH_2), 35.9 (SCH), 30.1 (SCH_2), 28.6 (CH_2), 24.1 (CH_3). δ (*trans-syn*, minor rotamer) 185.2 ($C_{carbene}$), 136.2, 136.0, 135.6, 129.3, 128.7, 128.4, 123.1, 123.0, 111.4, 110.7 (Ar-C), 53.4 (NCH_2Ph), 47.8 (NCH_2), 36.0 (SCH), 30.4 (SCH_2), 29.0 (CH_2), 24.2 (CH_3). MS (ESI) *m*/*z* 787 $[M - Br]^+$. Despite all efforts, no matching elemental analysis could be obtained for this complex.

trans-Dibromido-bis(1-isobutyl-3-(3-(isopropylthio)propyl)-benzimidazolin-2-ylidene)nickel(II) (237).

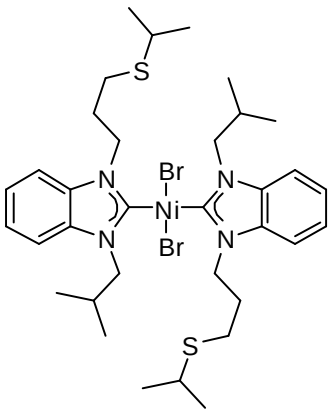

Benzimidazolium salt **209** (371 mg, 1.00 mmol, 2.0 equiv.), nickel(II) acetate (88 mg, 0.50 mmol, 1.0 equiv.) and TBAB (1.00 g) were dried under vaccum at 80 °C for 2 h. Then the temperature was brought slowly to 130 °C and maintained constant for 12 h. After this time the reaction mixture was allowed to cool to ambient temperature. Trituration with water and subsequent filtration gave the product as a red solid (351 mg, 0.40 mmoo, 81%, mixture of *trans-syn* and *trans-anti* rotamers). ^1H NMR (500 MHz, $CDCl_3$): δ (both rotamers) 7.54–7.45 (m, 2 H, Ar-H), 7.38–7.29 (m, 2 H, Ar-H), 7.24–7.15 (m, 4 H, Ar-H), 5.59–5.40 (m, 4 H, NCH_2), 4.97 (d, $^3J_{H\text{-}H}$ = 8 Hz, 4 H, NCH_2), 3.49–3.36 (m, 1 H, SCH), 3.30–3.19 (m, 1 H, SCH), 3.08–2.95 (m, 2 H, CH), 2.89–2.73 (m, 8 H, SCH_2, CH_2), 1.34–1.29 (m, 12 H, CH_3), 1.27–1.21 (m, 12 H, CH_3). $^{13}C\{^1H\}$ NMR (125 MHz, $CDCl_3$): δ (both rotamers) 184.0, 183.9 ($C_{carbene}$), 136.3, 136.1, 135.5, 135.4, 122.8, 111.0, 111.0, 110.7, 110.6 (Ar-C), 56.2, 56.1, 47.8, 47.7 (NCH_2), 35.8 (SCH), 30.2, 29.9, 29.5, 28.9, 28.7 (SCH_2, CH, CH_2), 24.1, 24.1 (CH_3), 21.7, 21.7 (CH_3). MS (ESI) *m*/*z* 719 $[M - Br]^+$. Despite all efforts, no matching elemental analysis could be obtained for this complex.

General procedure for the alkylation of pyrazoles with iodoethane.
The pyrazole was dissolved in iodoethane (2 mL per mmol) and the resulting mixture was heated to 90 °C for 3 d. Then, the solvent was removed under reduced pressure. The crude product was washed with diethyl ether and dried *in vacuo*.

General procedure for the alkylation of pyrazoles with trimethyloxonium tetrafluoroborate.
Trimethyl-oxonium tetrafluoroborate (1.2 equiv.) was suspended in anhydrous dichloromethane (6 mL per mmol) under nitrogen atmosphere. The pyrazole was added, and the mixture was heated to reflux for 15 h. The solvent was removed in vacuo, the residue taken up in THF, and the product was precipitated by addition of diethyl ether, isolated, and dried *in vacuo*.

General procedure for the preparation of *trans*-dibromido-(1,3-diisopropylbenzimidazolin-2-ylidene)(pyrazole)palladium(II) complexes.
The respective pyrazole (0.10 mmol, 2.0 equiv.) was added to a solution of dimer **30** (47 mg, 0.05 mmol, 1.0 equiv.) in dichloromethane (4 mL) and the resulting mixture was stirred at ambient temperature for 30 min. Then, the solvent was removed under reduced pressure and the remaining solid dried *in vacuo*.

General procedure for the alkylation of pyrazoles with bromoethane.
The pyrazole was dissolved in bromoethane (2 mL per mmol) and the resulting mixture was heated to 45 °C for 3 d. Then, the solvent was removed under reduced pressure. The crude product was washed with diethyl ether and dried *in vacuo*.

General procedure for the direct arylation of pentafluorobenzene.
A Schlenk tube was charged with precatalyst (3.0 µmol, 0.5 mol%), base (0.66 mmol, 1.1 equiv.) and aryl halide (0.60 mmol, 1.0 equiv.) if it was a solid. DMA (2 mL) was added and the vessel was evacuated and backfilled with dry nitrogen for three times. Pentafluorobenzene (74 µL, 0.66 mmol, 1.1 equiv.) and aryl halide (0.60 mmol, 1.0 equiv.), if it was a liquid, were added, and the mixture was immersed in a preheated oil bath for 24 h. After cooling to ambient temperature, dichloromethane (4 mL) was added, and the resulting suspension was filtered over a short plug of

Celite. The solution was concentrated under reduced pressure and the residue was purified by column chromatography (silica gel, hexane or hexane/diethyl ether).

General procedure for the catalytic hydroamination of phenylacetylene using Pd catalysts.
A Schlenk tube was charged with precatalyst (10 µmol, 1.0 mol%) under an atmosphere of dry nitrogen. Anhydrous toluene (3 mL) and triflic acid (2.0 µL, 20 µmol, 2.0 mol%) were added and the resulting suspension was stirred for 5 min at ambient temperature. Then phenylacetylene (219 µl, 2.00 mmol, 2.00 equiv.) and 2,6-dimethylaniline (123 µl, 1.00 mmol, 1.00 equiv.) were added, and the Schlenk tube was immersed in an oil bath preheated to 100 °C. The mixture was allowed to react for 15 h. After this time, the Schlenk tube was taken out of the oil bath, and the suspension was diluted with diethyl ether (10 mL), and decane as an internal standard was added. Samples were analyzed by GC-MS.

General procedure for Sonogashira cross-couplings.
Copper(I) iodide (10 mg, 50 µmol, 5.0 mol%), 4-bromoacetophenone (199 mg, 1.00 mmol, 1.00 equiv.) and precatalyst (10 µmol, 1.0 mol%) were placed in a Schlenk flask under an atmosphere of dry nitrogen. Degassed DMF (2 mL) was added, followed by phenylacteylene (219 µL, 2.00 mmol, 2.00 equiv.) and triethylamine (166 µL, 1.20 mmol, 1.20 equiv.). The Schlenk tube was immeres in an oil bath preheated to 80°C, and the mixture was allowed to react for 3 h. After this time, the mixture was allowed to cool to ambient temperature, and dichloromethane (25 mL) was added. The solution was extracted with water (3 × 25 mL), dried over Na_2SO_4, filtered, and concentrated under reduced pressure. The residue was analyzed by ^{1}H NMR spectroscopy.

General procedure for the direct arylation of 1-methylpyrrole.
A Schlenk tube was charged with precatalyst (10 µmol, 1.0 mol%), 4-bromoacetophenone (199 mg, 1.00 mmol, 1.00 equiv.) and potassium acetate (196 mg, 2.00 mmol, 2.00 equiv.) under an atmosphere of dry nitrogen. Degassed dimethyl acetamide (3 mL) was added, followed by 1-methylpyrrole (266 µL, 3.00 mmol, 3.00 equiv.). The tube was immersed in an oil bath preheated to 150 °C, and the mixture was allowed to react for 20 h. After this time, the Schlenk tube was taken out of the oil bath, the suspension was diluted with diethyl ether (10 mL) and decane as an internal standard was added. Samples were analyzed by GC-MS.

General procedure for Hartwig-Buchwald cross-couplings.

A Schlenk tube was charged with precatalyst (10 µmol, 1.0 mol%) under an atmosphere of dry nitrogen. Anhydrous THF (3 mL), bromobenzene (105 µL, 1.00 mmol, 1.00 equiv.) or chlorobenzene (102 µL, 1.00 mmol, 1.00 equiv.), pyrrolidine (124 µL, 1.50 mmol, 1.50 equiv.) and potassium *tert*-butoxide (168 mg, 1.50 mmol, 1.50 equiv.) were added, and the mixture was immersed into an oil bath preheated to 50 °C for 2 h. After this time, the tube was taken out of the oil bath, the reaction mixture was diluted with diethyl ether (10 mL), and decane as an internal standard was added. Samples were analyzed by GC-MS.

General procedure for the α-arylation of propiophenone.

A Schlenk tube was charged with precatalyst (5 µmol, 1.0 mol%) and sodium *tert*-butoxide (53 mg, 0.55 mmol, 1.10 equiv.) under an atmosphere of dry nitrogen. Anhydrous THF (2 mL), propiophenone (66 µL, 0.50 mmol, 1.00 equiv.) and bromobenzene (53 µL, 0.50 mmol, 1.00 equiv.) or chlorobenzene (51 µL, 0.50 mmol, 1.00 equiv.) were added, and the Schlenk tube was immersed into an oil bath preheated to 70 °C for 6 h. After this time, the tube was taken out of the oil bath, the reaction mixture was diluted with diethyl ether (10 mL). Samples were analyzed by GC-MS.

General procedure for the catalytic hydroamination of phenylacetylene using Pt catalysts.

A Schlenk tube was charged with precatalyst (10 µmol, 1.0 mol%) under an atmosphere of dry nitrogen. Anhydrous toluene (3 mL) and – in some cases – silver triflate (5.1 mg, 20 µmol, 2.0 mol%) were added and the resulting suspension was stirred for 5 min at ambient temperature. Then phenylacetylene (219 µL, 2.00 mmol, 2.00 equiv.) and 2,6-dimethylaniline (123 µL, 1.00 mmol, 1.00 equiv.) were added, and the Schlenk tube was immersed in an oil bath preheated to 80 °C. The mixture was allowed to react for 3 h. After this time, the Schlenk tube was taken out of the oil bath, the suspension was diluted with diethyl ether (10 mL) and decane as an internal standard was added. Samples were analyzed by GC-MS.

General procedure for the catalytic hydrosilylation of styrene.

A Schlenk tube was charged with precatalyst (20 µmol, 0.5 mol%) under an atmosphere of dry nitrogen. Styrene (459 µl, 4.00 mmol, 1.00 equiv.) and bis(trimethylsilyloxy)methylsilane

(1.20 mL, 4.40 mmol, 1.10 equiv.) were added, and the Schlenk tube was immersed in an oil bath preheated to 70 °C. After a reaction time of 5 h, the Schlenk tube was taken out of the oil bath. Diethyl ether (10 mL) and decane as an internal standard were added, and samples were analyzed by GC-MS.

General procedure for Suzuki-Miyaura cross-couplings.

A Schlenk tube was charged with precatalyst (10 µmol, 1.0 mol%), triphenylphosphine (5.2 mg, 20 µmol, 2.0 mol%), phenylboronic acid (158 mg, 1.30 mmol, 1.30 equiv.), potassium phosphate hydrate (461 mg, 2.00 mmol, 2.00 equiv.) and the respective bromo- or chloroarene if it was a solid (1.00 mmol, 1.00 equiv.) under inert nitrogen atmosphere. Anhydrous toluene (3 mL) was added, followed by bromo- or chloroarene if it was a liquid (1.00 mmol, 1.00 equiv.). The Schlenk tube was immersed into an oil bath preheated to 70 °C and the mixture was allowed to react for two hours. After this time, the Schlenk tube was taken out of the oil bath, the solution was diluted with dichloromethane (10 mL), and decane as an internal standard was added. Samples were analyzed by GC-MS.

Computational details

All calculations were carried out with the Gaussian 09 program at the B3LYP level.[78,79] For geometry optimizations, the nature of all stationary points was confirmed by frequency analysis, and all geometries were found to represent minima on the potential energy surface, with the exceptions of the titanium complexes **55b-Ti**, **55d-Ti**, and **56b-Ti**, which were found to be transition states, and the dications **58bHH** and **58dHH**, for which fixed bond lengths of 1.420 Å between N-2 and N-3 were imposed to prevent cleavage during optimization.

For the optimization of the singlet and triplet states of the free carbenes **55-58**, as well as the corresponding mono- and dications, hydrogen, carbon, and nitrogen atoms were described with the aug-cc-pVTZ basis set.[80] Zero-point-corrected energies for the calculation of relative stabilities and singlet-triplet gaps and enthalpies for the calculation of proton affinities were taken directly from these calculations. Kohn–Sham orbitals were calculated at the same level of theory for the optimized structures.

The geometries of the transition metal complexes NHC-AuCl and NHC-$TiCl_4$ with NHCs **55-58** were optimized using the cc-pVDZ basis set for hydrogen, carbon, nitrogen, chlorine, and

titanium,[80,91] and the Stuttgart-Köln ECP60MDF pseudopotential together with the adapted cc-pVDZ-PP basis set for the description of gold.[92] A C_S with the NHC lying in the mirror plane was imposed for these geometry optimizations.

Nucleus-independent chemical shifts (NICS) for the singlet and triplet states of the free carbenes **55**-**58** and the corresponding mono- and dications were calculated at the B3LYP/aug-cc-pVTZ level using the gauge invariant atomic orbital (GIAO) method with the probe at the ring center.[217,218]

Natural bond orbital (NBO) analysis was performed at the B3LYP/ aug-cc-pVTZ level of theory to obtain a localised form of the wavefunction.[219] Natural atomic orbitals (NAOs) were used to express natural localised molecular orbitals and obtain molecular charge distribution through natural population analysis (NPA). The p-electron population was obtained from the occupancy of the p_π NAO.

An energy decomposition analysis (EDA)[28] of the NHC-transition metal bond was done at the BP86 level by using the extended transition state (ETS) scheme with the ADF2012.01 program, based on the B3LYP/cc-pVDZ-(PP) geometries.[97,220,221] Uncontracted Slater-type orbitals were used as basis functions. All elements were described by basis sets of triple-ξ quality augmented by two sets of polarisation functions (basis set called TZ2P in ADF).[222] Core electrons (1s for carbon and nitrogen atoms, [He]2s2p for chlorine and titanium atoms and [Ar]4s4p4d for gold atoms) were treated with the frozen-core approximation. Scalar relativistic effects were accounted for by applying the zeroth-order regular approximation (ZORA).[223] The instantaneous interaction energy ΔE_{int} between NHC and transition metal fragments was decomposed into three main components using the equation $\Delta E_{int} = \Delta E_{elstat} + \Delta E_{Pauli} + \Delta E_{orb}$. The orbital interaction term ΔE_{orb} was further decomposed into components belonging to the irreducible representations of the C_S point group, i. e. the σ- and π-contributions according to $\Delta E_{orb} = \Delta E_\sigma + \Delta E_\pi$. By repeating the EDA after deleting the virtual orbitals on either the ligand or the transition metal fragment, estimates for π-donation $\Delta E_{\pi(LM)}$ and π-backdonation $\Delta E_{\pi(ML)}$ were obtained.[69e,90,96]

The ETS–NOCV (natural orbitals for chemical valence) scheme was used as an alternative approach to investigate the orbital interaction energy ΔE_{orb}.[100] The calculations were executed at the BP86/TZ2P level of theory. The orbital interaction term is decomposed into contributions by NOCV pairs, which describe charge-transfer channels between the fragments. By visual

inspection, these are classified as either donation, backdonation or internal reorganization processes.

For the geometry optimization of *trans-syn* and *trans-anti* rotamers of the simplified model of nickel(II) complex **233**, all elements were described with the cc-pVDZ basis set.[80,91b,c,194] Gibbs free energies wer taken directly from these calculations.

The geometry optimization of truncated NHC ligands **243**-**247** was carried out using a cc-pVDZ basis set to describe all elements, and Kohn-Sham orbitals were calculated for the optimised structures using the aug-cc-pVTZ basis set.[80,91a,208] For the optimization of pincer and pseudopincer complex geometries, and the calculation of their Gibbs free energies, palladium and bromine were described with a cc-pVDZ-PP basis set in combination with the corresponding electronic core potential, and the lighter elements were treated with the cc-pVDZ basis set.[80,91a,209]

All basis sets were retrieved from the EMSL Basis Set Library.[224]

X-ray Diffraction Studies.

X-ray data were collected with a Bruker AXS SMART APEX diffractometer, using Mo Kα radiation with the SMART suite of Programs.[225] Data were processed and corrected for Lorentz and polarization effects with SAINT,[226] and for absorption effect with SADABS.[227] Structural solution and refinement were carried out with the SHELXTL suite of programs.[228] The structure was solved by direct methods to locate the heavy atoms, followed by difference maps for the light, non-hydrogen atoms. All hydrogen atoms were put at calculated positions. All non-hydrogen atoms were generally given anisotropic displacement parameters in the final model. A summary of selected crystallographic data is given in the appendix, and CIF files are provided on the enclosed CD.

Appendix (Selected crystallographic data, data collection and refinement parameters)

	82	**84**	**89**·$CHCl_3$	**90**·$CHCl_3$
Formula	$C_{24}H_{30}Br_2ON_4Pd$	$C_{24}H_{30}Br_2N_4Pd$	$C_{25}H_{30}Br_3Cl_3N_4Pd$	$C_{25}H_{30}Br_2Cl_3IN_4Pd$
MW (g/mol)	656.75	640.76	839.01	886.00
crystal size (mm)	0.60 × 0.20 × 0.08	0.50 × 0.30 × 0.06	0.50 × 0.26 × 0.10	0.26 × 0.22 × 0.16
crystal system	Orthorhombic	Orthorhombic	Orthorhombic	Orthorhombic
space group	*Pbca*	*Pbca*	*P*2(1)2(1)2(1)	P2(1)2(1)2(1)
a (Å)	9.0465(6)	9.0480(3)	11.706(4)	11.741(2)
b (Å)	16.5328(10)	16.4781(6)	15.947(5)	15.964(3)
c (Å)	35.937(2)	35.4180(14)	16.887(6)	16.643(3)
α (°)	90	90	90	90
β (°)	90	90	90	90
γ (°)	90	90	90	90
V ($Å^3$)	5374.9(6)	5280.6(3)	3152.3(18)	3119.5(10)
Z	8	8	4	4
$\rho_{calculated}$ (g/cm^3)	1.623	1.612	1.768	1.886
temperature (K)	223(2)	223(2)	223(2)	100(2)
wavelength (Å)	0.71073	0.71073	0.71073	0.71073
θ (°)	2.27 to 27.50	1.15 to 27.49	1.76 to 27.50	1.77 to 27.50
no. of unique reflections	6171	6056	7213	7164
max. and min. transmission	0.7569, 0.2158	0.8064, 0.2559	0.6526, 0.2037	0.5379, 0.3925
final *R* indices [I>2σ(I)]	R_1 = 0.0697, wR_2 = 0.1552	R_1 = 0.0647, wR_2 = 0.1242	R_1 = 0.0538, wR_2 = 0.1173	R_1 = 0.0360, wR_2 = 0.0930
R indices (all data)	R_1 = 0.0987, wR_2 = 0.1648	R_1 = 0.0845, wR_2 = 0.1314	R_1 = 0.0953, wR_2 = 0.1337	R_1 = 0.0392, wR_2 = 0.0945
goodness-of-fit on F^2	1.141	1.199	0.943	1.068
peak/hole ($e.Å^{-3}$)	2.679 and -1.165	1.107 and -1.129	1.544 and -0.686	1.342 and -1.000

	112	**116**	**117**	**118**·CH_2Cl_2
Formula	$C_{47}H_{42}BClF_4N_2P_2Pd$	$C_{24}H_{30}Br_2N_4Pd$	$C_{13}H_{15}Br_2N_3Pd$	$C_{17}H_{19}Br_2Cl_2N_3Pd$
MW (g/mol)	925.43	640.74	479.50	602.47
crystal size (mm)	0.40 × 0.18 × 0.14	0.60 × 0.26 × 0.08	0.46 × 0.30 × 0.20	0.50 × 0.10 × 0.10
crystal system	Monoclinic	Orthorhombic	Monoclinic	Monoclinic
space group	*P2(1)/n*	*Pbca*	*P2(1)/n*	*P2(1)/n*
a (Å)	12.7835(6)	16.426(4)	7.4290(8)	9.2378(8)
b (Å)	19.6275(8)	9.501(3)	11.2598(12)	17.1028(15)
c (Å)	17.6761(8)	32.743(9)	18.300(2)	13.6570(12)
α (°)	90	90	90	90
β (°)	102.4180(10)	90	98.965(2)	108.2690(10)
γ (°)	90	90	90	90
V (Å^3)	4331.3(3)	5110(2)	1512.1(3)	2048.9(3)
Z	4	8	4	4
$\rho_{calculated}$ (g/cm^3)	1.419	1.666	2.106	1.953
temperature (K)	223(2)	100(2)	100(2)	100(2)
wavelength (Å)	0.71073	0.71073	0.71073	0.71073
θ (°)	1.57 to 27.50	1.76 to 27.50	2.13 to 27.50	2.38 to 27.50
no. of unique reflections	9920	5876	3475	4696
max. and min. transmission	0.9186, 0.7905	0.7470 and 0.2047	0.3563 and 0.1539	0.6310 and 0.1859
final *R* indices [I>2σ(I)]	R1 = 0.0546, wR2 = 0.1234	R1 = 0.0489, wR2 = 0.1238	R1 = 0.0226, wR2 = 0.0490	R1 = 0.0225, wR2 = 0.0532
R indices (all data)	R1 = 0.0775, wR2 = 0.1339	R1 = 0.0706, wR2 = 0.1350	R1 = 0.0250, wR2 = 0.0493	R1 = 0.0276, wR2 = 0.0548
goodness-of-fit on F^2	1.061	1.040	1.708	1.025
peak/hole (e.Å^{-3})	0.785 and -0.326	2.038 and -1.412	0.657 and -0.896	0.514 and -0.601

	119·CH_2Cl_2	**121**	**122** (cocrystal)	**124**·CH_2Cl_2
Formula	$C_{30}H_{30}Br_2Cl_3N_2PPd$	$C_{38}H_{48}Br_2N_4Pd$	$C_{133}H_{182}Br_8Cl_6N_{12}Pd_4$	$C_{23}H_{26}Br_2Cl_2N_4Pd$
MW (g/mol)	828.10	827.02	3226.49	695.60
crystal size (mm)	0.56 × 0.52 × 0.04	0.38 × 0.30 × 0.08	0.26 × 0.20 × 0.12	0.20 × 0.16 × 0.07
crystal system	Monoclinic	Triclinic	Triclinic	Monoclinic
space group	*P2(1)/n*	*P-1*	*P-1*	*P2(1)/n*
a (Å)	12.8293(17)	10.359(3)	12.1948(8)	10.1973(10)
b (Å)	14.4879(19)	12.225(3)	14.1073(9)	15.7552(16)
c (Å)	17.675(2)	14.926(4)	21.3296(14)	16.6958(17)
α (°)	90	83.575(5)	76.8260(10)	90
β (°)	101.964(2)	81.529(5)	84.0540(10)	103.881(2)
γ (°)	90	83.534(5)	79.2280(10)	90
V (Å^3)	3213.9(7)	1849.0(9)	3502.8(4)	2604.0(5)
Z	4	2	1	4
$\rho_{calculated}$ (g/cm^3)	1.711	1.485	1.530	1.774
temperature (K)	100(2)	100(2)	100(2)	100(2)
wavelength (Å)	0.71073	0.71073	0.71073	0.71073
θ (°)	1.80 to 27.50	2.07 to 27.50	1.96 to 27.50	1.80 to 27.50
no. of unique reflections	7364	8476	16079	5985
max. and min. transmission	0.8764 and 0.2528	0.8133 and 0.4275	0.7184 and 0.5141	0.7668 and 0.5013
final *R* indices [I>2σ(I)]	R1 = 0.0590, wR2 = 0.1540	R1 = 0.0519, wR2 = 0.1111	R1 = 0.0390, wR2 = 0.0740	R1 = 0.0440, wR2 = 0.0964
R indices (all data)	R1 = 0.0806, wR2 = 0.1685	R1 = 0.1061, wR2 = 0.1276	R1 = 0.0577, wR2 = 0.0773	R1 = 0.0626, wR2 = 0.1038
goodness-of-fit on F^2	1.091	0.952	1.320	1.027
peak/hole (e.Å^{-3})	6.500 and -2.160	1.115 and -1.011	1.282 and -0.944	1.397 and -0.711

	134	**135**·MeCN	**136**	**137**
Formula	$C_{12}H_{13}Br_2N_3Pd$	$C_{17}H_{18}Br_2Cl_{0.25}N_4Pd$	$C_{28}H_{25}Br_2N_2PPd$	$C_{32}H_{25}F_6N_2O_4PPd$
MW (g/mol)	465.47	553.44	686.69	752.91
crystal size (mm)	0.30 × 0.14 × 0.10	0.24 × 0.12 × 0.10	0.197 × 0.099 × 0.063	0.36 × 0.24 × 0.10
crystal system	Monoclinic	Monoclinic	Monoclinic	Monoclinic
space group	P2(1)/c	P 21/n	P 21/n	P 21/n
a (Å)	9.4099(17)	13.4325(6)	10.6153(8)	10.7241(8)
b (Å)	12.173(3)	10.2745(4)	16.6679(12)	16.5483(9)
c (Å)	12.280(2)	13.8594(6)	14.6369(12)	17.6106(12)
α (°)	90	90	90	90
β (°)	90.10(2)	98.377(2)	100.457(3)	96.812(2)
γ (°)	90	90	90	90
V (Å^3)	1406.6(5)	1892.36(14)	2546.8(3)	3103.2(4)
Z	4	4	4	2
$\rho_{calculated}$ (g/cm^3)	2.198	1.943	1.791	1.612
temperature (K)	100(2)	100(2)	100(2)	100(2)
wavelength (Å)	0.71073	0.71073	0.71073	0.71073
θ (°)	2.36 to 27.46	2.284 to 27.498	2.302 to 25.370	2.274 to 25.350
no. of unique reflections	4429	4337	4666	5669
max. and min. transmission	0.5418 and 0.2284	0.7457 and 0.5798	0.7452 and 0.6851	0.7457 and 0.6721
final *R* indices [I>2σ(I)]	R1 = 0.0243, wR2 = 0.0573	R1 = 0.0291, wR2 = 0.0663	R1 = 0.0369, wR2 = 0.0627	R1 = 0.0446, wR2 = 0.0953
R indices (all data)	R1 = 0.0278, wR2 = 0.0573	R1 = 0.0372, wR2 = 0.0693	R1 = 0.0672, wR2 = 0.0701	R1 = 0.0653, wR2 = 0.1018
goodness-of-fit on F^2	1.054	1.048	1.011	1.029
peak/hole (e.Å^{-3})	0.863 and -0.336	2.257 and -1.398	0.835 and -0.579	0.993 and -0.716

	2 **140'**·3 MeCN	**159**·HBr·2 $CHCl_3$	**160**	**161**
Formula	$C_{40}H_{40.50}Br_2N_{3.50}P_2Pd$	$C_{29}H_{52}Br_3Cl_6N_4Pd$	$C_{27}H_{50}Br_2N_4Pd$	$C_{19}H_{30}Br_2N_4O_2Pd$
MW (g/mol)	898.42	1015.57	696.93	612.69
crystal size (mm)	0.450 × 0.240 × 0.120	0.22 × 0.12 × 0.11	0.560 × 0.120 × 0.100	0.460 × 0.360 × 0.200
crystal system	Monoclinic	Triclinic	Monoclinic	Monoclinic
space group	P 21/n	P -1	P 21/n	P 21/n
a (Å)	16.9962(10)	12.4203(9)	9.813(3)	10.5073(12)
b (Å)	14.4727(10)	12.4948(9)	13.609(4)	12.8755(14)
c (Å)	30.934(2)	14.5961(11)	23.352(6)	17.273(2)
α (°)	90	82.908(3)	90	90
β (°)	96.906(2)	72.160(2)	96.238(6)	107.541(2)
γ (°)	90	71.533(3)	90	90
V ($Å^3$)	7553.9(9)	2044.3(3)	3100.1(14)	2228.2(5)
Z	8	2	4	4
$\rho_{calculated}$ (g/cm^3)	1.580	1.650	1.493	1.826
temperature (K)	100(2)	100(2)	100(2)	100(2)
wavelength (Å)	0.71073	0.71073	0.71073	0.71073
θ (°)	2.193 to 28.282	2.092 to 25.024	1.735 to 27.494	2.008 to 27.496
no. of unique reflections	18743	7172	7116	5114
max. and min. transmission	0.7457 and 0.6580	0.7457 and 0.5973	0.7456 and 0.5023	0.7457 and 0.6299
final *R* indices [I>2σ(I)]	R1 = 0.0558, wR2 = 0.1238	R1 = 0.0513, wR2 = 0.1348	R1 = 0.0437, wR2 = 0.1064	R1 = 0.0225, wR2 = 0.0545
R indices (all data)	R1 = 0.0889, wR2 = 0.1369	R1 = 0.0718, wR2 = 0.1477	R1 = 0.0717, wR2 = 0.1156	R1 = 0.0253, wR2 = 0.0556
goodness-of-fit on F^2	1.048	1.076	1.064	1.040
peak/hole ($e.Å^{-3}$)	2.944 and -2.419	1.544 and -2.421	1.332 and -1.075	0.580 and -0.422

	188	**190**	**211**	**212**
Formula	$C_{27}H_{36}Br_2N_4Pd$	$C_{16}H_{21}Br_2N_3Pd$	$C_{19}H_{22}$ Br_2N_2PtS	$C_{16}H_{24}Br_2N_2PtS$
MW (g/mol)	682.82	521.58	665.36	631.34
crystal size (mm)	0.340 × 0.270 × 0.100	0.120 × 0.260 × 0.460	0.44 × 0.16 × 0.02	0.38 × 0.26 × 0.16
crystal system	Orthorhombic	Monoclinic	Monoclinic	Monoclinic
space group	$P2_12_12_1$	P 21/c	*Cc*	*P2(1)/n*
a (Å)	8.6448(4)	14.328(4)	24.808(3)	10.0593(5)
b (Å)	9.4399(4)	8.534(3)	7.8191(11)	13.9747(7)
c (Å)	34.1094(12)	15.731(5)	11.2324(15)	14.2926(8)
α (°)	90	90	90	90
β (°)	90	111.507(5)	114.943(2)	110.1410(10)
γ (°)	90	90	90	90
V (Å^3)	2783.5(2)	1789.58	1975.6(5)	1886.33(17)
Z	4	4	4	4
$\rho_{calculated}$ (g/cm^3)	1.629	1.936	2.237	2.223
temperature (K)	100(2)	100(2)	100(2)	100(2)
wavelength (Å)	0.71073	0.71073	0.71073	0.71073
θ (°)	2.388 to 28.313	1.53 to 28.45	2.76 to 27.49	2.10 to 27.50
no. of unique reflections	6892	4483	3974	4315
max. and min. transmission	0.7457 and 0.5548	0.7457 and 0.5599	0.8062 and 0.0830	0.2543 and 0.0942
final *R* indices [I>2σ(I)]	R1 = 0.0288, wR2 = 0.0551	R1 = 0.0429, wR2 = 0.0899	R1 = 0.0331, wR2 = 0.0788	R1 = 0.0310, wR2 = 0.0773
R indices (all data)	R1 = 0.0352, wR2 = 0.0563	R1 = 0.0594, wR2 = 0.0991	R1 = 0.0345, wR2 = 0.0794	R1 = 0.0349, wR2 = 0.0788
goodness-of-fit on F^2	1.027	1.042	1.030	1.048
peak/hole (e.Å^{-3})	1.121 and -0.392	1.411 and -0.910	2.220 and -1.484	1.894 and -1.886

	213·MeCN	**214**	**215**·0.5 CH_2Cl_2	**216**
Formula	$C_{27}H_{29}Br_2N_3PtS$	$C_{20}H_{24}Br_2N_2PtS$	$C_{17.5}H_{27}Br_2ClN_2PtS$	$C_{26}H_{28}Br_2N_2PtS$
MW (g/mol)	782.50	679.38	687.83	755.47
crystal size (mm)	0.23 × 0.22 × 0.02	0.46 × 0.26 × 0.10	0.38 × 0.25 × 0.17	0.35 × 0.10 × 0.04
crystal system	Monoclinic	Monoclinic	Monoclinic	Monoclinic
space group	*P2(1)/c*	*P2(1)/c*	P2(1)/c	*P2(1)/n*
a (Å)	15.1236(10)	11.0917(15)	9.5460(13)	11.770(3)
b (Å)	11.4199(8)	16.445(2)	12.5982(17)	7.9153(18)
c (Å)	16.7775(11)	11.7723(16)	18.517(3)	27.695(6)
α (°)	90	90	90	90
β (°)	113.3190(10)	93.702(3)	97.310(3)	97.538(6)
γ (°)	90	90	90	90
V (Å^3)	2660.9(3)	2142.8(5)	2208.8(5)	2557.9(10)
Z	4	4	4	4
$\rho_{calculated}$ (g/cm^3)	1.953	2.106	2.068	1.962
temperature (K)	100(2)	100(2)	100(2)	100(2)
wavelength (Å)	0.71073	0.71073	0.71073	0.71073
θ (°)	2.22 to 27.50	1.84 to 27.50	2.15 to 27.50	1.48 to 27.50
no. of unique reflections	6111	4930	5075	5873
max. and min. transmission	0.8504 and 0.2489	0.5629 and 0.4259	0.2762 and 0.1128	0.7221 and 0.1505
final *R* indices [I>2σ(I)]	R1 = 0.0388, wR2 = 0.0744	R1 = 0.0314, wR2 = 0.0751	R1 = 0.0627, wR2 = 0.1230	R1 = 0.0360, wR2 = 0.0809
R indices (all data)	R1 = 0.0504, wR2 = 0.0787	R1 = 0.0391, wR2 = 0.0870	R1 = 0.0720, wR2 = 0.1264	R1 = 0.0483, wR2 = 0.0944
goodness-of-fit on F^2	0.971	1.088	1.229	1.079
peak/hole (e.Å^{-3})	1.840 and -1.129	2.278 and -1.076	2.056 and -3.482	1.916 and -1.171

	221	**222**	**223**·C_7H_8	**226**
Formula	$C_{19}H_{22}Br_2N_2PdS$	$C_{32}H_{48}Br_4N_4Pd_2S_2$	$C_{64}H_{68}Br_4N_4Pd_2S_2$	$C_{26}H_{28}Br_2N_2PdS$
MW (g/mol)	576.67	1085.30	1489.78	666.78
crystal size (mm)	0.52 × 0.10 × 0.09	0.10 × 0.06 × 0.02	0.20 × 0.13 × 0.12	0.46 × 0.36 × 0.20
crystal system	Orthorhombic	Monoclinic	Triclinic	Monoclinic
space group	P2(1)2(1)2(1)	P2(1)/n	P-1	Cc
a (Å)	8.8914(15)	11.5261(8)	8.9485(4)	15.038(3)
b (Å)	14.057(2)	36.043(3)	11.9417(6)	11.540(2)
c (Å)	16.137(3)	14.1629(9)	14.7246(7)	16.353(4)
α (°)	90	90	91.2520(10)	90
β (°)	90	102.121(2)	94.0830(10)	117.039(3)
γ (°)	90	90	101.6050(10)	90
V (Å^3)	2017.0(6)	5752.7(7)	1536.34(13)	2527.8(10)
Z	4	6	1	4
$\rho_{calculated}$ (g/cm^3)	1.899	1.880	1.610	1.752
temperature (K)	100(2)	100(2)	100(2)	100(2)
wavelength (Å)	0.71073	0.71073	0.71073	0.71073
θ (°)	2.52 to 27.49	1.13 to 25.00	1.74 to 27.50	2.33 to 27.50
no. of unique reflections	4626	10121	7047	4421
max. and min. transmission	0.6623 and 0.1812	0.5629 and 0.4618	0.5629 and 0.4603	0.5021 and 0.2608
final *R* indices [I>2σ(I)]	R1 = 0.0253, wR2 = 0.0533	R1 = 0.0716, wR2 = 0.1338	R1 = 0.0318, wR2 = 0.0712	R1 = 0.0331, wR2 = 0.0643
R indices (all data)	R1 = 0.0279, wR2 = 0.0539	R1 = 0.1345, wR2 = 0.1576	R1 = 0.0394, wR2 = 0.0738	R1 = 0.0427, wR2 = 0.0696
goodness-of-fit on F^2	0.988	0.995	1.030	0.985
peak/hole (e.Å^{-3})	0.767 and -0.428	3.538 and -1.763	0.828 and -0.442	0.824 and -0.568

	227	**228**	**229**·1.5 CH_2Cl_2	**230**
Formula	$C_{32}H_{40}Br_2N_4PdS$	$C_{29}H_{42}Br_2N_4PdS$	$C_{39.5}H_{47}Br_2Cl_3N_4PdS$	$C_{33}H_{42}Br_2N_4PdS$
MW (g/mol)	778.96	744.94	982.44	792.98
crystal size (mm)	0.46 × 0.26 × 0.10	0.26 × 0.18 × 0.02	0.50 × 0.20 × 0.10	0.56 × 0.40 × 0.10
crystal system	Triclinic	Triclinic	Monoclinic	Monoclinic
space group	P-1	P-1	P 21/n	P 21/n
a (Å)	10.844(13)	9.026(7)	9.299(4)	10.924(5)
b (Å)	13.184(15)	9.594(8)	33.216(15)	23.550(10)
c (Å)	13.233(16)	19.802(17)	13.877(6)	12.900(5)
α (°)	78.09(2)	89.396(18)	90	90
β (°)	70.73(2)	78.969(19)	102.034(11)	95.699(9)
γ (°)	65.88(2)	70.357(18)	90	90
V (Å^3)	1624(3)	1582(2)	4192(3)	3302(2)
Z	2	2	4	4
$\rho_{calculated}$ (g/cm^3)	1.593	1.563	1.557	1.595
temperature (K)	100(2)	100(2)	100(2)	100(2)
wavelength (Å)	0.71073	0.71073	0.71073	0.71073
θ (°)	1.70 to 27.50	2.10 to 27.59	1.23 to 27.50	1.81 to 27.50
no. of unique reflections	7423	7247	9594	7572
max. and min. transmission	0.7456 and 0.6149	0.7456 and 0.5853	0.7456 and 0.5449	0.7898 and 0.5117
final *R* indices [I>2σ(I)]	R1 = 0.0564, wR2 = 0.1435	R1 = 0.0903, wR2 = 0.1676	R1 = 0.0569, wR2 = 0.1346	R1 = 0.0447, wR2 = 0.1106
R indices (all data)	R1 = 0.0805, wR2 = 0.1549	R1 = 0.1356, wR2 = 0.1874	R1 = 0.0912, wR2 = 0.1508	R1 = 0.0639, wR2 = 0.1206
goodness-of-fit on F^2	1.092	1.096	1.051	1.050
peak/hole (e.Å^{-3})	3.640 and -1.137	2.074 and -2.445	1.590 and -1.410	1.351 and -0.800

	232	**233**
Formula	$C_{39}H_{46}Br_2N_4PdS$	$C_{38}H_{44}Br_2N_4NiS_2$
MW (g/mol)	869.08	839.42
crystal size (mm)	0.20 × 0.12 × 0.07	0.48 × 0.31 × 0.28
crystal system	Monoclinic	Monoclinic
space group	P 21/n	P2(1)/c
a (Å)	9.4352	10.682(3)
b (Å)	20.7414(16)	18.283(5)
c (Å)	19.2349(14)	9.480(3)
α (°)	90	90
β (°)	94.539(2)	91.825(6)
γ (°)	90	90
V (Å^3)	3752.4(5)	1850.6(8)
Z	4	2
$\rho_{calculated}$ (g/cm^3)	1.538	1.506
temperature (K)	100(2)	100(2)
wavelength (Å)	0.71073	0.71073
θ (°)	2.23 to 25.72	2.21 to 27.50
no. of unique reflections	7081	4243
max. and min. transmission	0.5621 and 0.4648	0.5629 and 0.4232
final *R* indices [I>2σ(I)]	R1 = 0.0387, wR2 = 0.0750	R1 = 0.0724, wR2 = 0.2133
R indices (all data)	R1 = 0.0707, wR2 = 0.0850	R1 = 0.1079, wR2 = 0.2390
goodness-of-fit on F^2	1.019	1.106
peak/hole (e.Å^{-3})	1.208 and -1.305	1.863 and -1.315

References

[1] Moss, G. P.; Smith, P. A. S.; Tavernier, D. *Pure Appl. Chem.* **1995**, *67*, 1307.

[2] (a) Hoffmann, R.; Zeiss, G. D.; Van Dine, G. W. *J. Am. Chem. Soc.* **1968**, *90*, 1485. (b) Tukov, A. A.; Normand, A. T.; Nechaev, M. S. *Dalton Trans.* **2009**, 7015.

[3] (a) Mueller, P. H.; Rondan, N. G.; Houk, K. N.; Gano, J. E.; Platz, M. S. *Tet. Lett.* **1983**, *24*, 485. (b) Richards, C A.; Kim, S.; Yamaguchi, Y.; Schaefer, H. F. *J. Am. Chem. Soc.* **1995**, *117*, 10104.

[4] (a) Harrison, J. F.; Liedtke, R. C.; Liebman, J. F. *J. Am. Chem. Soc.* **1979**, *101*, 7162. (b) Nemirowski, A.; Schreiner, P. R. *J. Org. Chem.* **2007**, *72*, 9533.

[5] (a) Schoeller, W. W. *J. Chem. Soc., Chem. Commun.* **1980**, 124. (b) Pauling. L. *J. Chem. Soc., Chem. Commun.* **1980**, 688. (c) Baird, N. C.; Taylor, K. F. *J. Am. Chem. Soc.* **1978**, *100*, 1333.

[6] Schuster, G. B. *Adv. Phys. Org. Chem.* **1986**, *22*, 311.

[7] (a) Simmons, H. E.; Smith, R. D. *J. Am. Chem. Soc.* **1958**, *80*, 5323. (b) Simmons, H. E.; Smith, R. D. *J. Am. Chem. Soc.* **1959**, 81, 4256.

[8] (a) Davies, H. M. L.; Beckwith, R. E. J. *Chem. Rev.* **2003**, *103*, 286. (b) Díaz-Requejo, M. M.; Belderrain, T. R.; Nicasio, M. C.; Pérez, P. J. *Dalton Trans.* **2006**, 5559. (c) Doyle, M. P.; Duffy, R.; Ratnikov, M.; Zhou, L. *Chem. Rev.* **2010**, *110*, 704. (d) Gillingham, D.; Fei, N. *Chem. Soc. Rev.* **2013**, *42*, 4918.

[9] Wanzlick, H.-W.; Schikora, E. Angew. Chem. 1960, 72, 494.

[10] (a) Hahn, F. E.; Wittenbecher, L.; Van, D. L.; Fröhlich, R. *Angew. Chem., Int. Ed.* **2000**, *39*, 541. (b) Böhm, V. P. W.; Herrmann, W. A. *Angew. Chem., Int. Ed.* **2000**, *39*, 4036. (c) Cheng, M.; Lai, C.; Hu, C. *Mol. Phys.* **2004**, *102*, 2617.

[11] Lemal, D. M.; Lovald, R. A.; Kawano, K. I. *J. Am. Chem. Soc.* **1964**, *86*, 2518.

[12] (a) Igau, A.; Grutzmacher, H.; Baceiredo, A.; Bertrand, G. *J. Am. Chem. Soc.* **1988**, *110*, 6463. (b) Igau, A.; Baceiredo, A.; Trinquier, G.; Bertrand, G. *Angew. Chem., Int. Ed.* **1989**, *28*, 621.

[13] (a) Arduengo, A. J.; Harlow, R. L.; Kline, M. *J. Am. Chem. Soc.* **1991**, *113*, 361. (b) Arduengo, A. J.; Goerlich, J. R.; Marshall, W. J. *J. Am. Chem. Soc.* **1995**, *117*, 11027.

[14] (a) Arduengo III, A. J.; Dias, H. V. R.; Harlow, R. L.; Kline, M. *J. Am. Chem. Soc.* **1992**, *114*, 5530. (b) Arduengo III., A. J.; Goerlich, J. R.; Marshall, W. J. *J. Am. Chem. Soc.* **1995**, *117*, 11027. (c) Alder, R. W.; Allen, P. R.; Murray, M.; Orpen, A. G. *Angew. Chem., Int. Ed.* **1996**, *35*, 1121. (d) Hahn, F. E.; Wittenbecher, L.; Boese, R.; Bläser, D. *Chem. Eur. J.* **1999**, *5*, 1931.

[15] (a) Boehme, C.; Frenking, G. *J. Am. Chem. Soc.* **1996**, *118*, 2039. (b) Poater, A.; Ragone, F.; Giudice, S.; Costabile, C.; Dorta, R.; Nolan, S. P.; Cavallo, L. *Organometallics* **2008**, *27*, 2679.

[16] (a) Tschugajeff, L.; Skanawy-Grigorjewa, M.; Posnjak, A. *Z. Anorg. Allg. Chem.* **1925**, *148*, 37. (b) Burke, A.; Balch, A. L.; Enemark, J. H. *J. Am. Chem. Soc.* **1970**, *92*, 2555. (c) Butler, W. M.; Enemark, J. H. *Inorg. Chem.* **1971**, *10*, 2416. (d) Butler, W. M.; Enemark, J. H.; Parks, J.; Balch, A. L. *Inorg. Chem.* **1973**, *12*, 451.

[17] Fischer, E. O.; Maasböl, A. *Angew. Chem., Int. Ed.* **1964**, *3*, 580.

[18] Schrock, R. R. *J. Am. Chem. Soc.* **1974**, *96*, 6796.

[19] de Frémont, P.; Marion, N.; Nolan, S. P. *Coord. Chem. Rev.* **2009**, *253*, 862.

[20] (a) Öfele, K. *J. Organomet. Chem.* **1968**, *12*, P42. (b) Wanzlick, H.-W.; Schönherr, H. *Angew. Chem., Int. Ed.* **1968**, *7*, 141.

[21] Cardin, D. J.; Cetinkaya, B.; Lappert, M. F.; Manojlović-Muir, L.; Muir, K. W. *J. Chem. Soc., Chem. Commun.* **1971**, 400.

[22] (a) Herrmann, W. A.; Köcher, C. *Angew. Chem., Int. Ed.* **1997**, *36*, 2162. (b) Bourissou, D.; Guerret, O.; Gabbaï, F. P.; Bertrand, G. *Chem. Rev.* **2000**, *100*, 39. (c) Herrmann, W. A. *Angew. Chem., Int. Ed.* **2002**, *41*, 1290. (d) Peris, E.; Crabtree, R. H. *Coord. Chem. Rev.* **2004**, *248*, 2239. (e) *N-Heterocyclic Carbenes in Synthesis*; Nolan, S. P., Ed.; Wiley-VCH: Weinheim, 2007. (f) Kantchev, E. A. B.; O'Brien, C. J.; Organ, M. G. *Angew. Chem., Int. Ed.* **2007**, *46*, 2768. (g) Díez-González, S.; Marion, N.; Nolan, S. P. *Chem. Rev.* **2009**, *109*, 3612. (h) Melaimi, M.; Soleilhavoup, M.; Bertrand, G. *Angew. Chem., Int. Ed.* **2010**, *49*, 8810. (i) Mata, J. A.; Poyatos, M. *Curr. Org. Chem.* **2011**, *15*, 3309. (j) Valente, C.; Çalimsiz, S.; Hoi, K. H.; Mallik, D.; Sayah, M.; Organ, M. G. *Angew. Chem., Int. Ed.* **2012**, *51*, 3314. (k) Bézier, D.; Sortais, J.-B.; Darcel, C. *Adv. Synth. Catal.* **2013**, *355*, 19.

[23] (a) Enders, D.; Balensiefer, T. *Acc. Chem. Res.* **2004**, *37*, 534. (b) Marion, N.; Díez-González, S.; Nolan, S. P. *Angew. Chem., Int. Ed.* **2007**, *46*, 2988. (c) Enders, D.; Niemeier, O.;

Henseler, A. *Chem. Rev.* **2007**, *107*, 5606. (d) Biju, A. T.; Kuhl, N.; Glorius, F. *Acc. Chem. Res.* **2011**, *44*, 1182.

[24] Hahn, F. E.; Jahnke, M. C. *Angew. Chem., Int. Ed.* **2008**, *47*, 3122.

[25] Benhamou, L.; Chardon, E.; Lavigne, G.; Bellemin-Laponnaz, S.; César V. *Chem. Rev.* **2011**, *111*, 2705.

[26] (a) Arduengo III, A. J. U. S. Patent No. 5077414 A, 1991. (b) Arduengo III, A. J.; Krafczyk, R.; Schmutzler, R.; Craig, H. A.; Goerlich, J. R.; Marshall, W. J.; Unverzagt, M. *Tetrahedron* **1999**, *55*, 14523.

[27] Hintermann, L. *Beilstein J. Org. Chem.* **2007**, *3*, 22.

[28] Kuhn, K. M.; Grubbs, R. H. *Org. Lett.* **2008**, *10*, 2075.

[29] Huynh, H. V.; Han, Y.; Ho, J. H. H.; Tan, G. K. *Organometallics* **2006**, *25*, 3267.

[30] Becker, H. G. O.; Hoffmann, G.; Gwan, K. M.; Knüpfer, L. *J. Prakt. Chem.* **1988**, *330*, 325.

[31] (a) Crudden, C. M.; Allen, D. P. *Coord. Chem. Rev.* **2004**, *248*, 2247. (b) Cavallo, L.; Correa, A.; Costabile, C.; Jacobsen, H. *J. Organomet. Chem.* **2005**, *690*, 5407. (c) Díez-González, S.; Nolan, S. P. *Coord. Chem. Rev.* **2007**, *251*, 874. (d) Dröge, T.; Glorius, F. *Angew. Chem., Int. Ed.* **2010**, *49*, 6940. (e) Kumar, A.; Ghosh, P. *Eur. J. Inorg. Chem.* **2012**, 3955. (f) Nelson, D. J.; Nolan, S. P. *Chem. Soc. Rev.* **2013**, *42*, 6723.

[32] Huynh, H. V.; Frison, G. *J. Org. Chem.* **2013**, *78*, 328.

[33] (a) Viciano, M.; Mas-Marzá, E.; Sanaú, M.; Peris, E. *Organometallics*, **2006**, *25*, 3063. (b) Hindi, K. M.; Siciliano, T. J.; Durmus, S.; Panzner, M. J.; Medvetz, D. A.; Reddy, D. V.; Hogue, L. A.; Hovis, C. E.; Hilliard, J. K.; Mallet, R. J.; Tessier, C. A.; Cannon, C. L.; Youngs, W. J. *J. Med. Chem.* **2008**, *51*, 1577. (c) MaGee, K. D. M.; Travers, G.; Skelton, B. W.; Massi, M.; Payne, A. D.; Brown, D. H. *Aust. J. Chem.* **2012**, *65*, 823.

[34] (a) Araki, S.; Wanibe, Y.; Uno, F.; Morikawa, A.; Yamamoto, K.; Chiba, K.; Butsu, Y. *Chem. Ber.* **1993**, *126*, 1149. (b) Wehlan, M.; Thiel, R.; Fuchs, J.; Beck, W.; Fehlhammer, W. P. *J. Organomet. Chem.* **2000**, *613*, 159. (c) Huynh, H. V.; Meier, N.; Pape, T.; Hahn, F. E. *Organometallics* **2006**, *25*, 3012. (d) Hahn, F. E.; Klusmann, D.; Pape, T. *Eur. J. Inorg. Chem.* **2008**, 4420. (e) Nogai, S. D.; McKenzie, J. M.; Cronje, S.; Raubenheimer, H. G.; *New J. Chem.* **2009**, *33*, 2208. (f) Yen, S. K.; Koh, L. L.; Huynh, H. V.; Hor, T. S. A. *Eur. J. Inorg. Chem.* **2009**, 4288. (g) Bellemin-Laponnaz, S. *Polyhedron* **2010**, *29*, 30.

[35] (a) Binobaid, A.; Iglesias, M.; Beetstra, D. J.; Kariuki, B.; Dervisi, A.; Fallis, I. A.; Cavell, K. J. *Dalton Trans.* **2009**, 7099. (b) Lu, W. Y.; Cavell, K. J.; Wixey, J. S.; Kariuki, B. *Organometallics* **2011**, *30*, 5649. (c) Dunsford, J. J.; Cavell, K. J.; Kariuki, B. M. *Organometallics* **2012**, *31*, 4118. (d) Iglesias, M.; Beetstra, D. J.; Knight, J. C.; Ooi, L.-L.; Stasch, A.; Coles, S.; Male, L.; Hursthouse, M. B.; Cavell, K. J.; Dervisi, A.; Fallis, I. A. *Organometallics* **2008**, *27*, 3279. (e) Dunsford, J. J.; Cavell, K. J. *Dalton Trans.* **2011**, *40*, 9131.

[36] (a) Gründemann, S.; Kovacevic, A.; Albrecht, M.; Faller, J. W.; Crabtree, R. H. *J. Am. Chem. Soc.* **2002**, *124*, 10473. (b) Chianese, A. R.; Kocacevic, A.; Zeglis, B. M.; Faller, J. W.; Crabtree, R. H. *Organometallics* **2004**, *23*, 2461. (c) Arnold, P. L.; Pearson, S. *Coord. Chem. Rev.* **2007**, *251*, 596. (d) Aldeco-Perez, E.; Rosenthal, A. J.; Donnadieu, B.; Parameswaran, P.; Frenking, G.; Bertrand, G. *Science* **2009**, *326*, 556. (d) Poulain, A.; Iglesias, M.; Albrecht, M. *Curr. Org. Chem.* **2011**, *15*, 3325. (e) Krüger, A.; Albrecht, M. *Aust. J. Chem.* **2011**, *64*, 1113.

[37] (a) Schneider, S. K.; Roembke, P.; Julius, G. R.; Loschen, C.; Raubenheimer, H. G.; Frenking, G.; Herrmann, W. A. *Eur. J. Inorg. Chem.* **2005**, 2973. (b) Schuster, O.; Wang, L.; Raubenheimer, H. G.; Albrecht, M. *Chem. Rev.* **2009**, *109*, 3445.

[38] (a) Lebel, H.; Janes, M. K.; Charette, A. B.; Nolan, S. P. *J. Am. Chem. Soc.* **2004**, *126*, 5046. (b) Xu, X.; Xu, B.; Li, Y.; Hong, S. H. *Organometallics* **2010**, *29*, 6343.

[39] (a) Mathew, P.; Neels, A.; Albrecht, M. *J. Am. Chem. Soc.* **2008**, *130*, 13534. (b) Guisado-barrios, G.; Bouffard, J.; Donnadieu, B.; Bertrand, G. *Angew. Chem., Int Ed.* **2010**, *49*, 4759. (c) Bouffard, J.; Keitz, B. K.; Tonner, R.; Guisado-Barrios, G.; Frenking, G.; Grubbs, R. H.; Bertrand, G. *Organometallics* **2011**, *30*, 261. (d) Kilpin, K. J.; Paul, U. S. D.; Lee, A.; Crowley, J. D. *Chem. Commun.* **2011**, *47*, 328. (e) Yuan, D.; Huynh, H. V. *Organometallics* **2012**, *31*, 405. (f) Donnelly, K. F.; Petronilho, A.; Albrecht, M. *Chem. Commun.* **2013**, *49*, 1145.

[40] (a) Schütz, J.; Herdtweck, E.; Herrmann, W. A. *Organometallics* **2004**, *23*, 6084. (b) Herrmann, W. A.; Schütz, J.; Frey, G. D.; Herdtweck, E. *Organometallics* **2006**, *25*, 2437. (c) Kessler, F.; Szesni, N.; Maaß, C.; Hohberger, C.; Weibert, B.; Fischer, H. *J. Organomet. Chem.* **2007**, *692*, 3005. (d) Prades, A.; Viciano, M.; Sanaú, M.; Peris, E. *Organometallics* **2008**, *27*, 4254. (e) Schmidt, A.; Guan, Z. *Synthesis* **2012**, *44*, 3251.

[41] (a) Jothibasu, R.; Huynh, H. V. *Chem. Commun.* **2010**, *46*, 2986. (b) Sivaram, H.; Jothibasu, R.; Huynh, H. V. *Organometallics* **2012**, *31*, 1195. (c) Zhou, Y.; Liu, Q.; Lv, W.; Pang, Q.; Ben,

R.; Qian, Y.; Zhao, J. *Organometallics* **2013**, *32*, 3753. (d) Guan, Z.; Namyslo, J. C.; Drafz, M. H. H.; Nieger, M.; Schmidt, A. *Beilstein J. Org. Chem.* **2014**, *10*, 832.

[42] (a) Han, Y.; Huynh, H. V. *Chem. Commun.* **2007**, 1089. (b) Han, Y.; Huynh, H. V.; Tan, G. K. *Organometallics* **2007**, *26*, 6581. (c) Lavallo, V.; Dyker, C. A.; Donnadieu, B.; Bertrand, G. *Angew. Chem., Int. Ed.* **2008**, *47*, 5411. (d) Han, Y.; Huynh, H. V. *Organometallics* **2009**, *28*, 2778. (e) Han, Y.; Lee, L. J.; Huynh, H. V. *Chem. Eur. J.* **2010**, *16*, 771.

[43] (a) Schneider, S. K.; Roembke, P.; Julius, G. R.; Raubenheimer, H. G.; Herrmann, W. A. *Adv. Synth. Catal.* **2006**, *348*, 1862. (b) Schneider, S. K.; Julius, G. R.; Loschen, C.; Raubenheimer, H. G.; Frenking, G.; Herrmann, W. A. *Dalton Trans.* **2006**, 1226. (c) Schneider, S. K.; Rentzsch, C. F.; Krüger, A.; Raubenheimer, H. G.; Herrmann, W. A. *J. Mol. Catal. A* **2007**, *265*, 50. (d) Raubenheimer, H. G.; Cronje, S. *Dalton Trans.* **2008**, 1265. (e) Strasser, C. E.; Stander-Grobler, E.; Schuster, O.; Cronje, S.; Raubenheimer, H. G. *Eur. J. Inorg. Chem.* **2009**, 1905.

[44] (a) Schuster, O.; Yang, L.; Raubenheimer, H. G.; Albrecht, M. *Chem. Rev.* **2009**, *109*, 3445. (b) Crabtree, R. H. *Coord. Chem. Rev.* **2013**, *257*, 755.

[45] (a) Ung, G.; Bertrand, G. *Chem. Eur. J.* **2011**, *17*, 8269. (b) Huynh, H. V.; Ong, H. L.; Bernhammer, J. C.; Frison, G. *Eur. J. Inorg. Chem.* **2013**, 4654.

[46] (a) Lever, A. B. P. *Inorg. Chem.* **1990**, *29*, 1271. (b) Lever, A. B. P. *Inorg. Chem.* **1991**, *30*, 1980.

[47] (a) Tolman, C. A. *J. Am. Chem. Soc.* **1970**, *92*, 2953. (b) Tolman, C. A. *J. Am. Chem. Soc.* **1970**, *92*, 2956. (c) Tolman, C. A. *Chem. Rev.* **1977**, *77*, 313.

[48] Huynh, H. V.; Han, Y.; Jothibasu, R;Yang, J. A. *Organometallics* **2009**, *28*, 5395.

[49] (a) Denk, K.; Sirsch, P.; Herrmann, W. A. *J. Organomet. Chem.* **2002**, *649*, 219. (b) Chianese, A. R.; Li, X.; Janzen, M. C.; Faller, J. W.; Crabtree, R. H. *Organometallics* **2003**, *22*, 1663. (c) Kelly III, R. A.; Clavier, H.; Giudice, S.; Scott, N. M.; Stevens, E. D.; Bordner, J.; Samardjiev, I.; Hoff, C. D.; Cavallo, L.; Nolan, S. P. *Organometallics* **2008**, *27*, 202.

[50] Poulain, A., Canseco-Gonzalez, D.; Hynes-Roche, R.; Müller-Bunz, H.; Schuster, O.; Stoeckli-Evans, H.; Neels A.; Albrecht, M. *Organometallics* **2011**, *30*, 1021.

[51] (a) Cardin, J.; Cetinkaya, B.; Cetinkaya, E.; Lappert, M. F.; Randall, E. W.; Rosenberg, E. *J. Chem. Soc., Dalton Trans.* **1973**, 1982. (b) Herrmann, W. A.; Runte, O.; Artus, G. *J. Organomet.*

Chem. **1995**, *501*, C1. (c) Baker, M. V.; Barnard, P. J.; Brayshaw, S. K.; Hickey, J. L.; Skelton, B. W.; White, A. H. *Dalton Trans.* **2005**, 37. (d) Chernyshova, E. S.; Goddard R.; Pörschke, K.-R. *Organometallics*, **2007**, *26*, 3236.

[52] (a) Valente, C.; Çalimsiz, S.; Hoi, K. H.; Mallik, D.; Sayah, M.; Organ, M. G. *Angew. Chem., Int. Ed.* **2012**, *51*, 3314. (b) Collado, A.; Balogh, J.; Meiries, S.; Slawin, A. M. Z.; Falivene, L.; Cavallo, L.; Nolan, S. P. *Organometallics* **2013**, *32*, 3249. (c) Dierick, S.; Dewez, D. F.; Markó, I. E. *Organometallics* **2014**, *33*, 677.

[53] (a) Altenhoff, G.; Goddard, R.; Lehmann, C. W.; Glorius, F. *J. Am. Chem. Soc.* **2004**, *126*, 15195. (b) Würtz, S.; Lohre, C.; Fröhlich, R.; Bergander, K.; Glorius, F. *J. Am. Chem. Soc.* **2009**, *131*, 8344.

[54] (a) Hillier, A. C.; Sommer, W. J.; Yong, B. S.; Petersen, J. L.; Cavallo, L.; Nolan, S. P. *Organometallics* **2003**, *22*, 4322. (b) Poater, A.; Cosenza, B.; Correa, A.; Giudice, S.; Ragone, F.; Scarano, V.; Cavallo, L. *Eur. J. Inorg. Chem.* **2009**, 1759. (c) Clavier, H.; Nolan, S. P. *Chem. Commun.* **2010**, *46*, 841.

[55] (a) Rubio, R. J.; Andavan, G. T. S.; Bauer, E. B.; Hollis, T. K.; Cho, J.; Tham, F. S.; Donnadieu, B. *J. Organomet. Chem.* **2005**, *690*, 5353. (b) Nielsen, D. J.; Cavell, K. J.; Skelton, B. W.; White, A. H. *Organometallics* **2006**, *25*, 4850. (c) Hahn, F. E.; Jahnke, M. C.; Pape, T. *Organometallics* **2006**, *25*, 5927. (d) Roseblade, S. J.; Ros, A.; Monge, D.; Alcarazo, M.; Álvarez, E.; Lassaletta, J. M.; Fernández, R. *Organometallics* **2007**, *26*, 2570. (e) Warsink, S.; Hauwert, P.; Siegler, M. A.; Spek A. L.; Elsevier, C. J. *Appl. Organomet. Chem.* **2009**, *23*, 225. (f) Huynh, H. V.; Yuan, D.; Han, Y. *Dalton Trans.* **2009**, 7262. (g) Unger, Y.; Meyer, D.; Molt, O.; Schildknecht, C.; Münster, I.; Wagenblast, G.; Strassner, T. *Angew. Chem., Int. Ed.* **2010**, *49*, 10214. (h) DePasquale, J.; Kumar, M.; Zeller, M.; Papish, E. T. *Organometallics* **2013**, *32*, 966. (i) Huynh, H. V.; Lee, C.-S. *Dalton Trans.* **2013**, *42*, 6803. (j) Liu, X.; Braunstein, P. *Inorg. Chem.* **2013**, *52*, 7367.

[56] (a) Kernbach, U.; Ramm, M.; Luger, P.; Fehlhammer, W. P. *Angew. Chem., Int. Ed.* **1996**, *35*, 310. (b) Hu, X.; Castro-Rodriguez, I.; Meyer, K. *Organometallics* **2003**, *22*, 3016. (c) Hu, X.; Castro-Rodriguez, I.; Meyer, K. *J. Am. Chem. Soc.* **2003**, *125*, 12237.

[57] (a) Jeffrey, J. C.; Rauchfuss, T. B. Inorg. Chem. 1979, 18, 2658. (b) Slone, C. S.; Weinberger, D. A.; Mirkin, C. A. Prog. Inorg. Chem. 1999, 48, 233. (c) Braunstein, P.; Naud, F.

Angew. Chem., Int. Ed. 2001, 40, 680. (d) Huynh, H. V.; Yeo, C. H.; Tan, G. K. Chem. Commun. 2006, 3833

[58] (a) O, W. W. N.; Lough, A. J.; Morris, R. H. *Organometallics* **2009**, *28*, 6755. (b) Busetto, L.; Cassani, M. C.; Femoni, C.; Macchioni, A.; Mazzoni, R.; Zuccaccia, D. *J. Organomet. Chem.* **2008**, *693*, 2579

[59] (a) Huynh, H. V.; Teng, Q. *Chem. Commun.* **2013**, *49*, 4244. (b) Teng, Q.; Upmann, D.; Ng Wijaya, S. A. Z.; Huynh, H. V. *Organometallics* **2014**, *33*, 3373.

[60] Schneider, S. K.; Herrmann, W. A.; Herdtweck, E. *J. Mol. Cat. A* **2006**, *245*, 248.

[61] Hahn, F. E.; Paas, M.; Van, D. L.; Fröhlich, R. *Chem. Eur. J.* **2005**, *11*, 5080.

[62] (a) Yamaguchi, Y.; Kashiwabara, T.; Ogata, K.; Miura, Y.; Nakamura, Y.; Kobayashi, K.; Ito, T. *Chem. Commun.* **2004**, 2160. (b) Voutchkova, A. M.; Feliz, M.; Clot, E.; Eisenstein, O.; Crabtree, R. H. *J. Am. Chem. Soc.* **2007**, *129*, 12834. (c) López-Gómez, M. J.; Martina, D.; Bertrand, G. *Chem. Commun.* **2013**, *49*, 4483.

[63] (a) Wang, H. M. J.; Lin, I. J. B. *Organometallics* **1998**, *17*, 972. (b) Chun, J.; Lee, H. S.; Jung, I. G.; Lee, S. W.; Kim, H. J.; Son, S. U. *Organometallics* **2010**, *29*, 1518.

[64] Hahn, F. E.; Klusmann, D.; Pape, T. *Eur. J. Inorg. Chem.* **2008**, 4420.

[65] (a) Enders, D.; Balensiefer, T. *Acc. Chem. Res.* **2004**, *37*, 534. (b) Marion, N.; Díez-González, S.; Nolan, S. P. Angew. Chem., Int. Ed. 2007, 46, 2988. (c) Enders, D.; Niemeier, O.; Henseler, A. *Chem. Rev.* **2007**, *107*, 5606. (d) Biju, A. T.; Kuhl, N.; Glorius, F. *Acc. Chem. Res.* **2011**, *44*, 1182. (e) Hopkinson, M. N.; Richter, C.; Schedler, M.; Glorius, F. *Nature* **2014**, *510*, 485.

[66] Fèvre, M.; Pinaud, J.; Gnanou, Y.; Vignolle, J.; Taton, D. *Chem. Soc. Rev.* **2013**, *42*, 2142.

[67] (a) Breslow, R. *J. Am. Chem. Soc.* **1958**, *80*, 3719. (b) Berkessel, A.; Elfert, S.; Yatham, V. R.; Neudörfl, J.-M.; Schlörer, N. E.; Teles, J. H. *Angew. Chem., Int. Ed.* **2012**, *51*, 12370.

[68] (a) Ema, T.; Oue, Y.; Akihara, K.; Miyazaki, Y.; Sakai, T. *Org. Lett.* **2009**, *11*, 4866. (b) Pinaud, J.; Vignolle, J.; Gnanou, Y.; Taton, D. *Macromolecules* **2011**, *44*, 1900. (c) Vora, H. U.; Wheeler, P.; Rovis, T. *Adv. Synth. Catal.* **2012**, *354*, 1617. (d) Lu, T.; Gu, L.; Kang, Q.; Zhang, Y. *Tet. Lett.* **2012**, *53*, 6602. (e) Jia, M.-Q.; Liu, C.; You, S.-L. *J. Org. Chem.* **2012**, *77*, 10996.

[69] (a) Lee, M.-T.; Hu, C.-H. *Organometallics* **2004**, *23*, 976. (b) Scott, N. M.; Nolan, S. P. *Eur. J. Inorg. Chem.* **2005**, 1815. (c) Crabtree, R. H. *J. Organomet. Chem.* **2005**, *690*, 5451. (d)

Glorius, F. *Top. Organomet. Chem.* **2007**, *21*, 1. (e) Tonner, R.; Heydenrych, G.; Frenking, G. *Chem. Asian J.* **2007**, *2*, 1555.

[70] (a) Frenking, G.; Solà, M.; Vyboishchikov S. F. *J. Organomet. Chem.* **2005**, *690*, 6178. (b) Jacobsen, H.; Correa, A.; Poater, A.; Costabile, C.; Cavallo, L. *Coord. Chem. Rev.* **2009**, *253*, 687.

[71] (a) Scholl, M.; Trnka, T. M.; Morgan, J. P.; Grubbs, R. H. *Tet. Lett.* **1999**, *40*, 2247. (b) Scholl, M.; Ding, S.; Lee, C. W.; Grubbs, R. H. *Org. Lett.* **1999**, *1*, 953. (c) Trnka, T. M.; Grubbs, R. H. *Acc. Chem. Res.* **2001**, *34*, 18.

[72] (a) Beletskaya, I. P.; Cheprakov, A. V. *Chem. Rev.* **2000**, *100*, 3009. (b) Hillier, A. C.; Grasa, G. A.; Viciu, M. S.; Lee, H. M.; Yang, C.; Nolan, S. P. *J. Organomet. Chem.* **2002**, *653*, 69. (c) Marion, N.; Nolan, S. P. *Acc. Chem. Res.* **2008**, *41*, 1440. (d) Fortman, G. C.; Nolan, S. P. *Chem. Soc. Rev.* **2011**, *40*, 5151.

[73] (a) Markó, I. E.; Stérin, S.; Buisine, O.; Mignani, R.; Branlard, P.; Tinant, B.; Declercq, J. P. *Science* **2002**, *298*, 204. (b) Marion, N.; Navarro, O.; Kelly, R. A., III; Nolan, S. P. *Synthesis* **2003**, *16*, 2590. (c) Budagumpi, S.; Haque, R. A.; Salman, A. W. *Coord. Chem. Rev.* **2012**, *256*, 1787. (d) Cao, P.; Cabrera, J.; Padilla, R.; Serra, D.; Rominger, F.; Limbach, M. *Organometallics* **2012**, *31*, 921.

[74] (a) Brien, C. J. O.; Kantchev, E. A. B.; Valente, C.; Hadei, N.; Chass, G. A.; Lough, A.; Hopkinson, A. C.; Organ, M. G. *Chem. Eur. J.* **2006**, 12, 4743. (b) Valente, C.; Çalimsiz, S.; Hoi, K. H.; Mallik, D.; Sayah, M.; Organ, M. G. *Angew. Chem., Int. Ed.* **2012**, *51*, 3314.

[75] (a) Enders, D.; Breuer, K.; Raabe, G.; Runsink, J.; Teles, J. H.; Melder, J.-P.; Ebel, K.; Brode, S. *Angew. Chem., Int. Ed.* **1995**, *34*, 1021. (b) Bertrand, G.; Díez-Barra, E.; Fernández-Baeza, J.; Gornitzka, H.; Moreno, A.; Otero, A.; Rodríguez-Curiel, R. I.; Tejeda, J. *Eur. J. Inorg. Chem.* **1999**, 1965. (c) Bouffard, J.; Keitz, B. K.; Tonner, R.; Guisado-Barrios, G.; Frenking, G.; Grubbs, R. H.; Bertrand, G. *Organometallics* **2011**, *30*, 2617. (d) Álvarez, C. M.; García-Escudero, L. A.; García-Rodíguez, R.; Miguel, D. *Chem. Commun.* **2012**, *48*, 7209. (e) Bagh, B.; McKinty, A. M.; Lough, A. J.; Stephan, D. W. *Dalton Trans.* **2014**, *43*, 12842.

[76] (a) Weiss, R.; Lowack, R. H. *Angew. Chem., Int. Ed.* **1991**, *30*, 1162. (b) Frey, G. D.; Öfele, K.; Krist, H. G.; Herdtweck, E.; Herrmann, W. A. *Inorg. Chim. Acta* **2006**, *359*, 2622. (c) Jothibasu, R.; Huynh, H. V. *Organometallics* **2009**, *28*, 2505.

[77] Bernhammer, J. C.; Frison, G.; Huynh, H. V. *Chem. Eur. J.* **2013**, *19*, 12892.

[78] Gaussian 09, Revision D.01, Frisch, M. J.; Trucks, G. W.; Schlegel, H. B.; Scuseria, G. E.; Robb, M. A.; Cheeseman, J. R.; Scalmani, G.; Barone, V.; Mennucci, B.; Petersson, G. A.; Nakatsuji, H.; Caricato, M.; Li, X.; Hratchian, H. P.; Izmaylov, A. F.; Bloino, J.; Zheng, G.; Sonnenberg, J. L.; Hada, M.; Ehara, M.; Toyota, K.; Fukuda, R.; Hasegawa, J.; Ishida, M.; Nakajima, T.; Honda, Y.; Kitao, O.; Nakai, H.; Vreven, T.; Montgomery, J. A., Jr.; Peralta, J. E.; Ogliaro, F.; Bearpark, M.; Heyd, J. J.; Brothers, E.; Kudin, K. N.; Staroverov, V. N.; Kobayashi, R.; Normand, J.; Raghavachari, K.; Rendell, A.; Burant, J. C.; Iyengar, S. S.; Tomasi, J.; Cossi, M.; Rega, N.; Millam, M. J.; Klene, M.; Knox, J. E.; Cross, J. B.; Bakken, V.; Adamo, C.; Jaramillo, J.; Gomperts, R.; Stratmann, R. E.; Yazyev, O.; Austin, A. J.; Cammi, R.; Pomelli, C.; Ochterski, J. W.; Martin, R. L.; Morokuma, K.; Zakrzewski, V. G.; Voth, G. A.; Salvador, P.; Dannenberg, J. J.; Dapprich, S.; Daniels, A. D.; Farkas, Ö.; Foresman, J. B.; Ortiz, J. V.; Cioslowski, J.; Fox, D. J. Gaussian, Inc., Wallingford CT, **2010**.

[79] (a) Becke, A. D. *Phys. Rev. A* **1988**, *38*, 3098. (b) Becke, A. D. *J. Chem. Phys.* **1993**, *98*, 5648. (c) Lee, C.; Yang, W.; Parr, R. G. *Phys. Rev. B* **1988**, *37*, 785.

[80] Dunning, T. H. *J. Chem. Phys.* **1989**, *90*, 1007.

[81] Han, Y.; Huynh, H. V. *Dalton Trans.* **2011**, *40*, 2141.

[82] (a) Carter, E. A.; Goddard III, W. A. *J. Phys. Chem.* **1986**, *90*, 998. (b) Heinemann, C.; Thiel, W. *Chem. Phys. Lett.* **1994**, *217*, 11. (c) Nyulászi, L.; Veszpremi, T.; Forro, A. *Phys. Chem. Chem. Phys.* **2000**, *2*, 3127. (d) Cheng, M.-J.; Hu, C.-H. *Chem. Phys. Lett.* **2000**, *322*, 83. (e) Cheng, M.-J.; Hu, C.-H. *Chem. Phys. Lett.* **2001**, *349*, 477. (f) Graham, D. C.; Cavell, K. J.; Yates, B. F. *J. Phys. Org. Chem.* **2005**, *18*, 298. (g) Gronert, S.; Keeffe, J. R.; O'Ferrall, R. A. M. *J. Am. Chem. Soc.* **2011**, *133*, 3381.

[83] von Ragué Schleyer, P. ; Maerker, C.; Dransfeld, A.; Jiao, H.; van Eikema Hommes, N. J. R. *J. Am. Chem. Soc.* **1996**, *118*, 6317.

[84] Wolinski, K.; Hinton, J. F.; Pulay, P. *J. Am. Chem. Soc.* **1990**, *112*, 8251.

[85] Tonner, R., Heydenrych, G., Frenking, G. *ChemPhysChem* **2008**, *9*, 1474.

[86] (a) Alder, R. W.; Allen, P. R.; Williams, S. J. *J. Chem. Soc., Chem. Commun.* **1995**, 1267. (b) Alder, R. W.; Blake, M. E.; Oliva, J. M. *J. Phys. Chem. A* **1999**, *103*, 11200. (c) Kim, Y.-J.;

Streiwieser, A. *J. Am. Chem. Soc.* **2002**, *124*, 5757. (d) Magill, A. M.; Yates, B. F. *Aust. J. Chem.* **2004**, *57*, 1205. (e) Magill, A. M.; Cavell, K. J.; Yates, B. F. *J. Am. Chem. Soc.* **2004**, *126*, 8717. (f) Amyes, T. L.; Diver, S. T.; Richard, J. P.; Rivas, F. M.; Toth, K. *J. Am. Chem. Soc.* **2004**, *126*, 4366. (g) Chen, H.; Justes, D. R.; Cooks, R. G. *Org. Lett.* **2005**, *7*, 3949. (h) Chu, Y.; Deng, H.; Cheng, J.-P. *J. Org. Chem.* **2007**, *72*, 7790. (i) Kassaee, M. Z.; Shakib, F. A.; Momeni, M. R.; Ghambarian, M.; Musavi, S. M. *J. Org. Chem.* **2010**, *75*, 2539. (j) Liu, M.; Yang, I.; Buckley, B.; Lee, J. K. *Org. Lett.* **2010**, *12*, 4764. (k) Hollczki, O.; Gerhard, D.; Massone, K.; Szarvas, L.; Nemeth, B.; Veszpremi, T.; Nyulaszi, L. *New J. Chem.* **2010**, *34*, 3004. (l) Hollczki, O.; Kelemen, Z.; Nyulaszi, L. *J. Org. Chem.* **2012**, *77*, 6014.

[87] Lavallo, V.; Canac, Y.; Präsang, C.; Donnadieu, B.; Bertrand, G. *Angew. Chem., Int. Ed.* **2005**, *44*, 5705.

[88] Weiss, R.; Reichel, S.; Handke, M.; Hampel, F. *Angew. Chem., Int. Ed.* **1998**, *37*, 344.

[89] (a) Reed, A. E.; Weinhold, F. *J. Chem. Phys.* **1985**, *83*, 1736. (b) Reed, A. E.; Weinstock, R. B.; Weinhold, F. *J. Chem. Phys.* **1985**, *83*, 735.

[90] Jacobsen, H.; Correa, A.; Costabile, C.; Cavallo, L. *J. Organomet. Chem.* **2006**, *691*, 4350.

[91] (a) Woon, D. E.; Dunning, T. H. *J. Chem. Phys.* **1993**, *98*, 1358. (b) Balabanov, N. B.; Peterson, K. A. *J. Chem. Phys.* **2005**, *123*, 064107. (c) Balabanov, N. B.; Peterson, K. A. *J. Chem. Phys.* **2006**, *125*, 074110.

[92] (a) Figgen, D.; Rauhut, G.; Dolg, M.; Stoll, H. *Chem. Phys.* **2005**, *311*, 227. (b) Peterson, K. A.; Puzzarini, C. *Theor. Chem. Acc.* **2005**, *114*, 283.

[93] (a) Herrmann, W. A.; Öfele, K.; Elison, M.; Kühn, F. E.; Roesky, P. W. *J. Organomet. Chem.* **1994**, *480*, c7. (b) Kuhn, N.; Kratz, T.; Bläser, D.; Boese, R. *Inorg. Chim. Acta* **1995**, *238*, 179. c) Hahn, F. E.; von Fehren, T.; Fröhlich, R. *Z. Naturforsch. B* **2004**, *59*, 348.

[94] (a) Wang, H. M. J.; Vasam, C. S.; Tsai, T. Y. R.; Chen, S.-H.; Chang, A. H. H.; Lin, I. J. B. *Organometallics* **2005**, *24*, 486. (b) de Frémont, P.; Scott, N. M.; Stevens, E. D.; Nolan, S. P. *Organometallics* **2005**, *24*, 2411. (c) Dash, C.; Shaikh, M. M.; Butcher, R. J.; Ghosh, P. *Inorg. Chem.* **2010**, *49*, 4972.

[95] (a) Morokuma, K. *J. Chem. Phys.* **1971**, *55*, 1236. (b) von Hopffgarten, M.; Frenking, G. *Comput. Mol. Sci.* **2012**, *2*, 43.

[96] Fernández, I.; Frenking, G. *Chem. Eur. J.* **2006**, *12*, 3617.

[97] (a) Fonseca Guerra, C.; Snijders, J. G.; Te Velde, G.; Baerends, E. J. *Theor. Chem. Acc.* **1998**, *99*, 391. (b) Te Velde, G.; Bickelhaupt, F. M.; Baerends, E. J.; Fonseca Guerra, C.; Van Gisbergen, S. J. A.; Snijders, J. G.; Ziegler, T. *J. Comput. Chem.* **2001**, *22*, 931. (c) *ADF2012*, *SCM*, Theoretical Chemistry, Vrije Universiteit, Amsterdam, The Netherlands, http://www.scm.com

[98] Perdew, J. P. *Phys. Rev. B* **1986**, *33*, 8822.

[99] Van Lenthe, E.; Baerends, E. J. *J. Comput. Chem.* **2003**, *24*, 1142.

[100] Mitoraj, M.; Michalak, A.; Ziegler, T. *J. Chem. Theory Comput.* **2009**, *5*, 962.

[101] (a) Abernethy, C. D.; Codd, G. M.; Spicer, M. D.; Taylor, M. K. *J. Am. Chem. Soc.* **2003**, *125*, 1128. (b) Shukla, P.; Johnson, J. A.; Vidovic, D.; Cowley, A. H.; Abernethy, C. D. *Chem. Commun.* **2004**, 360. (c) Mungur, S. A.; Blake, A. J.; Wilson, C.; McMaster, J.; Arnold, P. L. *Organometallics* **2006**, *25*, 1861. (d) Li, J.; Schulzke, C.; Merkel, S.; Roesky, H. W.; Samuel, P. P.; Döring, A.; Stalke, D. *Z. Anorg. Allg. Chem.* **2010**, *636*, 511.

[102] (a) Nemcsok, D.; Wichmann, K.; Frenking, G. *Organometallics* **2004**, *23*, 3640. (b) Penka, E. F.; Schläpfer, C. W.; Atanasov, M.; Albrecht, M.; Daul, C. *J. Organomet. Chem.* **2007**, *692*, 5709. (c) Fantasia, S.; Petersen, J. L.; Jacobsen, H.; Cavallo, L.; Nolan, S. P. *Organometallics* **2007**, *26*, 5880. (d) Khramov, D. M.; Lynch, V. M.; Bielawski, C. W. *Organometallics* **2007**, *26*, 6042. (e) Antonova, N. S.; Carb, J. J.; Poblet, J. M. *Organometallics* **2009**, *28*, 4283. (f) Alcarazo, M.; Stork, T.; Anoop, A.; Thiel, W.; Fürstner, A. *Angew. Chem., Int. Ed.* **2010**, *49*, 2542.

[103] (a) Christl, M.; Engels, B. *Angew. Chem., Int. Ed.* **2009**, **48**, 1538. (b) Lavallo, V.; Dyker, C. A.; Donnadieu, B.; Bertrand, G *Angew. Chem., Int. Ed.* **2009**, *48*, 1540. (c) Fernández, I.; Dyker, C. A.; DeHope, A.; Donnadieu, B.; Frenking, G.; Bertrand, G. *J. Am. Chem. Soc.* **2009**, *131*, 11875. (d) Klein, S.; Tonner, R.; Frenking, G. *Chem. Eur. J.* **2010**, *16*, 10160. (e) Peuronen, A.; Hänninen, M. M.; Tuononen, H. M. *Inorg. Chem.* **2012**, *51*, 2577.

[104] (a) DeHope, A.; Donnadieu, B.; Bertrand, G. *J. Organomet. Chem.* **2011**, *696*, 2899. (b) Pranckevicius, C.; Stephan, D. W. *Organometallics* **2013**, *32*, 2693

[105] (a) Makino1, K.; Kim, H. S.; Kurasawa, Y. *J. Heterocyclic Chem.* **1999**, 36, 321. (b) Yoon, J.-Y.; Lee, S.; Shin, H. *Curr. Org. Chem.* **2011**, *15*, 657.

[106] Guillou, S.; Bonhomme F. J.; Janin, Y. L. *Synthesis* **2008**, 3504.

[107] Dodd, D. S.; Martinez, R. L. *Tetrahedron Lett.* **2004**, *45*, 4265.

[108] Bieringer, S.; Holzer, W. *Heterocycles* **2006**, *68*, 1825.

[109] Michaelis, A.; Hepner, E. *Chem. Ber.* **1903**, *36*, 3271.

[110] Reddy, C. S.; Devi, M. V.; Sunitha, M.; Nagaraj, A. *Chem. Pharm. Bull.* **2010**, *58*, 1622.

[111] (a) Hüttel, R.; Schäfer O.; Jochum, P. *Liebigs Ann. Chem.* **1955**, *593*, 200. (b) Rodríguez-Franco, M. I.; Dorrosonro, I.; Hernández-Higueras, A. I.; Antequera, G. *Tet. Lett.* **2001**, *42*, 863. (c) Stauffer, S. R.; Huang, Y.; Coletta, C. J.; Tedesco R.; Katzenellenbogen, J. A. *Bioorg. Med. Chem.* **2001**, *9*, 141. (d) Lyalin, B. V.; Petrosyan,V. A. *Russ. Chem. Bull.* **2013**, *62*, 1044.

[112] Stefani, H. A.; Pereira, C. M. P.; Almeida, R. B.; Braga, R. C.; Guzen, K. P.; Cellac, R. *Tet. Lett.* **2005**, *46*, 6833.

[113] Bernhammer, J. C.; Huynh, H. V. *Dalton Trans.* **2012**, *41*, 8600.

[114] (a) Yuan, D.; Huynh, H. V. *Organometallics* **2012**, *31*, 405. (b) Teng, Q.; Huynh, H. V. *Inorg. Chem.* **2014**, *53*, 10964.

[115] Han, Y.; Huynh, H. V.; Tan, G. K. *Organometallics* **2007**, *26*, 6447.

[116] (a) Huynh, H. V.; Wu, J. *J. Organomet. Chem.* **2009**, *694*, 323. (b) Shibata, T.; Ito, S.; Doe, M.; Tanaka, R.; Hashimoto, H.; Kinoshita, I.; Yano, S.; Nishioka, T. *Dalton Trans.* **2011**, *40*, 6778.

[117] Han, Y. *Group 10 transition metal chemistry of benzannulated/remote N-hetereocyclic carbene ligands*, Ph.D. thesis, National University of Singapore, **2008**.

[118] (a) Raubenheimer, H. G.; Desmet, M.; Olivier, P.; Kruger, G. J. *J. Chem. Soc., Dalton* Trans. 1996, 4431. (b) Köcher, C.; Herrmann, W. A. *J. Organomet. Chem.* **1997**, *532*, 261.

[119] (a) Tafipolsky, M.; Scherer, W.; Öfele, K.; Artus, G.; Pedersen, B.; Herrmann, W. A.; McGrady, G. S. *J. Am. Chem. Soc.* **2002**, *124*, 5865. (b) Szesni, N.; Hohberger, C.; Mohamed, G. G.; Burzlaff, N.; Weibert, B.; Fischer, H. *J. Organomet. Chem.* **2006**, *691*, 5753.

[120] Bernhammer, J. C.; Huynh, H. V. *Organometallics* **2012**, *31*, 5121.

[121] (a) Michaelis, A.; Röhmer, H. *Chem. Ber.* **1898**, *31*, 2907. (b) Michaelis, A.; Pasternack, R. *Chem. Ber.* **1899**, *32*, 2398.

[122] Dvorak, C. A.; Rudolph, D. A.; Ma, S.; Carruthers, N. I. *J. Org. Chem.* **2005**, *70*, 4188.

[123] Matveeva, E. D.; Podrugina, T. A.; Taranova, M. A.; Ivanova, A. M.; Gleiter, R.; Zefirov, N. S. *J. Org. Chem.* **2012**, *77*, 5770.

[124] Huynh, H. V.; Wong, L. R.; Ng, P. S. *Organometallics* **2008**, *27*, 2231.

[125] (a) Ramnial, T.; Abernethy, C. D.; Spicer, M. D.; McKenzie, I. D.; Gay, I. D.; Clyburne, J. A. C. *Inorg. Chem.* **2003**, *42*, 1391. (b) de Fre´mont, P.; Scott, N. M.; Stevens, E. D.; Ramnial, T.; Lightbody, O. C.; Macdonald, C. L. B.; Clyburne, J. A. C.; Abernethy, C. D.; Nolan, S. P. *Organometallics* **2005**, *24*, 6301.

[126] Vicente, J; Arcas, A.; Bautista, D.; Jones, P. G.; *Organometallics* **1997**, *16*, 2127.

[127] (a) Lafrance, M.; Shore, D.; Fagnou, K. *Org. Lett.* **2006**, *8*, 5097. (b) Alberico, D.; Scott, M. E.; Lautens, M. *Chem. Rev.* **2007**, *107*, 174. (c) Ackermann, L.; Vicente, R.; Kapdi, A. R. *Angew. Chem., Int. Ed.* **2009**, *48*, 9792. (d) Rene´, O.; Fagnou, K. *Org. Lett.* **2010**, *12*, 2116. (e) Chen, F.; Min, Q.−Q.; Zhang, X. *J. Org. Chem.* **2012**, *77*, 2992. (f) He, M.; Soulé, J.-F.; Doucet, H. *ChemCatChem* **2014**, *6*, 1824.

[128] Lafrance, M.; Rowley, C. N.; Woo, T. K.; Fagnou, K. *J. Am. Chem. Soc.* **2006**, *128*, 8754.

[129] (a) Schmidt, A.; Snovydovych, B.; Habeck, T.; Dröttboom, P.; Gjikaj, M.; Adam, A. *Eur. J. Org. Chem.* **2007**, 4909. (b) Schmidt, A.; Beutler, A.; Snovydovych B. *Eur. J. Org. Chem.* **2008**, 4073. (c) Schmidt, A.; Snovydovych, B.; Hemmen, S. *Eur. J. Org. Chem.* **2008**, 4313. (d) Schmidt, A.; Snovydovych, B.; Casado, J.; Quirante, J. J.; Teodomiro, J.; Navarrete L.; Ramírez, F. J. *Phys. Chem. Chem. Phys.* **2009**, *11*, 341. (e) Schmidt, A.; Guan, Z. *Synthesis* **2012**, *44*, 3251.

[130] Lindner, A.; Schmidt, A. *Synlett* **2008**, 2961.

[131] Schmidt, A.; Habeck, T.; Snovydovych, B.; Eisfeld, W. *Org. Lett.* **2007**, *9*, 3515.

[132] (a) Sivaram, H.; Tan, J.; Huynh, H. V. *Organometallics* **2012**, *31*, 5875. (b) Guo, S.; Sivaram, H.; Yuan, D.; Huynh, H. V. *Organometallics* **2013**, *32*, 3685. (c) Sivaram, H.; Tan, J.; Huynh, H. V *Dalton Trans.* **2013**, *42*, 12421.

[133] (a) Han, Y.; Yuan, D.; Teng, Q.; Huynh, H. V. *Organometallics* **2011**, *30*, 1224. (b) Guo, S.; Lim, M. H.; Huynh H. V. *Organometallics* **2013**, *32*, 7225.

[134] (a) Yang, J.; Gharagozloo, P. *Synth. Commun.* **2005**, *35*, 409. (b) Sather, A. C.; Berryman, O. B.; Rebek, J. *Org. Lett.* **2012**, *14*, 1600.

[135] Jothibasu, R. *Group 10 and group 11 transition metal chemistry of benzimidazolin-2-ylidene and indazolin-3-ylidene ligands*, Ph.D. thesis, National University of Singapore, **2010**.

[136] Bernhammer, J. C.; Chong, N. X.; Jothibasu, R.; Zhou, B.; Huynh, H. V. *Organometallics* **2014**, *33*, 3607.

[137] (a) Huynh, H. V.; Van, D. L.; Hahn, F. E.; Hor, T. S. A. *J. Organomet. Chem.* **2004**, *689*, 1766. (b) Huynh, H. V.; Seow, H. X. *Aust. J. Chem.* **2009**, *62*, 983. (c) Yeung, A. D.; Ng, P. S.; Huynh, H. V. *J. Organomet. Chem.* **2011**, *696*, 112.

[138] (a) Magill, A. M.; Yates, B. F.; Cavell, K. J.; Skelton, B. W.; White, A. H. *Dalton Trans.* **2007**, 3398. (b) Guo, S.; Huynh, H. V. *Organometallics* **2014**, *33*, 2004

[139] Denmark, S. E.; Beutner, G. L. *Angew. Chem., Int. Ed.* **2008**, *47*, 1560.

[140] van Leeuwen, P. W. N. M.; Kamer, P. C. J.; Reek, J. N. H.; Dierkes, P. *Chem. Rev.* **2000**, *100*, 2741.

[141] Chong, N. X. *Indazolin-3-ylidenes: Complexes and applications*, M.Sc. thesis, National University of Singapore, **2014**.

[142] (a) Gischig, S.; Togni, A. *Eur. J. Inorg. Chem.* **2005**, 4745. (b) Houghton, J.; Dyson, G.; Douthwaite, R. E.; Whitwood, A. C.; Kariuki, B. M. *Dalton Trans.* **2007**, 3065. (c) Yuan, D.; Tang, H.; Xiao, L.; Huynh, H. V. *Dalton Trans.* **2011**, *40*, 8788. (d) Chen, Q.; Lv, L.; Yu, M.; Shi, Y.; Li, Y.; Pang, G.; Cao, C. *RSC Adv.* **2013**, *3*, 18359.

[143] (a) Müller, T. E.; Beller, M. *Chem. Rev.* **1998**, *98*, 675. (b) Müller, T. E.; Hultzsch, K. C.; Yus, M.; Foubelo, F.; Tada, M. *Chem. Rev.* **2008**, *108*, 3795. (c) Nishina, N.; Yamamoto, Y. *Top. Organomet. Chem.* **2013**, *43*, 115.

[144] Penzien, J.; Su, R. Q.; Mu¨ ller, T. E. *J. Mol. Catal. A: Chem.* **2002**, *182*, 489.

[145] Shimada, T.; Bajracharya, G. B.; Yamamoto, Y. *Eur. J. Org. Chem.* **2005**, 59.

[146] (a) Freixa, Z.; van Leeuwen, P. W. N. M. *Dalton Trans.* **2003**, 1890. (b) Johns, A. M.; Utsunomiya, M.; Incarvito, C. D.; Hartwig, J. F. *J. Am. Chem. Soc.* **2006**, *128*, 1828. (c) Birkholz, M.-N.; Freixa, Z.; van Leeuwen, P. W. N. M. *Chem. Soc. Rev.* **2009**, *38*, 1099.

[147] (a) Chinchilla, R.; Nájera, C. *Chem. Rev.* **2007**, *107*, 874. (b) Nicolaou, K. C.; Bulger, P. G.; Sarlah, D. *Angew. Chem., Int. Ed.* **2005**, *44*, 4442.

[148](a) Hillier, A. C.; Grasa, G. A.; Viciu, M. S.; Lee, H. M.; Yang, C.; Nolan, S. P. *J. Organomet. Chem.* **2002**, *653*, 69. (b) Fortman, G. C.; Nolan, S. P. *Chem. Soc. Rev.* **2011**, *40*, 5151. (c) John, A.; Modak, S.; Madasu, M.; Katari, M.; Ghosh, P. *Polyhedron* **2013**, *64*, 20.

[149] (a) an der Heiden, M.; Plenio, H. *Chem. Commun.* **2007**, 972. (b) Ananikov, V. P.; Musaev, D. G.; Morokuma, K. *Eur. J. Inorg. Chem.* **2007**, 5390. (c) Schilz, M.; Herbert Plenio, H. *J. Org. Chem.* **2012**, *77*, 2798.

[150] (a) da Costa, M. R. G.; Curto, M. J. M.; Davies, S. G.; Duarte, M. T.; Resende, C.; Teixeira, F. C. *J. Organomet. Chem.* **2000**, *604*, 157. (b) Jiang, X.; Tiwari, A.; Thompson, M.; Chen, Z.; Cleary, T. P.; Lee, T. B. K. *Org. Process Res. Dev.* **2001**, *5*, 604. (c) Ben-Yahia, A.; Naas, M.; El Kazzouli, S.; Essassi, E. M.; Guillaumet, G. *Eur. J. Org. Chem.* **2012**, 7075.

[151] Schreiber, S. L. *Nature* **2009**, *457*, 153.

[152] Cisnetti, F.; Gibard, C.; Gautier, A. *J. Organomet. Chem.* **2014**, doi: 10.1016/j.jorganchem.2014.10.012.

[153] Bernhammer, J. C.; Singh, H.; Huynh, H. V. *Organometallics* **2014**, *33*, 4295.

[154] Singh, H. *Indazolin-3-ylidenes: Complexes and applications*, BSc. (hons) thesis, National University of Singapore, **2014**.

[155] Huynh, H. V.; Jothibasu, R. *J. Organomet. Chem.* **2011**, *696*, 3369.

[156] (a) Chen, M.; Vicic, D. A.; Turner, M. L.; Navarro, O. *Organometallics* **2011**, *30*, 5052. (b) Chen, M.; Vicic, D. A.; Chain, W. J.; Turner, M. L.; Navarro, O. *Organometallics* **2011**, *30*, 6770.

[157] (a) Farran, R.; House, J. E., Jr. *J. Inorg. Nucl. Chem.* **1972**, *34*, 2219. (b) Enlow, P. D.; Woods, C. *Inorg. Chem.* **1985**, *24*, 1273. (c) Herrmann, W. A.; Kuˈhn, F. E.; Mattner, M. R.; Artus, G. R. J.; Geisberger, M. R.; Correia, J. D. G. *J. Organomet. Chem.* **1997**, *538*, 203. (d) Krogul, A.; Skupin´ska, J.; Litwinienko, G. *J. Mol. Catal. A* **2014**, *385*, 141.

[158] Hall, H. K. *J. Am. Chem. Soc.* **1957**, *79*, 5441.

[159] Bondi, A. *J. Phys. Chem.* **1964**, *68*, 441.

[160] (a) Satoh, T.; Miura, M. *Chem. Lett.* **2007**, *36*, 200. (b) Seregin, I. V.; Gevorgyan, V. *Chem. Soc. Rev.* **2007**, *36*, 1173. (c) McGlacken, G. P.; Bateman, L. M. *Chem. Soc. Rev.* **2009**, *38*, 2447. (d) Gryko, D. T.; Vakuliuk, O.; Gryko, D.; Koszarna, B. *J. Org. Chem.* **2009**, *74*, 9517. (e) Bensaid, S.; Doucet, H. *ChemSusChem* **2012**, *5*, 1559.

[161] Ghosh, D.; Lee, H. M. *Org. Lett.* **2012**, *14*, 5534. (b) O˙zdemir, I.; Guˈrbuˈz, N.; Kalogˇlu, N.; Dogˇan, O˙.; Kalogˇlu, M.; Bruneau, C.; Doucet, H. *Beilstein J. Org. Chem.* **2013**, *9*, 303.

[162] (a) Navarro, O.; Marion, N.; Mei, J.; Nolan, S. P. *Chem. Eur. J.* **2006**, *12*, 5142. (b) Organ, M. G; Abdel-Hadi, M.; Avola, S.; Dubovyk, I.; Hadei, N.; Kantchev, E. A. B.; O'Brien, C. J.; Sayah, M.; Valente, C. *Chem. Eur. J.* **2008**, *14*, 2443. (c) Zhu, L.; Gao, T.; Shao, L. *Tetrahedron* **2011**, *67*, 5150. (d) Tu, T.; Fang, W.; Jiang, J. *Chem. Commun.* **2011**, *47*, 12358. (e) Meiries, S.; Le Duc, G.; Chartoire, A.; Collado, A.; Speck, K.; Arachchige, K. S. A.; Slawin, A. M. Z.; Nolan, S. P. *Chem. Eur. J.* **2013**, *19*, 17358. (f) Krinsky, J. L.; Martínez, A.; Godard, C.; Castillón, S.; Claver, C. *Adv. Synth. Catal.* **2014**, *356*, 460. (g) Bastug G.; Nolan, S. P. *Organometallics* **2014**, *33*, 1253. (h) Huang, P.; Wang, Y.; Yu, H.; Lu, J. *Organometallics* **2014**, *33*, 1587. (i) Zhang, Y.; César, V.; Storch, G.; Lugan; N.; Lavigne, G. *Angew. Chem., Int. Ed.* **2014**, *53*, 6482.

[163] (a) Viciu, M. S.; Kelly, R. A.; Stevens, E. D.; Naud, F.; Studer, M.; Nolan, S. P. *Org. Lett.* **2003**, *5*, 1479. (b) Singh, R.; Nolan, S. P. *J. Organomet. Chem.* **2005**, *690*, 5832. (c) Luan, X.; Mariz, R.; Robert, C.; Gatti, M.; Blumentritt, S.; Linden, A.; Dorta, R. *Org. Lett.* **2008**, *10*, 5569. (d) Johansson, C. C. C.; Colacot, T. J. *Angew. Chem., Int. Ed.* **2010**, *49*, 676.

[164] (a) v. Auwers, K.; Allardt, H.-G. *Chem. Ber.* **1924**, *57*, 1098. (b) Georgarakis, E.; Schmid, H.; Hansen, H.-J. *Helv. Chim. Acta* **1979**, *62*, 234.

[165] Cadogan, J. I. G. *Q. Rev., Chem. Soc.* **1962**, *16*, 208.

[166] Kumar, M. R.; Park, A.; Park, N.; Lee, S. *Org. Lett.* **2011**, *13*, 3542.

[167] Sharghi, H.; Aberi, M. *Synlett* **2014**, *25*, 1111.

[168] (a) Arnold, P. L.; Scarisbrick, A. C.; Blake, A. J.; Wilson, C. *Chem. Commun.* **2001**, 2340. (b) Arnold, P. L.; Sanford, M. S.; Pearson, S. M. *J. Am. Chem. Soc.* **2009**, *131*, 13912. (c) del Pozo, C.; Iglesias, M.; Sánchez, F. *Organometallics* **2011**, *30*, 2180. (d) Naziruddin, A. R.; Hepp, A., Pape, T.; Hahn, F. E. *Organometallics* **2011**, *30*, 5859. (e) Cross, W. B.; Daly, C. G.; Boutadla, Y.; Singh, K. *Dalton Trans.* **2011**, *40*, 9722. (f) Nägele, P.; Herrlich, U.; Rominger, F.; Hofmann, P. *Organometallics* **2013**, *32*, 181.

[169] (a) Bierenstiel, M.; Cross, E. D. *Coord. Chem. Rev.* **2011**, *255*, 574. (b) Yuan, D.; Huynh, H. V. *Molecules* **2012**, *17*, 2491. (c) Fliedel, C.; Braunstein, P. *J. Organomet. Chem.* **2014**, *751*, 286.

[170] (a) McGuinness, D. S.; Suttil, J. A.; Gardiner, M. G.; Davies, N. W. *Organometallics* **2008**, *27*, 4238. (b) Gandolfi, C.; Heckenroth, M.; Neels, A.; Laurenczy, G.; Albrecht, M.

Organometallics **2009**, *28*, 5112. (c) Huynh, H.V.; Chew, Y.X. *Inorg. Chim. Acta* **2010**, *363*, 1979. (d) Yuan, D.; Huynh, H. V. *Organometallics* **2010**, *29*, 6020. (e) Zhou, X.; Jordan, R. F. *Organometallics* **2011**, *30*, 4632. (f) Syska, H.; Herrmann, W. A.; Kühn, F. E. *J. Organomet. Chem.* **2012**, *703*, 56. (g) Holm, S. C.; Rominger, F.; Straub, B. F. *J. Organomet. Chem.* **2012**, *719*, 54.

[171] (a) Wolf, J.; Labande, A.; Daran, J.-C.; Poli, R. *Eur. J. Inorg. Chem.* **2007**, 5069. (b) Fliedel, C.; Schnee, G.; Braunstein, P. *Dalton Trans.* **2009**, 2474. (c) Huynh, H. V.; Yeo, C. H.; Chew, Y. X. *Organometallics* **2010**, *29*, 1479. (d) Fliedel, C.; Braunstein, P. *Organometallics* **2010**, *29*, 5614. (e) Canovese, L.; Visentin, F.; Levi, C.; Santo, C.; Bertolasi, V. *J. Organomet. Chem.* **2013**, *732*, 27. (f) Rosen, M. S.; Stern, C. L.; Mirkin, C. A. *Chem. Sci.* **2013**, *4*, 4193. (g) Hohloch, S.; Hettmanczyk, L.; Sarkar, B. *Eur. J. Inorg. Chem.* **2014**, 3164.

[172] Bernhammer, J. C.; Huynh, H. V. *Organometallics* **2014**, *33*, 172.

[173] Starikova, O. V.; Dolgushin, G. V.; Larina, L. I.; Ushakov, P. E.; Komarova, T. N.; Lopyrev, V. A. *Russ. J. Org. Chem.* **2003**, *39*, 1467.

[174] (a) Ahrens, S.; Herdtweck, E.; Goutal, S.; Strassner, T. *Eur. J. Inorg. Chem.* **2006**, 1268. (b) Ahrens, S.; Strassner, T. *Inorg. Chim. Acta* **2006**, *359*, 4789.(b) Jahnke, M. C.; Pape, T.; Hahn, F. E. *Z. Naturforsch.* **2010**, *65b*, 341.

[175] (a) Han, Y.; Huynh, H. V.; Tan, G. K. *Organometallics* **2007**, *26*, 4612. (b) Hu, J. J.; Li, F.; Hor, T. S. A. *Organometallics* **2009**, *28*, 1212. (c) Hu, J. J.; Bai, S.-Q.; Yeh, H. H.; Young, D. J.; Chi, Y.; Hor, T. S. A. *Dalton Trans.* **2011**, *40*, 4402.

[176] Müller, T. E.; Pleier, A.-K. *J. Chem. Soc., Dalton Trans.* **1999**, 583.

[177] (a) Burling, S.; Field, L. D.; Li, H. L.; Messerle, B. A.; Turner, P. *Eur. J. Inorg. Chem.* **2003**, 3179. (b) Field, L. D.; Messerle, B. A.; Vuong, K. Q.; Turner, P. *Organometallics* **2005**, *24*, 4241. (c) Bauer, E. B.; Andavan, G. T. S.; Hollis, T. K.; Rubio, R. J.; Cho, J.; Kuchenbeiser, G. R.; Helgert, T. R.; Letko, C. S.; Tham, F. S. *Org. Lett.* **2008**, *10*, 1175. (d) Kinder, R. E.; Zhang, Z.; Widenhoefer, R. A. *Org. Lett.* **2008**, *10*, 3157. (e) Ogata, K.; Nagaya, T.; Fukuzawa, S.-I. *J. Organomet. Chem.* **2010**, *695*, 1675. (f) Barroso, S.; de Aguiar, S. R. M. M.; Munhá, R. F.; Martins, A. M. *J.Organomet. Chem.* **2014**, *760*, 60.

[178] (a) Brunet, J.-J.; Chu, N. C.; Diallo, O.; Vincendeau, S. *J. Mol. Catal. A: Chem.* **2005**, *240*, 245. (b) Severin, R.; Doye, S. *Chem. Soc. Rev.* **2007**, *36*, 1407. (c) Chianese, A. R.; Lee, S. J.; Gagné, M. R. *Angew. Chem., Int. Ed.* **2007**, *46*, 4042.

[179] Zhang, R.; Xu, Q.; Mei, L.-Y.; Li, S.-K.; Shi, M. *Tetrahedron* **2012**, *68*, 3172.

[180] (a) Dub, P. A.; Rodriguez-Zubiri, M.; Daran, J.-C.; Brunet, J.-J.; Poli, R. *Organometallics* **2009**, *28*, 4764. (b) Dub, P. A.; Poli, R. *J. Am. Chem. Soc.* **2010**, *132*, 13799. (c) Dub, P. A.; Béthegnies, A.; Poli, R. *Organometallics* **2012**, *31*, 294.

[181] (a) Weitershaus, K.; Ward, B. D.; Kubiak, R.; Müller, C.; Wadepohl, H.; Doye, S.; Gade, L. H. *Dalton Trans.* **2009**, 4586. (b) Alvarado, E.; Badaj, A. C.; Larocque, T. G.; Lavoie, G. G. *Chem. Eur. J.* **2012**, *18*, 12112.

[182] (a) Reichl, J. A.; Berry, D. H. *Adv. Organomet. Chem.* **1998**, *43*, 197. (b) Trost, B. M.; Ball, Z. T. *Synthesis* **2005**, 853. (c) Troegel, D.; Stohrer, J. *Coord. Chem. Rev.* **2011**, *255*, 1440.

[183] (a) Karstedt, B. D. Ger. Offen. DE 1941411, 1970. (b) Karstedt, B. D. Ger. Offen. DE 2307085, 1973. (c) Speier, J. L. *Adv. Organomet. Chem.* **1979**, *17*, 407.

[184] (a) Markó, I. E.; Stérin, S.; Buisine, O.; Berthon, G.; Michaud, G.; Tinant, B.; Declercq, J. P. *Adv. Synth. Catal.* **2004**, *346*, 1429. (b) Buisine, O.; Berthon-Gelloz, G.; Brière, J. F.; Stérin, S.; Mignani, G.; Branlard, P.; Tinant, B.; Declercq, J. P.; Markó, I. E. *Chem. Commun.* **2005**, 3856. (c) Berthon-Gelloz, G.; Buisine, O.; Brière, J.-F.; Michaud, G.; Stérin, S.; Mignani, G.; Tinant, B.; Declercq, J.-P.; Chapon, D.; Markó, I. E. *J. Organomet. Chem.* **2005**, *690*, 6156. (d) De Bo, G.; Berthon-Gelloz, G.; Tinant, B.; Markó, I. E. *Organometallics* **2006**, *25*, 1881. (e) Poyatos, M.; Maisse-Francois, A.; Bellemin-Laponnaz, S.; Gade, L. H. *Organometallics* **2006**, *25*, 2634. (f) Berthon-Gelloz, G.; Schumers, J. M.; De Bo, G.; Markó, I. E. *J. Org. Chem.* **2008**, *73*, 4190. (g) Lu, C.; Gu, S.; Chen, W.; Qiu, H. *Dalton Trans.* **2010**, *39*, 4198. (h) Dunsford, J. J.; Cavell, K. J.; Kariuki, B. *J. Organomet. Chem.* **2011**, *696*, 188. (i) Zanardi, A.; Mata, J. A.; Peris, E. *Eur. J. Inorg. Chem.* **2011**, 416. (j) Taige, M. A.; Ahrens, S.; Strassner, T. *J. Organomet. Chem.* **2011**, *696*, 2918. (k) Silbestri, G. F.; Flores, J. C.; de Jesús, E. *Organometallics* **2012**, *31*, 3355.

[185] Roy, A. K.; Taylor, R. B. *J. Am. Chem. Soc.* **2002**, *124*, 9510.

[186] Bernhammer, J. C.; Hunyn, H. V. *Organometallics* **2014**, *33*, 1266.

[187] Krishnan, D.; Wu, M.; Chiang, M.; Li, Y.; Leung, P.-H.; Pullarkat, S. A. *Organometallics* **2013**, *32*, 2389.

[188] (a) Han, Y.; Huynh, H. V.; Koh, L. L. *J. Organomet. Chem.* **2007**, *692*, 3606. (b) Doğan, Ö.; Gürbüz, N.; Özdemir, İ.; Çetinkaya, B.; Şahin, O.; Büyükgüngör, O. *Dalton Trans.* **2009**, 7087.

[189] Gorelsky, S. I. *Organometallics* **2012**, *31*, 4631.

[190] (a) Matsubara, K.; Ueno, K.; Shibata, Y. *Organometallics* **2006**, *25*, 3422. (b) Huynh, H. V.; Jothibasu, R. *Eur. J. Inorg. Chem.* **2009**, 1926. (c) Zhang, C.; Wang, Z. *Organometallics* **2009**, *28*, 6507. (d) Oertel, A. M.; Ritleng, V.; Chetcuti, M. J. *Organometallics* **2012**, *31*, 2829. (e) Hameury, S.; de Frémont, P.; Breuil, P.-A. R.; Olivier-Bourbigou, H.; Braunstein, P. *Dalton Trans.* **2014**, *43*, 4700.

[191] Huynh, H. V.; Holtgrewe, C.; Pape, T.; Koh, L. L.; Hahn, E. *Organometallics* **2006**, *25*, 245.

[192] Bernhammer, J. C.; Huynh, H. V. *Organometallics* **2014**, *33*, 5845.

[193] Berding, J.; van Paridon, J. A.; van Rixel, V. H. S.; Bouwman, E. *Eur. J. Inorg. Chem.* **2011**, 2450.

[194] Wilson, A. K.; Woon, D. E.; Peterson, K. A.; Dunning, T. H., Jr. *J. Chem. Phys.* **1999**, *110*, 7667.

[195] (a) Zim, D.; Gruber, A. S.; Ebeling, G.; Dupont, J.; Monteiro, A. L. *Org. Lett.* **2000**, *2*, 2881. (b) Littke, A. F.; Fu, G. C. *Angew. Chem., Int. Ed.* **2002**, *41*, 4176. (c) Suzuki, A. *Angew. Chem., Int. Ed.* **2011**, *50*, 6722. (d) Doucet, H. *Eur. J. Org. Chem.* **2008**, 2013. (e) Torborg, C.; Beller, M. *Adv. Synth. Catal.* **2009**, *351*, 3027. (f) Lennox, A. J. J.; Lloyd-Jones, G. C. *Chem. Soc. Rev.* **2014**, *43*, 412.

[196] (a) Lee, C.; Ke, W..; Chan, K.; Lai, C.; Hu, C.; Lee, H. M. *Chem. Eur. J.* **2007**, *13*, 582. (b) Liao, C..; Chan, K.; Chang, Y.; Chen, C..; Tu, C.; Hu, C.; Lee, H. M. *Organometallics* **2007**, *26*, 5826. (c) Xi, Z.; Zhang, X.; Chen, W.; Fu, W.; Wang, D. *Organometallics* **2007**, *26*, 6636. (d) Inamoto, K.; Kuroda, J.; Kwon, E.; Hiroya, K.; Doi, T. *J. Organomet. Chem.* **2009**, *694*, 389. (e) Kuroda, J.; Inamoto, K.; Hiroya, K.; Doi, T. *Eur. J. Org. Chem.* **2009**, 2251. (f) Ritleng, V.; Oertel, A. M.; Chetcuti, M. J. *Dalton Trans.* **2010**, *39*, 8153. (g) Rosen, B. M.; Quasdorf, K. W.; Wilson, D. A.; Zhang, N.; Resmerita, A.-M.; Garg, N. K.; Percec, V. *Chem. Rev.* **2011**, *111*,

1346. (h) Jana, R.; Pathak, T. P.; Sigman, M. S. *Chem. Rev.* **2011**, *111*, 1417. (i) Oertel, A. M.; Ritleng, V.; Burr, L.; Chetcuti, M. J. *Organometallics* **2011**, *30*, 6685. (j) Zell, T.; Fischer, P.; Schmidt, D.; Radius, U. *Organometallics* **2012**, *31*, 5065. (k) Han, F.-S. *Chem. Soc. Rev.* **2013**, *42*, 5270.

[197] (a) Li, Z.; Jiang, Y.-Y.; Fu, Y. *Chem. Eur. J.* **2012**, *18*, 4345. (b) Mesganaw, T.; Garg, N. K. *Org. Process Res. Dev.* **2013**, *17*, 29.

[198] Chiu, P. L.; Lai, C.-L.; Chang, C.-F.; Hu, C.-H.; Lee, H. M. *Organometallics* **2005**, *24*, 6169.

[199] (a) Amatore, C.; Jutand, A.; Le Duc, G. *Chem. Eur. J.* **2011**, *17*, 2492. (b) Liu, L.; Zhang, S.; Chen, H.; Lv, Y.; Zhu, J.; Zhao, Y. *Chem. Asian J.* **2013**, *8*, 2592.

[200] Zhou, Y.; Xi, Z.; Chen, W.; Wang, D. *Organometallics* **2008**, *27*, 5911.

[201] (a) Albrecht, M.; van Koten, G. *Angew. Chem., Int. Ed.* **2001**, *40*, 3750. (b) Pugh, D.; Danopoulos, A. A. *Coord. Chem. Rev.* **2007**, *251*, 610. (c) Selander, N.; Szabó, K. J. *Chem. Rev.* **2011**, *111*, 2048. (d) van Koten, G. *J. Organomet. Chem.* **2013**, *730*, 156. (e) Szabó, K. J. *Top. Organomet. Chem.* **2013**, *40*, 203. (f) Hawk, J. L.; Craig, S. L. *Top. Organomet. Chem.* **2013**, *40*, 319.

[202] (a) Lee, H. M.; Zeng, J. Y.; Hu, C.; Lee, M. *Inorg. Chem.* **2004**, *43*, 6822. (b) Danopoulos, A. A.; Wright, J. A.; Motherwell, W. B. *Chem. Commun.* **2005**, 784. (c) Wei, W.; Qin, Y.; Luo, M.; Xia, P.; Wong, M. S. *Organometallics* **2008**, *27*, 2268. (d) Fogler, E.; Balaraman, E.; Ben-David, Y.; Leitus, G.; Shimon, L. J. W.; Milstein, D. *Organometallics* **2011**, *30*, 3826. (e) Zhang, X.; Wright, A. M.; DeYonker, N. J.; Hollis, T. K.; Hammer, N. I.; Webster, C. E.; Valente, E. J. *Organometallics* **2012**, *31*, 1664. (f) Mancano, G.; Page, M. J.; Bhadbhade, M.; Messerle, B. A. *Inorg. Chem.* **2014**, *53*, 10159.

[203] (a) van Koten, G. *Pure Appl. Chem.* **1989**, *61*, 1681. (b) Moreno, I.; SanMartin, R.; Inés, B.; Churruca, F.; Domínguez, E. *Inorg. Chim. Acta* **2010**, *363*, 1903. (c) Gelman, D.; Musa, S. *ACS Catal.* **2012**, *2*, 2456. (d) Roddick, D. M. *Top. Organomet. Chem.* **2013**, *40*, 49.

[204] (a) Canovese, L.; Visentin, F.; Chessa, G.; Uguagliati, P.; Santo, C.; Bandoli, G.; Maini, L. *Organometallics* **2003**, *22*, 3230. (b) Bassetti, M.; Capone, A.; Salamone, M. *Organometallics* **2004**, *23*, 247. (c) Vuzman, D.; Poverenov, E.; Shimon, L. J. W.; Diskin-Posner, Y.; Milstein, D. *Organometallics* **2008**, *27*, 2627. (d) Fulmer, G. R.; Kaminsky, W.; Kemp, R. A.; Goldberg, K. I.

Organometallics **2011**, *30*, 1627. (e) Ruddy, A. J.; Mitton, S. J.; McDonald, R.; Turculet, L. *Chem. Commun.* **2012**, *48*, 1159.

[205] (a) Moxham, G. L.; Randell-Sly, H. E.; Brayshaw, S. K.; Woodward, R. L.; Weller, A. S.; Willis, M. C. *Angew. Chem., Int. Ed.* **2006**, *45*, 7618. (b) Zhao, C.; Jennings, M. C.; Puddephatt, R. J. *Dalton Trans.* **2008**, 1243. (c) Moxham, G. L.; Randell-Sly, H.; Brayshaw, S. K.; Weller, A. S.; Willis, M. C. *Chem. Eur. J.* **2008**, *14*, 8383.

[206] (a) Poverenov, E.; Gandelman, M.; Shimon, L. J. W.; Rozenberg, H.; Ben-David, Y.; Milstein, D. *Organometallics* **2005**, *24*, 1082. (b) Lindner, R.; van den Bosch, B.; Lutz, M.; Reek J. N. H.; van der Vlugt, J. I. *Organometallics* **2011**, *30*, 499.

[207] Bernhammer, J. C.; Frison, G.; Huynh, H. V. *Dalton Trans.* **2014**, *43*, 8591.

[208] Kendall, R. A.; Dunning, T. H. *J. Chem. Phys.* **1992**, *96*, 6796.

[209] (a) Peterson, K. A.; Figgen, D.; Goll, E.; Stoll H.; Dolg, M. *J. Chem. Phys.* **2003**, *119*, 11113. (b) Peterson, K. A.; Figgen, D.; Dolg, M. ; Stoll, H. *J. Chem. Phys.* **2007**, *126*, 124101.

[210] Denmark S. E.; Beutner, G. L. *Angew. Chem., Int. Ed.* **2008**, *47*, 1560.

[211] Venanzi, L. M. *J. Chem. Soc.* **1958**, 719.

[212] Kaleta, Z.; Tárkányi, G.; Golmolry, Á; Kálmán, F.; Nagy, T.; Soós, T. *Org. Lett.* **2006**, *8*, 1093.

[213] Kumar, A.; Maurya, R. A.; Sharma, S. *Bioorg. Med. Chem. Lett.* **2009**, *19*, 4432.

[214] Li, X.; He, L.; Chen, H.; Wu, W.; Jiang, H. *J. Org. Chem.* **2013**, *78*, 3636.

[215] Zora, M.; Kivrak, A.; Yazici, C. *J. Org. Chem.* **2011**, *76*, 6726.

[216] Eller, G. A.; Vilkauskaitė, G.; Arbačiauskienė, E.; Šačkus A.; Holzer, W. *Synth. Commun.* **2011**, *41*, 541.

[217] von Ragué Schleyer, P.; Maerker, C.; Dransfeld, A.; Jiao, H.; van Eikema Hommes, N. J. R. *J. Am. Chem. Soc.* **1996**, *118*, 6317.

[218] Wolinski, K.; Hinton, J. F.; Pulay, P. *J. Am. Chem. Soc.* **1990**, *112*, 8251.

[219] (a) Reed, A. E.; Weinhold, F. *J. Chem. Phys.* **1985**, *83*, 1736. (b) Reed, A. E.; Weinstock, R. B.; Weinhold, F. *J. Chem. Phys.* **1985**, *83*, 735. (c) Reed, A. E.; Curtis, L. A.; Weinhold, F. *Chem. Rev.* **1988**, *88*, 899.

[220] Perdew, J. P. *Phys. Rev. B* **1986**, *33*, 8822.

[221] (a) Ziegler, T.; Rauk, A. *Inorg. Chem.* **1979**, *18*, 1558. (b) Ziegler, T.; Rauk, A. *Inorg. Chem.* **1979**, *18*, 1755.

[222] van Lenthe, E.; Baerends, E. J. *J. Comput. Chem.* **2003**, *24*, 1142.

[223] (a) van Lenthe, E.; Baerends, E. J.; Snijders, J. G. *J. Chem. Phys.* **1994**, *101*, 9783. (b) van Lenthe, E.; Ehlers, A.; Baerends, E. J. *J. Chem. Phys.* **1999**, *110*, 8943.

[224] (a) Feller, D. *J. Comput. Chem.* **1996**, *17*, 1571. (b) Schuchardt, K. L.; Didier, B. T.; Elsethagen, T.; Sun, L.; Gurumoorthi, V.; Chase, J.; Li, J.; Windus, T. L. *J. Chem. Inf. Model.* **2007**, *47*, 1045.

[225] *SMART* version 5.628; Bruker AXS Inc.: Madison, WI, **2001**.

[226] *SAINT+* version 6.22a; Bruker AXS Inc.: Madison, WI, **2001**.

[227] Sheldrick, G. W. *SADABS* version 2.10; University of Göttingen, **2001**.

[228] *SHELXTL* version 6.14; Bruker AXS Inc.: Madison, WI, **2000**.